MSEL

Materials Science and Engineering Laboratory

CERAMICS

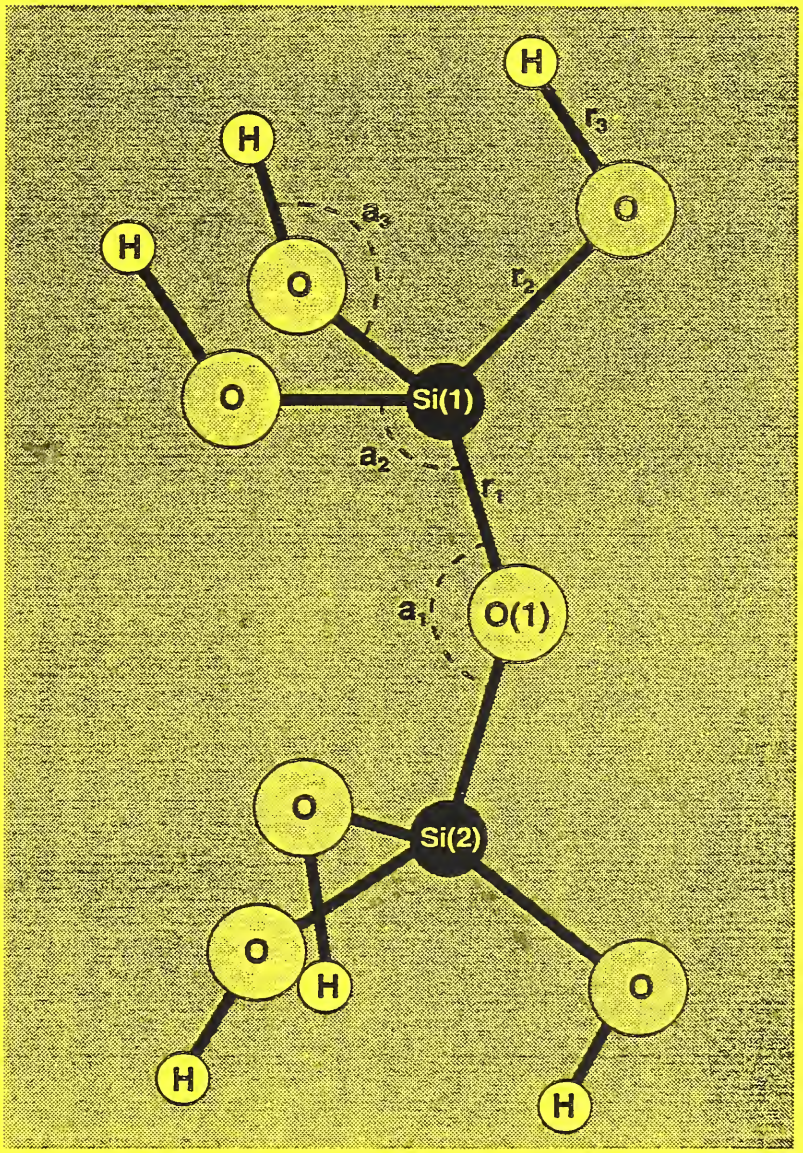

NAS-NRC
Assessment Panel
February 13-14, 1992

NISTIR 4694
U.S. Department of Commerce
National Institute of Standards
and Technology

Technical Activities 1991

Model of Si-O used in molecular orbital calculations illustrating how bond displacements in SiO_2 are being used to model stress corrosion.

MSEL

Materials Science and Engineering Laboratory

CERAMICS

S.W. Freiman, Acting Chief
S.J. Dapkunas, Deputy Chief

NAS-NRC
Assessment Panel
February 13-14, 1992

NISTIR 4694
U.S. Department of Commerce
National Institute of Standards
and Technology

Technical Activities 1991

U.S. DEPARTMENT OF COMMERCE, Robert A. Mosbacher,Secretary
National Institute of Standards and Technology, John W. Lyons, Director

TABLE OF CONTENTS

OVERVIEW

In 1991, the Ceramics Division continued its program of standards development, data generation and evaluation, and research focused on the characterization and understanding of material behavior. Our research program focuses on the critical issues which control the implementation of advanced ceramics and is developed through internal assessment and consultation with representatives from ceramic industries and academia.

The results of our program are provided to the ceramics community, in part, through collaborative programs with guest scientists from universities and industry. During this past year the Ceramics Division research program has led to three invention disclosures, 225 publications or submissions (papers, books, and standards), and over 150 talks.

We have maintained our leadership position with respect to national and international standards activities. In addition to ASTM committee participation, Division staff coordinated the International Energy Agency Round Robin on Ceramic Powder Characterization Techniques and the U. S. ceramic activities in the Versailles Advanced Materials and Standards (VAMAS) Project. Ceramics Division personnel, led by Dr. Subhas Malghan and Dr. Stephen Hsu, in collaboration with the participants of the IEA powder characterization program, have developed twenty-five procedures for analysis of ceramic powder properties. These data will provide a basis for powder specifications required for international commerce. Dr. Said Jahanmir is now serving as the leader of the VAMAS working group on tribology, while Mr. George Quinn leads the working group on ceramics. Participation in all of these areas has strengthened the U.S. position in international standards development.

In the way of data activities, three new volumes were completed as part of the joint NIST-American Ceramic Society program to develop and disseminate evaluated phase diagrams. These include Volume 9 in the series "Phase Diagrams for Ceramists," a 1991 Annual Volume, and a special monograph containing approximately 200 phase diagrams pertinent to high T_c superconductors. The Structural Ceramics Database became available in October 1990 as NIST Standard Reference Database Number 30 (SRD 30). This system is the first collection of evaluated thermal and mechanical property data for advanced ceramics that has been made available to the public in a computerized, user-friendly format. More than fifty industries, government laboratories, and academic research facilities purchased SRD 30 during fiscal year 1991. Work has continued on A Computerized Tribology Information System, ACTIS, which ultimately will consist of databases, design codes, searching capability, a product directory, and a newsletter.

During the past year, work significantly increased in the Ceramics Division in a number of areas related to photonic and optoelectronic materials:

- A NIST competence initiative awarded to Dr. Debra Kaiser has enabled her to begin efforts in constructing and operating a metal-organic chemical vapor deposition system for producing single-crystal ferroelectric oxide films.

- The superior performance of mercuric iodide gamma ray detectors grown in space over crystals grown on the ground has been shown via diffraction images. As a result, the growth in space of higher purity mercuric iodide now acquires particular interest in the improvement of these detectors.

- Two of the most commonly observed luminescence emission bands of CVD diamond occur in the red and blue-violet regions of the visible spectrum. Spectrally resolved cathodoluminescence imaging of isolated diamond particles has shown that for some choices of deposition conditions, the red emission band is associated with (111) crystal growth sectors and the blue-violet emission band is associated with (100) sectors. It may thus be possible to control the color of the luminescence by controlling the crystal growth habit. This is of interest for potential applications of CVD diamond in full-color luminescent displays.

- Oklahoma State University tests of glasses prepared at NIST showed absorption and thermal lensing properties that ensure reduction of very high intensity blue (457 nm wavelength) light to below the threshold for damage to the human retina in an apertured optical observation system such as a telescope. Studies of numerous borate, phosphate, silicate and germinate glass compositions prepared over the years by NIST provided the understanding that led to this breakthrough.

- Diffraction anomalous fine structure (DAFS) has been demonstrated with copper crystals and with $In_xGa_{1-x}As$ films. This new technique will enable the study of buried layers containing the same atomic species as surface layers in electronic devices.

We are continuing to expand our research efforts into unique processing methods applicable for both structural and functional ceramics. Experiments have demonstrated that a variety of magnetic nano-composite materials can be produced through molecular chemical processing in a modified sol-gel system, coprecipitation processes, and by metal-organo complex formation. Some examples of the magnetic nano-composite generated in bulk by these processes are iron-in-silica gel, iron-in-vitreous alumina, cobalt-in-copper and cobalt-zinc ferrites. In addition, continuing work on the compaction of nano-size, amorphous silicon nitride powders at low temperatures has led to the production of optically transparent, hard ceramics by sintering at much lower temperatures than could be achieved under normal conditions. The effects of compacting pressure and temperature on properties is being investigated, and scale-up issues are being considered.

The program in high T_c superconductivity remains strong. A particularly noteworthy result comes from joint work performed with the University of Wisconsin. Electrical transport measurements across individual grain boundaries in bulk-scale $YBa_2Cu_3O_{6+x}$ bicrystals at 77K have revealed a general trend for a transition from flux pinning to Josephson junction to resistive behavior with increasing misorientation angle. Subsequent transmission electron microscopy studies on several electromagnetically-characterized boundaries revealed a thin second phase layer at resistive boundaries which was absent from Josephson junction boundaries. Thus, the fine-scale microstructural features of a grain boundary are critical in determining the transport mechanism across it. In addition, considerable work was performed in delineating phase equilibria in the four-component Bi-Sr-Ca-Cu-O system. These data will be used to optimize processing procedures in this system.

As we expand our research efforts in the area of functional ceramics, we continue to address the key issues with respect to structural materials:

- New techniques for powder and compact characterization such as nuclear magnetic resonance (NMR) and electrokinetic sonic amplitude (ESA) measurements are leading to an increased understanding of powder processing. NMR techniques to spatially resolve distributions in silicon nitride slurries to the 40 micrometer level have been developed.

- A study was conducted to assess the current state-of-the-art in the machining of advanced ceramics, and to identify research areas which could lead to significant improvements in efficiency and surface finish.

- Significant progress has been realized in our program to design microstructures which provide optimize properties for specific applications. Specifically, anisotropic alumina/aluminum titanate has been utilized as a model material to demonstrate this predictive capability for fracture toughness. Research has continued to identify those microstructural features which control creep in both monolithic and composite ceramics.

In addition to the experimental programs, this past year has seen an increase in the modeling efforts in this Division. These studies range from molecular orbital calculations of water enhanced bond rupture, aimed at predicting stress corrosion of ceramics, to microstructural modeling which should lead to a greater understanding of how to achieve desired properties through sintering.

During this past year, both funding and staff levels have remained relatively stable; we were able to add two individuals to the Materials Microstructural Characterization Group (Dr. Charles Bouldin and Dr. Joseph Woicik), who are working extensively on optoelectronic materials. Both of these individuals transferred to the Ceramics Division from the NIST Electronics and Electrical Engineering Laboratory (EEEL). We recognize the need to replace key personnel who retired this year, and are actively searching for the most promising candidates.

As we enter 1992, we will continue to address those fundamental needs of cost, reliability and performance prediction for advanced ceramics. Our efforts will focus on powder processing/sintering and machining research required to achieve the above noted objectives for structural ceramics. In the area of functional materials, our efforts will focus on the development of processing-property relations for thin-film ferroelectrics and diamond films and on the development of test procedures to ensure the mechanical reliablility of piezoelectric and superconducting materials in both bulk and thin-film form.

A number of Ceramic Division members received external recognition for their work. Dr. Sheldon Wiederhorn was inducted as a member of the National Academy of Engineering. Dr. Robert Roth presented the Sosman Award Lecture for the Basic Science Division of the American Ceramic Society. Dr. Craig Carter was a co-recipient of the Ross Coffin Purdy Award of the American Ceramic Society, presented for the most outstanding scientific paper published in the previous year. Dr. Brian Lawn and Dr. Sheldon Wiederhorn were jointly presented with the Hobart M. Kraner Award by the Lehigh Valley Section of the American Ceramic Society and the Ceramics Laboratory at Lehigh University. Mr. Richard Gates and Dr. Stephen Hsu won the Al Sonntag Award for the best paper on solid lubrication published during the year in a journal of the Society of Tribologists and Lubrication Engineers.

Finally, in the latter part of FY-1991, Dr. Stephen Hsu, the first chief of the Ceramics Division, elected to resume active research. All of us in the Division appreciate the leadership he provided the Division and wish him success in his new endeavors.

Stephen W. Freiman
Acting Chief, Ceramics Division

1991 DIVISION RESOURCES

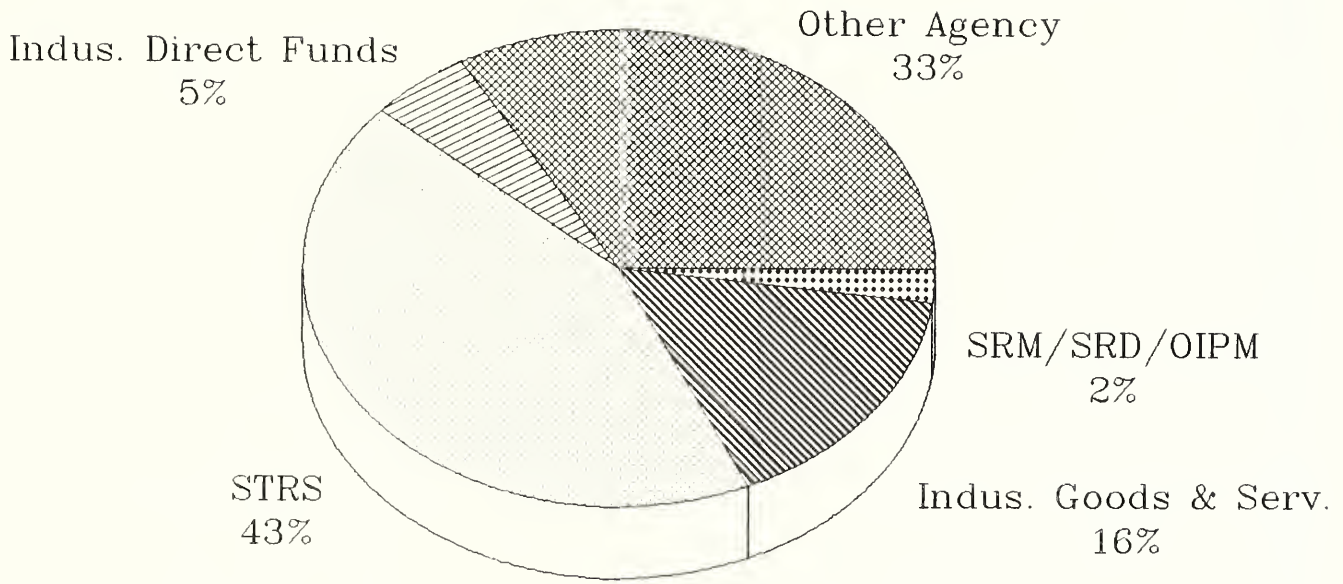

TECHNICAL ACTIVITIES*

Certain trade names and company products are mentioned in the text or identified in illustrations in order to adequately specify the experimental procedure and equipment used.

In no case does such identification imply recommendation or endorsement by the National Institute of Standards and Technology, nor does it imply that the products are necessarily the best available for that purpose.

TECHNICAL ACTIVITIES*

STANDARDS AND DATA ACTIVITIES

The ceramics industry requires the availability of carefully determined standard materials, techniques, and data. Division activities address these needs through the development of standard reference materials and the dissemination of evaluated data. A list of Standard Reference Materials that the Division has produced is given in OUTPUTS AND INTERACTIONS. Transfer to industry is implemented through the ASTM in the case of test methodologies, and through the American Ceramic Society and the NIST Offices of Standard Reference Data and Standard Reference Materials for data and materials.

Increasing international competition in the advanced ceramics field necessitates participation in multinational standards development activities. Techniques of measurement have been evaluated and developed through our powder characterization program conducted under the auspices of the International Energy Agency (described under Powder Characterization and Processing), and the Versailles Advanced Materials and Standards (VAMAS) Project for fracture and wear evaluation. We plan to continue our participation in these programs, serving as the domestic focal point.

Significant Accomplishments

- In collaboration with the participants of the International Energy Agency (IEA) powder characterization program, twenty-five procedures for analysis of ceramic powder properties were developed. Using these procedures, the participants have analyzed five powders, a silicon carbide, a zirconia, an aluminum nitride, and two silicon nitrides. The data collected by all participants have been compiled and organized into a report. Data analysis activity is in progress.

- Two standards for mechanical property tests were finalized and formally adopted. ASTM C 1161, "Flexural Strength of Advanced Ceramics at Ambient Temperature," is the first test method standard developed in ASTM Committee C-28, Advanced Ceramics. MIL STD 1942(A) "Flexural Strength of High Performance Ceramics at Ambient Temperature," an updated and revised version of an older MIL STD, is now a tri-service (Army, Navy, and Air Force) standard.

- A computerized database has been constructed containing over 350 records of material properties and tribological properties for a number of advanced ceramic materials. The data were obtained from NIST research programs, from other tribology experts, and from literature sources. Data evaluation was carried out both by NIST and by a contractor at Stevens Institute of Technology. The database has been configured as a numeric spreadsheet that can be used with commercial MS/DOS software. It represents the most extensive tribology database on ceramics presently available.

- Specifications were established and a contract was awarded by competitive means to develop the second state set of technical modules for the Computerized Tribology Information System (ACTIS). Delivery of the six modules is expected over an eighteen month period. The new modules include a lubricant database; an expert system lubricant selector; three software codes for design of gear, ball bearing, and roller bearing systems; and a central access module. The new set will significantly expand the first version of ACTIS that is currently being marketed.

- Three new volumes were completed as part of the joint NIST-American Ceramic Society program to develop and disseminate evaluated phase diagrams. These include Volume 9 in the series "Phase Diagrams for Ceramists," a 1991 Annual Volume, and a special monograph containing approximately 200 phase diagrams pertinent to high T_c superconductors.

The Structural Ceramics Database

R. G. Munro and E. F. Begley

The Structural Ceramics Database (SCD) Version 1.0, containing thermal and mechanical properties for silicon carbides and silicon nitrides, was released in October 1990 as NIST Standard Reference Database Number 30. This version was developed under funding from the Gas Research Institute and the Center for Advanced Materials at Pennsylvania State University, the NIST Ceramics Division, and the NIST Standard Reference Data Program.

The SCD project emphasizes the use of evaluated data. Evaluated property data are data that have been reviewed and found to be acceptable according to a set of rather basic criteria. For structural ceramics, there are usually four conditions that need to be satisfied before data are classified as "evaluated": (1) the material is adequately identified, (2) the measurement method is specified and sufficiently described with details concerning the specimen preparation and the measurement procedures and conditions, (3) a measure of the quality of the data is given or can be perceived, and (4) the reported values are reasonable.

The data for SCD 1.0, listed in Table 1, were obtained from publicly available technical literature and were evaluated at NIST. During FY-1991, new data acquisition and evaluation efforts were conducted in coordination with ongoing research projects at NIST and the Center for Advanced Materials. The latter efforts provided an opportunity to make the most current, state-of-the-art data accessible to users faster than has been possible previously using only the traditional publication of technical papers. Most notably, data on the creep characteristics and the corrosion resistance of selected commercial grades of silicon carbide were obtained in this manner.

Table 1: The thermal and mechanical properties contained in the Structural Ceramics Database Version 1.0

Thermal Conductivity	Thermal Diffusivity
Thermal Expansion	Thermal Shock Resistance
Specific Heat	Elastic Modulus
Shear Modulus	Bulk Modulus
Compressibility	Poisson's Ratio
Tensile Strength	Flexural Strength
Hardness	Fracture Toughness
Fracture Energy	Creep Rate
Creep Exponent	Creep Activation Energy

The effectiveness of the technology transfer accomplished by the SCD project also depends on the ease with which users can access the data. The SCD is designed to be used on personal computers and is issued as a stand-alone program that can be executed directly from DOS. The features of the software package are designed to help the user to find and understand the needed data as easily as possible.

The features in SCD 1.0 allowed the user to construct queries of the database using computer-assisted specifications in a query-by-example format. The results of a query were then displayed in tabular formats. To enhance the user's perception of the results, a new graphics capability was developed during FY-1991.

```
Name: silicon nitride (Norton Company NCX-34)          Record: 3 of 35
                                Flexural Strength
 Temperature °C      Flexural Strength MPa
          20         851
         400         807
         500         799
         600         719
         700         636
         800         653
        1000         656
     Method: Four-point bend
      Notes: Self-aligning fixture, 1/4-point load, Instron test
             machine (Model 1125), crosshead speed = 0.5 mm/min.
Preparation: Heated at temperature for 30-45 min before testing.
    Quality: Stand. dev. (MPa) = 85; 65; 74; 143; 157; 140; 104.
   Cautions: Authors suggested that failure strength is
             independent of temperature up to 500 °C.
Environment: Air

[F1] Help                [PgDn] Next property   [Home] Description
[F2] Choose properties   [PgUp] Prior property    [F8] Graph
```

Figure 1. An example of a property data table in the Structural Ceramics Database.

The new option to view data graphically is available whenever a table of data, such as Figure 1, is being examined. The user merely presses a designated function key, and the system displays the property data as a function of temperature, such as Figure 2.

The current design of the SCD, therefore, is particularly well suited to materials research efforts. If the performance of structural ceramics were dependent only on the values of the materials properties, then the SCD would also be well suited to the needs of design engineers. The performance of structural ceramics, however, often depends on technical details of the fabrication process, the application environment, and the operating conditions. Indeed, this dependence is so significant that even the measured values of the materials properties can vary with measurement details. Consequently, the use of structural ceramics may require a greater depth of experience with the materials than is commonly expected of design engineers. Such a demand may result in a significant barrier to the commercial use of advance ceramics.

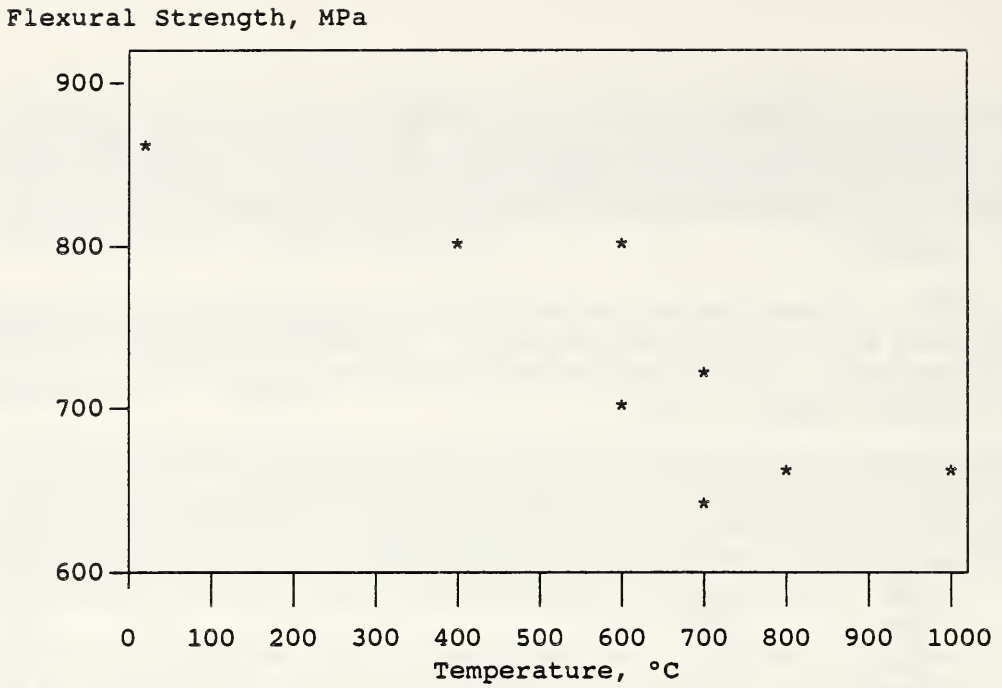

Figure 2. An illustration of the graph produced by pressing function key F8 in the case depicted in Figure 1.

A potential resolution of this barrier may be provided through the use of expert system technology. The SCD project, therefore, has initiated a new effort to develop expert systems that will assist design engineers in using structural ceramics. Two projects are underway: an assessment of the potential applications of expert systems in the natural gas industry, and the development of a materials selector expert system. The latter project is in the initial phase in which a demonstration system will be constructed as a preliminary step towards the development of a prototype.

The more than fifty industries, government laboratories, and academic research facilities that have purchased SCD 1.0 during FY-1991 are evidence of the broad interest in structural ceramics and the pressing need for evaluated data. Future versions of the SCD and its associated expert systems may, therefore, have a significant impact on the competitiveness of U.S. industries and the development of commercial applications of structural ceramics.

Powder Characterization Round Robin

S. G. Malghan, S. M. Hsu, J. F. Kelly, L. -S. Lum, E. F. Begley and D. B. Minor

As structural ceramic components are beginning to establish their presence in a variety of applications, the need to establish internationally accepted standard procedures for analysis of the starting raw materials is becoming more urgent. At present, there are no acceptable standard characterization procedures for fine powders used in the manufacture of ceramic components. This lack of procedures is one of the reasons for problems such as low reproducibility, low reliability, and high cost in the manufacture of ceramics. The powder characterization program, in its second phase, is an attempt to address this situation.

The program is conducted under the auspices of the International Energy Agency (IEA). The focus of the powder characterization interlaboratory comparison program is on research and development of high-temperature structural ceramics for advanced heat engines and other energy conservation applications. The major objective of the IEA programs is the evolution of standardized testing and characterization methods for these new materials.

Four participating countries in the program are: Germany, Japan, Sweden and the U.S. In each country, the participants represent industrial, academic and research organizations. In all, there are forty-five participants in the four countries. Researchers from these organizations have worked closely to define the technical scope of work.

In Subtask 6, which is the current phase of the IEA powder characterization program, the primary focus is to enhance the quality, repeatability, and reproducibility of measurements on five ceramic powders (two silicon nitrides, a silicon carbide, an yttria-stabilized zirconia, and an aluminum nitride) through a program of interlaboratory comparison of measurements. The participants are engaged in the analysis of the above mentioned powders by using specific procedures developed in this program.

The powder samples were prepared under controlled environment and shipped to the participants. During the past year, all the participants have analyzed the powder samples using essentially the same procedures. Some of the technical problems observed in the procedures were identified. The data were sent to NIST where compilation and preliminary analysis is underway. A report on the compilation of data available up to June 1991 was prepared and distributed to the participants for their review. Currently, efforts are underway to analyze the data and prepare graphical plots of data. In addition, simple statistics are also being calculated to help in the data analysis. Based on this analysis, preliminary conclusions will be developed.

The data analysis carried out until now shows that a significant improvement has been achieved in both repeatability and reproducibility of several measurement procedures. Size distribution by sedimentation using Sedigraph; size distribution by light scattering; specific surface area by multipoint and single point nitrogen BET absorption; and carbon, oxygen and nitrogen determination by combustion appear to provide significantly improved data over those used in the previous Subtask 2 program. In Subtask 2, the procedures were not recommended, whereas, as mentioned earlier, one of the major efforts in Subtask 6 was to develop procedures in collaboration with the participants and use them for analysis.

In the coming year, data analysis will be completed and the final report will be prepared. The report will contain data, data analysis, procedures, conclusions, and recommendations.

Mechanical Property Standardization

G. D. Quinn

Mechanical property standard test methods are a requisite for obtaining high quality, reliable test data for materials development, materials characterization, and design. Standards are important for establishment of specifications and data bases for design. This project is driven by the need for standards for heat engine programs, but the standards are generic and suitable for all advanced ceramics.

The work in this program includes conducting experiments with conventional or new methods, studying the technical literature, interacting with American industry to assess their needs and preferences, cooperating with international standardization programs, drafting standards, and shepherding standards through the appropriate standardization process.

In 1991, two standards were finalized and formally adopted:

1. ASTM C 1161, "Flexural Strength of Advanced Ceramics at Ambient Temperature." This is the first test method standard developed in ASTM Committee C-28, Advanced Ceramics.

2. MIL STD 1942(A) "Flexural Strength of High Performance Ceramics at Ambient Temperature." This is an updated and revised version of the original MIL STD. Revisions were made in cooperation with the U. S. Army MTL to correct some minor tolerances, to bring the document more into alignment with the ASTM version, and to reorganize it to make it more readable. The document is now a tri-service (Army, Navy, and Air Force) standard.

Four additional standards are under development:

1. "Flexure Strength of Advanced Ceramics at Elevated Temperatures." This document is at an advanced balloting stage in the ASTM C-28 process and should be adopted in 1992.

2. "Young's Modulus, Shear Modulus, and Poisson's Ratio for Advanced Ceramics by Resonance." This document was prepared in collaboration with S. Gonczy of Allied Signal and J. Helfinstine of Corning. It is now up for an ASTM Society ballot and should be adopted in 1992.

3. "Standard Practice for the Characterization of Strength Limiting Defects in Advanced Structural Ceramics." This is an original standard and is being prepared in cooperation with the U. S. Army MTL. It is estimated that it will be formally adopted as a MIL HBK in late 1991.

4. "Standard Practice for Reporting Strength Data and Estimating Weibull Distribution Parameters for Advanced Ceramics." This practice is being prepared in cooperation with Dr. S. Duffy of NASA-Lewis. The goal is to rationalize the way Weibull strength data is analyzed and reported. Several preliminary drafts have been prepared and it will be submitted for an ASTM C-28 subcommittee ballot in late 1991.

In addition, work is underway on a series of areas that will eventually lead to preparation of draft standards. Fracture toughness experiments have been completed as part of an internationally coordinated VAMAS round-robin project. Analysis of these experiments is underway, and, coupled with a literature review, consultation with industry and international leaders, a draft standard will be prepared in cooperation with Dr. E. Fuller in late 1991.

This project also leads to publications on testing methodologies, or guides to the interpretation of results. This includes papers ranging from a note on the effect of friction constraint of fixed load pins in flexure, to two comprehensive review papers. One is a review of the value of flexure data for design and is to be considered the definitive paper on the subject, and the other is an overview of strength and proof testing written for an ASM handbook. In addition, two sets of users guides have been prepared on how to make and use flexure fixtures for room and elevated temperature.

VAMAS Prestandardization Research

G. D. Quinn, E. R. Fuller and S. W. Freiman

During 1991, G. Quinn was appointed international leader of Technical Working Area #3, Ceramics, in the Versailles Advanced Materials and Standards (VAMAS) Project. This program has as its objective international cooperation on research on prestandardization topics.

NIST completed experiments on a fracture toughness round robin set up by the Japan Fine Ceramics Center (JFCC) and coordinated in the USA by NIST. Results were obtained from five of the six USA participants. Testing included indentation fracture (Vickers indent and measure crack lengths), indentation strength (indent a bend bar and break it), and single-edge precracked beam (bridge indentation to precrack a single edge notch beam specimen). Analysis of the results is underway and could lead to a USA draft standard.

A high temperature fracture toughness round robin is also underway in cooperation with JFCC and NASA-Lewis. A final report on the dynamic fatigue round robin coordinated by S. Freiman and E. Fuller is in preparation. New initiatives are pictured in the area of fractographic analysis, quantitative microscopy and fracture toughness.

A Computerized Tribology Information System

A. W. Ruff, S. Jahanmir and S. M. Hsu

Development has continued on the computerized tribology information system, ACTIS. The overall plan for the PC-based system was developed from a workshop held at NIST in 1985. The work has been funded by NIST, other federal agencies (Department of Energy Office of Energy Conversion and Utilization Technologies, Air Force Wright Aeronautical Labs, Army Belvoir Research and Development Center, and the National Science Foundation), and professional societies (Society of Tribologists and Lubrication Engineers and the American Society of Mechanical Engineers).

The complete ACTIS system will consist of six components: numeric databases, design calculation codes, a newsletter, bibliographic searching, a research-in-progress database, and a product and services directory. The first stage of the system is presently being marketed. It consists of six modules that include a central control module; a numeric database on tribological materials; and four design calculation codes for contact stress, gear, and journal bearing systems. Recently, a contract was awarded competitively to proceed with the second stage of the ACTIS System. Work is currently underway on six modules: an improved central access module, two rolling element bearing modules, an advanced gear module, a lubricant database, and a lubricant expert system selector module.

The Tribology Data Center, established at NIST with support from the Ceramics Division and the Standard Reference Data Office, continues efforts to obtain, evaluate, and disseminate critical data on tribomaterials. The emphasis this year has been on ceramic tribological materials. Data have been gathered from NIST research activities, from other tribology experts, and from the literature. Data validation has been carried out at NIST and by a contractor at the Stevens Institute of Technology. The database will be made available in the form of a PC spreadsheet containing over 350 records of material and tribological information.

Tribological Standards and Measurement Activities

A. W. Ruff

A new subcommittee on Computerization was formed in 1990 by the ASTM G-2 Committee on Wear and Erosion. The subcommittee is chaired by a NIST staff member. Standards development has begun in areas of computer control of wear test systems, databases of tribology information, statistical analysis of wear data, and expert systems for tribomaterial selection. A draft standard has been written on a format for databases on wear, and will be sent for subcommittee ballot soon. The work is also coordinated with ASTM Committees E49 on Computerization of Material Property Data.

A project has been proposed to the Versailles Advanced Materials and Standards (VAMAS) Project's Wear Test Method group to establish a uniform methodology for organizing wear test data. The effort will probably involve 10-25 laboratories around the world, and would be a first attempt to reach an international consensus in the important area of tribological data. A valuable technical benefit would be the opportunity to evaluate wear data obtained from a variety of different test methods as used in different laboratories.

Another project nearing completion concerns an effort to assemble a set of micrographs and associated information for the purpose of preparing an atlas of worn surfaces. The work involves tribology groups at NIST, Battelle Columbus Labs, and BAM in Germany. The atlas will consist of two parts; one is a collection of data and micrographs of worn surfaces on a variety of materials under different exposure conditions. There will be about eighty examples drawn from work of the staff at the three laboratories. The second part will be a computerized database of 313 records drawn from publications in the ASME series from the International Conference on Wear of Materials, 1977-1991. Most of the work comprising the wear atlas was originally published in this series. The database will permit searching that literature source for particular tribology information.

VAMAS Wear Test Methods

S. Jahanmir

The objectives of the Wear Test Methods Technical Working Area of Versailles Advanced Materials and Standards (VAMAS) are: (1) improvements in the reproducibility and comparability of wear test methods and (2) characterization of the wear behavior of advanced materials. Two round-robin interlaboratory comparisons, based on the first objective, resulted in several publications and standard test methods adopted by ASTM and DIN. Current activities of this committee, under NIST leadership, are concerned mostly with the second objective.

In two recent meetings twelve proposed projects were discussed and evaluated with respect to the goals of VAMAS. Four projects were selected: 1) uniform format for reporting tribological data for computerized databases, 2) wear volume measurement comparison, 3) survey of present standard test methods for wear, and 4) round-robin wear tests on hard coatings.

The goal of project No. 1 (organized by A. W. Ruff) is to define a uniform format for organizing and reporting wear data with application to computerized databases. This project is very important and timely, because of recent interests in using computer databases for storing materials property data and searching the databases to retrieve data for research, design, and material selection. There are large differences between the database formats being used by different organizations in the U. S. and also in other countries. If a uniform format is developed, then it will be much easier to exchange data among organizations interested in the same type of data. In fact, a recent international effort on data exchange, Product Data Exchange using STEP (PDES), is an excellent example, indicating the need for a standardized database format. Other benefits of the proposed project include agreements on important variables and units, as well as methods for reporting data precision. At the completion of this project, a VAMAS report will be issued which will contain recommendations for a uniform format for reporting of wear data.

The goal of project No. 2 is to evaluate and compare different methods used for wear volume measurements. Several specimens worn under different loads will be prepared to produce a range of wear volumes. These specimens will then be circulated among the participating laboratories with instructions for wear volume measurements by two or three different techniques.

The purpose of project No. 3 is to gather and disseminate a listing of currently available standards for wear testing. This project has received a preliminary approval by a VAMAS steering committee. A questionnaire has been prepared for distribution to the participating laboratories. The results of this project will be compiled in a VAMAS report.

The goal of project No. 4 is to evaluate the effect of test variables on wear, in order to develop recommendations for testing of hard coatings. A pin on disk geometry, similar to the previous round-robin exercise, will be used. The specific details for the materials and test conditions are currently being formulated.

Ceramic Phase Equilibria Program

H. M. Ondik, S. W. Freiman, M. A. Clevinger, T. R. Green[1], K. M. Kessell[1], N. Swanson[1], N. Asmail[1], C. L. Cedeno[1], and C. G. Messina[1]

[1]American Ceramic Society Industrial Research Associates

The Ceramic Phase Equilibria Program continues to provide the ceramics user community with evaluated phase equilibria data covering all non-alloy, inorganic systems. This past year has been the sixth full year of operation of the Ceramics Phase Diagram Data Center under the expansion plan sponsored cooperatively by NIST and the American Ceramic Society (ACerS). Over $2,500,000 has been raised by the ACerS from industry and universities for the support of the program.

The first in a new series of phase diagram publications was introduced this year. Phase Diagrams for Ceramists, Annual '91, a soft-cover volume, was completed in June. This volume covers a large variety of chemical systems. Although the diagrams are properly evaluated, they do not have the cross-referencing and comparison of similar diagrams which occur in the regular topically-oriented volumes. The annual volumes are intended to help catch up with the backlog of diagrams currently in the Data Center files and to provide a medium for more rapid publication of new work that might wait several years for a suitable topically-oriented volume.

A monograph, Phase Diagrams for High T_c Superconductors, was prepared in the Data Center. It includes most new diagrams developed world-wide for the systems of interest, $\approx$200, and also some pertinent diagrams from early volumes of the phase diagrams series.

These two books were printed entirely within the Data Center by the staff using a newly acquired desk-top publishing system. A new laser printer permits printing of the diagrams in a quality that rivals that of the ink-plotter system used for Volumes 6, 7, and 8. The total control of the printing process has accelerated book production, avoiding the need to wait for time on the part of the NIST Standard Reference Data (SRD) Office, the Government Printing Office (GOP) staff, and ACerS Headquarters staff to prepare final pages for approval by the editors and Data Center staff.

Examination, evaluation, and digitization of diagrams for inclusion in Volume 9 of Phase Diagrams for Ceramists has been completed. This topically-oriented hardcover volume contains systems of interest to the semiconductor community (systems containing Groups IVa, Va, and VIa elements). It is expected to be completed and available for distribution in early 1992.

The database system for use on DOS-based personal computers (PC) will soon be ready for marketing by NIST and the ACerS. The original version has undergone extensive revision based on beta-test results, comments received when demonstrated at meetings, and advice from the Standard Reference Data Program staff. Installation programming and a user manual are in the final stages of preparation. The system provides for search and manipulation of both

textual and graphics information. The textual portion covers the bibliographic and chemical system information for Volumes 1 through 8 and is contained in and operated by a customized commercial database system. The graphics portion uses programs written by NIST staff and operates within the system to permit diagrams to be plotted and manipulated on screen. The database will include the diagrams of Volumes 6, 7, and 8, the only volumes which have been produced using digitized diagrams.

Papers likely to contain phase diagrams of interest to the Data Center continue to be delivered by the Data Abstract Search Service (DASS) under a contract with the ACerS. They cover all chemical systems currently being included: oxide and salt systems; boride, carbide, and nitride systems; systems containing elements of Groups IVa, Va, and VIa of the Periodic Table; and aqueous systems. At one time it was planned that the ACerS would publish bibliographic updates regularly as a portion of Ceramic Abstracts. It has since been decided that preparation of separate bibliographic publications was more useful and it is anticipated that another such volume will appear in early 1992. The last such publication, printed in March 1990, provided chemical system and author indexes and bibliographic references for over 12,000 diagrams in the Data Center computer files which had not yet appeared in any volume of Phase Diagrams for Ceramists.

Standard Reference Materials (SRMs) for X-ray Diffraction

J. P. Cline

At present, three x-ray diffraction SRMs are under development. These are briefly described below:

SRM 1976, Instrument Sensitivity SRM

Intensity measurements by x-ray diffraction, the basis for a quantitative analysis by this method, have always been prone to measurement errors of such magnitude that the instrumental contributions have never been evaluated. Recent round-robin studies initiated by the International Centre for Diffraction Data, ICDD, have indicated the optical characteristics of powder diffraction equipment may affect intensity measurements by up to 30%. In response to this study, a SRM is being produced to allow for calibration of equipment with respect to sensitivity, or diffraction intensity as a function of two-theta angle.

In order to remove the variable of sample loading technique from intensity measurements, the SRM is in the form of sintered alumina plates. These plates consist of a highly uniform, though oriented, microstructure consisting of alumina platelets measuring 5 to 8 micrometers in diameter by 1 to 2 micrometers in thickness. Twelve relative intensity values have been certified, for integrated intensity as well as peak height measurements, through a two-theta range of 25.5 to 145.0 degrees. Certification was performed on a conventional powder diffractometer using Cu Kα radiation which was verified to be operating properly during the round robin study. Use of the SRM entails the collection of data in a manner analogous to the certification method and generation of a correction curve from the comparison of the experimental data to that of the certified values. Subsequent, corrected data from various laboratories will be placed on the same scale and the instrumental contribution to the variations in quantitative measurements will be removed.

SRM 676, Alumina Internal Standard SRM

To accomplish quantitative analysis of multi-phase samples, the user must first know the relative diffracting power of the various phases. The ICDD has reviewed this problem and adopted the concept of the I/I_c to serve as an indicator of phase diffracting power. The I/I_c is the diffracting power of a given phase, I, relative to that of alumina, or corundum, I_c. Knowledge of this value for each phase in the experimental pattern, listed in the ICDD data base, will allow for meaningful quantitative assessment of routinely collected XRD data. An alumina SRM has been developed for use as an internal standard in I/I_c determinations, which has been determined to offer a diffraction intensity as close to the theoretical as possible.

The investigated phenomena consisted of powder characteristics which would affect diffraction intensity. The powder characteristics included: extinction, particle size broadening, phase purity, degree of preferred orientation, and overall diffraction intensity. Extinction effects were determined with the Rietveld refinements, in conjunction with the Sabine model for primary extinction of neutron time-of-flight (TOF) data. Phase purity, preferred orientation, particle size broadening, and overall diffraction intensity were determined with the Rietveld refinements of high quality XRD data collected on mixtures of candidate materials and silicon, SRM 640b. Preferred orientation was eliminated with some preparations by spray drying of the samples, allowing for the most accurate and precise determination of candidate materials' diffracting power. Orientation effects were determined by utilizing the March-Dollase model in Rietveld refinements of conventionally loaded samples. The ideal material was determined to be an alumina designed as a polishing compound, the particles of which are equiaxed and range from 1 to 2 micrometers in diameter.

SRM 656, Silicon Nitride Quantitative Analysis SRM

Silicon nitride is a non-oxide ceramic of considerable interest due to its toughness and strength at elevated temperatures. Ubiquitous to the processing of silicon nitride is the transformation from the α to the β phase. Commercially available powders generally consist of approximately 92% α, 4% β, and the remainder as an amorphous material. Upon sintering, the metastable α phase transforms to the β phase, forming acicular, interlocking grains which impart the desired properties to the finished piece. The degree to which this transformation reaches completion, as well as the composition of the starting material, are of considerable importance to the investigation of microstructure/property relationships of this material.

The difficulty with the analysis of the this material rests with the complete overlap of the β phase's diffraction pattern with that of the α. Thus, the accepted approach involves the use of peak heights which do not account for shifts in height versus area caused by size and strain broadening. Furthermore, analysis of the amorphous content cannot be accomplished in this manner. The Rietveld method, which is unaffected by peak overlap, was employed to obtain the most accurate measurement of diffraction intensity from the phases of this system. Both the SRM itself and the test specimens were spray dried to eliminate preferred orientation. Equations concerning the analysis of data collected in conjunction with the spiking method were developed to determine amorphous content of the starting material. Data were collected with both XRD and TOF for the development of this SRM.

POWDER CHARACTERIZATION AND PROCESSING

Subhas Malghan

The manufacture of reliable, cost-effective, advanced ceramics depends upon the availability and controlled processing of fine powders. These requirements are addressed through development of techniques of powder analysis and data required by industry. This capability is extended to characterization of slurries and microstructural development during consolidation and sintering. The group carries out an integrated effort from the early steps of synthesis of well-characterized, deagglomerated powders to the understanding of processing effects on the microstructure of ceramics.

The group continues to play a key role in an international interlaboratory comparison of powder characterization methods conducted under the auspices of the International Energy Agency (IEA). The results have provided an important basis for the establishment of measurement procedures and standards that are vitally needed for the international commerce of advanced ceramic powders and materials. These activities are discussed in STANDARDS AND DATA ACTIVITIES.

Significant Accomplishments

- Experimental research has demonstrated that a variety of magnetic nano-composite materials can be produced through molecular chemical processing in systems based on modified sol-gel, advanced coprecipitation, and metal-organo complex formation. Some examples of the magnetic nano-composite generated in bulk by these processes are iron-in-silica gel, iron-in-vitreous alumina, cobalt-in-copper, and cobalt-zinc ferrites.

- A unique NMR imaging facility was assembled for study of solids. In this system a large gradient in the stray field under the edge of the superconducting-coil, 9.394 tesla magnet of the Bruker MSL-400 system is utilized. A field gradient of 0.5 tesla per centimeter is measured at this location. Using this system, 80 micrometer resolution was obtained in the imaging of binder distribution in a green ceramic body.

- The existence of predominantly electrostatic adsorption under acidic conditions (pH = 4.0) in silicon nitride powder - polymethacrylic acid (PMAA) - water was established. The PMAA surfactant adsorption was found to increase as a function of its bulk concentration. On the other hand, under alkaline pH conditions (pH = 8.0), very little adsorption of the surfactant was observed.

- Compaction of nano-size, amorphous silicon nitride powders at low temperatures has been able to produce optically transparent ceramics. Significant progress is being made with respect to the study of process variables and the understanding of fundamental mechanisms of densification. The effects of compacting pressure and temperature on hardness, microstructure, and optical properties have been investigated. The physics of low-temperature compaction of nano-size particles is also being examined.

- By the application of electrokinetic sonic amplitude (ESA) measurement, the surface properties of zirconia powders in aqueous environment were distinguished. The ESA technique was used for the measurement of isoelectric points (pH_{iep}) of the powders. A correlation was found to exist between the pH_{iep} and performance of the powders in a plasma spray coating process.

- Differences were identified between the nano-size, amorphous and micrometer-size crystalline silicon nitride powders with respect to the rate of oxidation, activation energy during oxidation, and formation of oxidation products. The oxidation rate of nano-size, amorphous powder was higher. The activation energies were 113 $\pm$ 20 kJ/mol and 63 $\pm$ 4 kJ/mol for amorphous and crystalline powders, respectively, as determined by photoelectron data. Oxynitride formation during oxidation was exclusive to the amorphous powder.

Nano-composite Materials for Magnetic Refrigeration

J. J. Ritter

Increasing national and international concerns about the environmental impacts of volatile chlorofluorocarbon refrigerants has prompted investigations into alternative approaches to refrigeration. The possible use of the magnetocaloric effect to this end is under serious consideration.

Magnetocaloric systems are attractive since the refrigerant can be a self-contained solid material, with appropriate assemblies of magnetic spins. In the absence of a magnetic field, the magnetic spins are thermally randomized and the entropy of the spin system is high. When a magnetic field is applied, the spins are aligned with the field, and the entropy of the spin system decreases. Concomitant with these entropy changes are changes in the heat content of the refrigerant. When the spins are aligned in the field, the heat is released from the refrigerant to the environment and the temperature of the environment increases. When removed from the field, the spins are thermally randomized as the refrigerant absorbs heat from its surroundings. Consequently, the environment suffers a decrease in temperature. Thus, by moving the refrigerant in and out of a magnetic field, and with suitably arranged heat exchangers, a refrigeration cycle can be established. Refrigerators using this principle have been constructed, but because of the types of materials currently available as magnetic refrigerants, the operational range is below 20 K. The development of new refrigerants with operational capabilities between 20 and 200 K is critical to the expansion of this field.

Recent theoretical work at NIST suggests that enhanced magnetocaloric effects may be derived from superparamagnetic nanocomposite materials where the magnetic component is present in clusters 5 to 10 nm in size. The development of synthetic techniques to generate this type of material with a variety of operational ranges is essential for the implementation of magnetic refrigeration. Experimental work in the Ceramics Division at NIST has demonstrated that different varieties of magnetic nano-composite materials can be produced through molecular chemical processing in systems based on modified sol-gel, advanced coprecipitation, and metal-organo complex formation. Examples of magnetic nanocomposites generated in bulk by these processes include iron in silica gel, iron in vitreous alumina, cobalt in copper, and cobalt-zinc ferrites. Both control of the magnetic state and nanoparticulate size of the magnetic regions in these materials is achieved through judicious chemical processing.

Surfactant-Powder Interactions in Ceramic Suspensions

S. G. Malghan and U. Paik[1]

[1]Clemson University

Processing of silicon nitride powders in aqueous or non-aqueous solvents involves the use of a number of surface-active agents to serve different functions such as dispersion, agglomeration, green strength, and moldability. The surface-active agents influence the interparticle interactions through the control of interfacial chemistry in a given solvent. Current understanding of the surface-active agents adsorption on silicon nitride powder, especially when the surfactants have different chemical composition, is insufficient. Published data on

polymethacrylic acid and polyethylene glycol interactions, when present together, show that these species interact and produce complex iono-molecular species depending on the pH of the bulk solution. The increased viscosity and agglomerates formation in the suspensions could be related to the formation of complex surface-active species. To prevent the formation of agglomerates, an improved understanding of the interactions between the silicon nitride powder, sintering aid powders, and surfactants in aqueous environment should be developed.

In our study, for experimental simplification, a spray drying powder system constituting Si_3N_4 powder - Y_2O_3 powder - polymethacrylic acid (PMAA) - polyethylene glycol (PEG) - water is being examined. However, the complexity of the system is being simplified by studying the individual constituents and in groups of two and three constituents at a time. In the past year, we have been studying the following systems in aqueous environments:

- silicon nitride powder
- silicon nitride powder with PMAA
- silicon nitride powder with PMAA and PEG

In the final stages, the entire system will be examined and interpretations will be developed.

The analytical techniques utilized to study these systems are electrokinetic sonic amplitude (ESA), adsorption isotherms, agglomerate size distribution, and specific surface area. The ESA analysis of individual components such as Si_3N_4 powder (Ube SNE-3 powder), PMAA and PEG was carried out to determine the variation of ESA as a function of pH of the bulk solution and isoelectric point (pH_{iep}). The powder selected for this study has a pH_{iep} of 4.9 in the as-received form. After adsorption of PMAA, the pH_{iep} shifted to as low as 2.8 at an equilibrium concentration of 1.0% by weight of PMAA. At 0.01 and 0.1% PMAA, the pH_{iep} was at 4.4 and 3.3, respectively, showing that significant increase in the PMAA adsorption takes place by increasing the bulk concentration from 0.01 to 0.1%. As expected, the adsorption of PEG does not affect the pH_{iep}, whereas the ESA decreased as a function of PEG concentration. This decrease in the ESA could be related to loss of active adsorption sites on the powder.

The adsorption studies have indicated a total lack of adsorption of PMAA at alkaline pH (8.0) and increased adsorption at acidic pH (4.5). The increase of PMAA adsorption under acidic environment is an indication of the existence of primarily electrostatic adsorption and, to a lesser extent, hydrogen bonding. Though there may not be any measurable adsorption at pH = 8.0, a stable dispersion could be produced, which indicates that other mechanisms of surfactant effectiveness, such as steric stabilization may be present. Tests are in progress to evaluate relative differences of dispersions at pH 4.5 and 8.0.

Binder Distribution in Ceramic Green Body by NMR

P. S. Wang

Failures in advanced ceramics often occur due to structural defects undetectable by conventional methods. Nuclear magnetic resonance (NMR) imaging is an emerging technology which provides a unique material diagnostic technique by in-situ, internal mapping. It can provide information not only on the material distribution (nuclear spin density), but also on the chemical and physical characteristics of these materials (nuclear spin relaxation times). In a ceramic green body, the binder distribution is a critical parameter that affects the final ceramic's mechanical, thermal and electrical properties and reliability. Understanding of the interfacial reactions between the binder and ceramic powders under various processing parameters is essential to alleviate binder distribution related problems in the ceramic processing technology.

In biological systems and medical diagnosis, NMR imaging is a well-established technique. The imaging method uses a magnetic field gradient generated by a set of gradient coils to encode the positions of the nuclear spins with a spatially varying Larmor frequency. Once the variations in resonant frequency have been decoded, an NMR image can be constructed. However, due to the nuclear spin dipole-dipole interaction in solid state, the NMR spectroscopic signal will be very broad. To perform NMR imaging based on these unresolved broad lines is extremely difficult and the resolution is poor.

In "hard solids" such as ceramics, the linewidth due to the nuclear dipolar interaction because of the restriction in atomic motion is often a few hundred times larger than that in the mobile samples. Consequently, line-narrowing and large field gradient are the two critical factors to a successful NMR imaging technique for solids.

In the past year, we assembled a unique NMR imaging facility for study of solids utilizing the huge gradient in the stray field. A planar surface under the edge of the superconducting coil in the 9.394 tesla magnet of our Bruker MSL-400 system is utilized for this purpose. At this surface, a static field gradient strength of approximately 0.5 tesla centimeter was measured. Since it is static in nature, the sample which is placed in the center of a spherical resonant coil of 163 MHz has to be moved to get the spatial information. When the sample (together with coil) is moved up through this surface along the z-axis of the magnet (parallel to the gradient direction), a maximum of 512 points will be irradiated by a solid echo multipulse train (usually 8 pulses of 4 μs each) to detect the nuclear echo signal. This linear movement can be repeated many times (number of scans) as desired and echo signals accumulated to achieve a good signal-to-noise ratio. When this "one-dimensional" mapping is complete, the sample rotates in the YZ plane and then continues scanning for its nuclear echo signals. After the sample completes a 360 degree rotation in the YZ plane, a two-dimensional map can be constructed by back projection of these echo signals. To construct a three-dimensional picture, the sample has to rotate away from the YZ plane. All these movements are controlled automatically by an ASPECT 3000 computer. Figure 3 shows the schematic of sample motion and the principal functions.

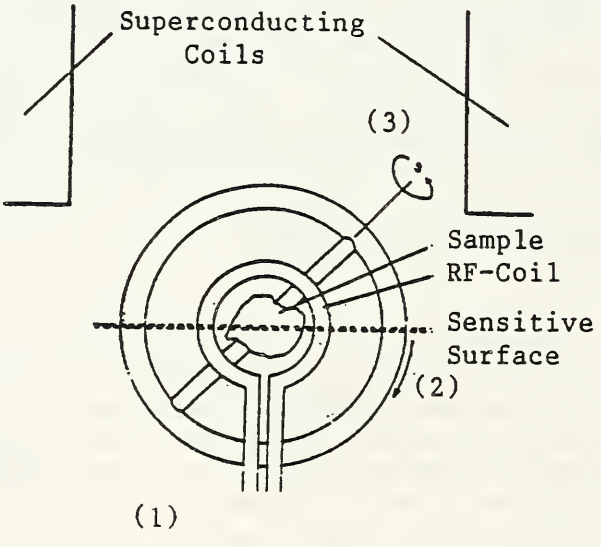

Figure 3. Schematic of sample motion (1) linear motion along Z-axis, (2) sample rotation in YZ-plane, (3) second rotation of the sample for three dimension imaging.

The binder distribution in a ceramic green body containing silicon nitride/polyethylene glycol (binder)/polyacrylic acid (dispersant)/water system was studied. A cylindrical sample 12 mm in diameter and 10 mm thick was sliced 64 times each along X, Y, and Z directions. ^{1}H echo signals at 162.7 MHz were backprojected to construct 192 pictures. Figure 4 shows two examples of these pictures. This sample contains 10.4 wt. % binder. Figure 4(a) is a cross section of an internal slice which shows the binder is fairly well distributed. Figure 4(b) is a vertical slice; a low binder region was detected. The white spot on each of the two pictures is due to epoxy, a high proton-containing polymer, used to glue the sample on the sample holder.

Since we are observing proton magnetic resonance outside of the magnet, the resonance was observed at 162.7 MHz instead of 400.13 MHz. Calculation shows that the same resonance coil can also be used for ^{19}F resonance. Since ^{19}F resonance occurs at a frequency 4% lower than that of ^{1}H, moving the probe 4mm closer to the center of the magnet may compensate the difference. This is important because ^{19}F is also an undesired impurity in many ceramic materials. Next year, we plan to extend the application of NMR imaging to other systems and develop resonance facility to cover ^{27}Al and ^{89}Y, as well.

Fabrication and Characterization of Nano-phase Ceramic Materials

A. Pechenik

This research program concentrates on the understanding of fundamental processes involved in the fabrication of nano-phase ceramic materials from atomic clusters smaller than 100 nm in size. Though size-selected atomic clusters of many ceramic materials in the range of 1-100 nm can be readily synthesized by a variety of techniques, little is known about the methods for production of materials from fine powders consisting of such small particles. Superplasticity, supermodulus, low-temperature ductility, tunable band-gap width, large electro-optic coefficients and other exciting properties are predicted for ceramic materials comprised of nano-size crystalline grains. Unfortunately, there are currently no known techniques, on an industrial or laboratory scale, which would allow fabrication of full-density nanophase ceramic materials without losing the novel properties entailed by the small size of the individual grains. The main difficulty in the fabrication of nanophase materials is that the high-temperature sintering commonly utilized for processing of conventional ceramics cannot be used with nano-size particles, because it causes recrystallization and loss of desired properties. In this project we investigate a fundamentally new approach to fabrication of nano-phase ceramic materials utilizing **low temperatures and high pressures**.

To show the usefulness of our approach, we have investigated compaction and densification of an ultra-fine powder of Si_3N_4, a material which is justly termed "unsinterable" in its pure state. We studied compaction of the nano-size silicon nitride powder at industrially accessible conditions of temperatures below 500°C and pressures not exceeding 5 GPa. The starting powder for this investigation was synthesized at Rutgers University by Prof. Danforth via CO_2-laser-driven gaseous reaction. The powder consisted of 17 nm particles of stoichiometric silicon nitride and was amorphous according to x-ray and electron diffraction characterization. We compacted this powder under vacuum at room temperature and subsequently sintered it at 500°C for 2 hours under 5 GPa pressure using diamond anvils. This procedure yielded a material with hardness of 700 kg/mm^2. The material was translucent in the visible range and showed high transmittance in the IR range up to 10 μm. Both the hardness and optical transparency of the material significantly improved when, prior to hot-pressing, the powder was compacted at liquid nitrogen temperature. Optically transparent samples were fabricated by utilizing compaction at liquid nitrogen temperatures followed by sintering at 500°C under 5 GPa. The hardness of these materials increased to 1200 kg/mm^2.

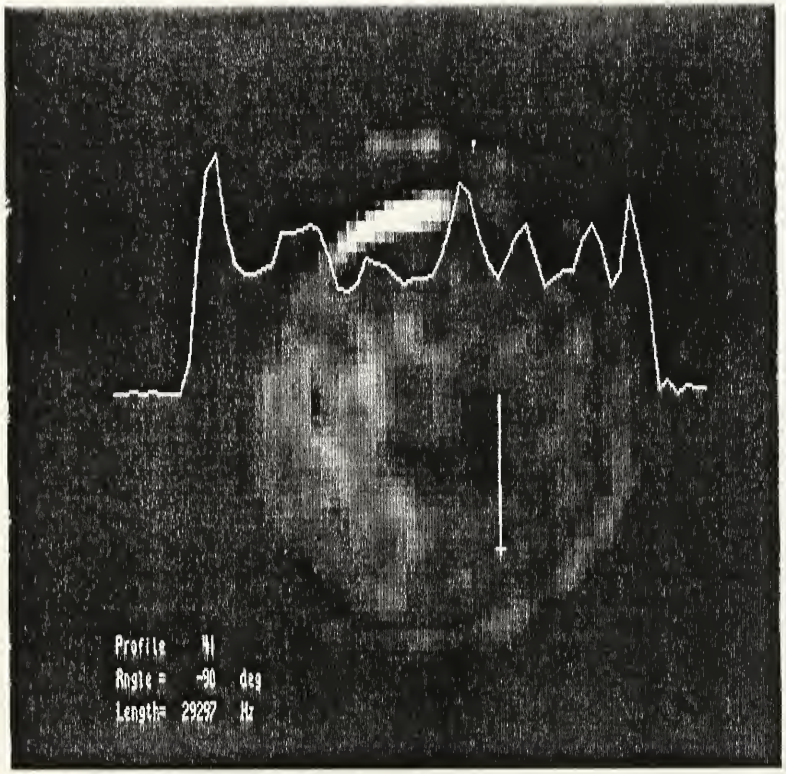

(a)

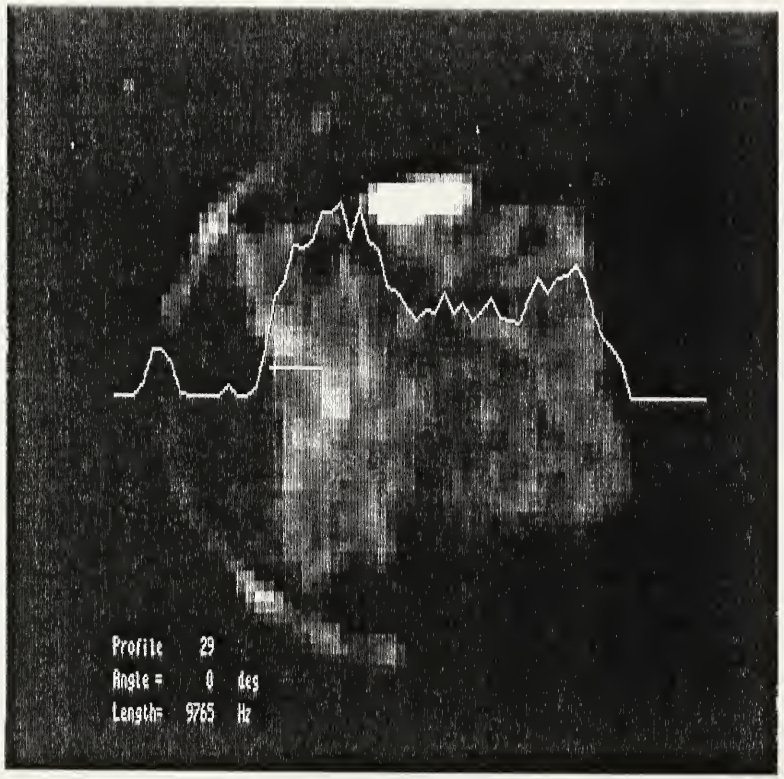

(b)

Figure 4. (a) Cross section and (b) vertical slice of a silicon nitride ceramic green body with 10.4 wt. % polyethylene glycol to show the binder distribution.

Transmission electron microscopy (TEM) examination of the compacts revealed that the small amorphous particles did not change their morphology during compaction, and no recrystallization or grain growth occurred. The particles were compacted into a matrix of densely packed grains. Some small pores are observed in the TEM micrographs, 5-10 nm in size, but no larger pores were detected in TEM, scanning electron microscope (SEM), and optical observations. This unique microstructure is responsible for high, hardness and transparency in the visible range of the nano-phase amorphous silicon nitride.

When subsequently these samples were sintered **without using pressure** at 1300°C for 2 hours, crystallization took place, the material lost its transparency, and hardness increased to nearly 1800 kg/mm^2, which is essentially equal to hardness of fully-dense polycrystalline silicon nitride sintered with the help of additives called sintering aids. No sintering aids were used in our work except for some oxygen contamination introduced by the exposure to ambient atmosphere. We also started our work on compaction of powders never exposed to the ambient atmosphere. The **unexposed** powders, which were nearly free of oxygen or moisture, showed improved compacting properties, as manifested by the improved optical transparency of the samples after processing. The prepared materials clearly possess high fracture toughness, as can be emphasized from the fact that no cracks were produced at the corners of Vickers diamond indentations under loads up to 2 kg (the maximum loads that we were able to put on these small samples). Under similar testing conditions, conventional silicon nitride would produce penny-like cracks around the diamond indentation even under loads well below 1 kg.

Aside from its possible industrial significance, this work on nano-size silicon nitride materials has raised a number of fundamental questions about the mechanisms of densification of the fine particles under pressure. The unexpected result that compaction is improved at low temperatures goes somewhat against the common intuition, but can be reasoned as manifestation of the slowing down of diffusion and chemical reactions at the interfaces of compacting particles. The diffusion leads to creation of bridges between particles that come in contact and this process is extremely rapid for nano-size particles. In a way, low temperatures decrease the friction forces between particles when the surfaces of the particles are free of impurities. **Low temperature compaction of nano-size clusters** is a fundamentally new concept which came from this work. We plan to investigate further the physics of this process.

Our future goals are:

- Investigate sintering of the nano-phase silicon nitride to produce polycrystalline material. If the high density of the amorphous compacts can be retained in the polycrystalline state, this could open the opportunity for fabrication of silicon nitride without using sintering aids.
- Study mechanical properties of the prepared compacts at various temperatures and measure creep rates.
- Characterize optical properties of the amorphous silicon nitride to assess its possible applications in the field of electro-optics.
- Understand and model the physics of low-temperature compaction.
- Scale-up the process.

Surface Characterization of Alumina-Coated Silicon Carbide Platelets

P. T. Pei, J. F. Kelly and S. G. Malghan

Alumina composites reinforced with silicon carbide platelets (SiCp) are being developed as wear resistant materials. Some of these materials exhibit outstanding toughness and flexural strength combination. However, basic understanding of the surface chemical interactions and microstructure at the interface between the reinforcement and matrix is insufficient.

The chemistry and microstructure of the interface between the SiCp reinforcement and alumina matrix must fulfill several functions. It may be necessary for the SiCp to have a coating which minimizes reaction with the alumina matrix during processing and with the environment during service. In addition, the interface should have microstructural properties which optimize fracture toughness, strength and slow crack growth. The optimum chemistry of coating and interface microstructure for SiCp reinforced alumina have not been presently determined; however, the role of the interface is well recognized. The interface is known to control the onset of stresses during sintering due to differential shrinkage in SiCp-reinforced alumina composites.

A colloidal chemistry based technique was developed for coating SiCp with alumina particles of different sizes, ranging from 0.04 to 0.7 micrometers. The goal of this research was to evaluate the interfacial chemistry parameters in the coating of SiCp with alumina particles. The ultimate goals are to gain sufficient understanding of sintering stresses by controlling the interfacial chemistry and structure and to obtain optimum properties of the sintered composite. During the coating process, surface preparation of SiCp is important. The SiCp were surface cleaned by washing in trichloroethylene followed by sequential washing in solutions of HNO_3 (0.01N) and NH_4OH (0.1N) in distilled-deionized water. The coating process was as follows. A slurry of SiCp in water was first made at 2.5 volume% and was sonicated for deagglomeration. The pH of the slurry was then adjusted to 5.8. The alumina slurry was made in a similar manner. At pH 5.8, the SiCp surface carried a net negative charge and that of alumina, a net positive charge. Aliquots of alumina slurry were added to the SiCp slurry in increments of one unit surface area of the SiCp slurry. The mixture was stirred to equilibrate the adsorption process. After each equilibration, interfacial characteristics of SiCp and alumina particulates in aqueous suspensions were determined by the measurement of electrokinetic sonic amplitude (ESA) using a Matec 8000 apparatus by Matec Applied Sciences. Figure 5 shows the ESA measurements after each addition of $A\ell_2O_3$. Figure 6 shows SEM micrographs of alumina coating on a SiCp surface.

Scanning electron microscopy (SEM) and digital image analysis have been used to study the degree of surface coverage obtained in the deposition of alumina powder particles on silicon carbide platelets. We have found that SEM-based image analysis is an excellent technique both for obtaining a quantitative measure of surface coverage and for evaluating the formation of the alumina coating. Digitized images are obtained by collecting the signal from the SEM secondary electron detector for each point in a 512 by 256 pixel grid covering an area of approximately 40 μm^2 on an individual silicon carbide platelet. The resulting image intensity maps show regions of high intensity (alumina) and regions of lower intensity (silicon carbide). The computer analysis of these grey-scale images gives a quantitative measure of the fraction of the area coverage. The fractional surface coverage is found to increase with increasing alumina concentration with 50% coverage obtained with a 200% alumina to SiCp surface area ratio. The morphology of the alumina powder particles is observed to be blocky with dimension ratios of roughly 1:2:3. This is consistent with the measured covering effectiveness of approximately 25%. The SEM imaging shows visually the approach to full surface coverage as the ratio of alumina surface area to silicon carbide platelet area increases.

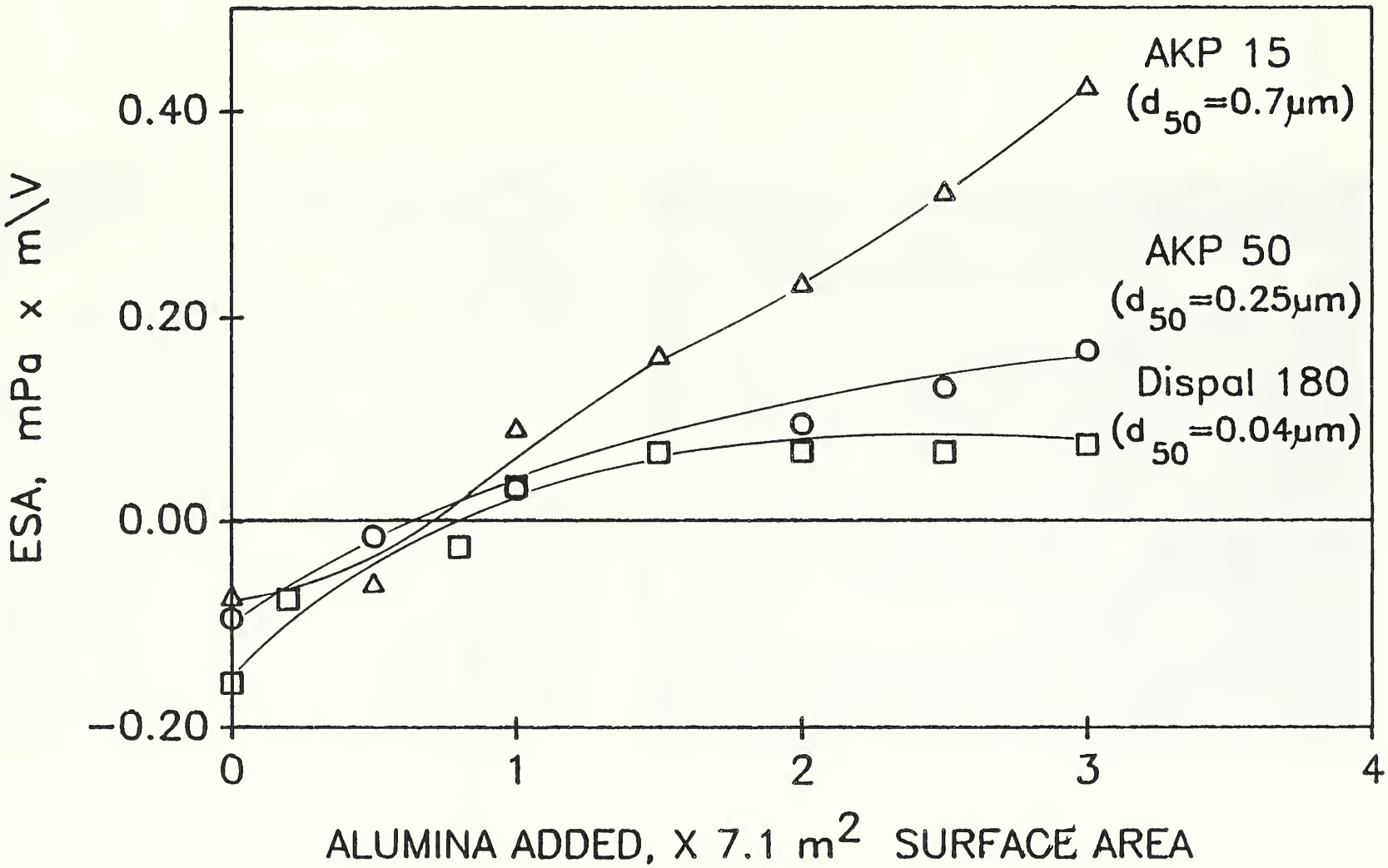

Figure 5. ESA of SiCp in the presence of increasing concentration of $A\ell_2O_3$ with different particle sizes varying from 0.04 μm to 0.7 μm.

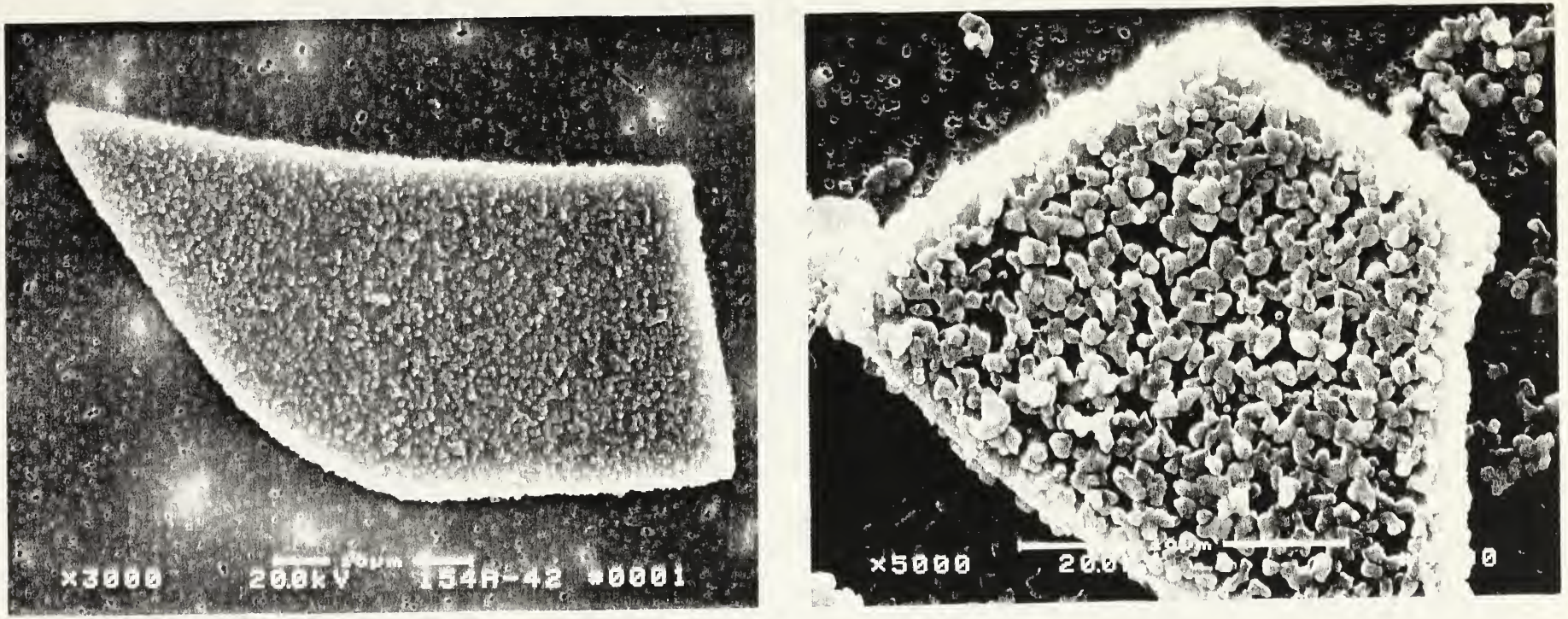

(a) (b)

Figure 6. SEMs of coated SiCp with alumina of different particle sizes: (a) 0.25 μm and (b) 0.7 μm alumina on SiCp.

Characterization of Spray Dried Zirconia Powders

P. T. Pei, P. Zajchowski[1] and S. G. Malghan

[1]Pratt and Whitney

Plasma sprayed coatings of metallic and ceramic materials are used effectively for a variety of gas turbine engine applications including abradable seals and wear resistant and thermal barrier coatings. Variations are found in the coatings. Two possible approaches to decrease the frequency of variations are by (1) improvement of the plasma spray equipment and optimization of appropriate plasma spray parameters and (2) characterization of the powder used in the spray process so that interrelationships can be developed between powder properties and variations in the coatings. At NIST, the second approach was examined.

Zirconia powders of different lots were received from Pratt and Whitney (PW) for characterization. The frequency of coating variations was determined by PW as percent passing a thermal rupture test. A high value of thermal rupture test passing was desired for obtaining high quality coatings.

The following powder characterization tests were addressed: (1) particle size distribution, 2) binder content and chemical composition, 3) optical microscopy, 4) tap density, 5) pH_{iep} by electrokinetic sonic amplitude (ESA), and 6) thermal gravimetric analysis (TGA). Each property of the powder revealed a different type of information about its characteristics. The measurement of certain properties such as particle/agglomerate size distribution and morphology presented technical difficulties due to the fragile nature of the agglomerates. Though significantly more effort is required in the development of reliable test techniques for the methods mentioned above, certain techniques provided useful information. Some of the powder properties found to exhibit differences between the performance of the plasma spray powders were optical microscopy, thermal gravimetric analysis, pH of suspensions in water at which the particles carry a net zero charge, pH_{iep} and binder concentration. However, not all of these properties showed interrelationships with behavior of the powders in the plasma spray coating process. An inverse relationship was found to exist between the binder concentration and % passing of the thermal rupture test data. Some of the powders containing a high concentration of the binder indicated segregation of the binder which resulted in its nonuniform distribution. The binder concentration and/or distribution in the powders was found to affect the interfacial chemistry of the powders when the powders were present in aqueous suspensions. The interfacial chemical parameters such as ESA and pH_{iep} were obtained by using the ESA measurement technique. This type of interrelationship between the binder concentration, interfacial chemistry and thermal rupture data indicates the importance of the steps involved in the preparation of spray dried powders in determining the performance of the powders in the plasma spray coating process. Differences in the binder concentration and interfacial chemical parameters provide a measure of variation in the flowability of the powders in the plasma coating process. The powder flow is expected to be affected not only by agglomerates morphology but also by their size distribution. However, the determination of these properties of the powders is affected by lack of availability of reproducible and accurate measurement techniques. We are continuing research to identify methods of characterization of spray dried powders and factors affecting these measurements.

Microstructural Development in Self Reinforced Silicon Nitride

J. S. Wallace and J. F. Kelly

Recently, silicon nitride materials with remarkably high fracture toughness at room and elevated temperatures have been developed. The extraordinary mechanical properties are related to development of rod-shaped, ß-silicon nitride grains during densification, resulting in a composite-like, fibrous microstructure. The end result is improved reliability of the ceramic

with a flaw tolerance not commonly associated with brittle ceramic materials. The properties of these materials are strongly influenced by the grain size and grain shape. The factors influencing the development of the desired rod-shaped Si_3N_4 grains are poorly understood. Furthermore, accurate analysis of the grain shape and grain size distribution in these non-equiaxed materials is difficult.

To overcome these problems, two different approaches are being taken. First, the factors which influence the development of microstructure, namely, chemical composition, impurities, time, temperature, and pressure, are being investigated. Because of the large number of experimental variables, some of which are interactive, statistically designed experiments are being utilized. These experiments on grain growth are being performed on a model oxynitride glass -Si_3N_4 system for which the variables such as composition and impurity levels can be carefully controlled and, for the dilute systems investigated, are relatively insensitive to contaminants on the Si_3N_4 powder used. The effect of specific intentional dopants, such as carbon, on the morphology and growth rate of Si_3N_4 grains will also be investigated. Microstructural evolution will be evaluated with respect to the size and morphology of the silicon nitride grains for the chosen process variables, and the relationships determined and will be compared to theoretical models of grain growth in the presence of a liquid phase.

Microstructural development as well as characterization of the microstructure are basic parts of the program. Analysis of the stereological parameters associated with this model system as well as those of monolithic Si_3N_4 bodies will be performed. Techniques are being developed for characterizing the three-dimensional morphology and size of individual Si_3N_4 grains. First, chemical techniques for removing Si_3N_4 grains from the monolithic body which do not affect the size and shape of the grains, are being investigated. These grains will be characterized for true size and shape using the scanning electron microscope. From these measurements, the stereological parameters for two dimensional polished surfaces can be mathematically derived. This information is expected to provide a useful tool for analyzing non-equiaxed grain structures. Also, this data will be compared to that of the glass-Si_3N_4 model system study to assure that the appropriate parameters are being evaluated in each study.

Surface Oxidation of Amorphous Versus Crystalline Silicon Nitride Powders by XPS and AES

P. S. Wang

X-ray photoelectron spectroscopy (XPS) and Bremstrahlung-excited Auger spectroscopy (AES) have been used previously in our studies to characterize high temperature oxidation of SiC whiskers, SiC platelets, and a Si_3N_4 containing a 4 wt. % Y_2O_3. For the SiC whiskers, the oxidation rate was linear in the temperature range 600 to 800°C, with an activation energy of 71 kJ/mol. On the SiC platelets, XPS showed that boron impurity segregated to the surface to form boron oxide during oxidation at temperatures between 500°C and 800°C. The presence of this boron impurity appeared to alter the oxidation kinetics. For the Si_3N_4-4%Y_2O_3 powder, XPS did show that the oxidation was linear at temperatures between 900° and 1000°C. It also showed that silicon nitride and yttrium oxide particles reacted, resulting in the formation of an yttrium-rich phase at the interface between the surface SiO_2 layer and the underlying silicon nitride.

The oxidation of silicon nitride powders and hot-pressed samples at temperatures above 1000°C has been studied using thermal gravimetric analysis (TGA). These studies showed the formation of silicon oxide follows a parabolic rate, as expected for diffusion controlled oxidation. In the present study, XPS and AES have been used to measure and compare the initial oxidation kinetics of a crystalline powder containing up to 95% α-Si_3N_4 and a nano-size powder containing mostly an amorphous phase. Samples were oxidized in air at temperatures between 850°C and 1000°C.

The crystalline powder used in this study was from Ube Industries and the nano-powder was from Union Carbide Corp. Respective specific surface areas of these powders were 10.0 m^2/g and 80 m^2/g. Samples were heated in air for 0.5, 1.0, 2.0 and 4.0 hours at 850, 900, 950, or 1000°C. A Leco furnace model 542-27 with an Omega model CN2011K temperature controller was used. The XPS instrument and data system have been described previously.

The Si KLL spectra for both powders were obtained at four temperatures and times. The oxide and the nitride Si KLL peak positions were in good agreement with those found previously.

The oxide layer was measured to be 0.7 nm thick on the as-received crystalline powder and 1.0 nm on the nano-size powder. In both cases, there is a good agreement between the oxide thicknesses calculated from the KLL Auger electron data with those calculated from the 1s photoelectron data, although the thickness values calculated from the 1s data are systematically ~10% higher. The rate constants have been used to make the Arrhenius plots. An example is shown in Figure 7. For the nanopowder, the activation energies of 113 $\pm$ 20 and 105 $\pm$ 13 kJ/mol have been calculated from the KLL data and 1s data, respectively. For the crystalline powder, an activation energy of 63 $\pm$ 4 kJ/mol was determined from both sets of data.

On the crystalline powder, there was no evidence of oxynitride formation during oxidation. The N 1s spectra for the nanosize powder heated at 1000°C are shown in Figure 8. The peak at 402 eV, which increases with heating time, can be attributed to an oxynitride. The formation of an oxynitride has been observed previously during the oxidation of aluminum nitride.

Agitation Milling of Silicon Nitride Powder

S. G. Malghan and D. B. Minor

Milling of silicon nitride powders is an integral part of conventional and colloidal-techniques-based processing. However, currently used methods such as tumbling and vibratory ball milling suffer from inherent deficiencies. These include slow milling and mixing kinetics, limited range of flexibility to control particle and powder morphology, and low concentration of solids in the slurry. High energy agitation milling has shown promise in overcoming some of these deficiencies. The current program is directed towards the development of interrelationships between the major milling parameters and their influence on the resulting powder properties. In addition, the application of a mathematical model for simulation of milling was investigated.

During this past year, the influence of concentration of solids in the slurry and milling media diameter were examined. High energy agitation milling tests were conducted in a specially designed mill consisting of silicon nitride chamber, rotors, spacers and media. Milling kinetics tests were conducted at 34 and 44 vol. % of solids in the slurry containing 150 ppm (with respect to solids) polyacrylate surfactant of an average molecular weight of 7500. First, these results indicate a significant interaction between the rotor speed, slurry flow rate and solids concentration in the slurry. Second, solids concentration in the slurry was found to have a significant influence on the particle morphology (shape, texture, and size).

By milling at a high concentration of solids, 44 vol. %, the particles can be either rounded with a minimum amount of size reduction at low rotor speeds or fractured to produce a significant size reduction at high rotor speeds. Since the particle morphology of the Ube powders has been an issue, detailed investigations have been conducted using scanning electron microscopy (SEM). Two examples of particle morphology modification are presented in Figures 9(a) and 9(b). As shown in Figure 9(a), the SNE-3 powder milled at 44 vol. % solids in the slurry, 480 cc/min slurry flow rate and 2000 rpm, the resulting particles are rounded. The change of sharp-blocky to rounded morphology of particles is enhanced at low rotor speeds and high solids concentration. The effect of slurry flow rate appears to be minimal. On the other hand, at high solids concentration and high rotor speed, intergranular fracture of particles is enhanced. As shown in Figure 9(b), the blocky particles are almost absent and a large number small particles

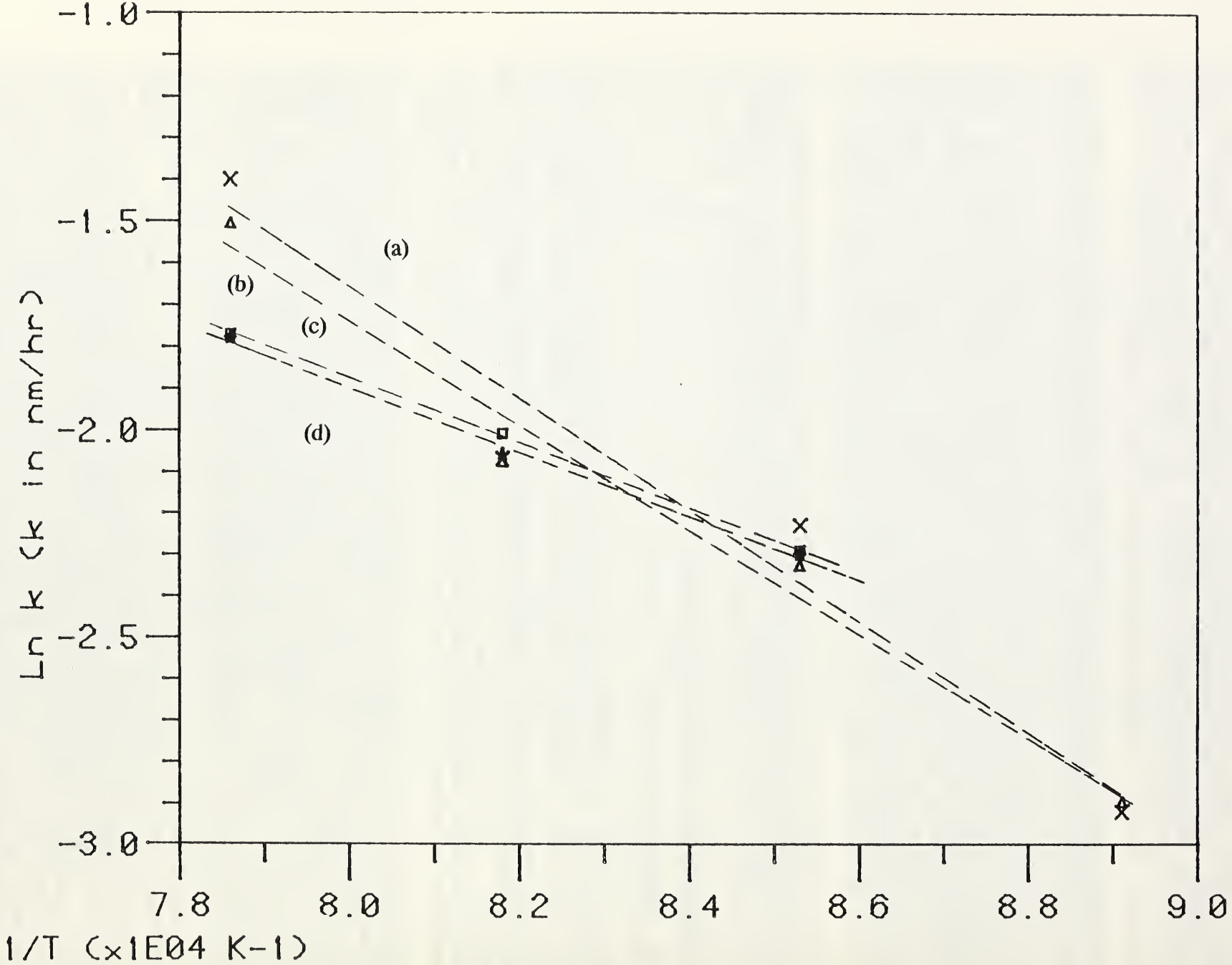

Figure 7. Arrhenius plot of rate constant, k, for α-Si_3N_4 crystallites [(a) KLL data and (b) XPS 1s data] and for nano-size powders [(c) KLL data and (d) XPS 1s data].

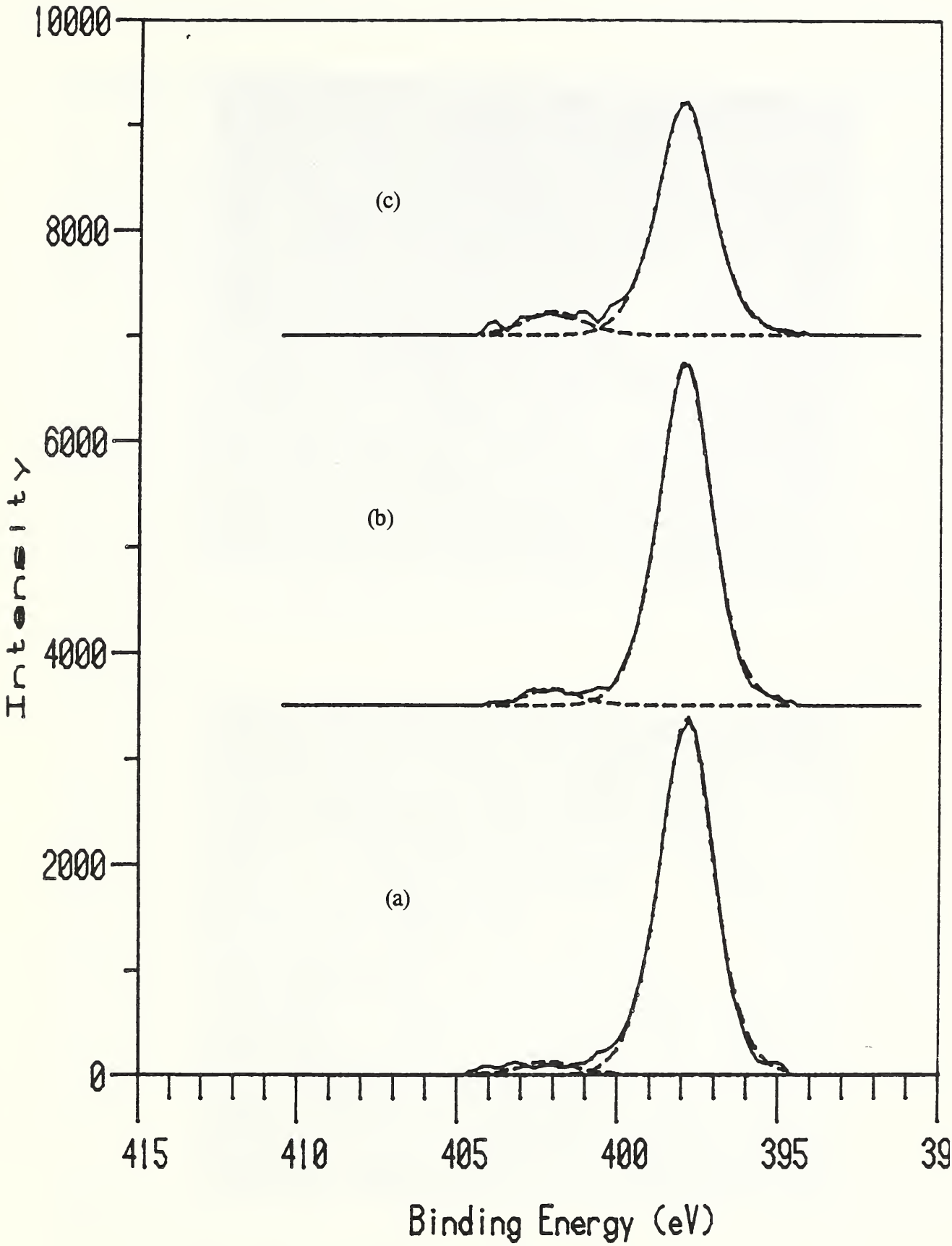

Figure 8. N 1s scans for nano-size, amorphous Si_3N_4 powders heated in air at 1,000° C. for (a) 1.0 hr., (b) 2.0 hrs., and (c) 4.0 hrs.

(a)

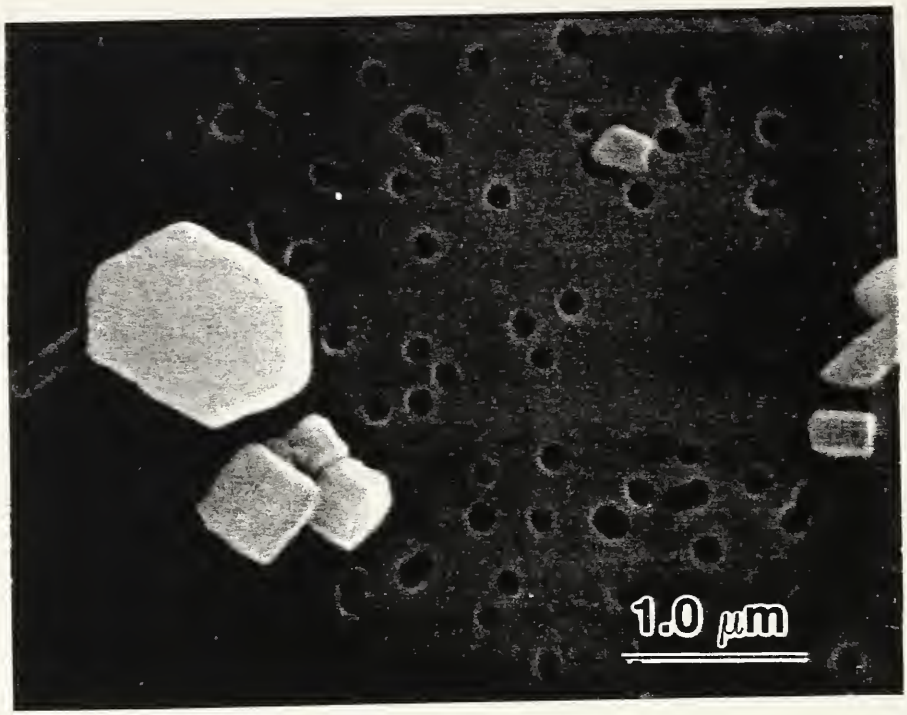

(b)

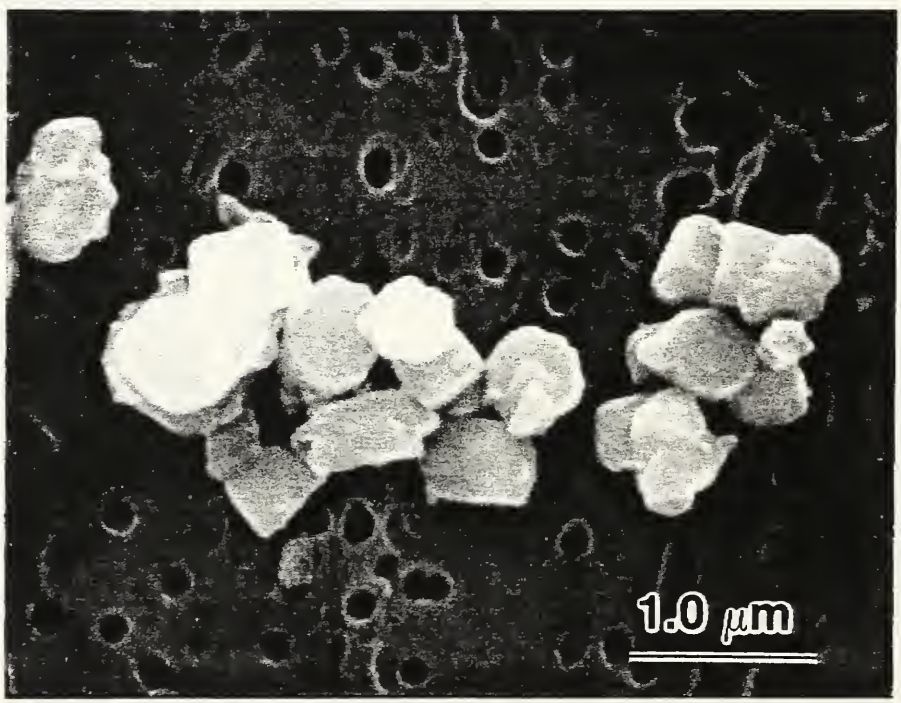

Figure 9. SEM micrographs of: (a) powder milled 26 min., showing appearance of small fragments from the edges of larger particles and (b) powder milled 120 min. showing extensive rounding of particles.

are present. In either case, high concentration of solids is essential to produce compression and impact related size reduction mechanisms at low and high rotor speeds, respectively.

The results of milling with 3.0 mm diameter media were compared with those of 2.0 mm media. The milling rate significantly decreased when using the 3.0 mm media. The decrease in milling rate is related to an effective decrease in the surface area of media that come in contact with the particles in a given time interval. When the total weight of media is fixed, the larger media offer fewer contacts with the particles per unit time and, hence, the slower milling kinetics. However, if the feed particles are much larger in relation to the media size, then the larger size media offer an advantage.

A kinetic milling model, ESTIMILL, was used for simulating the behavior of the high energy agitation ball mill. The ESTIMILL is a Fortran program developed for the purpose of simulating tumbling mill behavior for a specified set of milling model parameters and estimating the required model parameters from the experimental data. The program, which is based on a linear-kinetic size reduction model, is capable of carrying out simulation and/or parameter estimation for a variety of steady state milling configurations. This model is particularly well suited for simulation applications including off-line optimization, on-line optimization, and scale-up of milling circuits. This model was used to carry out analysis of the milling data obtained under a variety of conditions and determine the model parameters. Specifically, the parameters of breakage rate function and breakage distribution function were determined. These parameters are considered to be unique to this material and milling system. Milling of this powder under other conditions not experimentally investigated was studied by using the parameters developed by simulation. These simulation results were later confirmed by experiments.

Automaton Algorithm for Surface Mass Transport Due to Curvature Gradients: Simulations of Sintering.

P. J. P. Pimienta[1], W. C. Carter[2] and E. J. Garboczi[3]

[1]Guest scientist
[2]Postdoc
[3]Building Materials Division

A number of physical phenomena and technological processes involve the evolution of a surface due to its curvature. For example, a surface scratch will gradually smooth when temperatures are high enough for mass transport; or, a system of loose particles will form inter-particle necks and sinter due to surface diffusion. Strictly speaking, such rearrangement is driven by gradients in chemical potential along the surface. When the surface tension is isotropic, the potential is proportional to curvature. Mathematically tracking a surface under the influence of its own dynamics is notoriously difficult. The velocity of the surface in the direction of its normal is proportional to the divergence of the gradient (in the coordinates of the surface) of the curvature: the result is a non-linear, fourth-order partial differential equation with moving boundary conditions. Calculations have either employed useful approximations or numerical techniques and are always limited to simple cases.

A simulation of sintering of many particles will require a new approach. Analysis begins by replacing an atomically stepped surface with a continuous representation, which is then represented digitally by pixels. The size of a pixel is a small fraction of a particle, but is far above atomic length scales. We illustrate a useful algorithm which calculates an approximation to the curvature of a discrete representation of a surface and then updates the surface according to simple rearrangement rules. The algorithm is a cellular automaton, consisting of: 1) curvature calculation via local neighbor-counting rules for each surface pixel, and 2) rules to rearrange the pixels. It is relatively easy to develop such schemes. Since each pixel only responds to its local environment, a simulation program is not limited to simple geometric shapes, but can operate on structures that are arbitrarily complicated at the continuum particle

level. It is anticipated that cellular automaton techniques will be useful in investigating the behavior of many-particle sintering compacts and may lead to new understanding of these processes.

The effort, thus far, has been to establish and demonstrate the local rules of counting which simulate curvature and to show pixel-moving rules which simulate transport via a vapor phase. We have compared our results to known scratch-smoothing calculations and have demonstrated the technique for sintering of one or more particles and for pore closure due to vapor diffusion, all in two dimensions. The algorithm is easily generalized to large random collections of particles in 2-D, and to 3-D problems as well. For three-dimensional problems, one simply redefines the curvature counting box to be a cube, and then the air pixel count will be a linear function of the total curvature at a surface pixel. Of course, 3-D pixels are now cubes. It would also be possible to look at orthogonal planar slices within the curvature counting box, to determine the curvature in each plane.

Other physical features can also be built into the model. Grain boundary energies can be handled by checking whether a given pixel is at a boundary or not. When measuring the curvature at such a pixel, a mismatch term can be put into the curvature box to bring in a grain boundary difference. Anisotropy in the surface energy can be handled by calculating the surface normal at a given surface site, and then appropriately weighing the probability of pixel removal with the surface energy terms combined with the curvature terms. It is important eventually to be able to build-in elastic forces, so that stresses are taken into account as sintering proceeds. Simple methods for using elastic spring networks realistically mapped into digital images of model materials have been developed, and can be applied with little further development to the sintering problem.

MECHANICAL PROPERTIES

David Cranmer

The reliable application of structural ceramics depends upon the ability to control and predict mechanical properties. Knowledge of processing - microstructure - property - performance relationships is the basis for this control and is the focus of our program in mechanical properties. Our program on mechanical properties has as its broad objectives: (1) the generation of new theories and data to elucidate fracture and deformation mechanisms in brittle materials; (2) the development of fracture methodology for studying the fundamental forces that exist between two near surfaces; (3) the investigation of ceramic microstructures and their relationship to mechanical behavior; and (4) the understanding of the deformation and fracture properties that govern the mechanical response of ceramics at high temperatures. Specific projects are focussed on the processing-property relations between microstructural features and resulting properties including toughening behavior in structural ceramics and development of models for the fracture behavior of continuous fiber-reinforced, ceramic matrix composites. This latter work involves test development as well as preparation, characterization, and testing of composite systems.

Significant Accomplishments

- Surface Force Apparatus (SFA) measurements of dissimilar ceramic surfaces immersed in aqueous media have shown the existence of an attractive electrical double-layer force between silica and sapphire at neutral pH. This is believed to be the first ever direct measurement of this type of attraction. The measurements also show the existence of a strong repulsive force at short-range which prevents the surfaces from sticking together when they come very close to contact. Until now it was not known whether the repulsion would occur between dissimilar materials.

- It has been observed that when dry ceramic surfaces are brought into contact and then separated, discrete discharges occur at particular surface separations in the micrometer range. The tentative explanation for these discharges is that they are triggered when the electrostatic potential between the surfaces reaches a certain critical value, but the mechanism appears unrelated to the usual dielectric breakdown of gases which occurs across larger gaps. It is intended to study this effect further, and to explore its implications for static electrical phenomena and fractoemission effects.

- Cathodoluminescence studies of residual stresses have been applied, probably for the first time, to observations of the residual stresses at and near the fiber/matrix interface of fiber reinforced ceramic matrix composites.

- An improved computational program was developed to estimate creep-curvature rate in flexure from implicit functions of the power-law parameters of compressive and tensile creep.

- Oklahoma State University tests of glasses prepared at NIST showed absorption and thermal lensing properties that ensure reduction of very high intensity blue (457 nm wavelength) light to below the threshold for damage to the human retina in an apertured optical observation system such as a telescope. Studies of numerous borate, phosphate, silicate and germanate glass compositions prepared over the years by NIST provided the understanding that led to this breakthrough.

- A study of cyclic fatigue in nontransforming ceramics was completed. It was shown that ceramics with strong R-curve characteristics are subject to modest degradation in cyclic fatigue. For the first time, a mechanism of cyclic fatigue in ceramics, namely, frictional degradation of bridging grains at crack interface, was identified.

- Creep and creep rupture data have been obtained for four different grades of silicon nitride. By specifying both the creep deformation and creep rupture behavior, the results have allowed preliminary lifetime predictions, which specify service life under combined stress and temperature conditions. Comparison of the results on this basis clearly establishes significant differences in high temperature behavior and provides a useful criterion for material selection.

Microstructural Design of Ceramics

B. R. Lawn, S. J. Bennison[1], J. Rödel[1], L. Braun[1], N. Padture[1],
S. Thanomkul, J. Runyan[2] and K-T. Wan[3]

[1]Guest Scientist, Lehigh University
[2]Co-op Student, Virginia Polytechnic and State University
[3]Guest Scientist, University of Maryland

The major part of our research program is directed toward a fundamental understanding of the governing role of microstructure in the strength and toughness properties of multi-phase structural ceramics. Specifically, our aims are twofold: (i) identify the underlying micromechanical processes responsible or crack-resistance (R-curve) behavior in monophase and multi-phase ceramics, and thereby establish fracture mechanics models for predicting strength responses of ceramics; and (ii) in accordance with these predictions, tailor ceramic microstructure so as to optimize strength and reliability characteristics. These aims form our basis for microstructural design.

A second part of our program is to examine brittle fracture properties in terms of fundamental intersurface interactions, of the kind measured in the Israelachvili surface force apparatus. This research bears strongly on materials problems as diverse as adhesion states between coatings and substrates, grain boundary energies, colloidal chemistry, and tribology.

Guided by our previous modeling of grain-bridging toughening, we fabricated and tested a "designed" two-phase alumina/aluminum-titanate composite with unprecedented flaw tolerance (strength independent of flaw size). The micromechanism of toughening in this material was elucidated by following crack evolution to failure using a specially designed in situ device for operation in the scanning electron microscope. This establishes the fundamental basis for future microstructural design of ceramics with optimum toughness properties.

We developed an entirely objective way of determining the underlying short-crack R-curve for such materials directly from indentation-strength data, without need for any prior knowledge of the analytical form of this curve.

A study of cyclic fatigue in nontransforming ceramics was also completed. It was shown that ceramics with strong R-curve characteristics are subject to modest degradation in cyclic fatigue. For the first time, a mechanism of cyclic fatigue in ceramics, namely, frictional degradation of bridging grains at crack interface, was identified.

A new analysis of equilibrium crack growth in brittle materials in interactive atmospheres, based on surface forces concepts, was developed. Experimental data on mica-silica interfaces were correlated with measurements in the surface force apparatus. These data allow uniquely simple evaluation of interfacial energies at virgin and healed interfaces.

Our goals for FY-1992 are as follows.

- To strengthen our in-house processing to provide a unique processing-properties approach to designing stronger tougher ceramics. To this end, we will reinforce our formal link with Lehigh and Carnegie-Mellon Universities.

- To continue developing the R-curve principles systematically to even more complex two-phase composites, in light of the growing evidence that the bridging mechanism may be a primary source of toughening in most (non-transforming) ceramics. Also, to continue to investigate the micromechanics of bridging using our scanning electron microscope fixture for in situ observations or propagating cracks, with particular focus on the micromechanisms of grain and second phase particle pull out.

- To focus even more closely on short-crack responses in these material systems, including damage cumulation and thermal shock. The stabilizing effect of R-curves offers major advantages to such properties.

- To continue studies on the interrelation between fracture and surface forces, with extensions to dissimilar surfaces.

Surface Forces Between Dissimilar Ceramic Materials

D. T. Smith, R. G. Horn and A. Grabbe

The Surface Force Apparatus has been used very successfully for more than a decade now to make fundamental measurements of forces between molecularly smooth mica surfaces in a variety of liquid and vapor environments. Recently at NIST, a method has been devised to extend these measurements to silica surfaces. This development greatly extends the range of possible studies which can be made with the apparatus, and in particular it has opened the way to investigating surface forces between dissimilar materials. Such forces play a vital role in areas such as intergranular fracture, the mechanical properties of composite materials, colloidal processing of mixed powders and composites, and the adhesion of coatings.

In addition to silica, there is the possibility of using thin single crystals of sapphire (alumina) for these measurements. Experiments between silica-sapphire and mica-sapphire couples immersed in aqueous electrolyte solutions have now been carried out. Both silica and mica acquire a negative charge in water. The sapphire surface is known to be positively charged when the solution pH is below 8, and negatively charged at higher pH values.

Our results clearly show an attractive electrical double-layer force between silica and sapphire at neutral pH. This is believed to be the first ever direct measurement of this type of attraction. At high pH the double-layer force becomes repulsive, as expected from the charging behavior described above. More importantly, the measurements clearly show the presence of a strong

repulsive force which operates at short-range, and prevents the surfaces from sticking together when they come very close to contact. This hydration force has previously been observed between two silica surfaces but does not occur between two sapphire surfaces. Until now it was not known whether the repulsion would occur between dissimilar materials when only one surface is "hydrated."

The conclusion is substantiated by measurements between mica and sapphire. Previous work has shown that there is a hydration force between two mica surfaces in concentrated electrolyte solutions, but not in dilute solutions. With mica-sapphire, in addition to a double-layer attraction measured at long range, no hydration force occurs in dilute electrolyte. However, there is a hydration force in concentrated electrolyte solutions. Once again, it appears that only one surface needs to be hydrated in order for a hydration repulsion to occur. This has important ramifications for colloidal processing of mixed powders, since the hydration force prevents the powders from adhering to each other, which is in contrast to classical theoretical expectations.

A different set of experiments has been conducted on silica-mica in a dry atmosphere. In this situation a new and dramatic contribution to the force between these materials has been identified. When the two different materials come into contact, electrical charge transfers across the interface from one to the other. Thus one of the materials (mica) acquires a positive charge and the other (silica) becomes negative. When the materials are subsequently pulled apart, the two layers of charge must be separated from each other, and a large amount of work must be done against the electrostatic attraction between the oppositely charged surfaces. This means that the adhesion is considerably stronger than it would have been in the absence of the charge transfer effect.

In order to explore this phenomenon further, a method of quantifying the charge transferred between silica and mica was developed. This involved building two sensitive electrometers which measure the charge on each material by integrating current flow into proof planes very close to the surfaces. The technique also allows investigation of the rate at which charge dissipates from the surfaces after they have been separated.

The familiar phenomenon of static electricity is another manifestation of charge transfer between different insulating materials. As everyone knows, static electrical effects are much reduced in humid air, and we have confirmed that the same is true in our experiments. We are able to keep very close control over the liquid or vapor surrounding the two surfaces. Initial tests conducted in a nitrogen atmosphere show that as the humidity of the atmosphere increases, less electrical charge is transferred when the surfaces are initially separated, and the charge persists for a shorter time.

Force measurements show very little force between the two initially uncharged materials when they first approach, but a very strong attraction after they have touched. The data fit a simple model of the electrostatic attraction between two capacitor plates, if the presence of the electrometer proof planes is taken into account. The attractive force has a longer range than other surface forces, so that the integral of the force, equal to the work of adhesion between these two materials in the dry atmosphere, is unusually large. In fact the result, 6 J/m^2, is comparable to the cohesive strength of many ionic single crystals, such as sapphire.

An additional effect is observed when the charged surfaces are separated. Discrete discharges occur at particular surface separations in the micrometer range. The tentative explanation for these discharges is that they are triggered when the electrostatic potential between the surfaces reaches a certain critical value, but the mechanism appears unrelated to the usual dielectric breakdown of gases which occurs across larger gaps. It is intended to study this effect further, and to explore its implications for static electrical phenomena and fractoemission effects.

Toughening Mechanisms in High Performance Ceramic Matrix Composites

C. P. Ostertag, D. C. Cranmer and S. M. Wiederhorn[1]

[1]MSEL Scientist

One of the advantages of ceramic matrix composites is their ability to tolerate damage without failing catastrophically. Our knowledge and understanding of the toughening mechanisms by which this happens is, however, limited. Recently, we have made a number of advances to more clearly elucidate these mechanisms in fiber-reinforced ceramic composites. Specific parameters of interest include how fiber length and/or orientation affect the frictional stresses, the fiber debonding and the fiber pull-out length at the matrix-fiber interface, as well as changes in the crack profile. The effect of incidence angle of the propagating crack on the reinforcement orientation plane is also being studied to determine the optimum angle of incidence for maximum toughening.

Model ceramic composites were produced by a controlled low-cost fabrication technique. Samples with different fiber volume fraction and fiber spacing were processed and sintered. The processing of these composites involved tape-casting and pressure squeeze casting. To reduce the damage (crack formation) during sintering, the fibers were coated with different materials in order to reduce or avoid the stress development. The coated fiber-reinforced composites were then tested to study their influence on crack propagation and cracking mechanisms at room temperature and elevated temperatures.

a) Crack propagation measurements at room temperature

A device for in-situ SEM examination is being used to measure crack propagation in fiber-reinforced ceramic composites during loading. The matrix crack initiation and propagation including both the crack tip and the crack wake zones were studied as a function of fiber volume fraction. The interaction of the crack front and wake with the reinforcement was observed in-situ using compact tension specimens. The interactions were videotaped and analyzed in detail to quantitatively determine the effects of the reinforcement on the crack tip and crack wake zones. Preliminary results show a strong interaction of the crack tip with the reinforcing fibers. The crack stopped after approaching the fiber matrix interface. Despite a load increase and a dramatic increase in the crack opening displacement, the crack initially did not propagate. Only after a load increase of approximately three to five times the amount needed to propagate the crack far from the reinforcements, did further crack propagation occur. The crack tip interaction with the reinforcements was observed as a function of fiber volume fraction. The higher the fiber volume fraction, the higher was the load necessary to propagate the crack. Furthermore, the toughness of the composites scaled as a function of fiber volume fraction. These experiments were performed on composites reinforced with fibers both uncoated and polymer- and metal-coated, and will be extended to composites reinforced with alumina-coated fibers. The magnitude of the residual stresses (clamping stresses) will vary with fiber coating and coating thickness.

b) Crack propagation measurements at elevated temperature

There is unfortunately an overly simplistic view of the creep rupture process in the scientific community even for microstructurally simple monolithic ceramics. Moreover, there are several aspects of the creep process in monolithic materials that are not well understood, mostly due to the lack of experimental data. Furthermore, few attempts have been made to test composite materials at elevated temperature. Therefore we have been exploring the mechanisms responsible for creep damage in both monolithic and composite materials. The monolithic samples were fabricated the same way as the fiber-reinforced composites. The same sample

configuration (compact tension) used for the room temperature experiments was chosen for the elevated temperature experiments in order to directly compare the results. Preliminary results were obtained on monolithic alumina samples and on two uncoated fiber-reinforced composites. The measurements were performed at 1200° C at various time intervals. The samples were cooled down under load and photographed. An unexpected event occurred during the crack propagation in the composite samples. The crack propagated at first towards the fibers and then changed its direction 90 degrees to propagate parallel to the fiber plane. In the monolithic sample, failure occurred by the competitive growth of several microcracks ahead of the crack tip until one becomes critical.

Measurement of Residual Stresses by Cathodoluminescence

C. P. Ostertag, L. Robins and L. P. Cook

Residual stresses are present in both monolithic and composite materials and have a strong influence on their mechanical behavior. As an example, the increasing resistance to crack propagation with crack length (R-curve behavior) in alumina is attributed to the interlocking grains which are clamped into the matrix on either side of the crack interface by internal thermal expansion mismatch stresses. In composite materials, the toughness depends strongly on residual stresses (clamping stresses) between reinforcement and matrix, and hence, recent discussions have identified the need to assess the residual stress field effect on fiber debonding. Knowledge of these stresses, specifically their magnitude, is important. Unfortunately, there are few nondestructive evaluation (NDE) methods to measure residual stresses in ceramic materials with high spatial resolution.

Cathodoluminescence (CL) was used as a tool to measure residual stresses with high precision and with a spatial resolution of better than 5 μm. This is a phenomenon of light emission from specimens as a result of an interaction with an electron beam. In insulating crystals, the origin of the luminescence arises from impurity atoms (e.g., transition metals or rare earths) in the lattice. Using an electron microscope to produce the electron beam, the spatial distribution of luminescence sites can be observed with sub-micrometer resolution, and correlated with features of the specimen morphology or microstructure.

In previous work, we used CL imaging and spectroscopy in a scanning electron microscope to investigate residual stresses around indentations in alumina single crystals. This year, the work has been extended to measurements of residual stresses at and near the matrix/fiber interfaces in actual fiber reinforced ceramic matrix composites utilizing the stress-induced frequency shifts of the ruby lines. Both hydrostatic and non-hydrostatic stresses were measured. The magnitude of the stresses was observed to vary with distance from the interface of the matrix/fiber. The experiments were conducted on composites reinforced with gold-coated fibers, and will be extended to uncoated and Ni- and alumina-coated fibers.

Tensile Creep and Creep Rupture of Structural Ceramics

B. J. Hockey, S. M. Wiederhorn[1] and D. C. Cranmer

[1]MSEL Scientist

Structural ceramics are generally recognized as viable materials for components in heat engines for transportation and power generation. In these applications expected operating temperatures generally range from the ambient to ~ 1400°C. Currently, silicon nitride-based ceramics are regarded as prime candidates for these applications, due to their excellent thermal shock and oxidation resistance in combination with relatively high strength and toughness under ambient

conditions. However, as successful application requires service for extended periods under load at high temperatures, the evaluation of these materials ultimately depends on their creep/creep rupture behavior.

In this program, we are investigating the creep/creep rupture behavior of various commercial grades of silicon nitride in collaboration with their industrial producers and users (Norton, Allied Signal and Allison). The aim of this effort is both to assist in the evaluation of current grades of this material and to help guide the development of improved grades of material.

The approach adopted divides the program into three tasks. As ceramics are not commonly tested under uniaxial tension, the first task involved development of a tensile test configuration and methodology suitable for ceramics. Current capabilities allow measurement of tensile strains of $\sim 10^{-10}$ s^{-1} at temperatures up to 1500°C; at 1400°C, reliable test data have been obtained for periods exceeding 4,000 hour. Currently, work on this part of the program is directed toward test standardization. A draft standard for creep including this technology is now being prepared for consideration by ASTM Committee C28. A commercial version of the equipment developed at NIST is available from Applied Test Systems (ATS).

In the second task, tensile strain is measured as a function of time over regions of stress and temperature appropriate to the material. These tests are generally continued until rupture occurs to determine creep lifetime under the imposed conditions. To date, creep and creep rupture data have been obtained for four different grades of silicon nitride. By specifying both the creep deformation and creep rupture behavior, the results have allowed preliminary lifetime predictions, which specify service life under combined stress and temperature conditions. Comparison of the results on this basis clearly establishes significant differences in high temperature behavior and provides a useful criterion for material selection. The results have also established that the tensile creep of these materials occurs in a transient manner, in that strain rate continuously decreases with time throughout the duration of the tests. The occurrence of prolonged transient behavior is significant because it complicates determination of the effect of stress and temperature on creep rate, which are traditionally made on basis of steady state creep behavior. As a consequence, creep results obtained over different regions of stress and temperature can not be readily normalized to provide a global description of differences in creep and creep rupture behavior. Therefore, as our database is augmented by results from still other materials, the development of a transient creep model will be emphasized.

In the third task of this program, microstructural analyses, primarily by Analytical Transmission Electron Microscopy (ATEM) are used to determine the effect of microstructure on creep behavior. Comparison of the various grades of silicon nitride both before and after creep has shown that the microstructures differ primarily in the amount and composition of intergranular glass, which is retained in these materials as a remnant of liquid phase sintering. At high temperatures this glassy phase softens and also allows rapid diffusive transport, and thus effectively controls creep behavior. In this regard, our results have verified that differences in creep and creep rupture relate to differences in the thickness and composition of interfacial glass that separates silicon nitride grains. In particular, differences in the thickness and composition of interfacial glass have been shown to have a significant effect on the nucleation and growth of cavities, which ultimately results in creep rupture.

Analysis of Flexural Creep of Ceramics that Behave Differently in Compressive and Tensile Creep

R. F. Krause, Jr. and T.-J. Chuang

An improved computational program was developed to estimate creep-curvature rate in flexure from implicit functions of the power-law parameters of compressive and tensile creep. The program was applied to published displacement measurements for both an alumina ceramic at 1,000° C. and for a silicon nitride ceramic at 1,200° C. in separate tension, compression, and four-point flexure tests. Satisfactory agreement of the observed and estimated creep curvature rates in the flexure tests can be used to verify the accuracy of the tension and compression tests. Alternatively, observed displacement measurements in flexure tests can be combined with those in either compression or tension tests to predict by a least-squares method the power-law parameters for both compression and tensile creep of the test material. The program was applied to observed displacement measurements in both four-point flexure tests and compression tests to predict the power-law parameters for tensile creep of 99% silicon carbide ceramic at 1,500° C.

Statistically Planned Experiments on Silicon Carbide Whisker-Reinforced Alumina Composite

R. F. Krause, Jr. D. C. Cranmer, and E. R. Fuller, Jr.

In cooperation with the Statistical Engineering Division, statistically planned experiments are being conducted on silicon carbide whisker-reinforced alumina composites, candidates for cutting tool materials, to estimate the empirical relationships between the input factors of the processing conditions and the response variable of the product properties. Selected sizes and volume fractions of whiskers were blended by different procedures with an alumina powder and subsequently hot pressed in vacuum at selected stresses, elevated temperatures, and reaction times to fabricate respective billets of sintered materials. Specimens were diamond cut from billets and examined for the microstructural properties of density, grain size, and homogeneity; for the mechanical properties of flexural strength, hardness, and fracture toughness; and for the machine performance properties of flank and nose wear. The experiments were conducted under two-level factorial plans with six controllable factors. Regression analyses of the multi-dimensional variables can identify the important input factors, interactions among factors and optimum settings of factors to make improved cutting tool materials.

Glass Science and Technology

D. C. Cranmer, D. H. Blackburn[1], and D. A. Kauffman

[1]Consultant

NIST has been involved in glass science and technology since 1910-11 including (during World War II) large-scale production of glass for a variety of lenses and mirrors. At present the main efforts are the formulation and preparation of special glasses for test and evaluation by others and for use as standards; NIST is a unique national facility for supply of such glasses.

Collaboration with Oklahoma State University (OSU) on the optical properties of glasses continued. OSU tests of glasses prepared at NIST showed absorption and thermal lensing properties that ensure reduction of very high intensity blue (457 nm wavelength) light to below the threshold for damage to the human retina in an apertured optical observation system such as a telescope. Work continues on formulations that can do the same thing for other wavelengths. These glasses have optimal combinations of index of refraction, absorption coefficient and thermal coefficient of refractive index so that if a laser beam of high enough

intensity impinges, it will be defocused due to thermal lensing. Studies of numerous borate, phosphate, silicate and germanate glass compositions prepared over the years by NIST provided the understanding that led to this breakthrough. The optimal properties were found in Pb-modified silicates. Analyses indicate that the network atoms primarily determine the refractive index and its thermal coefficient while the modifier ions primarily determine the absorption.

Investigations of Eu-doped silicate glasses for optical storage also continued at OSU. Studies of NIST-supplied glasses indicate that the ability to write on the glasses is optimal when the strength of the chemical bonds and the local fields around the constituent atoms are weak.

Researchers at the NIST Reactor Radiation Division have confirmed the superiority of our ^{6}Li-loaded silicate glass as a thermal neutron shielding material, for which a patent application was filed this year. This material has the distinct advantage of stopping thermal neutrons but not producing large amounts of gamma-radiation. NIST researchers at the Cold Neutron Research Facility (CNRF) have begun using the material as neutron beam-defining apertures and beam stops; increased usage is expected as industrial users of the CNRF become aware of the material.

Collaborative research continued with the Center of Excellence for Materials Science Research located in the NIST Polymers Division. Funded by the National Institute of Dental Research and the American Dental Association Health Foundation (ADAHF), the Center conducts research associated with dentistry. A beta-quartz microcrystalline glass that can be molded into shapes and shades very similar to natural teeth has been developed. The ADAHF has licensed patents on it to a dental manufacturer that plans to market inserts to dentists before the end of calendar 1991 and anticipates initial sales on the order of 1.2 million units. Other research seeks to lower the viscosity of the material to achieve better casting properties and make them more compatible with CAD/CAM techniques.

Creep Rupture Lifetime Assessment on Fibrous Ceramic Composites

T.-J. Chuang, A.M. Glaeser[1] and S. Lee[2]

[1]University of California at Berkeley
[2]National Tsing Hua University

This research program is directed toward establishing a predictive methodology on creep rupture lifetime of fiber reinforced ceramic composites. If a reliable theory becomes available which enables the service life to be confidently estimated, premature component failure and unnecessary replacement can be avoided during service. In the fabrication phase, on the other hand, the material's microstructure can be tailored under the guidance of the theory in such a way as to maximize the service life. In general, the lifetime of a fibrous composite subjected to creep rupture conditions is a function of microcrack propagation rate along matrix/matrix as well as fiber/matrix interfaces, volume fraction of the fibers and fiber architecture. The crack growth rate, in turn, is a function of temperature, stress state and materials properties. Part of our project over the past year has been spent in developing a generic model for lifetime estimation on the composites subjected to long-term sustained loading conditions. Our results indicate that, contrary to the prevailing wisdom in the ceramics community, addition of fibers may actually shorten the life, while enhancing the toughness. Therefore, it becomes a challenging task for the processing engineer to strike a balance between short-term benefits and long-term losses.

Our achievements in this area are summarized as follows. The creep rupture lifetime in a generic fiber reinforced composite is predicted to be inversely proportional to the volume fraction of fibers to a power of one third and to the applied stress to a power of twelve. This prediction seems to agree with the preliminary data collected so far on silicon nitride composite reinforced with silicon carbide whiskers at 1250° C. To predict the speed of a microcrack propagating along a fiber/matrix interface, the crack-tip conditions must be ascertained first. Because of dissimilar properties between the two phases, the crack tip morphology becomes asymmetric in which it was shown that four cases are possible depending on the specific surface free energies and surface diffusivities of the adjoining phases. A tip morphology map in the space of surface energy was constructed in which domains applicable to each case are identified for a given set of surface diffusivities.

Our future goals are:

- To develop a diffusive crack growth theory at a bimaterials interface taking into account the distinct elastic and diffusive properties of the dissimilar phases. In this regard, we will continue a NIST-Tsing Hua University collaboration.

- To develop a stress intensity-crack velocity database in single-phase media. To this end, we will perform four-point bend creep tests on alumina bend bars of bamboo structure and attempt to measure crack lengths using optical microscopy.

- To prepare simple tension creep specimens containing implanted microdefects at the interfaces. Using lithographic technology, a predetermined pattern of microcracks can be implanted at the interface.

Workshop on Carbon/Carbon Composites

D. C. Cranmer

The "Fundamentals of Carbon/Carbon" workshop, sponsored by the U.S. Air Force Office of Scientific Research and NIST, was held at NIST in Gaithersburg on December 6 and 7, 1990. The primary purposes were to assess the state-of-the-science in carbon/carbon composites, and develop a basic research program based on the issues identified during the workshop. It consisted of twelve invited presentations and a poster session on the first day, followed by a half-day panel discussion on the second day.

The topics covered included U.S. Air Force needs, chemical synthesis and analysis, microstructure development, oxidation protection, and composite properties and modeling. A number of issues were identified which form the basis of a research program and are expected to provide significant advances in the understanding and use of carbon/carbon materials.

Growth Morphologies of Diffusion-Induced Recrystallized Grains

W. C. Carter[1] and C. A. Handwerker[2]

[1]Postdoc
[2]Metallurgy Division

Gradients in lattice parameter between coherently bonded regions of a solid result in internal strains. Such coherency strains develop under many different situations, e.g., during a coherent phase transformation such as spinodal decomposition or coherent nucleation, during diffusion of a misfit solute from an interface, or due to differences in thermal expansion coefficients, such as in the cooling of a thin film on a dissimilar substrate. These strains profoundly influence the thermodynamic stability of phases, the microstructure, and the composition distributions in the system. Effects of coherency strains depend on crystal structure and elastic properties.

We have examined a simple case in which a misfit solute diffuses from a grain boundary, or liquid, into a semi-infinite solid and produces coherency strains in the diffusion zone. When the diffusion depth is small compared with interfacial curvature, the diffusion geometry can be approximated as planar. Accordingly, the conditions for local equilibrium of the stressed solid at the interface depend on the difference between the interface and far-field compositions and not on details of the composition gradient. If two grains separated by a grain boundary or liquid film have different crystallographic orientations or different far-field compositions, diffusion of a misfit solute will produce different equilibrium compositions across the grain boundary or liquid film. This difference in composition across the interface provides a driving force for interface migration. This type of interface migration induced by diffusion of a misfit solute is known as diffusion-induced grain boundary migration (DIGM), liquid film migration (LFM), and diffusion-induced recrystallization (DIR), depending on the type of migrating interface.

The migration velocity can be written as a one-dimensional diffusion problem across the grain boundary or liquid film. (In this approximation, all other possible driving forces for migration, including the effects of curvature, are assumed to be negligible.) We have examined the specific case of diffusion-induced recrystallization (DIR), in which diffusion leads to formation of new grains which are enriched in solute. The composition of the new grains is approximately uniform and equal to that of the unstressed solid; therefore, the coherency strain in the new grains is zero. After nucleation, these new grains grow by solute diffusion down the grain boundary and into the dissolving grain. The velocity of DIR grains is proportional to the coherency strain-energy-density of the dissolving grain alone. An analytic expression for this orientation-dependence of elastic parameter and, hence, the migration velocity, was derived for DIR in cubic systems as a function of interface normal and the cubic elastic coefficients.

Previously, the limiting DIR growth morphologies for selected cubic systems were calculated by producing a polar plot of the coherency strain-energy-density, and, by analogy with the Wulff construction for surface energy, by finding the inner envelope of planes normal to a given direction at a given distance from the origin. A recent analysis of the method of characteristics by Cahn et al. and Taylor et al. makes it possible to make precise statements about limiting growth morphologies for DIR grains for a given migration velocity. They showed that the method of characteristics gives the proper solution to the growth problem, which in some cases is identical to the Wulff construction, such as the DIR case presented here.

We have used the method of characteristics to examine the grain morphology as a function of time for an initial grain of arbitrary shape and the range of limiting growth morphologies possible for growing DIR grains for cubic systems as a function of s11, s12, and s44. For an isotropic crystal, the energy density is independent of direction and the growth morphology will be a sphere. For cubic crystals, when the anisotropy factor, $\alpha = 2(s11 - s12)/s44$, is greater than unity, the fastest growth is parallel to $<111>$, the slowest growth is parallel to $<001>$ and the limiting growth morphology is cuboidal; when $\alpha < 1$, the fastest growth is parallel to $<100>$, the slowest growth is parallel to $<111>$ and the limiting shape is octahedral. This analysis serves to establish the physical and computational techniques for subsequent application to the other nine anisotropic sets of elastic coefficients and to anisotropic coherency strain.

Computer Simulations of Anisotropic Ceramic Microstructures in Two Dimensions.

O. Ito[1] and E. R. Fuller, Jr.

[1] Guest scientist, Hitachi Research Laboratory, Hitachi Ltd.

A major obstacle to an enhanced understanding of the physical properties of ceramic materials is the geometrical complexity of their polycrystalline microstructures. Since many of the physical properties of ceramics are determined by their microstructure, prediction and control of microstructural development is an important aspect of ceramic processing. Unlike most metals, which usually have cubic symmetry, ceramics typically have a lower crystalline symmetry.

Although many computer simulations have been performed to simulate microstructural development, most assume isotropic growth conditions. One such method for grain generation, which considers grain geometry and topology, is the model known as Voronoi polyhedra. In the Voronoi model, two neighboring grains nucleate simultaneously, and grow outward uniformly at the same rate. The grain boundary at which the two grains meet will be a straight line which is the perpendicular bisector between the two grain centers. If two neighboring grains nucleate at different times, however, which means nucleation occurs continuously, but still grow outward uniformly at the same rate, they will impinge along a boundary which forms a curve. This case is known as Johnson-Mehl model.

Most microstructure simulations have been based on these two models, both of which employ isotropic grain growth rate. This is typically not the case in most ceramic materials. Ceramic materials typically have crystallographically anisotropic properties. To study effects of this anisotropy on ceramic microstructure and properties, anisotropic factors were incorporated into geometric simulations of microstructure, such as the Voronoi and Johnson-Mehl models, to produce two-dimensional anisotropic microstructures. Instead of the usual circular (isotropic) growth seeds, various anisotropic nucleation seeds, such as ellipses, rectangles and selected polygons, were employed in a growth and impingement model with both simultaneous and continuous nucleation. Nine different microstructures were generated by varying the aspect ratio of the seeds. The morphology of these microstructures was analyzed for grain-size distributions, aspect-ratio distributions, and number of grain edges.

TRIBOLOGY

Said Jahanmir

Advanced structural ceramics are increasingly used in a variety of applications in which wear resistance is required. However, their reliable use depends upon the availability of data which describe performance and provide guidelines for material design. The primary focus in our research is on the characterization of the tribological interface including analysis of chemical reactions and formation of tribochemical films, physical and mechanical behavior of surface films, and the microstructural aspects of deformation and fracture processes leading to wear and failure.

Significant Accomplishments

- A wear transition diagram for a bearing grade HIP'ed silicon nitride was completed. The diagram shows that the tribological behavior of this material can be divided into four regimes:tribochemical reactions with atmospheric humidity, selective oxidation and diffusion of secondary constituents,oxidation of silicon nitride, and microfracture. The information obtained in this project can be used for determining the usable range of conditions for this material, and for making microstructural modifications to avoid severe wear under operating conditions.

- The NIST nanoindention and scratch tester apparatus has been used successfully in experiments to determine the effects of chemical environments on the process of scratching ceramic materials. The scratching process is being used as a slow speed analog for some processes that occur during machining and grinding of ceramics. The apparatus permits application of a controlled load to a diamond indenter while at the same time translating the test specimen. CVD silicon carbide was studied in three different environments: laboratory air, light mineral oil, and the mineral oil with stearic acid. Surface cracking of the specimen (associated with the scratching) varied with both load and enviornment. The results indicate that environment can have a significant effect on damage produced by indentation and scratching; similar effects could be expected associated with machining of ceramics.

- A study was conducted to assess the current state-of-the-art in the machining of advanced ceramics and to identify research areas which could lead to significant improvements. In conducting this assessment, a comprehensive literature search was carried out, visits and discussions were held with industrial companies interested in ceramic machining, a telephone survey was conducted of ceramic machining shops, a research in progress database was consulted, and individuals were invited to visit NIST and discuss different aspects of the ceramic machining.

- A workshop was held to assess the current status of ceramic bearing technology and identify the key research topics needed to expand the range of applications for silicon nitride bearings. The workshop was attended by 75 representatives from industry, government and universities. The summary of the presentations, discussions and recommendations is being prepared and will be issued as a NIST-SP.

Wear Transition Diagram for Silicon Nitride

S. Jahanmir and X. Dong[1]

[1]Guest Scientist, University of Maryland

Silicon nitride has emerged as a promising ceramic material for tribological applications. However, published research results indicate wide scatter in both the coefficient of friction and the wear rate data. The goal of our study is to elucidate the mechanisms of wear in this material, and other ceramics, as a function of contact conditions, and to disseminate this information in simple diagrams. Our recently published results on a high purity alumina indicated that the tribological behavior of this material can be divided into four regimes: tribochemical reactions between alumina and moisture, plowing, microfracture, and flow of glassy grain boundary phase. The coefficient of friction and the wear rate were relatively high in the microfracture regime. These four regimes were represented in a diagram with temperature and load as axes.

The wear transition diagram for a bearing grade, HIP'ed silicon nitride is shown in Figure 10. Similar to alumina, the tribological behavior of this material can be divided into four regimes. However, some of the mechanisms are different from those observed for alumina. Another important difference between the behavior of the two materials is that the wear transitions occur over a much broader region for silicon nitride compared to alumina. At low loads and relatively low temperatures, the tribological behavior of silicon nitride is controlled by formation of silicon hydroxide on the wear track. In this regime, the average coefficient of friction is 0.25, and the wear coefficient ranges from $1x10^{-4}$ to $4x10^{-4}$. In region II, selective oxidation and diffusion of WC and MgO control the wear behavior. The average coefficient of friction is 0.4 and the wear coefficient ranges from $2x10^{-4}$ to $4x10^{-4}$. The tribological behavior in region III is dominated by oxidation of silicon nitride. The average coefficient of friction is 0.65 and the wear coefficient ranges from $3x10^{-3}$ to $2x10^{-2}$. In region IV, similar to alumina, the primary mechanism of wear is microfracture. The average coefficient of friction in this region is approximately 0.8 and the wear coefficient ranges from $7x10^{-3}$ to $5x10^{-2}$. The wear transition diagram can be used for determining the usable range of conditions for a given material, and for the prediction of tribological behavior. The detailed understanding on the fundamental mechanisms can provide guidelines for microstructural modifications to avoid severe wear under operating conditions.

Assessment of Current Practice and Research Needs in Ceramic Machining

S. Jahanmir, L. K. Ives, A. W. Ruff and M. B. Peterson

Advanced structural ceramics, such as silicon nitride, are attractive for many applications due to their high strength at elevated temperatures, resistance to chemical degradation, abrasive wear resistance, and low density. Despite these advantages, there are considerable impediments to the introduction of advanced structural ceramics. With current technology, fabrication costs are high and component reliability is uncertain. The cost of machining can be as high as 90% of the total cost of some high precision components. Damage produced during machining can be detrimental to the performance and produce premature failure.

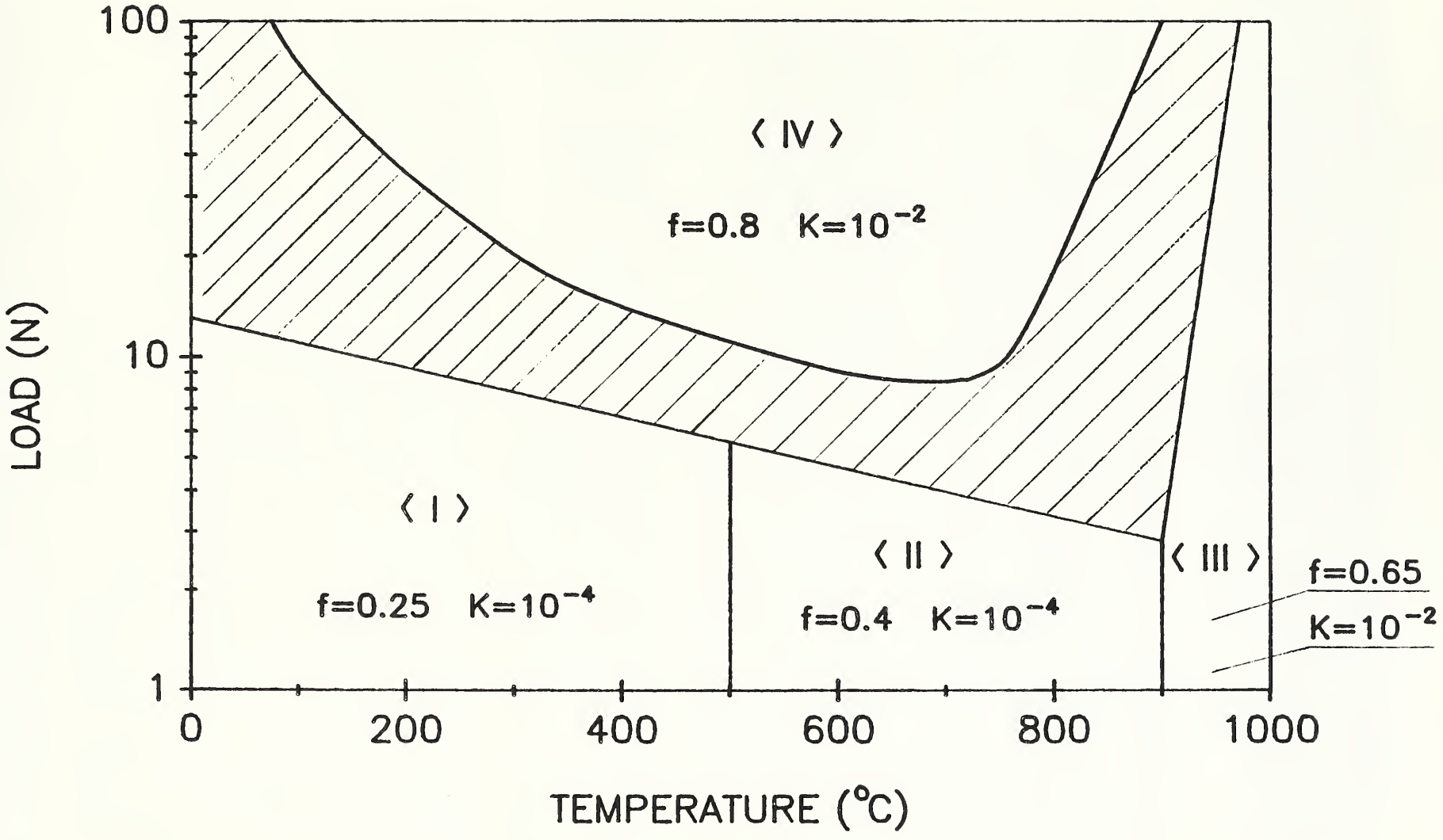

Figure 10. Wear transition diagram for NBD-100 silicon nitride showing four distinct regimes and a transition region: (I) tribochemical reactions, (II) selective oxidation and diffusion, (III) oxidation, and (IV) microfracture.

A study was conducted to assess the current state-of-the-art in the machining of advanced structural ceramics and to identify research areas which could lead to significant improvements. In conducting the assessment a comprehensive literature search was carried out, visits and discussions were held with industrial companies interested in ceramic machining, a telephone survey was conducted of ceramic machining shops, a research-in-progress database was consulted, and individuals were invited to visit NIST to discuss different aspects of ceramic machining.

The results of the assessment with regards to the needs in the machining and production of parts made from advanced ceramics is summarized as follows:

Reduction in Cost: The cost associated with machining is a major contributor to the overall cost of advanced structural ceramic components. Although, significant costs are also associated with raw materials, processing, and quality control, the primary impediment to the introduction of ceramic parts into the market place is the high cost of machining. Therefore, research efforts should be focused on developing methods and procedures for production of cost-effective advanced structural ceramic components.

Rapid Machining Methods: Advanced ceramic materials are difficult to machine with most conventional methods, with the exception of abrasive machining utilizing diamond. Abrasive machining of ceramics, however, is a slow process compared to metals. Innovative techniques are needed to increase the rate of material removal. But, it is extremely important to recognize that increases in the machining rate may introduce a larger level of surface and subsurface damage in the finished part. Therefore, developments of rapid machining methods must accompany damage assessment and control.

Optimization Data: With the exception of a few publications, there is little machining data available for advanced structural ceramics. There is a critical need for data to be used for the purpose of cost estimating, component design optimization, and selection of machining parameters. In the absence of such information, the operator takes the most conservative route, i.e., slow removal rates, which translates to a high cost of machining.

Damage Assessment: Performance and reliability of ceramic components are strongly influenced by damage introduced during machining. Surface finish and machining damage are especially sensitive to small changes in machining conditions. There is a need for reliable and fast in-situ, and post-machining damage assessment techniques. Development of sensors for real-time measurement of surface finish and damage assessment has the potential to increase manufacturing productivity significantly.

In order to take advantage of the unique properties of ceramics and assure their introduction into the market place, a coordinated research program is needed. The overall objectives of this program should be to develop an advanced technology for ceramic machining and remove the barriers that machining presents to widespread introduction of advanced structural ceramics.

Nanoindentation and Scratch Testing

A. W. Ruff and E. P. Whitenton

A new test and measurement system has been constructed that permits nano-indentation and controlled load or depth scratching of materials. The system is capable of characterization of thin surface films and coatings, as well as bulk materials that are inhomogeneous in structure and properties. The load range of the instrument is from 0.01 g to 500 g, permitting study over

a wide range of material properties. Depth sensitivity of about 1 nm is realized. Both the instantaneous load and the penetration of the indenter into the sample are measured continuously. The specimen can be translated under load to produce controlled scratches. The load can be held constant during the translation, or it can be varied in a preset pattern. Feedback electronic circuitry permits scratching at a controlled depth by adjusting the load in proportion to the material response. The scratching resistance force can be measured. All control functions and data analysis are carried out by a dedicated computer.

The system is being used to measure material properties such as microhardness, elastic modulus, ductility, toughness, and resistance to plowing deformation. Microscopic examination of the indentations and scratches afterward provides further information on the mechanisms involved. An example is shown in Figures 11(a) and 11(b) from a study underway of machined surfaces on silicon carbide. Load versus indentation depth results are shown in Figure 11(a) for two values of maximum force, carried out in a mineral oil environment. The loading curve (marked L) indicates a combined elastic and plastic response of the material, with good agreement between the results for the two loads. As the load on the diamond pyramid indenter is reduced (curves UL), the material first relaxes elastically, and then in the last stages plastically. Comparison of the two results indicates that elastic behavior is more significant at the low (10 g) load. The plastic indentation is only about 40 nm deep (for 10 g) at the test conclusion. Figure 11(b) shows a scanning electron micrograph of a scratch formed in the same material at 40 g load. Considerable cracking of the silicon carbide occurs adjacent to the scratch which is about 1200 nm wide (180 nm deep). This method is being used to investigate the nature of machining damage in materials having different plastic and fracture properties, and to understand the effects of different environments.

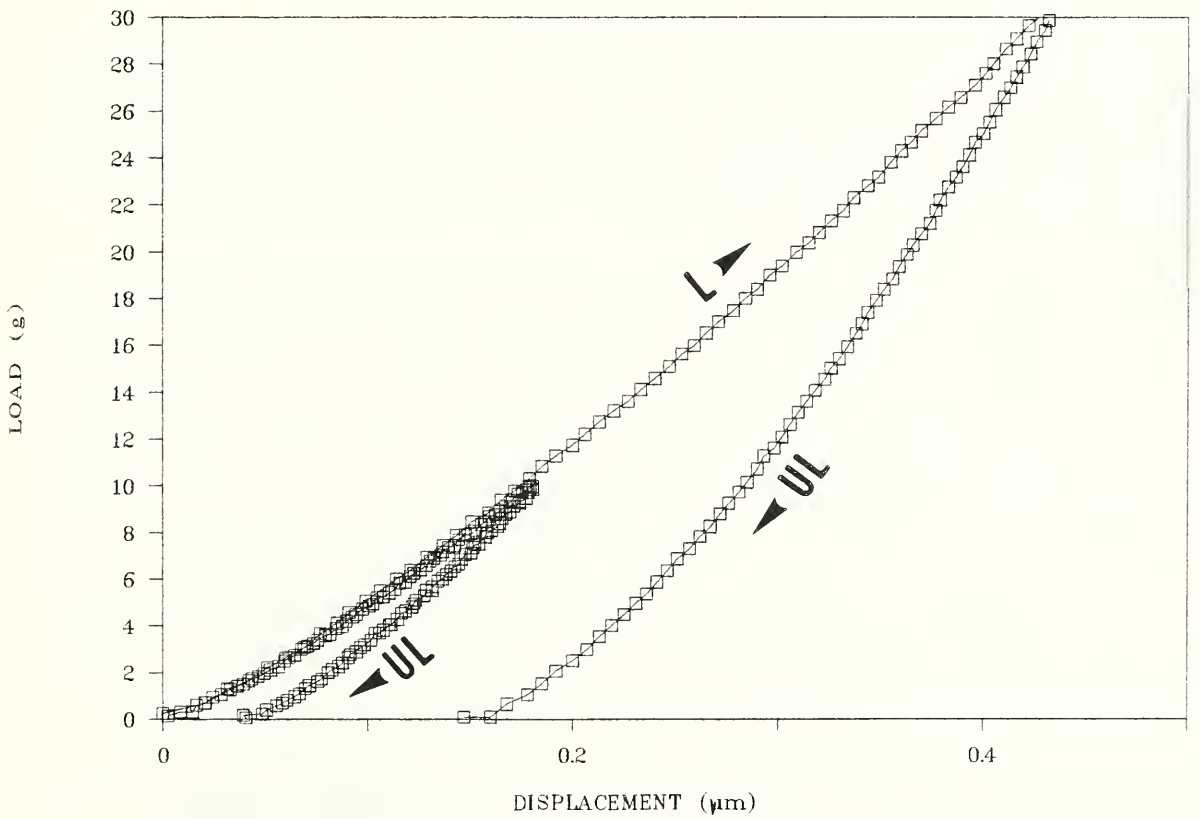

Figure 11(a). Nanoindentation results in silicon carbide tested in a mineral oil environment.

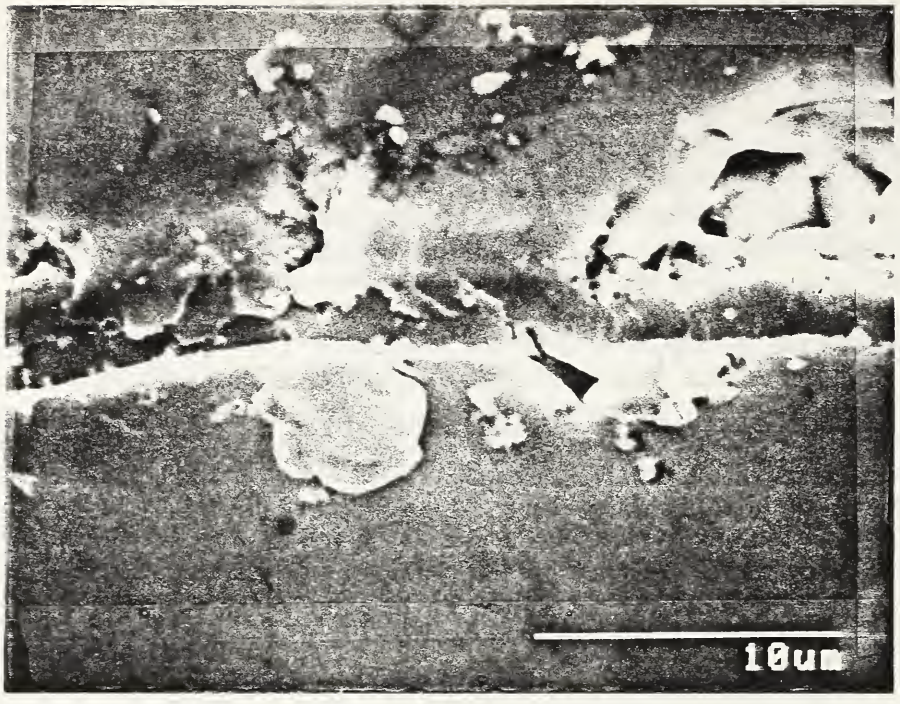

Figure 11(b). Scratch damage in silicon carbide tested in a mineral oil environment.

Mechanisms of Abrasive Wear in Lubricated Contacts

L. K. Ives, M. B. Peterson and E. P. Whitenton

Wear by extraneous abrasive particles is the predominant mode of wear experienced by lubricated components. The purpose of this project is to study the mechanisms which are responsible for this form of wear. A number of different mechanisms can be postulated. These include direct abrasion of the surfaces by hard particles, enhanced wear due to surface roughening and mechanisms involving effects associated with the disruption or prevention of the formation of protective lubricating films.

Current research in this project is sponsored by the Fossil Energy Materials Program of the Department of Energy. The Department of Energy is supporting the development of diesel engines capable of operating directly on pulverized coal, primarily in the form of a slurry consisting of 50% water and 50% coal. Efficient combustion has been demonstrated with this fuel; however, operating engines have experienced an extremely high rate of wear. Piston ring and cylinder liner wear is especially important in this connection. The high wear rate is directly associated with the presence of coal-fuel and combustion particles which enter the contact during sliding. Mineral matter in the coal rather than the coal itself is generally thought to be the main agent responsible for wear.

Previously, work on this project has focused on determining the nature of combustion particles that are responsible for wear. By examining particles obtained from prototype diesel engines operating on different types of coal-fuel, it was established that several different types of particles were present. The hardest and probably the most aggressive in terms of abrasion were found to be silicates and quartz, with quartz usually being the hardest mineral present.

The primary emphasis of current research is on the determination of the influence of contact parameters, the assessment of the effect of different lubricants, and the determination of the effect of different types of particles and component materials on wear processes. Relatively simple laboratory wear test methods are used in the investigation. Figure 12 shows results obtained with a pin-on-disk test. Wear rates were determined for a variety of different materials utilizing lubricant containing particles that were removed from the oil filter of an experimental

diesel engine that had been operated on coal-fuel. In general, the wear rate is relatively high for materials with hardness less than about 10 GPa. This is consistent with the fact that quartz with a hardness of about 10 GPa and silicates of similar hardness are the hardest particulate materials present. The wear rates obtained for sintered tungsten carbide (WC-6Co) and sapphire are extremely low. Coatings of sintered tungsten carbide are currently being considered as a means of increasing the wear life of piston rings and cylinder liners in coal-fueled diesel engines.

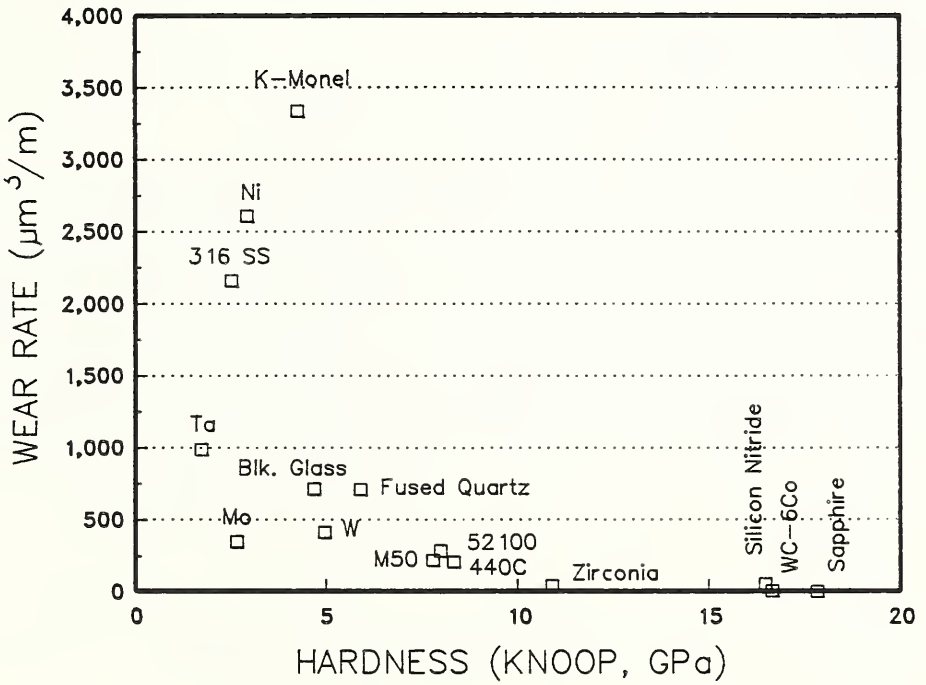

Figure 12. Wear rate of materials determined by means of pin-on-disk tests. The lubricant contained particles from the oil filter of a diesel engine which was operated with coal-fuel.

Tribology of Self-lubricating Composites

A. W. Ruff and M. B. Peterson

This project, sponsored by the Air Force Materials Laboratory, is concerned with the use of advanced, vacuum deposited solid lubricant coatings in bearing systems associated with mechanical components in space satellites. Research has been carried out to develop an understanding of the tribology of self-lubricating composites and to identify potential materials for actual hardware systems. Several key processes responsible for wear and friction in such materials have been identified.

NIST has prepared and examined a number of candidate materials. Composite materials consisting of both copper-matrix and bronze-matrix with solid lubricant phases of either intercalated ($NiCl_2$) graphite or molybdenum disulfide have been studied in sliding wear. Both uncoated and MoS_2 pre-coated type 440C stainless steel rings were used as counterface materials. Friction and wear tests were carried out using a pin-on-ring tribological test system at normal temperatures in both air and dry argon gas. Different effective area and volume percentages of solid lubricant were studied with controlled phase shape and spacing. Selected commercial composites were also studied for comparison.

In general, wear of the composite led to the establishment of an interfacial film, to the generation of wear debris particles some of which remained in the contact gap, and to surface recession at the location of the soft phase. Each of these characteristic features is important in determining the wear and friction mechanisms involved in the tribology of self-lubricating composites. Recommendations are being made to the Air Force for deciding on hardware design and production procedures. Project work continues to better understand the fundamental tribology at work, and to optimize the composites in other respects such as processing and mechanical strength.

Tribological Films and Coatings

M. B. Peterson, A. W. Ruff, L. K. Ives and E. P. Whitenton

This project examines the role of tribological films in sliding contacts and determines the principal mechanisms and the effects of material variables. Studies are being conducted to identify the nature and reactions of oxide films formed at sliding contacts. The purpose of this work is to identify the important properties of effective films (either lubricating or wear resisting) to provide the technology base for improved tribological materials. Studies have been conducted with glass and ceramic substrates in a variety of environments to generate tribological reaction films. These films have been analyzed as to composition and morphology. Friction behavior of mixed reactants have been compared with applied films of known composition to identify which films control friction behavior. Some reactions being considered are as follows:

$$MoO_2 + Sb_2S_3 \longrightarrow MoS_2 + Sb_2O_3$$

$$Mo + 2S \longrightarrow MoS_2$$

$$CuO + MoO_3 \longrightarrow CuMoO_4$$

$$NiO + WO_3 \longrightarrow NiWO_4$$

Friction behavior of mixed powders representing both sides of these equations have been compared under a variety of operating conditions and those conditions defined when both sides of the equations yield identical frictional behavior.

One aspect of this program has been to identify the frictional behavior of oxide films as a function of temperature and compare the results with alloys which form such oxides.

Figure 13 shows the friction-temperature behavior of nickel and nickel-chromium alloys. Friction decreases significantly at about 700°C. This is essentially the temperature where NiO becomes an effective lubricant.

When molybdenum and copper are added to Ni-Co alloys (Figure 14) the friction temperature behavior is quite different. Friction decreases at about 300°C; this is the temperature where MoO_3 becomes an effective lubricant. This behavior persists even with only 5 percent molybdenum addition. It is interesting to note that MoO_3 controls the friction behavior even though CuO (and also Cu_2O) give lower friction at lower temperature. Further investigations have shown that copper molybdate has essentially the same friction-temperature properties as molybdenum oxide. Thus, the tentative explanation is that a tribological reaction occurs to form copper molybdate which controls the friction properties of Ni-Mo-Cu alloy. Future efforts will be directed to study such tribo-reactions.

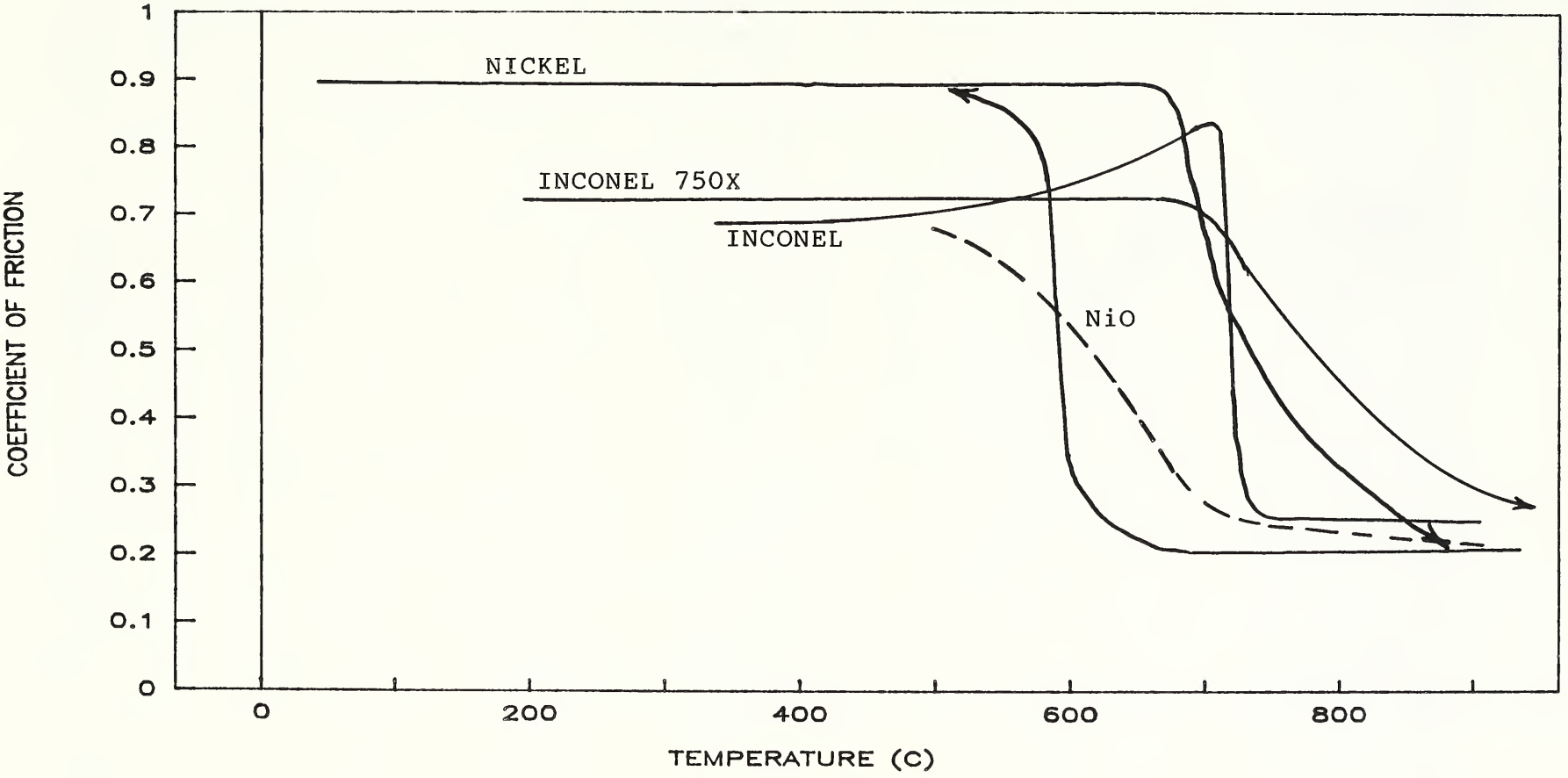

Figure 13. Effect of temperature on the coefficient of friction of nickel and nickel base alloys compared with NiO. Data points are not shown for sake of clarity.

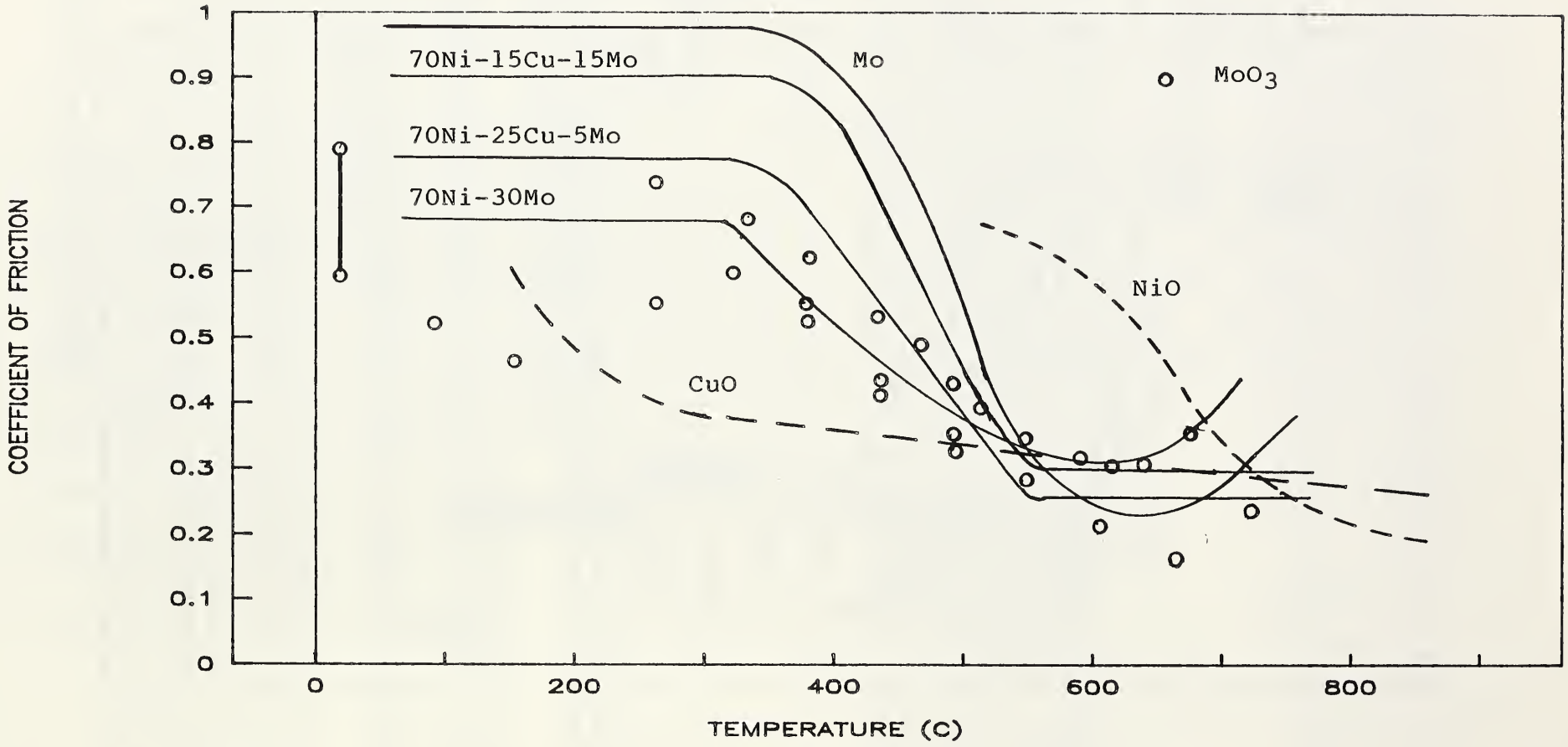

Figure 14. Effects of temperature on the coefficient of friction for molybdenum and nickel molybdenum alloys compared with MoO_3, CuO and NiO oxide powders.

Workshop on Ceramic Bearing Technology

S. Jahanmir

The principal advantages of components of advanced structural ceramics, such as silicon nitride, over metallic counterparts are lower density, higher abrasion resistance, higher chemical inertness, and electrical and magnetic insulation. Advanced structural ceramics have been evaluated during the past twenty years as balls, rollers and races in bearing applications. Currently, silicon nitride hybrid bearings (ceramic balls with steel races) are being used quite successfully as instrument bearings and as machine tool spindle bearings. In general, progress in research and in implementation of research results in utilization of ceramic bearings has been slow. Therefore, this workshop was organized to identify the major impediments and recommend possible solutions.

The objectives of the workshop were to assess the status of ceramic bearing technology, and identify the key research topics needed to expand the range of applications for ceramic bearings. A total of eleven invited presentations were given at the workshop which was attended by seventy-five representatives from industry, government and universities. The presentations and subsequent discussions covered present and potential future applications of ceramic bearings, and topics related to processing, machining, quality control, design, testing and performance evaluation. Based on the presentations and the subsequent discussions by the workshop participants, recommendations for future work were made.

Chemical Interactions of Advanced Materials and Lubricants

R. S. Gates, D. Deckman and S. M. Hsu

The implementation of advanced materials in many applications often requires an understanding of our ability to lubricate these materials. In many cases, conditions are so severe that boundary lubrication takes place, and the understanding must extend to the chemical interactions between the lubricant and the surface. This project has been investigating the chemical interactions between advanced materials and lubricants and lubricant additives to develop such an understanding.

In the past year, several chemical compound classes have been evaluated for their ability to lubricate Si_3N_4 and SiC, two of the most promising structural ceramics. More recently, research on the lubrication of Si_3N_4 has revealed the mechanism by which a specific oxygen-containing compound boundary lubricates this material. Additionally, a new sulfur-containing, antiwear additive for SiC has been discovered. Patent applications are being formulated; therefore, the exact structures cannot be revealed at this time.

Wear testing using several selected long-chain, oxygen-containing compounds revealed that these compounds have the ability to lubricate Si_3N_4 under the very high pressures encountered in boundary lubrication ($>$ 1 GPa). A comparison of friction traces from oxygen-containing compound "A" and paraffin oil lubricated tests (Figure 15) reveals that the compound A provides half the friction level, in addition to lower wear. This information, coupled with the observation of reaction products on and near the worn surface indicates chemical reaction between the surface and the compound. Analysis of the lubricant after the wear test using gel permeation - graphite furnace atomic absorption (GPC-GFAA) revealed that a high molecular weight, silicon-containing product was formed, indicating the direct formation of chemical bonds between the Si_3N_4 surface and the compound. Subsequent surface analysis of some of this high molecular weight reaction product using secondary ion mass spectroscopy (SIMS) disclosed more detailed information on its structure and has allowed us to propose a reaction mechanism between the Si_3N_4 surface and the compound.

Wear tests conducted using SiC determined that a specific sulfur-containing compound was able to reduce wear. Wear test results for several organic sulfides, some of which are considered as conventional antiwear additives in ferrous based tribological systems, confirmed that sulfur-containing compound "B" was unique in its ability to provide lower wear than any of these compounds. The mechanism for the antiwear activity of this compound is thought to involve modification of the stresses associated with asperity contact through the formation of a thin (0.1 μm), cohesive, protective film. Sulfur-containing compound "B" was found to be effective for a variety of SiC materials, regardless of sintering aids and microstructure. It has not been reported previously in the literature as having any antiwear capability, even in ferrous-based tribological systems.

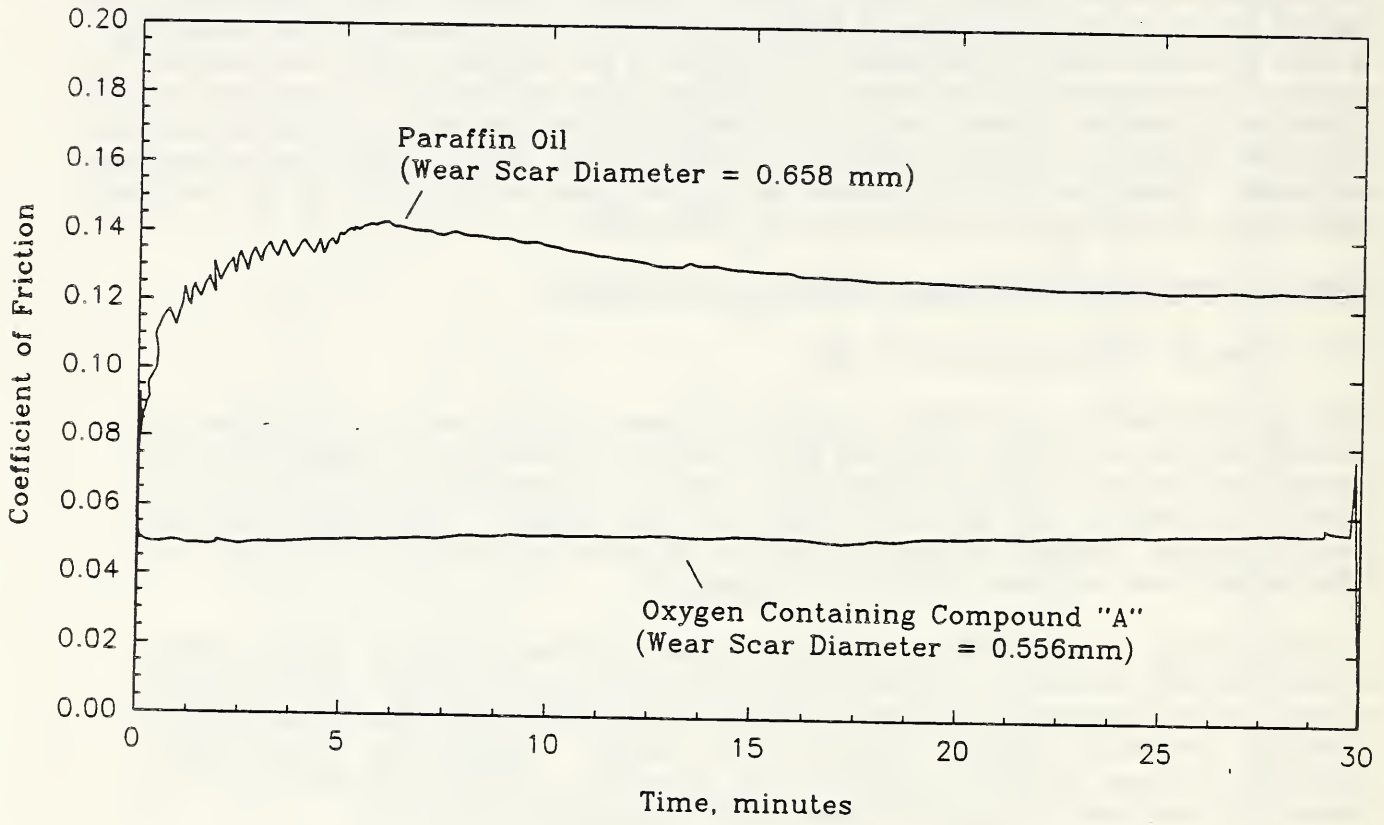

Figure 15. Friction reduction due to tribochemical reaction on the surface of Si_3N_4.

Chemically Assisted Ceramic Machining

J. C. Wang[1] and S. M. Hsu

[1]Guest Scientist, Pennsylvania State University

The purposes of this project are to improve the machining rate and to reduce surface damage of ceramic materials by introducing interfacial chemistry to modify the machining contact conditions. This project aims to resolve the difficulty that contributes to the major source of cost of manufacturing ceramic components.

The first phase of this project is to screen candidate compounds and to study the reaction mechanism and reaction rate of compounds in interest. A diamond wheel cutting tester equipped with a force measurement device has been set up. With the introduction of simple model compounds, it is clear from Figure 16 that the machining rate and surface finish could vary by over a factor of three. The mode of fracture and wear, and the cutting force also vary over a factor of wide range. It can be seen that typical commercial fluids do not offer obvious advantages over model compounds, which indicates the lack of progress in this important area.

To understand the correlation between chemical interaction and machining performance, it is necessary to examine the reaction mechanism, the reaction products, the property of the modified material surface, and the change of mechanical strength and wear mode resulting from these factors.

Several possibly useful mechanisms have been postulated; these include the formation of a softer surface (film), stress corrosion cracking, and reduction of friction force and maintenance of cutting efficiency. A preliminary study on reaction products confirm the oxidation and decomposition of chemical compounds in the contact to have produced lubricous films that maintain cutting angle and cutting force. The reaction products also help to redistribute the machining stresses and to change the direction and degree of fracture and crack propagation. Some chemical compounds anneal the machined damage by lightly corroding the surface in situ. Halogenated hydrocarbons offer the most promising results so far.

Currently, two directions are being pursued. One is to identify the most promising mechanism for different machining processes, since the emphasis on cutting is very different from grinding etc., and vice versa. The other is to carefully prove exactly how each mechanism functions, and what are the dominant parameters. At the same time, screening of new compounds and improvement of existing chemicals continue.

Lubricants for Heat Engines

J. M. Perez, P. Pei, C. S. Ku, Y. Sun[1], Z. Hu[1], Y. Zhang and S. M. Hsu

[1]Guest Scientist

This project explores novel chemical structural concepts to provide a superstable lubricant suitable to be used in heat engines. As new materials are developed, the chemistry and the mechanisms of lubrication change and an understanding of these systems is required to implement them. The low heat rejection engine (LHRE) concept is an example of an advanced technology, energy efficient conversion system in which the availability of high-temperature liquid lubricants is a critical barrier for successful implementation of the technology. Also, increased pressure on environmental issues support the need for more efficient and cleaner burning diesel engines. The fuels and lubricants play a role in this issue. Other future technologies, such as magnetic recording in the computer industry,

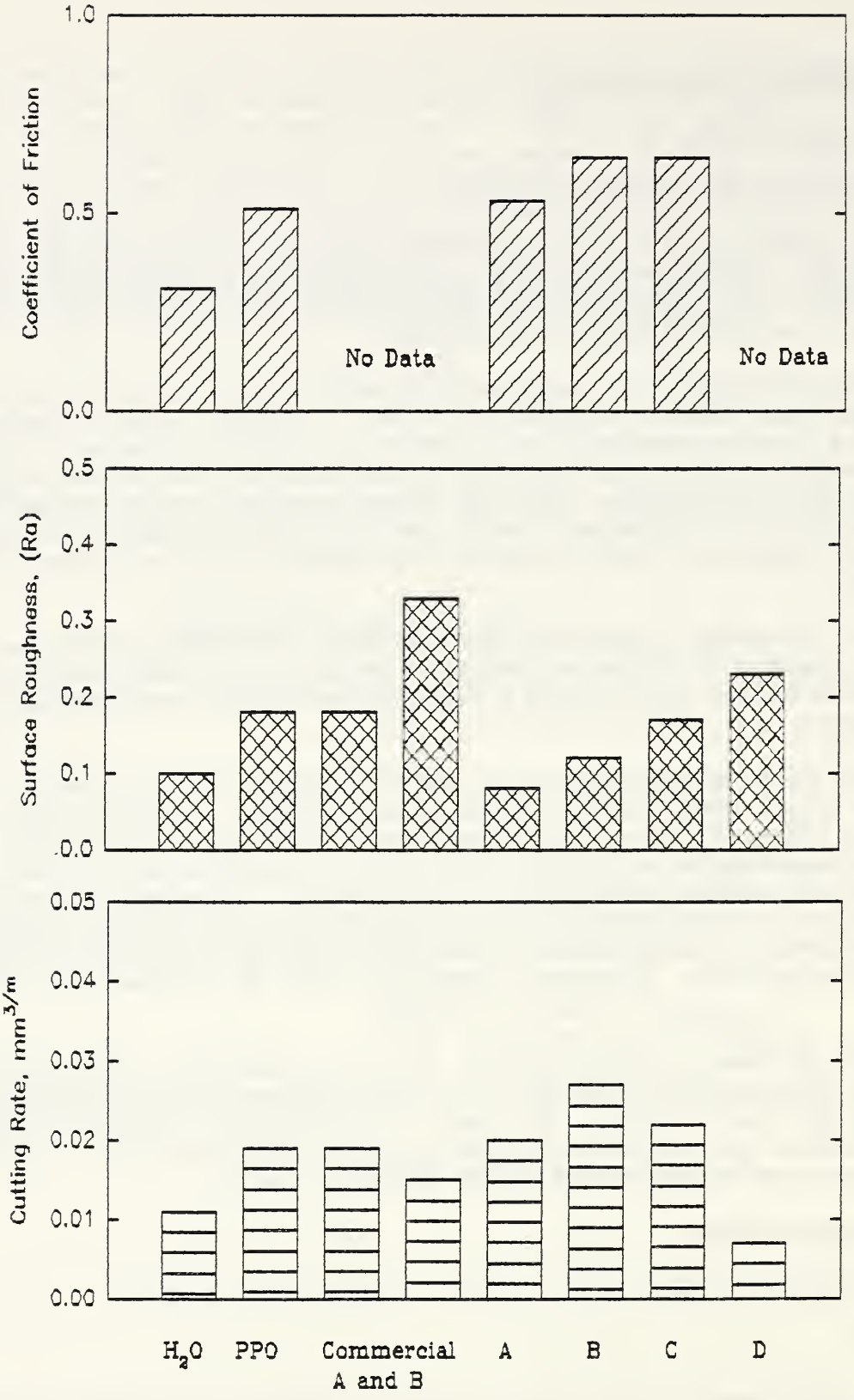

Figure 16. Chemical effects on force (upper figure), finish (middle figure, and rate (lower figure) of machining of silicon nitride. PPO and Commercial A and B are commercial cutting fluids. A, B, C and D are NIST development fluids.

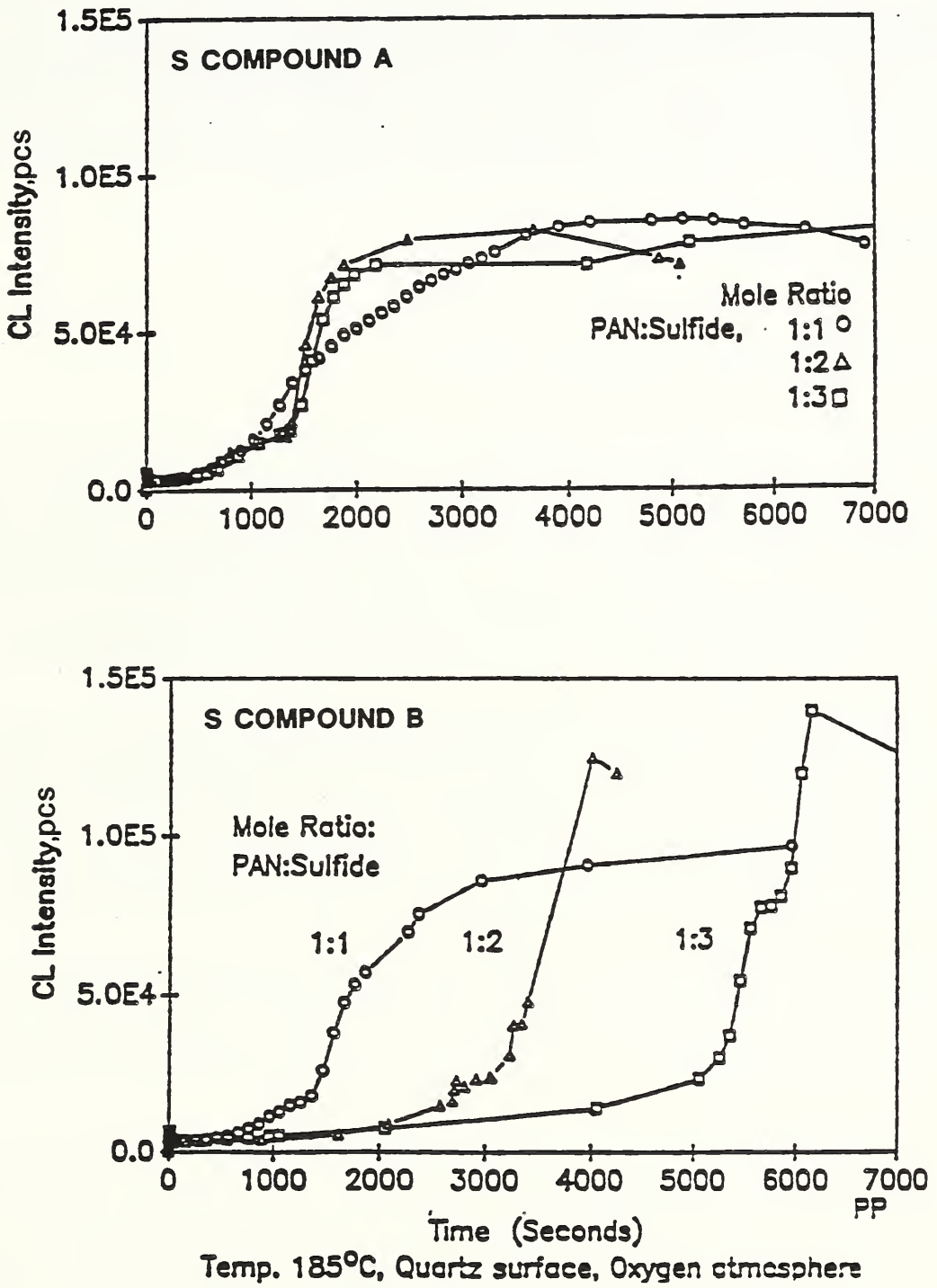

Figure 17. Chemical interactions - synergistic effect of PAN and sulfur compounds with different chemical structures.

precision engineering and reliability of robotic devices in manufacturing technology, clean-room electronic integrated-circuits manufacturing, and biomedical engineering are important technological areas where lubrication is a major or limiting factor.

This project has generated information on a number of synthetic fluids and chemical interactions with various materials for the LHRE system. Information on the chemistries and their influence on engine operations have been developed. The selection of materials plays a significant role on the interactions between the lubricant and surfaces. Research on surface active compounds demonstrates this dramatically. An example of the effect of proper selection of the chemistries is demonstrated on Figure 17. As the surface additive chemistry improved for a particular materials system, the oxidation stability is improved and the deposit forming tendencies at high temperatures are reduced.

Wear Maps

S. M. Hsu, M. C. Shen[1], S. W. Lee[1], and Y. Wang[2]

[1]Guest Scientist, University of Illinois at Chicago
[2]Guest Scientist, University of Maryland

The increasing utilization of advanced materials in engineering designs promotes technology advances. Ceramics are commonly considered to be one group of materials which meets the industrial needs because of their high compressive strength, low density, and chemical inertness, compared to conventional metallic materials. The friction and wear behaviors of a material are not intrinsic properties, rather they are strongly dependent upon operating conditions such as load, speed, lubrication, environment, etc. Before the ceramics can be successfully applied, their friction and wear behaviors need to be well characterized. A ceramics wear database is therefore required to provide adequate information for the material selections in design.

Because of the complicated dependencies of friction and wear upon the operating conditions, a wear map methodology has been developed from the current project not only to present the database but also to reveal the influencing parameters on the wear behavior of specific ceramics. This methodology presents the wear database in three-dimensional maps by plotting the wear data against two parameters. The most common selection of the two parameters is applied load and sliding speed. Other parameters include temperature, stress, and certain combinations of these parameters.

The current ceramics wear database includes five different ceramics, alumina, silicon nitride, silicon carbide, yttria stabilized zirconia (Y-TZP), and a silicon carbide whisker reinforced alumina composite (SiC_w/Al_2O_3). These materials were evaluated under various lubrication conditions including dry air, elevated temperature (up to 500°C), water, paraffin oil, and commercial lubricant.

Figure 18 presents the wear maps of five ceramics under dry air condition. The wear rate is defined by the wear volume divided by the distance slid. A relatively mild wear regime is commonly displayed at the low load and low speed corner in these maps, except for the composite. With increasing load and/or speed, a wear transition will occur. The wear transition is most strongly exhibited in the alumina case. The friction data normally indicates a transitional behavior as well. The blank areas at the high speed and high load corners represent where the wear is too severe for the test to continue.

These maps indicate that the wear rate under the same load and same speed may be very comparable with different materials, for example, the mild wear regimes in Si_3N_4, SiC, and Y-TZP. However, the wear transition as a simultaneous function of load and speed appears to vary with different materials. This indicates that the serviceable range for specific material is material dependent.

The current ceramics wear database demonstrates its capability of offering material selections guidelines for engineering applications. It also offers opportunities for innovative material designs for better wear resistance, since the database covers ceramics with various properties and microstructures. Detailed wear mechanism studies and modeling are currently being pursued to provide design guidelines.

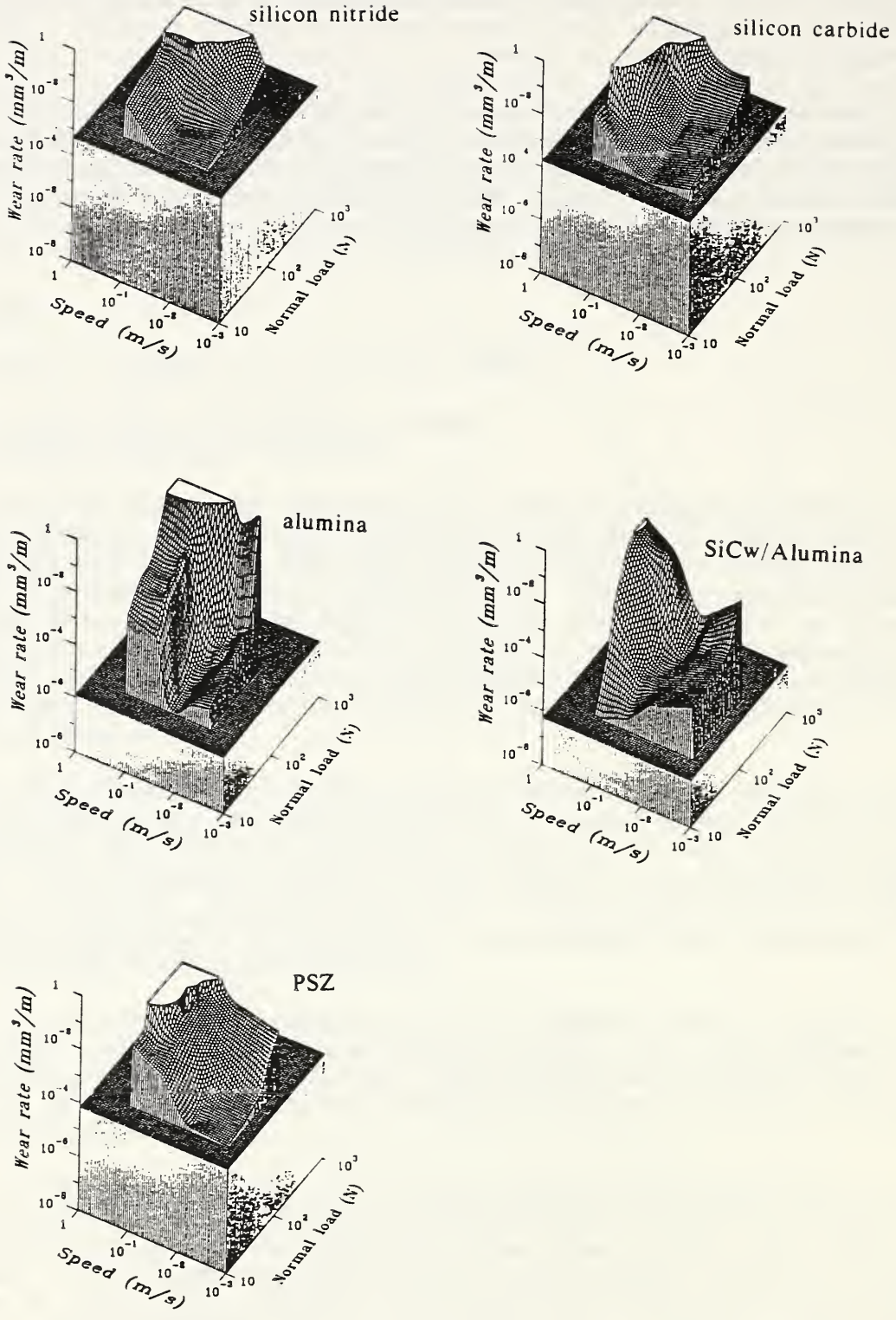

Figure 18. Wear maps for various ceramics under dry sliding conditions.

ELECTRONIC MATERIALS

Grady White

Increased application of ceramics as electronic materials has brought about a broad spectrum of research in this group, ranging from phase diagram determinations and processing studies of high temperature superconductors, through mechanical and electric-field/stress-field interaction investigations of actuator materials to compositional, mechanical, and electrical analysis of electronic films.

Significant Accomplishments

- Microcrack formation during cyclic loading was identified as a damage mechanism leading to mechanical failure. This mechanism also exhibited a temperature dependence which is presently not understood. These results make a major advance in our understanding of why cyclically loaded lead zirconate titanate (PZT) transducers are sometimes weaker than statically loaded PZT. This work is significant for determining long term reliability of these materials.

- Strain energy associated with a change in lattice parameter in a coherent surface layer for hexagonal crystal systems was calculated. This strain energy is the driving force got Diffusion Induced Grain-boundary Migration (DIGM). Results for the Al_2O_3-Cr_2O_3 system have been compared to experimental results (shape and growth rate) during DIGM. These results improve our basic understanding of diffusion processes in ceramics as well as provide a possible technique for composite generation on the individual grain scale.

- Both hardware to make backscattered Kikuchi patterns (BKP) and software to analyze the patterns have been applied to determine grain orientation to within 0.5° for grains down to 0.25 μm in size. These capabilities provide textural information on a size scale previously unavailable for ceramics.

- A single crystal diffractometer has been obtained and used to investigate high T_c materials for structure determination of the individual phases in the phase equilibrium diagrams. This instrument is expected to provide critical crystal structural information for research programs in the Ceramics, Reactor Radiation, and Polymer Divisions.

- High temperature melting behavior of BaY_2CuO_5 and $Ba_2YCu_3O_{6+x}$ have been investigated using a variety of special techniques designed to overcome difficulties of corrosion, environmental contamination and problems quenching the liquid phases at different temperatures. The results have detected errors in published results of peritectic reactions concerning the melting of the two phases. Continuing work in this area is expected to lead to a quantitative liquidus diagram resulting in improved melt processing procedures.

- Melt processing studies of a variety of high T_c materials have demonstrated that flux pinning can be increased substantially over that for the same materials formed by normal sintering processes. Both the amount of pinning and the temperature range over which the pinning occurs have been increased, with pinning observed up to 91 K.

- Molecular orbital ab initio calculations of strained Si-O bonds have been made which show that the process of strain results in an increased charge on both the O and the Si atoms and, simultaneously, a decreased number of electrons involved in the silica bond. When a water molecule is situated next to a silica bond, strain increases electron overlap between the water and the Si-O atoms at both the O and the Si. These results may help provide an explanation for environmentally enhanced fracture of brittle materials.

- An instrumented indenter has been used to obtain hardness values of a 5 μm thick high T_c film on an MgO substrate. The analysis, which was developed by workers primarily investigating metallic films, was shown to need improvements for use with brittle materials. Nevertheless, the data were found to be very reproducible, suggesting that the procedure could be very valuable for analyzing mechanical properties of ceramic films.

Applications of Statistical Methods to Superconductor Processing

C. K. Chiang, S. W. Freiman and N. M. Hwang

For most material processing studies, one or two independent variables are chosen and all other variables are implicitly assumed to be fixed. Since interactions between the chosen and the unchosen variables do exist in ceramic material, the experimental results obtained have a very narrow validity region, typically only within a specified range for fixed variables. In preparation for scientific studies, we need to know that the material is good material, which means the independent variable we chose to study is a good parameter with known relation to other uncontrolled variables. This criteria is very important for interpreting the research results especially for new materials. This program is attempting to integrate quality engineering methods into material research programs.

Modern experimental design methods, which have been proven to be successful in handling complicated engineering projects, were applied to investigate the bismuth-base superconductors. The bismuth-based superconductors, which consist of four to six composition components and many processing parameters such as composition and heat-treatment conditions, appear to be classical examples where statistical methods could be applied. A large number of variables, together with lack of knowledge about phase equilibria, made understanding of this system very difficult. Therefore, much controversial data exists in the literature. By using the Taguchi orthogonal array approach to design the experiments, we reduced the number of samples to eighteen and still provided enough essential information for scientific study. By integrating statistical methods into scientific research we were able to manage the large number of variables and to help understand the relationship between the superconductivity properties and processing in those materials.

Damage Identification in Cyclically Loaded PZT

G. S. White and M. Vaudin

Catastrophic failure without warning has seriously limited the application of brittle materials. Consequently, the fracture behavior of ceramics under static or monotonically increasing loading conditions has been intensely investigated. There exist a number of applications of ceramics, however, in which the material is subjected to cyclic, rather than static or monotonically increasing, loading. One such application is the use of piezoelectric ceramics as transducers, an application in which the ceramic undergoes large amounts of cyclic strain, often at its resonance frequency. It has been found previously that the strength of a piezoelectric material exposed to resonant cyclic loading can be noticeably less than that measured statically.

Our investigations of lead zirconate titanate (PZT) loaded at resonance frequency have found that microcracks are generated during the loading. These cracks apparently do not link up at lower temperatures (e.g., at $T < 80$ °C, in this work) but, at higher temperatures, do interact with macroscopic cracks which may be present and cause hundreds of micrometers of crack extension over the course of a few hours of excitation. This crack extension eventually leads to mechanical failure of the material. At the lower temperature range, although the microcracks do not link up, they are generated in a dense cloud about large flaws in the highest stress region of the material. If the temperature of the material is allowed to increase while load is applied, subsequent to microcrack generation, the material fails catastrophically without observable macrocrack generation or extension.

While these results explain the lower strength observed in PZT driven at resonance frequency relative to semi-static strength tests, we do not yet understand the microcrack generation mechanisms involved or the temperature dependence of the fracture process. Four-point bend measurements at both room temperature and at 150 °C have shown that observed crack extension cannot be due to environmentally enhanced fracture, so microcrack interactions must involve a different mechanism. Transmission electron microscopy (TEM) images show distinct differences in the domain structure of specimens cyclically loaded at $T > 150$ °C and those loaded at $T < 80$ °C, with the domain structure of specimens loaded at the higher temperature much less ordered. These results suggest that there is possibly a relation between temperature-enhanced domain reorientation and microcrack interactions. Such a connection, however, has not yet been shown to exist.

Molecular Orbital Calculations of Strained Silica Bonds

W. Wong-Ng, G. S. White, S. W. Freiman and C. Lindsay[1]

[1]Postdoc

In order to understand the reactions between different classes of environmental molecules and ceramic materials at the atomic level, information such as electron density distribution and atomic charges around strained crack-tip bonds is needed. Since it is difficult to use experimental techniques to obtain this type of information, we have begun ab initio molecular orbital calculations with the goal of elucidating some of the basic features and consequences of strain for the electronic properties of a model silica molecule in both the absence and presence of an active environment. We hope to combine the knowledge of quantum chemistry with results of crack growth experiments to learn about the mechanism by which environmental molecules assist crack growth. Initially, we have been investigating the effect of strain in silica, in the absence of active environmental molecules, to determine the sensitivity of the bond character to the method in which strain is applied to the model molecule.

In order to model the effect of strain on $H_6Si_2O_7$, the model molecule used to mimic silica, we used an idealized geometry (Figure 19) with a linear arrangement of the crack-tip Si-O(bridge)-Si bond. For these calculations, a tensile stress was applied along the longitudinal axis of the molecule. Since there is a lack of knowledge as to whether the external strain is distributed uniformly over all bonds and angles or is actually more localized at a particular center, a combination of geometric distortions was investigated. In principle, a symmetric system, such as the pyrosilicic acid molecule used for the calculations in this work, would undergo a symmetric strain when a far-field load is applied. However, this symmetry, beyond the Si-O-Si bridging bonds, results from the starting geometry we assumed. In the relatively random structure of a real glass, it is not clear whether the crack tip symmetry should be expected to extend beyond the bridging bonds. Consequently, we have investigated both symmetric and non-symmetric systems to see how sensitive the electronic structure of the Si-O bond is to symmetry. The strain geometries investigated range from an extremely localized, asymmetric

strain to distributed symmetric strains. Our purpose in these calculations was to evaluate the sensitivity of the electron distribution in the critical bridging Si-O bond to the manner in which the strains are applied. In our study, four different levels of strain, 5, 10, 15 and 20%, were employed.

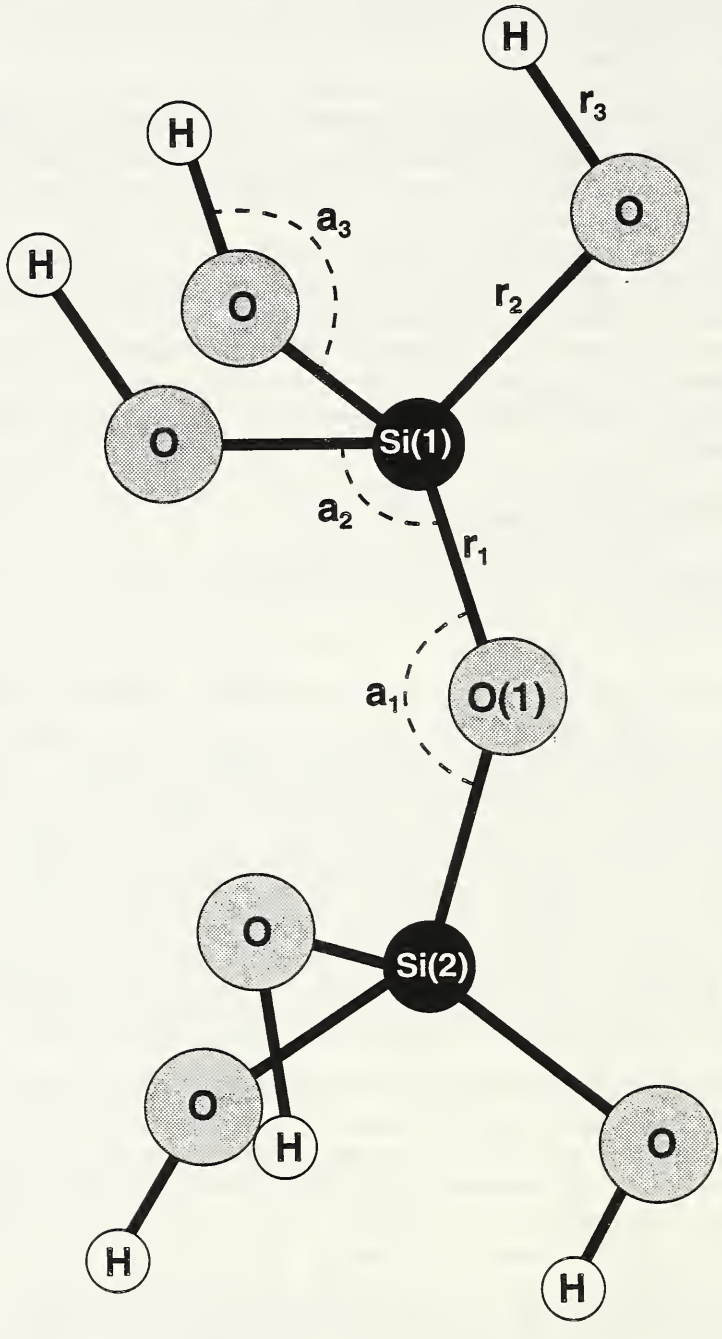

Figure 19. Model of Si-O used in molecular orbital calculations illustrating how bond displacements in SiO_2 are being used to model stress corrosion.

Using the Mulliken electron partition scheme, a method for estimating the electron populations on each atom involved in either covalent or ionic bonds, we found that the bonding electrons associated with the bridging Si and O atoms decrease as the strain increases. At the same time the total partitioned electrons associated with oxygen increases, suggesting that more electrons may be available during strain to interact with an environmental molecule.

We have investigated how varying the application of stress to the crack tip bonds affects the electronic behavior of the Si-O bonds. Although we have not determined which form of strain is the most physically realistic, we have demonstrated that all of the strain geometries have similar effects on the Si and O atoms' behavior.

Processing of Laser-Deposited Ferroelectric Ceramic Thin Films

L. P. Cook, C. K. Chiang, W. Wong-Ng, P. K. Schenck[1] and S. Brody[2]

[1]Metallurgy Division
[2]Harry Diamond Laboratories

Substantial progress was made toward the goal of producing electronic quality ferroelectric ceramic thin films by the pulsed laser deposition method. The laser method offers an attractive alternative to conventional methods such as sol-gel, because of its relative simplicity, its applicability to a wide variety of ceramic materials, and its compatibility with semiconductor processing methodology. However, many fundamental materials issues must be addressed before this important method can be extensively applied in production. The physics of the laser/target interaction, including plume diagnostics, is being addressed by the Metallurgy Division. We in the Ceramics Division are primarily interested in the physics and chemistry of deposition on the substrate, the materials science of the evolving thin film ceramic microstructure, how it is influenced by post processing, and the net effect on properties.

Much of the improvement in the quality of our films is related to the use of excimer (193 nm) rather than the NdYAG (1.06 μm) irradiation used initially. It was found that the excimer produces substantially less particulate material than the NdYAG, thus resulting in films with much smoother surfaces. A second factor is the use of carefully controlled substrate heating. This produces a very dense, hard film with few pinholes, a very important aspect for ferroelectric applications.

We have investigated thin film processing of two ferroelectric materials, barium titanate ($BaTiO_3$), and lead zirconate titanate (PZT) of composition near the morphotropic boundary, $PbZr_{0.57}Ti_{0.43}O_3$. PZT is currently of intense interest as a material for nonvolatile ferroelectric thin film memory. Barium titanate in thin film form has several potential applications, including ferroelectric memory, capacitors, and photonic devices. Ferroelectric and optical properties of the films have been measured in collaboration with the U.S. Army Harry Diamond Laboratories, where films are patterned and electroded, and properties are measured with a variety of instrumentation associated with a basic Sawyer-Tower circuit.

We have produced oriented films of $BaTiO_3$ on Pt-coated silicon wafers by depositing onto substrates heated at $\sim$750°C using a novel self-heating method, developed in our laboratory, which takes advantage of the resistive heating characteristics of silicon. Temperature is held constant by maintaining constant current. Using this technique, we have produced both ferroelectric and nonferroelectric barium titanate. To our knowledge, the ferroelectric thin film barium titanate is among the first reported. Curiously, this material does not show the peak splitting in the x-ray diffraction pattern required for tetragonal symmetry. Yet, the observation of ferroelectric hysteresis indicates a substantial fraction of the material must be non-cubic. Possibly, this relates to a preferred orientation observed in the transmission electron microscopy

(TEM) work such that tetragonal a-axes are oriented perpendicular to the plane of the substrate, with the result that the c-axes are in the plane of the substrate. The intensity of the ferroelectric effect may be inversely related to the uniformity of this orientation. The measured dielectric properties of the barium titanate films are comparable with those of the bulk. We are continuing studies of texturing and orientation in the barium titantate thin films, with the ultimate goal of producing single crystal epitaxial thin films. These should possess optimal properties for ferroelectric, dielectric, and photonic applications.

The processing of PZT thin films has proven more complex, due to the volatility of lead and also the kinetic factors associated with the crystallization of PZT versus the nonferroelectric pyroclore phase. Lead volatility requires the use of lower substrate temperatures, usually in conjunction with a post-depositional processing step. We have achieved the best results by post-annealing at ~550°C. In the future, we hope to avoid the post-annealing step by use of more accurate substrate temperature control during deposition. The ferroelectric properties of the PZT thin films are comparable to those prepared by sol-gel methods. Unfortunately, this also extends to the problem of ferroelectric fatigue, one of the major obstacles to full commercialization of these materials. After about 10^{11} cycles, the value of the switched remanent polarization begins to decrease, for reasons which are not fully understood. By careful study of the microstructural and crystallographic evolution of these films during processing and during testing, it is anticipated that greatly improved understanding of the correlation between such characteristics and the properties of the films, including fatigue, will result. While the PZT films also show lack of tetragonal splitting in the x-ray pattern, we know they are non-cubic because of their ferroelectric behavior. It appears that small particle size and strain may provide the explanation. Studies of orientational effects in the PZT thin films are ongoing.

We have designed and are constructing a deposition chamber which will allow the improved geometry necessary for producing laser-deposited thin films of high uniformity over 7.62 cm (3 inch) wafers. This will facilitate characterization of films by a variety of techniques simultaneously, since individual wafers can be sectioned into numerous areas of suitable size. It will also demonstrate the viability of the method for commercial application.

Materials for Stored Chemical Energy

L. P. Cook and E. Plante[1]

[1]Metallurgy Division

During the past year, extensive thermodynamic modeling and calculations have been completed of phase equilibria pertaining to stored chemical energy propulsion reactions. Using a multicomponent complex chemical equilibrium code (based on the program SOLGASMIX), we have been able to calculate the reaction products and enthalpy yield as a function of reaction completion for two stored chemical energy reaction schemes. In the first scheme, a mixture of liquid lithium is reacted with gaseous SF_6, resulting in a mixture of lithium sulfide and lithium fluoride at reaction completion. In the second scheme, a ternary liquid lithium-aluminum-magnesium alloy is reacted with gaseous perchloryl fluoride to produce a complex mixture of salts and oxides. Detailed calculations show that, for equilibrium to be maintained as progressive reaction occurs, a complex series of crystallization and dissolution reactions must occur. For example, phases such as $LiAlO_2$ and MgO are present near the midpoint of reaction and must react with residual product/fuel mix to produce $MgAl_2O_4$ as one of the final reaction products. These and other features of the complex phase equilibria must be carefully considered in the engineering and operation of practical stored chemical energy reactors.

Many of the stored chemical energy schemes involve oxidation of Li-based fuels, resulting in lithium aluminate products, and so we have spent substantial effort under ONR sponsorship to experimentally determine the Li_2O-Al_2O_3 phase diagram. This year, we were able to analyze and model the data thermodynamically and have prepared a phase diagram for the Li_2O-Al_2O_3 system. This diagram is also of interest to the nuclear fusion community and to lithium fuel cell researchers. Major features of the diagram include a revised liquidus on the high alumina end, an accurate determination of the phase transition in $LiAl_5O_8$, a postulated solid solution based on Li_2O, and a postulated nonquenchable high-temperature phase near the hypothetical beta-alumina composition.

Ceramic Fiber Growth

L. P. Cook, C. K. Chiang and W. Wong-Ng

During the final quarter of the year a new effort was begun to investigate the possibility of forming alumina fibers by a directed solidification method. A process for producing continuous, single crystal alumina fibers in the 5-10 μm diameter range would have major technological and economic impact. Our approach uses the cryolite (Na_3AlF_6)-alumina eutectic, which contains 10 wt % alumina, about the right proportion to produce a eutectic microstructure with non-interconnected alumina crystals. Experiments are underway to determine the proper conditions of growth of single crystal fibers. For this purpose, we have constructed a directed solidification apparatus capable of achieving high thermal gradients and slow pull rates. Results to date have emphasized the need for completing the process in an inert atmosphere, in order to avoid the formation of beta alumina. Future experiments will assess the influence of thermal gradients, pull rates, and melt composition on the process of fiber growth.

Thallia Superconductors

L. P. Cook, W. Wong-Ng and C. K. Chiang

The major goal was to determine if a solid solution exists in the 2122 Tl:Ca:Ba:Cu oxide phase, and to determine the relation between stoichiometry and critical transition temperature, T_c. Earlier data for this system had hinted at the existence of solid solutions based on the two-layered (2122) structure. This was suggested by a rough correlation between observed T_c and the amount of Tl lost from the bulk composition during extended annealing. A series of 42 experiments between 700 and 900 °C along the join between the 0122 Tl:Ca:Ba:Cu oxide composition and Tl_2O_3 (which encompasses the 1122 and 2122 high T_c stoichiometries) was planned and completed to verify the proposed relation between stoichiometry and T_c. This was indeed confirmed; at 860°C a nearly single phase region extending from ~ 12 to 20 mol % was observed. Furthermore, T_c varied across the range of bulk composition, achieving the maximum T_c for compositions near 5 mol %, appreciably away from the ideal 2122 stoichiometry at 16.7 mol % Tl_2O_3 on the join. As this composition was not single phase and yet the T_c was apparently associated with the 2122 present in the sample, it is concluded that appreciable solid solutions exist in another region of compositional space away from the join studied. Possible solid solution mechanisms have been proposed.

Processing High T_c Superconductors

M. D. Hill, J. E. Blendell and C. K. Chiang

The emphasis of the superconductor processing effort has been on the dual goals of enhancing the transport current densities by the elimination of weak links in sintered Ba-Ln-Cu-O materials (Ln=Y or the lanthanides) and on creating flux pinning centers in melt processed Ba-Ln-Cu-O materials. At present we have had more success in the former goal by examining

compositions in the Ba-Y-Sm-Cu-O system. Although intriguing developments have presented themselves in the area of melt-processed materials, no enhancement of critical current density has yet occurred.

High critical current densities (J_c) in $Ba_2YCu_3O_{6+x}$ (213) materials are limited by three factors: anisotropy of superconducting properties, weak links such as microcracks and insulating phases at the grain boundaries, and giant flux creep. In order to improve J_c, the material must be processed to minimize these effects. Thus, materials should be aligned, free of second phases and cracks, and have pinning sites to prevent flux creep. We have been investigating different processing methods and material compositions to determine their effects on properties. The table below compares sintering and melt processing methods relative to these three factors which control J_c.

Processing Method	Clean Grain Boundaries	Micro-cracks	Grain Alignment	Flux Pinning
Sintering of Powders	yes	no	no	?
Melt Processing	yes	yes	yes	yes

Sintering. The homogeneity and composition of the starting powder has a large effect upon the amount of impurities (especially amorphous CuO-rich material) that form at grain boundaries of the sintered material. A powder that exhibits a differential thermal analysis (DTA) endotherm between 920 and 945°C (depending upon the Po_2) will have impurities and second phases in the sintered material. This endotherm is associated with the reaction:

$$Ba_2YCu_3O_{6+x} + CuO \rightarrow BaY_2CuO_5 + \text{liquid}$$

When the composition is Ba-poor, either due to incomplete decomposition of the $BaCO_3$ or due to the formation of $BaCO_3$ during processing, the material is in a three-phase region containing 123 as well as BaY_2CuO_5 (121) and CuO.

Transmission electron microscopy (TEM) results clearly show a CuO-rich liquid phase at grain boundaries, which causes them to be weak links. To avoid the formation of a liquid phase in sintered Ba-Y-Cu (BYC) material, excess green phase was added to the starting powder and it was processed under conditions (temperature and Po_2) unfavorable for the formation of liquid phases. In addition, the green phase, (121), will react with excess liquid to form the 123 phase, favoring the reverse of the reaction shown above. Rather than adding Y-211 to Y-123 material, Sm-211 was added to the Y-123 compound, thus putting the composition in the quaternary Y_2O_3-Sm_2O_3-BaO-CuO system.

In the Sm-Ba-Cu-O phase diagram no tie-line exists between 211 and CuO. Instead, a tie-line exists between 123 and Sm_2CuO_4. This allows for processing in a region where CuO-rich liquid phases are unstable. The presence of the Sm-121 can be detected by energy dispersive x-ray (EDX) analysis since the Sm can be distinguished from the Y and, thus, composition maps are easily developed.

For samples sintered at 950°C in oxygen, the critical current density increased to 375 A/cm^2 for additions of 5 mol % of the Sm-211 phase, as shown in Figure 20. Scanning electron microscopy (SEM) results show that surrounding each particle of the Sm green phase is a patina containing a Sm-rich, Y-poor phase believed to be the 123 phase, thus indicating that the Sm-211 phase reacts with CuO-rich liquid phases to form the superconducting 123 phase. Work is underway in adding sub-micrometer Sm-211 or Y-211 particles to the Y-123 to increase the surface area of the 211 particles, making them more efficient at reacting with the liquid to form the 123 superconducting phase. Y-123 samples containing chemically synthesized Y-211 and Sm-211 particles have been sintered and the critical current density measurements are pending.

Melt Processing. A statistical experiment has been carried out which examined the effects of processing temperature, cooling rate, temperature gradient and oxygen partial pressure on the transport current density. Vibrating sample magnetometer (VSM) measurements provided data on the effect of processing parameters on flux pinning, and microstructural analysis yielded data on microcracking and the dynamics of the liquid front.

A variety of starting compositions, heat treatments and Po_2 were examined to optimize the superconducting properties of the melt-processed material. Novel microstructures have been produced in melt-processed samples of compositions $(Y_{0.75},Eu_{0.25})Ba_2Cu_3O_{6+x}$ and $(Dy_{0.75},Eu_{0.25})Ba_2Cu_3O_{6+x}$. It was found that for the Y-based material, only the cooling rate during solidification had any effect on J_c. For the Dy-based material, we found the opposite, i. e., that a 10°C/cm gradient during cooling and the Po_2 were important but the cooling rate had no effect. We are currently trying to correlate various microstructures with flux pinning by using VSM measurements.

In addition, several compositions were synthesized with barium stannate ($BaSnO_3$) as an additive. Other work in the literature reports that additions of fine grained $BaSnO_3$ to melt-processed BYC reduces the grain size of the green phase inclusions and enhances flux pinning. Barium stannate is believed to behave as a seed for the green phase material which may or may not involve epitaxy. We have prepared materials containing barium stannate and measurements of J_c and flux pinning by VSM are pending.

Bi-based Superconductors

M. D. Hill and C. K. Chiang

With extensive research into the phase equilibria of Bi-containing superconductors ongoing at NIST, research into the processing of the 80K (4:3:3:4) phase Bi superconductor has naturally followed. It has been determined that the blending and firing of alkaline earth oxides, bismuth oxide and copper oxide will not produce a homogenous superconductor. Upon heating, the bismuth oxide will melt at a lower temperature than that at which copper oxide reacts with the alkaline earth oxides. Thus, a route was devised in which a strontium calcium copper oxide ($SrCaCu_2O_3$) will react with a strontium bismuth oxide (1:2) and a calcium bismuth oxide (1:2) to form the (3:3:4:4) superconducting phase. The strontium and calcium bismuth oxides were easily prepared in single phase by solid state reaction at 720°C for 72 h in air. The $SrCaCu_2O_3$ is made single phase by a citrate chemical route. The ternary cuprate and the bismuthates are blended in the correct proportion, calcined in air at 810 and 845°C and single phase (by x-ray diffraction) material results.

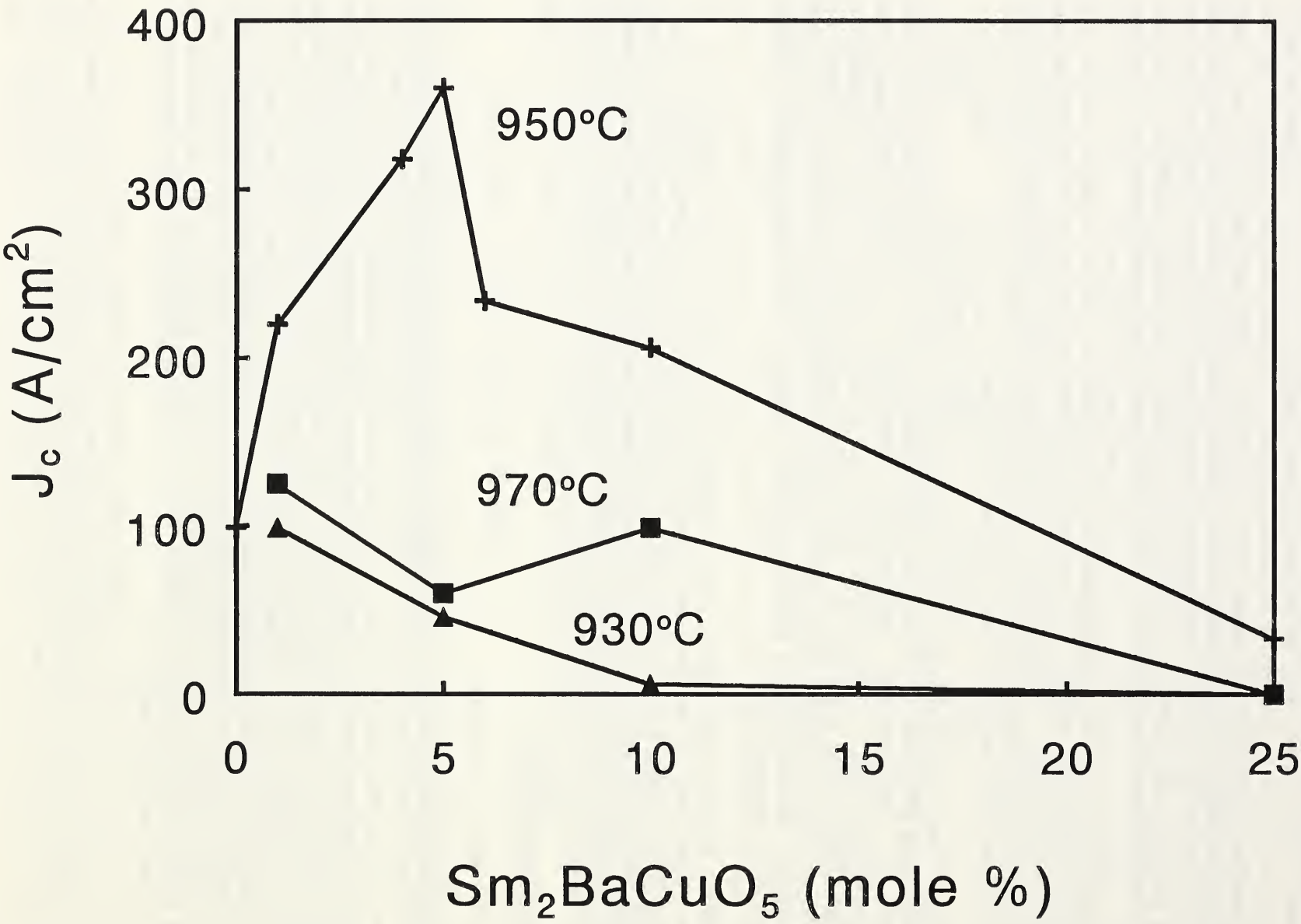

Figure 20. Effect of Sm_2BaCuO_5 additions on the critical current density, J_c, of $Ba_2YCu_3O_{6+x}$, for different sintering temperatures. It is seen that for sintering at 950°C, there is a three-fold increase in J_c for 5 mol % additions, but further additions have decreasingly less enhancement. At both 930°C there is little if any effect of Sm_2BaCuO_5 additions.

DTA was performed on the 3:3:4:4 powder in air to determine the solidus temperature. Using this as a starting point, several samples were uniaxially pressed into bars and heated at selected temperatures for 36 h in air to determine an optimal sintering temperature. An AC susceptibility test was performed on each of the samples to determine the T_c and the superconducting fraction.

The optimum sintering temperature was determined to be 847°C for Bi-rich, Ca-poor 3:3:4:4 material. Aligned material may be synthesized by alternating sintering steps with uniaxial pressing. If a material is sintered with a low percent theoretical density, it may be uniaxially pressed to align the micaceous Bi-superconductor grains and be refired. The results of resistivity and transport current density measurements are pending.

Sol-Gel Processing of Doped Barium Titanates for Infrared Detector Applications

M. D. Hill and R. S Roth

An alkoxide precursor route was chosen to synthesize a number of compositions containing barium titanate with controlled additions of zirconium, hafnium, tin or neodymium. These are candidate materials for pyroelectric infrared detectors being developed by K. Deb at Ft. Belvoir. Of all of the materials synthesized, those with the most promising figure of merit for infrared detector applications are based on a barium titanate - barium zirconate solid solution.
The synthesis phase of this effort has been completed.

Studies of Ceramics Using Backscattered Kikuchi Patterns in the Scanning Electron Microscope

M. D. Vaudin, J. E. Blendell, W. C. Carter and J. F. Kelly

Kikuchi patterns are commonly obtained in the transmission electron microscope (TEM); they are divergent beam electron diffraction patterns from which the crystallographic orientation of a grain in a material can be accurately measured. In the backscattered Kikuchi pattern (BKP) technique, Kikuchi patterns can be obtained using the scanning electron microscope (SEM) from grains as small as 0.25 μm in bulk samples. This is the highest spatial resolution of any bulk crystal orientation technique and has the advantage over the TEM technique that specimen preparation is much simpler. The pattern is recorded on a phosphor in the SEM, imaged with a low-light television camera and digitized using a frame grabber for subsequent enhancement. The image is displayed on a computer monitor together with a cursor which is used to measure the position of zone axes in the diffraction pattern. Computer analysis of the zone axis positions is used to determine crystal orientation to within 0.5°; comparative dislocation density information can also be obtained. The orientation and local texture information provided by the technique can be invaluable when studying grain boundaries, interfaces, thin films and materials produced by novel processing methods.

One of the particular difficulties encountered when studying ceramics as compared to metals and semiconductors arises because many ceramics are of relatively low symmetry. BKP patterns from non-cubic materials cannot be indexed by inspection, and therefore an efficient algorithm for automatically indexing diffraction patterns from any crystal system has been developed. The indexing is practically instantaneous once the zone axis positions have been recorded using the cursor; for example, an 8 MHz 286 IBM AT personal computer takes about 0.5 seconds to index a diffraction pattern from Al_2O_3. The accuracy of both orientation determination and indexing depend to a large degree on the uncertainty in the position of the pattern source, i.e., the position of the stationary electron probe on the specimen. A least squares algorithm has been developed to calculate the source position. In addition, the video camera introduces up to 5% distortion into the pattern at the edges, so a method of calibrating the video camera has been developed.

Ceramic materials from which diffraction patterns have been obtained and grain misorientations measured include pure alumina, alumina-chromia solid solutions, $Ba_2YCu_3O_{6+x}$ in both bulk and thin film form, PZT and silicon nitride. In experiments on diffusion-induced grain boundary migration in the alumina-chromia system, it was observed that different grains in alumina that had been polished and exposed to chromia vapor were found to develop different surface morphologies and varying chromia concentrations depending on the surface orientation. Those grains further from (0001) orientation had higher chromia concentrations and rougher surfaces. In other experiments, alumina in which discontinuous grain growth had occurred was investigated to see whether the misorientations in colonies of anomalously large grains were "special", e.g., twin-related. No special relationships were found.

When single crystals of the high temperature superconductor, $Ba_2YCu_3O_{6+x}$, are grown, clusters consisting of several crystals with approximately aligned c-axes are often formed. As part of a study of the nature of the [001] tilt boundaries that form between the crystals in the cluster, the angle between the [001] axes either side of each boundary was measured. Typically the angle was 2° or less and the boundary was therefore almost pure tilt in nature, but it was found that the [001] axes of grains at the edge of a cluster were frequently more misaligned with their neighbors, in places up to 10°.

In all these studies the BKP method provided useful information on absolute and relative grain orientations which it would be either difficult or impossible to obtain in any other way. Future work will be directed towards further improvements in the accuracy of the technique and the application of the technique to areas of ceramics research where local texture information is of major interest such as thin films of electronic and structural ceramics and the production of ceramic whiskers by novel processing techniques.

Phase Equilibria and Crystal Chemistry in Ceramic Systems

R. S. Roth, C. J. Rawn and C. Lindsay[1]

[1]Postdoc

During 1991, NIST continued its tradition as a principal experimental investigator of phase equilibria in ceramic systems. Some of the systems studied included the binary and ternary systems that make up the edges and faces of the SrO:CaO:½Bi_2O_3:CuO tetrahedron where high T_c superconductivity has been reported.

During the past year the CaO:½Bi_2O_3 binary was studied in detail. The highlights include: 1) structure determinations were made on both the $Ca_2Bi_2O_5$ and $Ca_4Bi_6O_{13}$ phases using x-ray and neutron diffractometry (collaborations with J.B. Parise, SUNY and C.C. Torardi, E.I. duPont de Nemours); 2) a metastable phase $\approx Ca_6Bi_7O_{16.5}$ was formed at about 925°C on the CaO-rich side of $Ca_2Bi_2O_5$, but at about 885°C on the CaO-poor side; 3) melting relations have been determined in the region of 20-50 mol percent CaO; 4) powder x-ray diffraction clearly shows that specimens with a 1:6 ratio of CaO:½Bi_2O_3 quenched from 750°C are rhombohedral, but samples quenched from $\leq$735°C exhibit peak splitting and faint superstructure reflections; 5) evidence of a rhombohedrally distorted phase (α') quenched from the stable "fcc" region with a c/a ratio slightly smaller than the cubic value and a metastable lower-temperature phase (α'') quenched from below the "fcc" region with a c/a ratio considerably larger than the cubic value.

In the SrO:CaO:½Bi_2O_3 ternary system high and low temperature oxidized phases were studied in specimens with a 49.5:16.5:34.0 ratio. Single crystal x-ray diffraction precession photographs (a complete structure determination has been performed in collaboration with T. Siegrist of AT&T Bell Laboratories) indicate that the high temperature phase is monoclinic (space group Pc) and powder diffraction data yield least squared values of a=11.227(1), b=5.9062(5), c=20.045(2)Å, β=101.789(8). The more oxidized low temperature phase was

synthesized using high temperature phase material and holding the powder in an oxygen atmosphere at 620°C for 5 h. Upon removal visual inspection revealed that the powder changed from yellow in color to black. The x-ray powder diffraction pattern has been indexed on an orthorhombic cell (space group Pmmm) with least squared values of a=5.9979(3), b=5.8966(3), c=8.3907(4)Å. Differential thermal analysis (DTA) data also confirm the presence of a phase transformation. Thermal gravimetric analysis (TGA) measurements during oxidation and calculations based on completely reducing the high temperature phase concludes that the low temperature phase has the perovskite structural formula: $(Sr_{2.97}Ca_{0.03})(Ca_{0.96}Bi_{0.18}^{3+}Bi_{1.86}^{5+})O_{8.88}$.

Recent interest has branched out to systems containing ZnO. Preliminary experimental phase equilibria studies of optical amplifiers have included collaborations with AT&T Bell Laboratories by studying the $ZnO:GeO_2:½Cr_2O_3$ and $ZnO:SiO_2:½Cr_2O_3$ systems and microwave dielectrics with Trans-Tech by studying the $BaO:TiO_2:ZnO$ system.

Phase equilibria in other systems containing microwave dielectric materials have also received considerable study this year. Ceramics with high dielectric constants are useful for fabricating dielectric components used in compact microwave equipment such as hand-held radar units and cellular telephones. Other applications require close control ("tuning") of the dielectric constant, the resonant frequency, and/or the temperature coefficients of these properties. Such control is achieved by varying the chemical composition of the material. The electrical properties of a material are functions of the crystal structure of the material, which in turn is a function of the chemical composition of the material. It is possible that increasing the content of a particular chemical element might have a beneficial effect on the electrical property of interest, but when the content of that element exceeds a certain value, a different crystal structure forms whose electrical properties are not suitable to the desired application.

Oxide ceramics adopting perovskite-like crystal structures with certain transition-metal atoms (e.g., niobium, titanium, strontium, or zinc) in the octahedral sites are known to have electrical properties useful for microwave dielectric applications. Lanthanum titanate, $La_{2/3}TiO_3$, is one example of such a material; it is not stable in a perovskite-like structure unless some of the titanium atoms are replaced by atoms of another element such as aluminum. Lanthanum niobate, $La_{1/3}NbO_3$, is stable in a perovskite-like structure without replacement of the niobium atoms by atoms of another element, and given its crystal structure and chemistry, it would be expected to have electrical properties useful for microwave applications. If it were possible to vary the composition of a perovskite-structure ceramic continuously from $La_{1/3}NbO_3$ to $La_{2/3}TiO_3$ without changing the crystal structure, it might be possible to produce a class of dielectric ceramics with useful and easily controlled electrical properties.

Study of the phase relations in the system $La_{1/3}NbO_3$-$La_{2/3}TiO_3$ this year has shown that this system is neither a solid solution nor a simple combination of the two perovskite-like end-members. Lanthanum niobium titanate, $LaNbTiO_6$, occurs at compositions around 50 mol% $La_{1/3}NbO_3$: 50 mol % $La_{2/3}TiO_3$, and adopts either of two aeschynite-like crystal structures, one monoclinic and one orthorhombic. Neither the temperature-composition relations between these two phases nor their electrical properties are widely known; the former are currently under study and the latter will eventually be studied in detail. Study of the $La_{1/3}NbO_3$-$La_{2/3}TiO_3$ system also indicates that $La_{2/3}TiO_3$ is not stabilized by adding niobium as it is by adding aluminum, and that probably about 10 mol % $La_{2/3}TiO_3$ can be added to $La_{1/3}NbO_3$ without forming $LaNbTiO_6$ as a second phase. This suggests that the electrical properties of $La_{1/3}NbO_3$ can be tuned over a narrow range by addition of titanium. When $LaAlO_3$ is added to $La_{1/3}NbO_3$, a perovskite-like structure is stable only for $LaAlO_3$ contents less than about 5 mol %, although $LaAlO_3$ also adopts a perovskite-like structure. However, when $LaAlO_3$ is added to $La_{2/3}TiO_3$, perovskite-like structures are stable from about 3 to 100 mol % $LaAlO_3$.

Superconducting Ceramics: Crystal Chemistry and Melting Studies of the Ba-Y-Cu-O System

W. Wong-Ng, L. P. Cook and B. Paretzkin[1]

[1] Guest Scientist

Our previous studies of the Ba-R-Cu-O systems, where R=lanthanides and yttrium, showed two important factors, namely, the progressively decreasing size of the lanthanides, known as the lanthanide contraction, as well as the role which the stability of different oxidation states of these elements plays in governing compound formation. In the past year, in addition to continuing our efforts to systematically investigate the effect of the above two factors, we also initiated an effort to study the liquidus phase diagram of the Ba-Y-Cu-O system.

The melting relationships of phases in the yttrium-containing system at high temperature have not been studied extensively. In general, most published liquidus diagrams have been constructed with limited quantitative compositional data on liquids participating in eutectic or peritectic equilibria. Even with the published data, there are apparent conflicts concerning the location and size of primary phase fields of solids and the location of eutectic and perieutectic reaction points. Studies of melting in these systems have been complicated by experimental problems such as corrosion of containers, difficulty in quenching the liquid phase, difficulties in interpreting x-ray patterns of complex phase assemblages, atmospheric contamination, and the tendency of the liquid to creep out of experimental containers.

Since compositional data of the liquid is important for constructing a quantitative phase diagram, we have devised a procedure using a combination of experimental methods to circumvent some of these difficulties. This procedure includes: (1) calcination and materials handling in special furnace and dry box assemblages, (2) differential thermal analysis (DTA) / thermal gravimetric analysis (TGA) studies to obtain indication of thermal events, (3) annealing of samples with porous wick materials in order to capture the liquid formed, (4) fast quenching of samples in liquid nitrogen cooled environment for preserving the oxygen stoichiometry of material, (5) powder x-ray characterization of solid phases present, (6) scanning electron microscopy (SEM) studies and x-ray mapping to study the microstructure of the quenched materials, (7) quantitative SEM / energy dispersive x-ray (EDX) analysis of the composition of melts, and (8) hydrogen reduction to obtain the oxygen content.

Application of this procedure so far has included studies of the melting of the green phase, BaY_2CuO_5, and the high T_c superconductor phase, $Ba_2YCu_3O_{6+x}$(213). These results show that the peritectic reactions reported in literature concerning the melting of the green phase and the 213 phase were incorrect. For example, the green phase melts according to the equilibrium: $2BaY_2CuO_5 \rightleftarrows Y_2O_3 + BaY_2O_4$ + liquid, instead of reported Y_2O_3 and liquid. The 213 sample appeared to melt to green phase and two immiscible liquids; we are in the process of confirming this. These results have significant impact on the processing of high T_c superconductors. So far, the melt compositions of these samples have shown extremely small contents of yttrium (the green phase melt gives the atomic percentage of cations as: Ba 40.9%, Y 2.4% and Cu 56.7%). Oxidation-reduction also plays an important role in melting. For example, when the green phase melts at 1268°C, oxygen is lost, corresponding to a change in bulk CuO_x from $CuO_{1.0}$ to $CuO_{.48}$. Current work continues to investigate other peritectic and eutectic reactions in the system which will eventually lead to a quantitative liquidus diagram.

Single Crystal X-ray Diffraction Studies

W. Wong-Ng, R. S. Roth, C. Rawn, L. P. Cook, B. Paretzkin[1] and B. Burton[2]

[1]Guest Scientist
[2]Metallurgy Division

A single crystal x-ray diffractometer has been purchased and installed. This is a research facility which is available to x-ray crystallographers in the Ceramics, Reactor Radiation and Polymers Divisions to investigate crystal structures of materials.

Crystallographic structural characterization has been shown to be essential for understanding phase equilibrium. Up to now, the majority of investigated phases have been those relevant to the superconductor systems Ba-R-Cu-O and Sr-Bi-Ca-Cu-O. In the Ba-R-Cu-O system, we have grown and studied the crystals of the "brown phase," $BaNd_2CuO_5$, and the "green phase," $BaDy_2CuO_5$. Despite similar formulae, the two structures are totally different. The different coordination environment around the lanthanide atoms (NdO_8 and DyO_7) gives rise to their different structures. Again, the size of the lanthanide elements governs the crystallography. It was also interesting to observe that in the brown phase, the CuO_4 units, although planar, are isolated and are orthogonal to the neighboring CuO_4 groups. This isolation presumably precludes superconductivity, and the orthogonal arrangement suggests a possible ferromagnetic coupling interaction. Currently, a joint study is being conducted with L. Bennett and L. Swartzendruber of the Metallurgy Division to investigate the magnetic properties of this material and of the solid solutions $Ba(Nd,La)_2CuO_5$.

With regard to bismuthinate phase equilibria, two new crystal structures, $CaBi_2O_4$ and $SrBi_2O_4$, in the CaO-Bi_2O_3 and SrO-Bi_2O_3 systems have been investigated in order to compare the Bi coordination. The two structures are rather different. In the strontium case, thin Sr-Bi-O slabs are formed parallel to the ab-plane of the unit cell, which accounts for the weaker forces in the direction perpendicular to these planes and promotes the formation a thin, layer-like morphology. In the Ca case, the Ca-Bi-O network is three-dimensional. In both structures, Bi atoms are bonded to four oxygens, leaving a large open space to accommodate the lone-pair electrons.

OPTICAL MATERIALS

Al Feldman

The objectives of the Optical Materials Group are to provide data, measurement methods, standards and reference materials, concepts, evaluated data, and other technical information on the fundamental aspects of processing, structure, properties and performance of optical and optoelectronic materials for industry, government agencies, universities, and other scientific organizations. The program supports generic technologies in crystalline, glassy, and thin film inorganic optical materials in order to foster their safe, efficient and economical use. Research in the group addresses the science base underlying new advanced optical materials technologies together with associated measurements methodology. The effort of the Optical Materials Group has been directed into three principal areas: diamond film processing and characterization, metalorganic chemical vapor deposition (CVD) of ferroelectric oxides, and single-crystal high-temperature superconducting ceramics.

Significant Accomplishments

- Hot filament CVD is an important process for growing diamond films. Deposition rate and film morphology can be affected by the geometry of the filaments. Increasing the filament turn density in helical filaments and depositing with two filaments instead of a single filament resulted in an unexpected decline in film growth rate and resulted in film morphologies typical of single filament depositions conducted at lower methane concentrations. A possible explanation suggests that the dual, high turn-density filaments impede the flow of activated methane to the substrate.

- Active electronics made of semiconducting diamond will require doped diamond films. Diamond films doped with boron have been grown in a hot filament CVD reactor, where the boron source was a solution of B_2O_3 in ethanol. A correlation between the B_2O_3 concentration in the ethanol and the boron doping level in the films was established.

- Two of the most commonly observed luminescence emission bands of CVD diamond occur in the red and blue-violet regions of the visible spectrum. Spectrally resolved cathodoluminescence imaging of isolated diamond particles has shown that, for some choices of deposition conditions, the red emission band is associated with {111} crystal growth sectors, and the blue-violet emission band is associated with {100} sectors. It may thus be possible to control the color of the luminescence by controlling the crystal growth habit. This is of interest for potential applications of CVD diamond in full-color luminescent displays.

- The optical transmittance and reflectance spectra of thin (~ 1 μm) CVD diamond windows were measured at photon energies from 0.5 eV in the infrared to 6.5 eV in the ultraviolet. The refractive indices, absorption coefficients, and surface roughnesses of these windows were calculated from the experimental data. The most defective windows (the least like single-crystal diamond) gave rise to significant optical absorption above 1 eV, but were relatively free of both bulk absorption and surface scatter below 1 eV. Diamond films with these properties might be useful as infrared-transmissive optical coatings if the problem of maintaining uniform film thickness over a large area could be solved.

- The performance of CVD diamond films will require control of defect structure. The twin defect structure of microwave plasma CVD diamond films has been examined by high resolution electron microscopy and the types of twins and twin interactions were observed with unprecedented resolution and detail. Based on these observations, a model for the growth of diamond CVD has been proposed which should prove useful in devising means to minimize the number of defects during film growth.

- Construction of a metalorganic chemical vapor deposition system for the growth of ferroelectric oxide thin films has been completed. The system will be used to fabricate films as part of a new program on ferroelectric oxide films for photonics.

- Flux pinning by twin boundaries in $YBa_2Cu_3O_{6+x}$ single crystals was found to be strongly dependent upon temperature and the orientation and magnitude of the applied magnetic field. Twin boundaries enhance flux pinning at 60-85 K for low fields applied parallel to the c-axis; under these field conditions at 77 K, twinned crystals have critical current densities approximately one order of magnitude greater than comparable twin-free crystals. In contrast, twin boundaries have no measurable effect on flux pinning at any temperature for applied fields perpendicular to the c-axis.

- Mechanical measurements on twinned and detwinned $YBa_2Cu_3O_{6+x}$ single crystals have shown that twin boundaries increase fracture toughness by about 25%. Fracture toughness was found to be anisotropic with the average value for cracks perpendicular to the basal plane being twice that of cracks parallel to the basal plane, indicating easier cleavage along basal planes. In addition, a small anisotropy in fracture toughness between the a and b directions was measured in detwinned crystals.

- Electrical transport measurements across individual grain boundaries in bulk-scale $YBa_2Cu_3O_{6+x}$ bicrystals at 77 K have revealed a general trend for a transition from flux pinning to Josephson junction to resistive behavior with increasing misorientation angle. However, some high-angle grain boundaries displayed flux pinning character and thus transmitted significant supercurrents even in high magnetic fields. Subsequent transmission electron microscopy studies on several electromagnetically-characterized boundaries revealed a thin second phase layer at resistive boundaries which was absent from Josephson junction boundaries. Thus, the fine-scale microstructural features of a grain boundary are critical in determining the transport mechanism across the boundary.

Chemical Vapor Deposition of Diamond

E. N. Farabaugh

Effect of filament geometry on growth rate and morphology: Hot filament chemical vapor deposition (HFCVD) is a important method for growing diamond films. In order to increase the deposition area in HFCVD reactors, one must understand how the filament geometry affects the growth rate and morphology of the deposited films. Our HFCVD reactor utilizes tungsten filaments in the form of helical coils 2.5 cm long suspended approximately 5 mm above a substrate heated by a substrate holder. We can operate our system either with a single filament or with two filaments side-by side. Gases used in the diamond deposition are methane and hydrogen.

In this most recent study, we have examined how three deposition parameters affected the morphologies and growth rates of the films produced. The parameters varied were: the turn density in the filaments -- 2, 4 or 6 turns/cm (5, 10, or 15 total turns, respectively); the number of filaments used -- 1 or 2; and the fraction of methane in the feed gas -- 0.25%, 0.50%, 0.75% or 1.0%. A minimum of 24 depositions was carried out. Each of the films was examined in a scanning electron microscope for the purpose of determining the surface morphology. The substrates were weighed before and after deposition in order to calculate a mean diamond film thickness and a mean growth rate.

For a given filament geometry, increasing the methane fraction in the feed gas yielded higher deposition rates, a result consistent with prior work. Furthermore, the areal coverage in a dual filament system was twice that of the single filament system. In the single filament system, the growth rate at a give gas mixture varied approximately linearly with the turn density; however, in the dual filament system, the growth rate was approximately independent of the turn density or even showed a decrease with increasing turn density, a result that was unexpectedly low. Furthermore, the morphologies of films grown with dual filaments having 4 and 6 turn/cm densities, displayed morphologies typical of films produced at lower methane fractions with single filaments. This effect cannot be simply explained or modeled because of complex flow patterns, temperature gradients, and numerous reaction products. One possible explanation suggests that the dual, high turn-density filaments impede the flow of activated methane to the substrate, resulting in growth rates and morphologies typical of growths with lower methane fractions.

Doped diamond films: Diamond films doped with boron have been deposited in a HFCVD reactor. A solution of boron trioxide in ethanol was the source of both carbon for the diamond growth and boron for the doping. Argon, which served as a carrier gas, was bubbled through the B_2O_3:ethanol solution at a controlled rate, typically 8 cm^3/s, and fed into a gas mixer. Hydrogen flowing at a rate of 100 cm^3/s was mixed with the carrier gas in the mixer. Diamond films were produce under typical conditions: substrate temperature --800 °C; filament temperature --1800 °C; chamber pressure --5.23 x 10^3 Pa (40 torr).

Secondary Ion Mass Spectroscopy (SIMS) was used to measure the concentration of boron in the diamond films. A correlation between the B_2O_3 concentration in the ethanol and the boron doping level in the films was established. It was noted that doped films grew at a somewhat higher growth rate (0.5μm/hr) than non-doped films grown under similar conditions.

Optical and Optoelectronic Characterization of CVD Diamond Films

L. H. Robins, E. N. Farabaugh and A. Feldman

Synthetic diamond is potentially a superior optical material for a number of applications because of its wide transparency range, from deep-ultraviolet to far-infrared, and because of its great mechanical strength, high thermal conductivity, and chemical inertness, which lead to good survivability in severe environments. Diamond also shows promise for optoelectronic applications that would be based on the visible light emission (luminescence) from defects, such as a full-color solid-state displays. Chemical vapor deposition (CVD) techniques developed in the last decade have enabled the growth of diamond particles and films at low pressure. In our research, we utilize several types of optical spectroscopy to investigate the relationships between the optical properties of CVD diamond specimens and the deposition conditions for these specimens. The goal of this research is to optimize the properties of CVD diamond for selected optical or optoelectronic applications. A major theme of this work has been the influence of imperfections in the diamond crystal structure, such as point defects, extended lattice defects, chemical impurities, and non-diamond phases, on the optical properties.

Cathodoluminescence (CL) imaging and spectroscopy in a scanning electron microscope (SEM) is one of the most informative methods developed at NIST for characterizing CVD diamond films. CL spectroscopy is a sensitive probe for identifying many types of defects and impurities. When these experiments are conducted in an SEM, the imaging capability of the SEM allows us to map the spatial distribution of the luminescence on a sub-micrometer scale. Features in the CL images can then be matched to features in the standard SEM images allowing us to correlate the position of luminescent defects with microstructural features.

We have used CL imaging and spectroscopy to study relatively large ($\sim$30 μm), well-faceted diamond crystallites. CL spectra of these crystallites revealed two dominant emission bands, a red band due to a nitrogen-vacancy complex (one or more atomic vacancies bound to a nitrogen atom) and a blue-violet band due to a dislocation-related defect. The results show that in particles grown at low temperatures ($\sim$600 °C), the nitrogen-vacancy emission is associated with {111} growth sectors, and the dislocation-related emission is associated sometimes with {100} and sometimes with {111} sectors. Spectrally resolved CL images of the red emission and of the blue-violet emission from a selected diamond particle are displayed in Figure 21. The most intense emission in the red region ($\sim$600 nm) arises from the triangular {111} facets while the most intense emission from the blue-violet region ($\sim$450 nm) arises from the large {100} facet. The secondary-electron emission image of the same diamond particle is also shown in the figure. The CL images appear blurred, compared to the secondary-electron image, because the CL originates from depths as far as 2 μm below the particle surface, where there is significant spreading of the incident electron beam. In particles grown at an intermediate temperature ($\sim$750 °C), the overall luminescence intensity is lower and both emission bands are associated with {100} sectors. We have interpreted these results with a model of competing recombination between distinct types of luminescence centers and also between luminescence and non-radiative recombination centers.

CL imaging of polycrystalline diamond films grown on silicon wafers shows that a near-infrared emission band due to a silicon impurity center is most intense in a thin ($\sim$2 μm) region of the film adjacent to the substrate. This observation implies that silicon atoms are incorporated in the diamond film a short distance from the substrate. These results add to our knowledge of how deposition conditions affect the spatial and spectral distributions of the luminescence of CVD diamond specimens. Good control of the spectral distribution of the luminescence (i.e., for visible wavelengths, the color) is needed if CVD diamond is to be used in full-color luminescent displays.

Wear-resistant transparent coatings for use at visible and near infrared wavelengths are possible optical applications of thin diamond films. To determine the suitability of a given film for such applications, it is necessary to study the spectral dependence of the optical properties, including transmittance, reflectance, absorptance, and optical scatter. We had previously demonstrated a technique for producing thin (0.3-2 μm) transparent diamond windows. First, a substrate (e.g., a silicon wafer) is polished with diamond powder to produce a high density of diamond nucleation sites. Next, a thin, dense polycrystalline diamond film is grown on the substrate. Finally, a portion of the substrate is removed by acid etching to provide a diamond window. We have developed a method for calculating the refractive index and absorption coefficient of such windows as a function of wavelength, and for distinguishing between transmission losses due to bulk absorption and transmission losses due to surface scatter. The method requires the measurement of the transmittance spectrum of a specimen and two reflectance spectra, one from each surface of the window.

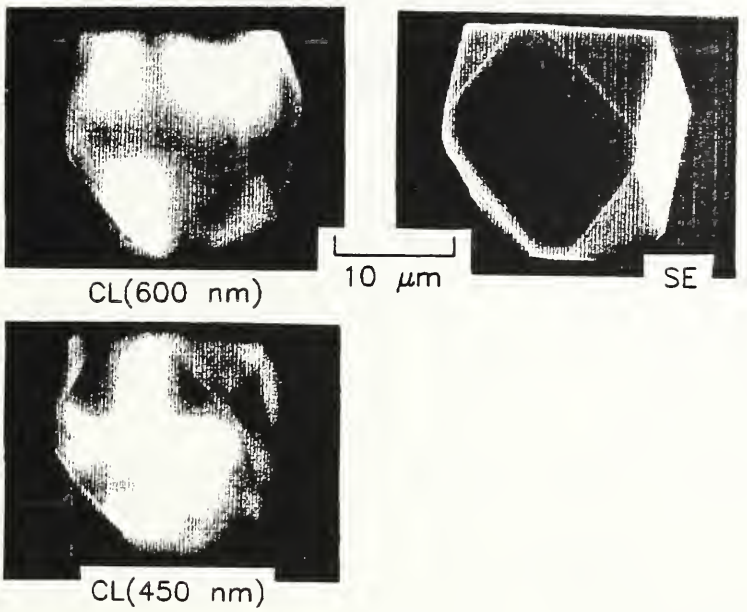

Figure 21. SEM images of a diamond particle grown by hot-filament CVD at low deposition temperature (nominally 600° C). Upper left: red CL image, taken with a 600 nm optical bandpass filter. Lower left: blue-violet CL image, taken with taken with a 450 nm optical bandpass filter. Upper right: secondary-electron (SE) image.

We have measured the optical properties of several CVD diamond windows that we had prepared by microwave plasma CVD and have obtained the following results. The optical scatter, which is known to be exponentially dependent on the mean squared surface roughness, increases with increasing film thickness and decreases with increasing methane fraction used in the film deposition. The wavelength-dependent refractive indices of the windows are approximately equal to or slightly less than the refractive index of single-crystal gem diamond. The absorption coefficients of the windows increase monotonically with increasing photon energy, and are larger than the absorption coefficient of a defect-free single crystal in the range 1 to 6.5 electron-volts (eV). The film absorption spectra contain two components, a gradual rise from 1 to 5.5 eV, and a noticeably steeper increase above 5.5 eV. The first component appears similar to the absorption spectra of "diamondlike" amorphous carbon or hydrocarbon films. The second component, the steep increase above the indirect bandgap of diamond (5.5 eV), has an exponential shape characteristic of highly defective crystalline materials. The absorption spectra of two diamond windows are plotted in Figure 22. At each wavelength, the specimen prepared from a 2.0% methane/hydrogen feed gas mixture showed a higher absorption coefficient that the specimen prepared from a 0.5% methane/hydrogen feed gas mixture. The absorption spectrum of a single-crystal diamond with a low defect and impurity content, obtained from previously published results, is also plotted in Figure 22 for comparison.

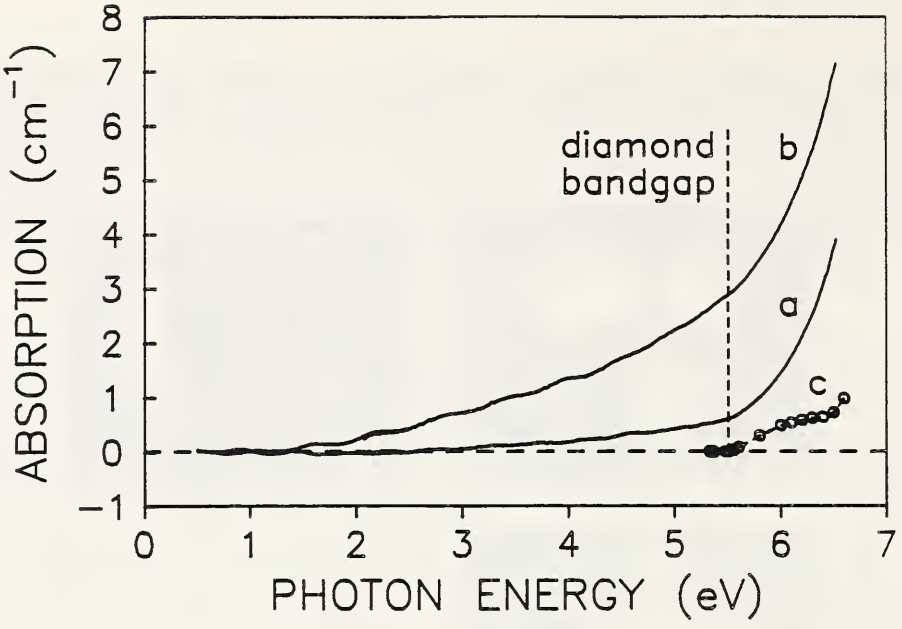

Figure 22. Calculated absorption spectra of two CVD diamond windows, grown by microwave-plasma-assisted CVD from methane-hydrogen gas mixtures: (a) 0.5% methane; (b) 2.0% methane. (c) Absorption spectrum of a high-quality single-crystal diamond. The indirect bandgap of diamond at 5.5 eV is indicated by a vertical dashed line. The windows with the smoothest surfaces show little surface scatter or bulk absorption at photon energies below 1 eV, and should thus perform well as infrared optical coatings.

High Resolution Electron Microscopy of Diamond Film Growth Defects and Their Interactions

D. Shechtman,[1] J. L. Hutchison,[2] E. N. Farabaugh, L. H. Robins and A. Feldman

[1]Technion (Israel), Guest Scientist at NIST and at the Johns Hopkins University
[2]Oxford University (UK)

High resolution electron microscopy of plasma-assisted chemical vapor deposition (CVD) diamond films was performed. One film studied was fine grained with a grain size of about 0.1 micrometer. Several features of the microstructure were studied and their importance to the understanding of the diamond film growth was evaluated. The variety of twins boundaries which were studied and analyzed include four types, some of which have never been observed or have never been studied in diamond before. The twin boundaries are denoted by the nomenclature: $\Sigma=3$, $\Sigma=9$, $\Sigma=27$ and $\Sigma=81$.

Figure 23 shows the twinning structure of a CVD diamond film. The twinning structure, which are more frequently found at the periphery of the crystal, consists of coherent twin boundaries and misfit twin boundaries (twin boundaries of type $\Sigma=9$ and higher order, which are not coherently matched). The local growth direction is indicated by the hollow arrows. New planes tend to nucleate and grow on reentrant planes (recessed or valley areas) on the crystal growth surface. Local growth proceeds from the apex of the "V"s, shown in the figure, along the direction shown by the hollow arrows.

Because a quintuplet twin point maximizes the number of reentrant surfaces, it becomes a probable nucleation point for new planes. When tracing the growth in a diamond crystallite, one often finds a quintuplet twin point to be the growth origin. Figure 24 shows such a quintuplet twin point. Around this point are 4 coherent twin boundaries of type $\Sigma=3$ and one misfit twin boundary of type $\Sigma=81$. The misfit angle is 7.5°, as indicated in the inset.

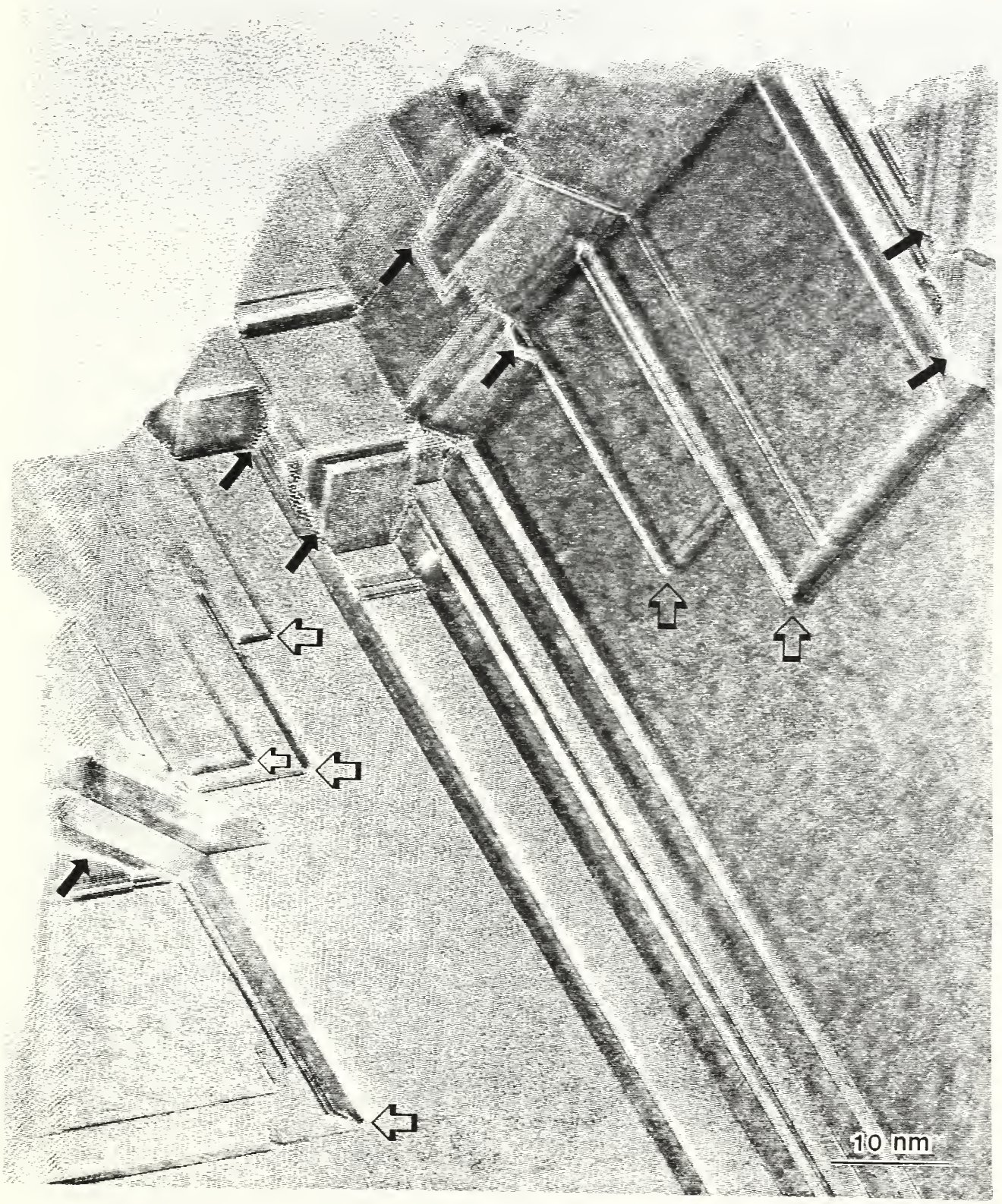

Figure 23. Twinning structure of a CVD diamond crystallite. Misfit boundaries, indicated by all of the arrows in the figure, are more frequently found in the periphery of a crystallite. The hollow arrows indicate the local growth direction.

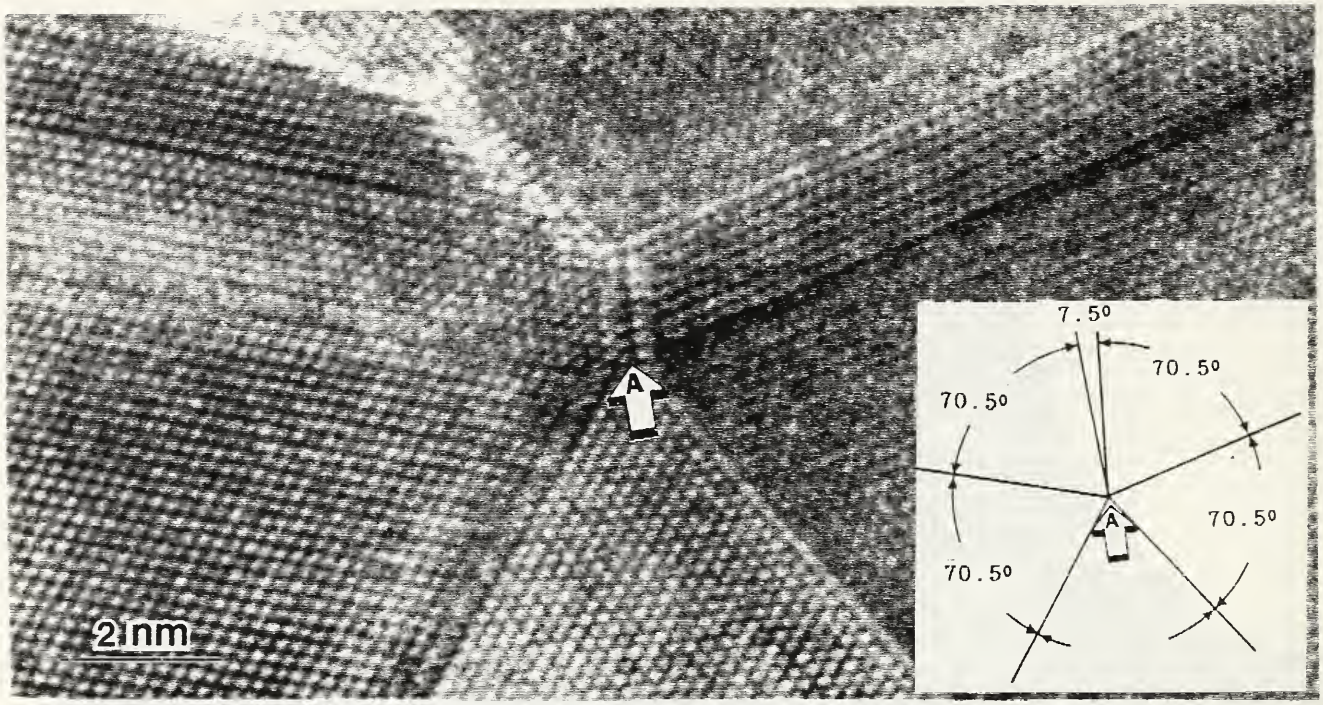

Figure 24. High resolution electron micrograph of a CVD diamond crystallite. A twin quintuplet is indicated by the hollow arrow, A. The arrow points to the misfit boundary, where the misfit angle is 7.5° as indicated in the inset.

General conclusions to be drawn from these observations include:

1. Twinning density rises with increasing distance from the center of the crystal.

2. The twins play an important role in the rapid growth of this type of film. The reentrant angle between intersecting twins serves as a nucleation site for the growth of new {111} planes.

3. A twin quintuplet has five reentrant angles and thus serves as a preferred nucleation site for new planes. An icosahedral crystallite contains 12 such quintuplet twins and thus has high probability for rapid growth.

4. Misfit boundaries, being the locus of intersection points of the growing planes on two adjacent twins, can serve as an indicator for the local crystal growth direction. The central nucleation site for the growing planes can be traced back in many cases to a quintuplet twin point.

Ferroelectric Oxide Thin Films for Photonics

D. L. Kaiser

This program addresses key scientific issues vital to the development of ferroelectric oxide thin films for photonic devices in future telecommunications, optical computing and image processing systems through a detailed study of the complex relationships between thin film deposition, microstructural features and electro-optical properties. The advancement of ferroelectric oxides for photonics is limited by two factors: 1) a practical thin film deposition

process for the mass production of optical-quality films; and 2) characterization of the nature of defect structures in the material and their effects on the electrical and electro-optical properties. In Phase I of the program, thin films will be deposited by metalorganic chemical vapor deposition (MOCVD). This technique is presently used for the commercial manufacture of GaAs-based epitaxial films for electronics and the fabrication of high quality superconducting oxide films. $BaTiO_3$ will be the first deposition material. Phase II of the program will involve detailed characterization of the films by a variety of chemical, structural, electrical, optical and electro-optical techniques to relate defect structures to key properties of interest to device applications. The final phase of the program will be a collaborative effort with the Electromagnetic Technology Division (Boulder) to fabricate and test devices from high-quality films.

In FY-1991, the construction of the MOCVD system was completed and operational testing and modifications were begun. Phase I efforts will commence in FY-1992 under funding of a NIST Competence Program award.

Superconducting $YBa_2Cu_3O_{6+x}$ Crystals

Detwinned and Twinned Single Crystals

D. L. Kaiser, F. W. Gayle[1], L. J. Swartzendruber[1], A. Roitburd[2], L. H. Bennett[1], J. Bohandy[3], B. F. Kim[3], K. Moorjani[3] and F. J. Adrian[3]

[1] Metallurgy Division
[2] University of Maryland
[3] The Johns Hopkins Applied Physics Laboratory

An understanding of the role of twin boundaries in superconducting properties of $YBa_2Cu_3O_{6+x}$ is essential to the technological advancement of this material for both electronic and high-field applications. The development of a thermomechanical process for detwinning $YBa_2Cu_3O_{6+x}$ single crystals in FY-1989 has presented opportunities for critical measurements to explore this issue. In this program, the effect of twin boundaries on superconducting properties of single crystals was studied via magnetometry. Flux pinning by twin boundaries was found to be strongly dependent upon temperature and the magnitude and orientation of the applied magnetic field with respect to the crystallographic orientation. Twin boundaries enhance flux pinning at 60-85 K for low fields applied parallel to the c-axis; under these field conditions at 77 K, twinned crystals have critical current densities of $\approx$ 7400 A/cm^2, approximately one order of magnitude greater than comparable twin-free crystals. In contrast, for applied magnetic fields (H) perpendicular to the c-axis, no effect of twin boundaries on flux pinning was found at any temperature. Magnetically modulated microwave absorption (MAMMA) measurements revealed that twin boundaries do not affect the transition temperature (T_c) or width of the superconducting transition. An anisotropy in dT_c/dH of 10-15% was observed in the a-b plane of detwinned crystals. MAMMA measurements on a crystal containing small amounts of Na, Mg, Al, Ca and Sr revealed a broader superconducting transition at a lower temperature compared to high-purity crystals, and a secondary transition due most likely to the segregation of the impurities at the twin boundaries.

Bicrystals

D. L. Kaiser, S. E. Babcock[1], X. Y. Cai[1] and D. C. Larbalestier[1]

[1] University of Wisconsin

The role of grain boundaries in electrical transport in polycrystalline samples of the high temperature superconductor $YBa_2Cu_3O_{6+x}$ (YBCO) is not well defined, although an understanding of this role is a key element to the application of these materials. In this program, electrical transport across grain boundaries in bulk-scale multi-crystals of known misorientation at 77 K has been measured to deduce the nature of the coupling across the boundaries. For [001] tilt boundaries, there was a general tendency for transport to change from flux pinning to Josephson junction to resistive character with increasing misorientation angle between the two crystals. However, some high angle (> 10° misorientation) grain boundaries exhibited flux pinning character, i.e., transmitted significant supercurrents even in high (up to 7 Tesla) magnetic fields. High resolution transmission electron microscopy studies were performed on the electromagnetically-characterized bicrystals to explore possible correlations between microstructural features and transport behavior. A 2.5 nm thick layer of second phase was observed in a resistive boundary whereas no such phase was detected at a Josephson junction boundary. These results suggest strongly that local-scale microstructural features of the boundary control the mechanism of transport across the boundary.

MATERIALS MICROSTRUCTURE CHARACTERIZATION

Gabrielle Long

Microstructure characterization is the fundamental link in the processing/structure/properties chain. Indeed, it can be said to supply the key element in providing the possibility of understanding the central relationships that exist between fabrication processes and materials properties.

Scientists in the Materials Microstructure Characterization group have constructed and currently maintain two beam ports on the National Institute of Standards and Technology /Materials Science and Engineering Laboratory beamline at the National Synchrotron Light Source. These experimental stations support small-angle x-ray scattering, x-ray topography and x-ray absorption spectroscopy measurements of material microstructure. The group also has an active program on in situ neutron scattering studies of microstructure evolution during ceramic sintering and in situ neutron reflectometry. Finally, there is a state-of-the-art program in ultraviolet photoemission and x-ray standing wave measurement on semiconductor surfaces and interfaces.

Significant Accomplishments

- Neutron scattering measurements of the evolution of the porous phase during the sintering of glassy silica and polycrystalline alumina were used to characterize sintering mechanisms. It was demonstrated that viscous flow and surface and volume diffusion lead to very different microstructure evolution signatures in terms of the average pore size as a function of density. These results yield a direct measure of the microstructure, which in turn drives the sintering.

- X-ray scattering measurements of the porous phase evolution during final stage sintering of alumina has been studied as a function of doping with sintering aid. The results indicate that, independent of the presence or absence of sintering aid, the pore-size distribution becomes broader as the material densifies, although to a lesser degree when MgO is present. Further, it was proven that the median pore size increases monotonically with increasing density, contrary to theoretical predictions.

- Anomalous small-angle x-ray scattering measurements have been carried out successfully for the first time on a material of technological importance. The size distribution and volume fraction of $Cr_{23}C_6$ precipitates in a reactor-grade material have been isolated from the distribution of all other precipitates. This enabled an analysis of the coarsening of these particular carbides as a function of isothermal aging temperature, in the presence of other microstructure populations.

- A high-resolution small-angle x-ray scattering diffractometer was commissioned at the National Synchrotron Light Source. This instrument, which is located on the NIST/MSEL beamport X23A3, is currently being used to measure ceramic microstructure in the previously inaccessible size range up to 1 μm.

- Artificial (man-made) diamonds have been examined by means of x-ray diffraction topography. The results elucidate the relationships that exist between the growth conditions, the perfection of the seed, isotopic purity and the quality of the product material.

- Energy dispersive x-ray diffraction was used to measure the thermally-induced residual strain in a SiC reinforced-TiAlNb matrix composite material. The radial and tangential components of the strain have been measured with a spatial resolution of better than 100 μm and compared to model calculations. These results have led to an improvement in the finite element calculations of in-service strain expected from components manufactured from this material.

- Si_3N_4 single-grain images have been achieved using monochromatic synchrotron radiation topography. This new method includes an analysis technique which permits the direct measurement of residual strain in a powder compact.

- Diffraction anomalous fine structure (DAFS) has been demonstrated with copper crystals and with $In_xGa_{1-x}As$ films. This new technique will enable the study of buried layers containing the same atomic species as surface layers in electronic devices.

- The x-ray standing wave (XRSW) method has been extended to the back-diffraction geometry for the purpose of studying clean semiconductor surfaces and metal-semiconductor interfaces. This is the first time that XRSW has been applied to real systems. It was proven that Sb completely passivates the surface of InP(110).

- The superior performance of mercuric iodide gamma ray detectors grown in space has been shown to be closely associated with a dramatic reduction in the occurrence of impurity precipitates, which apparently act as electron traps. This observation has been made in the diffraction images of a space-grown crystal, a second crystal grown on the ground from identical material, and a third crystal grown on the ground from specially purified material. As a result, the growth in space of higher purity mercuric iodide now acquires particular interest in the improvement of these detectors.

- Formation of a second phase in Bridgman-grown lead tin telluride crystal has been found to be suppressed by growth in space. This difference has been observed in high resolution diffraction images of a crystal grown in space and another grown from identical material on the ground. The growth of single phase material now being planned as a result of these experiments is expected to lead to important insight on the effects of microgravity on the growth of systems that are thermosolutally unstable in full gravitational fields.

- The choice between within-grain lattice regularity and new grain formation in cadmium zinc telluride has been shown to be strongly affected by growth protocols relevant to future space shuttle flights. As a result, it appears likely that cadmium telluride growth protocols for space flights now scheduled may be substantially modified. Future experiments should thus prove far more successful than would otherwise have been the case.

- Residual (110) interfaces in a high quality poled single crystal of barium titanate appear in high resolution diffraction images to delineate the boundaries of the 90° domains that had been removed by the poling. These images show that the interfaces consist of an atomic phase shift in the direction of the poling. This is the first time that such interfaces have been observed directly in barium titanate. This is also the first observation of the precise direction of such a phase shift, detectable only with high resolution diffraction imaging, in any material. The presence of these interfaces explains why domains in subsequent depoling of perovskite crystals tend to recur at the same locations that delineated domains before initial poling.

Small-Angle Scattering Measurement of the Densification of Glassy Silica and Polycrystalline Alumina

G. G. Long, S. Krueger[1], R. A. Gerhardt[2] and R. A. Page[3]

[1]Reactor Radiation Division
[2]Georgia Technological Institute
[3]Southwest Research Institute

The sintering behavior and the properties of ceramics depend on their internal structure. Until now, there have been very few methods for the characterization of ceramic microstructure that are truly convincing. One such method is electron microscopy, which can be used to measure statistically significant samples. However, three-dimensional stereology of ceramics can be very time consuming and labor intensive. Against this backdrop, it was of interest to develop techniques that are both practical and theoretically sound that could be used for the statistically significant characterization of ceramic microstructure.

This suggested a small-angle scattering (SAS) method which, before this research began, was very rare in ceramics research. The reason for this is that traditional SAS experiments measure microstructure in the 1 to 100 nm size range, below the size range of traditional interest in ceramics. Therefore, we brought to practical use the multiple small-angle neutron scattering (MSANS) method which can be used to study microstructures involving sizes up to 10 μm. The formalism for MSANS was developed at NIST in the late 1980's by Berk and Hardman-Rhyne. Starting with their formalism, we applied it to such questions as: what is the role of the green-body density, and what is the effect of MgO additive on the sintering of alumina?

Current research has focused on the microstructure evolution of glassy silica and polycrystalline alumina during sintering. It was found that, where viscous flow mechanisms are operative, i.e., for the silica, the smallest pores closed first and the largest pores coarsened well into the intermediate stage. It was found, quite surprisingly, that even late in the final-stage sintering of silica (where the density had reached 95% of theoretical) the porosity was open with a collapsed ribbon-like morphology. Where diffusion mechanisms are operative, i.e., for the alumina, the diameter of the open-channel porosity was constant throughout intermediate-stage sintering, and then there was significant coarsening of the isolated pores during final-stage sintering. The pore size results for both systems are shown in Figure 25. Perhaps most surprising of all, when the microstructure evolution was examined from a topological point of view, the major differences that were observed between systems evolving by viscous flow or evolving by diffusion mechanisms disappeared and the systems were found to be topologically equivalent (Figure 26). This result supports a theory of Rhines and DeHoff which had been developed earlier and which until now has not received the attention it may deserve.

High-Resolution Small-Angle X-ray Scattering by Ceramic Materials

G. G. Long, P. R. Jemian[1], J. R. Weertman[2] and D. R. Black

[1]Argonne National Laboratory
[2]Northwestern University

A high-resolution small-angle x-ray scattering instrument, capable of measuring material microstructure in the 3 nm to 1 μm size range, was designed, constructed and commissioned on the X23A3 beamline at the National Synchrotron Light Source. This new instrument was used to examine the effect of starting chemistry on microporous silica precursor bodies, and was used to follow the evolution of the pore-size distribution in the final-stage sintering of alumina.

The porous silica samples were prepared from mixtures containing 10 to 30 wt % colloidal silica sol and 90 to 70 wt % potassium silicate. Particle-size distributions were derived using a maximum-entropy technique. It was found that the lower the fraction of colloidal silica, the larger the median size of the aggregates and the broader their size distribution (Figure 27).

The evolution of the pore-size distribution in the final-stage sintering of alumina was studied in material that was 97 to more than 99.5% of theoretical density. It was learned that, with or without sintering aid, the size of the median pores coarsens and the pore-size distribution broadens as late-stage sintering proceeds (Figure 28). The median pore-size, contrary to theoretical predictions, was never observed to decrease as densification proceeded. The size of the remaining pores as well as the width of the pore-size distribution were smaller in the case where MgO had been added.

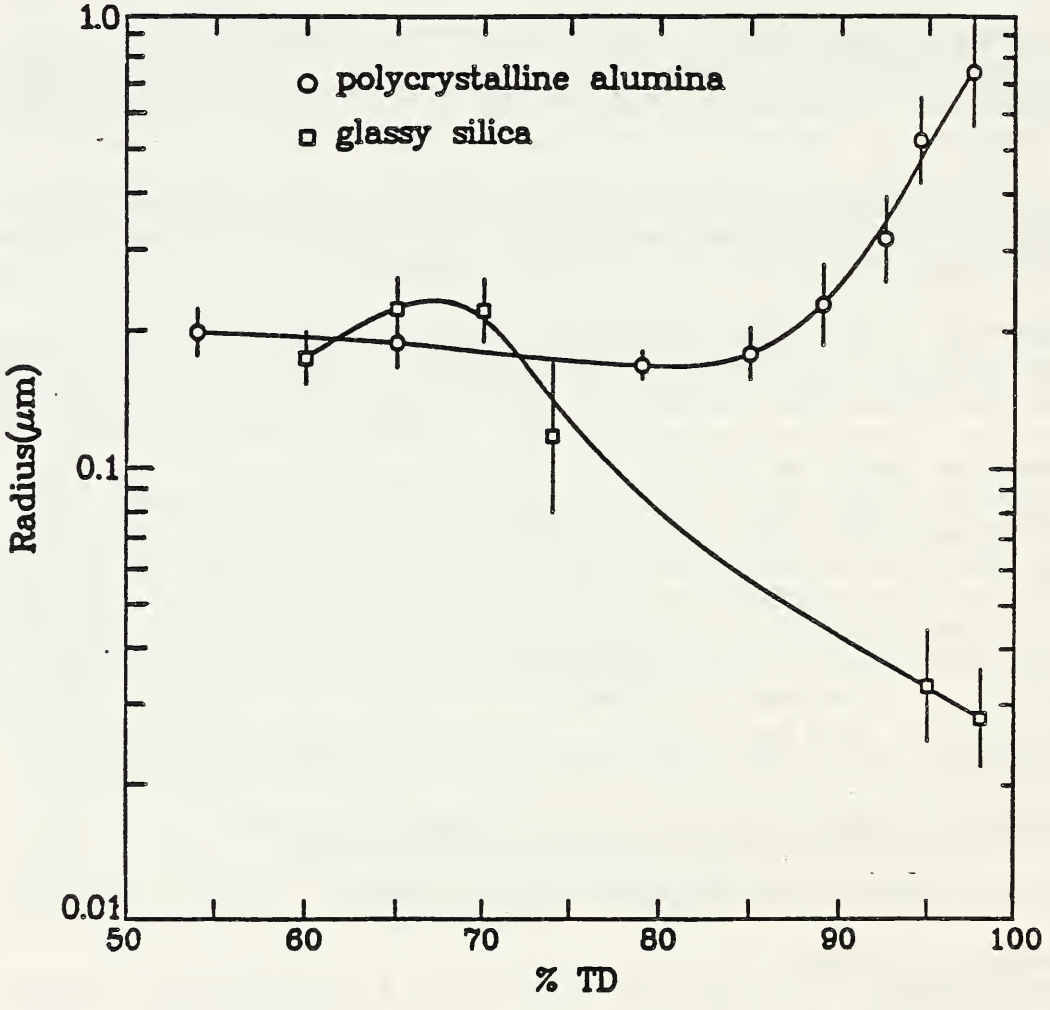

Figure 25. Median pore radius during sintering of alumina and silica as a function of the percent of theoretical density.

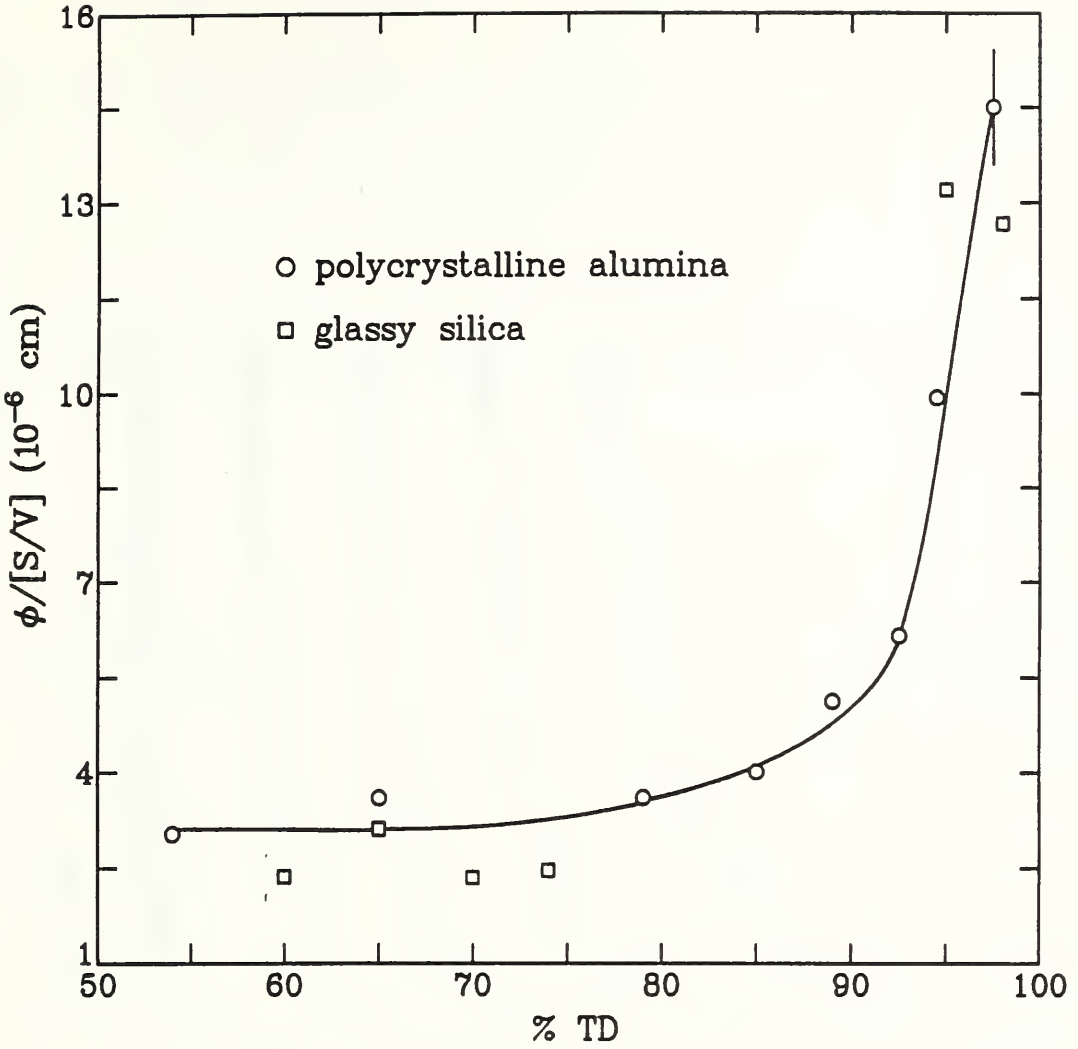

Figure 26. Pore volume fraction, ϕ, normalized to the pore surface area per unit volume, S/V, as a function of densification of alumina and silica.

Microstructure of Artificial Diamond

D. R. Black and H. E. Burdette

The availability of high-quality diamond will impact several commercial areas. These crystals will provide consistency in the field of precision diamond machining. High-quality defect-free single crystals will be required for high-temperature diamond electronic devices. The improved thermal properties of defect-free material will offer an opportunity to produce much better windows for high power lasers.

High-resolution x-ray diffraction topography is currently being used to examine the defect microstructure of natural and man-made diamonds. Until very recently, the highest quality diamonds available were natural type IIa (nitrogen concentration <50 ppm) crystals. In current technology, natural diamonds are generally used as substrates for homoepitaxial growth of thin diamond films by chemical vapor deposition. X-ray topography of such structures has demonstrated that type Ia diamond (with nitrogen concentration of $\sim 2 \times 10^3$ ppm in platelets) is nevertheless superior to type IIa as a substrate. The topographs of these type Ia diamonds are more crisp with much less strain.

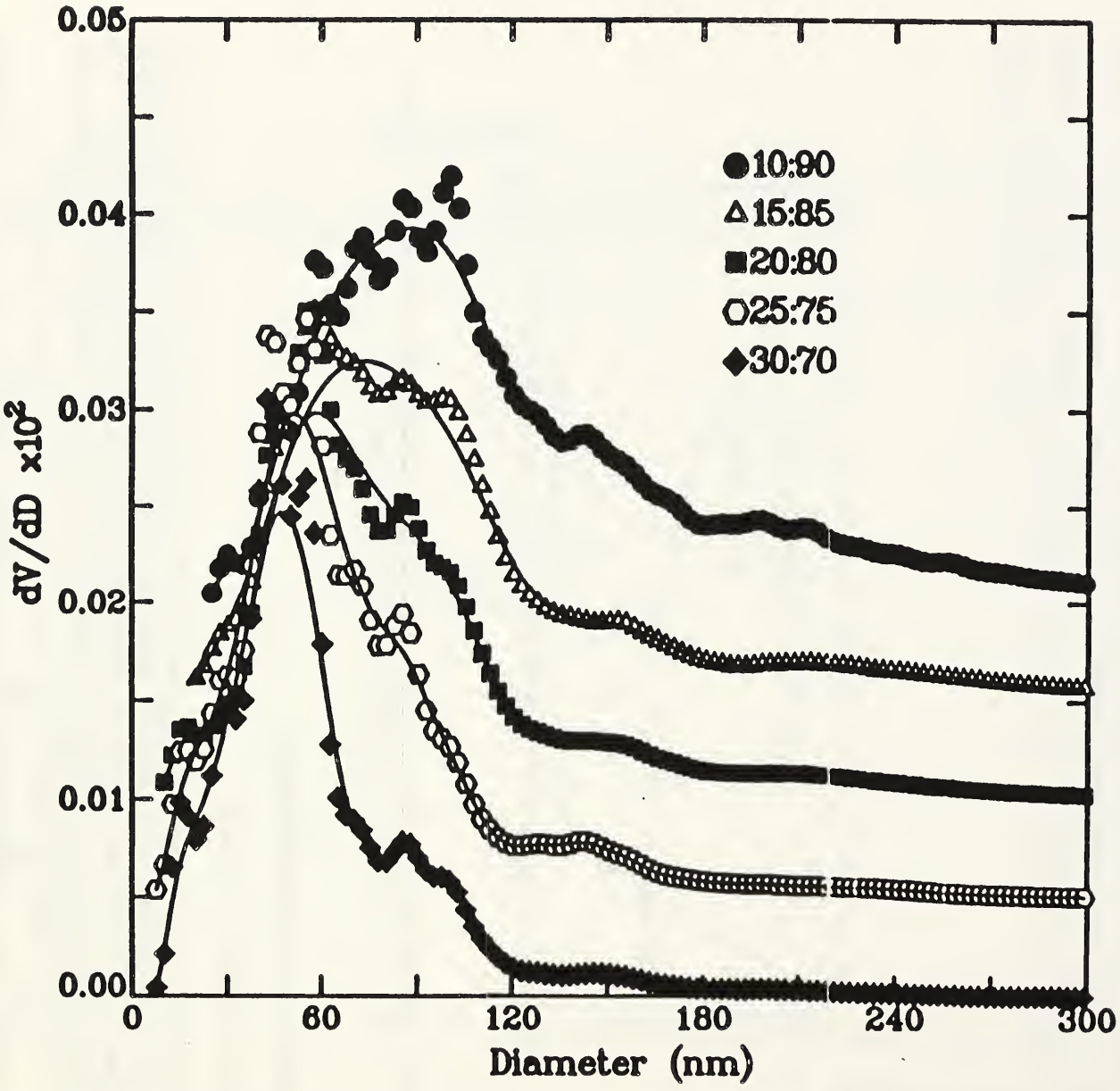

Figure 27. Volume distribution of particles and aggregates in microporous silica. Five results are shown, offset from each other for clarity. Each result is for a different colloid:silicate fraction, as indicated.

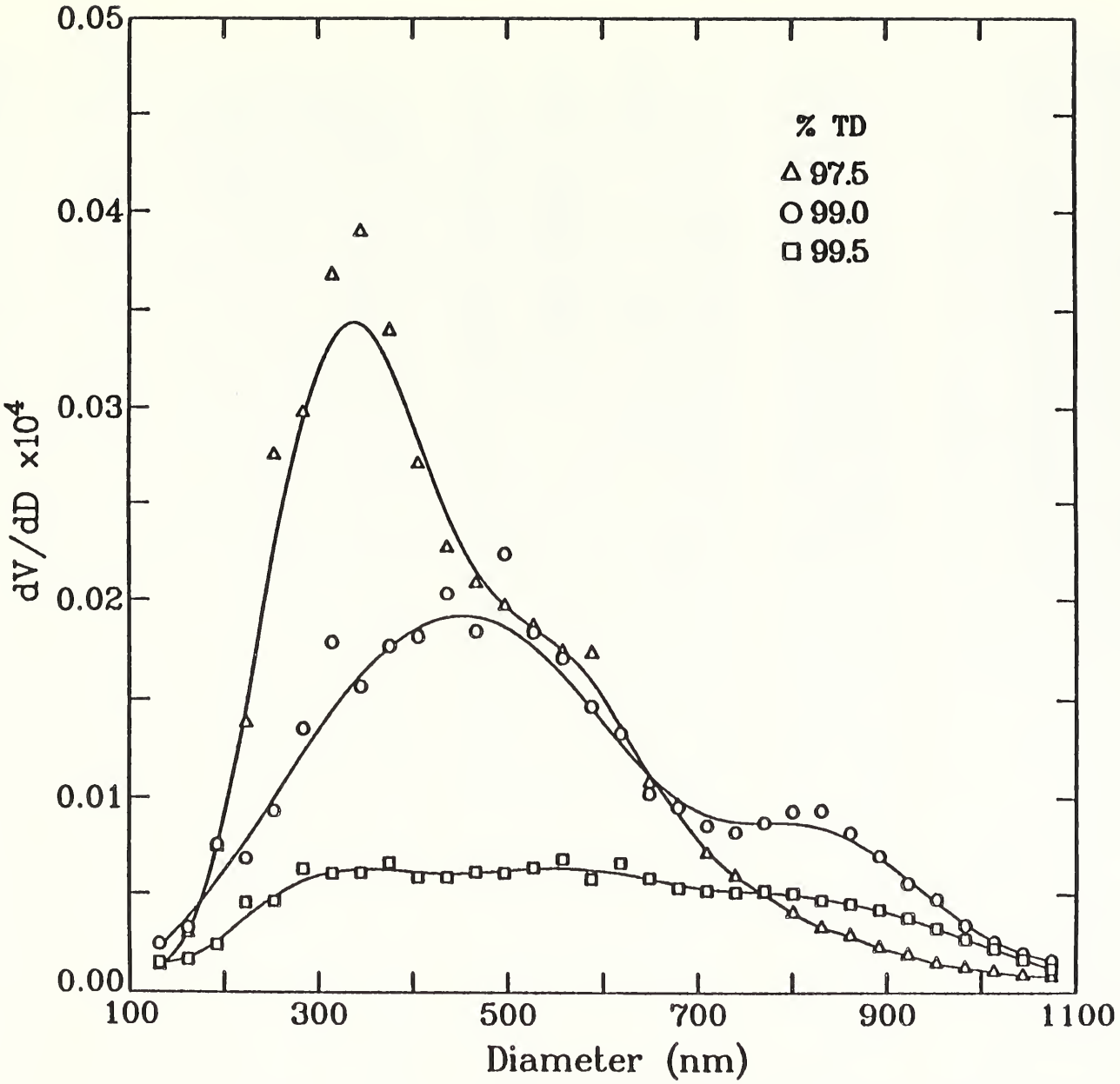

Figure 28. Volume distribution of pores for 97.5%, 99% and 99.7% dense alumina that had been doped with 0.25 wt % Mgo.

The high temperature/high pressure process patented by General Electric (GE) has opened the door to the possibility of producing high-quality artificial diamonds. In collaboration with scientists from GE, we have now demonstrated that good man-made diamonds are indeed superior to the best natural diamonds. We usually find that single dislocations and stacking faults are seen in artificial diamond, whereas such observations are very rare in natural material. Furthermore, it was unexpectedly found that new growth can be misoriented from the seed by approximately 0.2°. Whether or not this is a general requirement for artificial growth is now under investigation. This research has also been able to demonstrate that the best man-made material is found in the isotopically pure ^{12}C crystals.

Diffraction Topography and High-Resolution Diffraction Microscopy of Amethystine α-Quartz

R. D. Spal, H. H. Schloessin[1] and R. A. Secco[1]

[1]University of Western Ontario

The growth history, impurity intake and fracture of a Zambian α-quartz single crystal were studied in the general context of metallogenic and mineralic deposition processes. Topographs in **O**-beam and several complementary **H**-beam settings were recorded covering the entire ~1 mm thick crystal plate. The images show repeated optical (Brazil-law) and electrical (Dauphine-law) twinning.

The individually varying contributions of each part of the crystal to the integrated intensity determine the spread $\Delta\Theta_o$ of reflections about the precise Bragg angle Θ_o. These variations were determined in detail by a series of photographic **O**- and **H**-beam images, taken in discrete steps of 0.003-0.006° through $\Delta\Theta_o$ for $20\bar{2}0$, $30\bar{3}1$ and $11\bar{2}0$ reflection settings. The successive distributions of changing and vanishing contrasts, contributed to the integrated intensity by different parts of the crystal, map out its three-dimensional lattice strains $(\Delta d/d)_{hkl}$ and/or rotations $\delta\theta_{hkl}$. Enhanced reflectivity, evidently related to growth sectors, is found to originate from optical twin lamellae, dispersed impurity distributions, and large particulate impurity inclusions, aligned, some with preferred orientation, along apparent, probably healed, fracture surfaces.

The high resolution x-ray microscope was used to obtain images of 0.16-0.25 mm^2 areas, with 20x magnification, at 27 closely neighboring sites along a path within ~3mm radius from a conspicuous crack bifurcation. Digital records were taken of the **O**-beam images. The digital records lend themselves to quantitative topography and analysis by derived image representations. These include contour and vector maps, lattice strains and stresses, at all or specified levels, as well as their derivatives and resolved components in specific crystallographic directions. The strain fields of an arrested crack tip and of a large, crystallographically bounded, fluid inclusion (negative crystal) with a bubble inside it, have been of particular interest.

Development of Diffraction Anomalous Fine Structure Spectroscopy

C. E. Bouldin, J. C. Woicik and L. B. Sorensen[1]

[1]University of Washington

Diffraction anomalous fine structure (DAFS) spectroscopy is under development as a new method to obtain x-ray absorption fine structure (XAFS) information by examining the diffracted intensity just above the absorption edge of an element in a crystal. Preliminary studies on copper crystals have shown that DAFS can be interpreted using exactly the same formalism as in XAFS. Measurements on $In_xGa_{1-x}As$ have shown that DAFS can be used as a spatially and chemically selective probe. Studies of 1-2-3 superconductors have shown that DAFS can differentiate between the two copper sites in that material. This attribute of distinguishing chemically equivalent but crystallographically inequivalent sites adds a powerful new capability to XAFS.

Currently, we are studying the possibility of measuring the structure of a buried monolayer. The system is a GeSi high electron mobility transistor that is delta-doped with boron at the GeSi-Si interface. DAFS is measured from the silicon surface reconstruction peak to achieve interface specificity.

Synchrotron X-ray Standing-Wave Study of Sb on GaAs(110) and InP(110)

J. C. Woicik, T. Kendelewicz[1], K. E. Miyano[1], P. L. Cowan[2], C. E. Bouldin and W. E. Spicer[1]

[1]Stanford University
[2]Argonne National Laboratory

Much progress in understanding the geometric aspects of adsorption has followed the recent invention and development of the scanning tunneling microscope (STM). However, the STM does not readily provide information on distances perpendicular to the surface. These can be, in principle, obtained from techniques such as surface extended x-ray absorption fine structure (SEXAFS) or elastic low energy electron diffraction (ELEED). However, due to experimental constraints, the collection of high quality SEXAFS data for overlayers on heteropolar semiconductors is difficult, and no successful structural determination for these systems has been published yet. Additionally, a multishell analysis of SEXAFS would be required if structural parameters are to be determined, and the complexity of data analysis employing multiple-scattering theory is a limiting factor in ELEED studies which have been applied to only a handful of model systems.

In this research, structural data were obtained on Sb overlayers on InP(110) and GaAs(110) with the soft x-ray standing-wave (XSW) technique. This technique is an ideal complement to the STM studies because it can easily establish perpendicular distances. XSW can also provide the complete adatom geometry if a set of independent diffracting planes is used.

Although XSW experiments have been performed for some time, application to well-characterized vacuum-prepared interfaces began only recently. The realization that XSW can be performed in the back-diffraction geometry by scanning the photon energy rather than the incidence angle through the Bragg condition has facilitated this effort. Not only does this make the technique compatible with SEXAFS, it also allows the use of standard ultra-high vacuum (UHV) equipment.

Sb overlayers on GaAs and InP(110) are among the simplest interfaces on heteropolar semiconductors and are therefore a prime choice for these state-of-the-art experiments. Other methods of studying these interfaces have established their epitaxial and nonreactive character. However, questions on the exact geometry still exist. Recent STM results indicated the presence of Sb zig-zag chains at the Sb/GaAs interface. However, even within this class of models there remain several possible choices. Our new XSW results resolve these ambiguities.

Through a unique combination of EXAFS and XSW measurements, we have determined the pertinent structural parameters for these systems and compare these with theoretical calculations and ELEED determinations. Using ultraviolet photoemission measurements, we establish that there are two distinct Sb adsorption sites: $^{+}$Sb-In^{-} and $^{-}$Sb-P^{+}. We found that Sb occupies each 1/2 lattice site which is reasonable since InP is of the zincblende structure (Figure 29). Thus Sb completely passivates the semiconductor surface. It forms an ideal epitaxial continuous layer structure with covalent bonding on the InP(110) surface. Indeed, Sb passivates III-V surfaces both chemically and electronically.

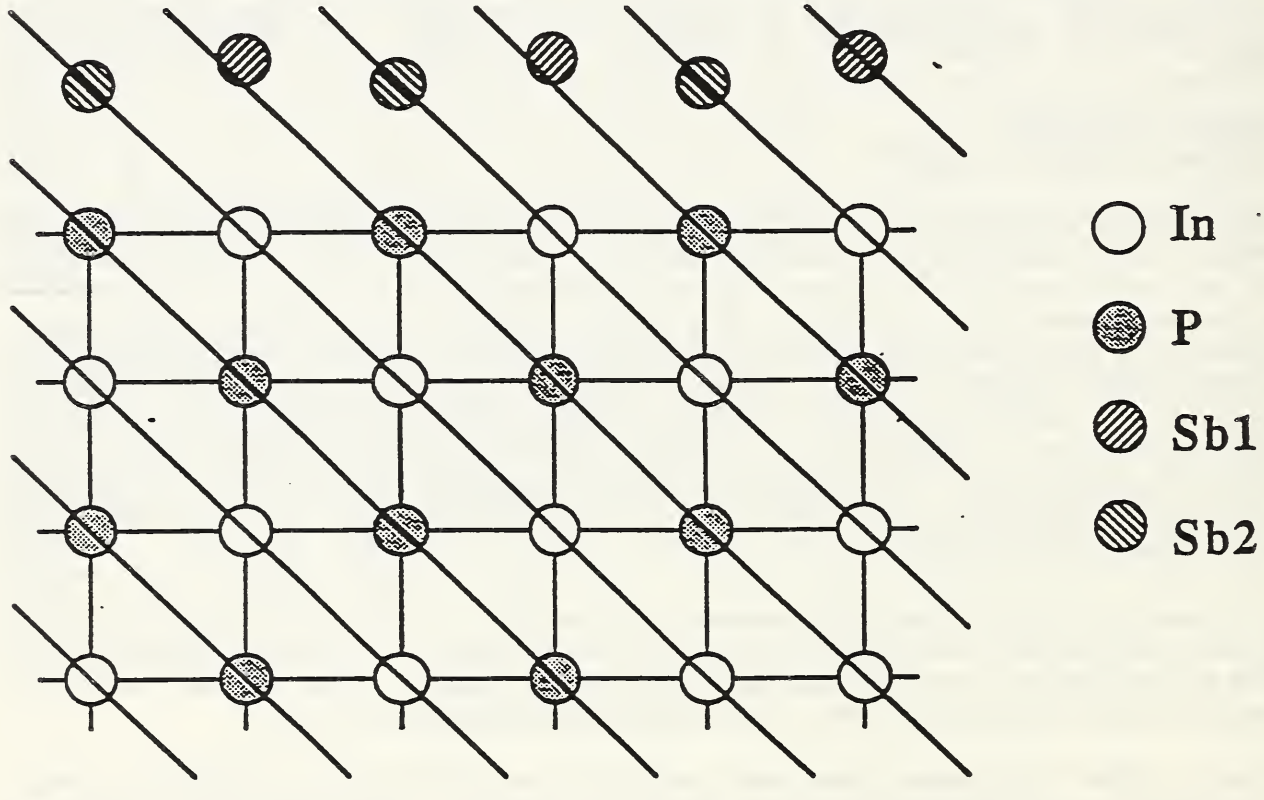

Figure 29. Diagram of Sb on InP(110). The lines indicate the 200 planes, where it can be seen that Sb occupies each 1/2 lattice site and thus can completely passivate the surface.

Irregularities in Crystals Grown in Microgravity and Related Terrestrial Crystals: Their Nature, Genesis, and Effects on Device Performance

B. Steiner, L. van den Berg,[1] A. Fripp,[2] R. Simchick,[2] D. Matthiesen,[3] B. Ditchek,[3] R. Lal,[4] A. Batra,[4] D. Larson,[5] K. Rajan,[6] U. Laor,[7] R. C. Dobbyn[8]

[1]EG&G Energy Systems
[2]NASA Langley Research Center
[3]GTE Laboratories
[4]Alabama A&M University
[5]Grumman
[6]Rensselaer Polytechnic Insititute
[7]Guest Scientist from the Nuclear Research Center of the Negev
[8]Consultant

Crystals grown in microgravity have previously been found to have properties superior to those of directly comparable terrestrial crystals and have led to substantial interest in crystal growth in space. For example, the charge carrier mobility of x- and gamma-ray mercuric iodide detectors made from space-grown crystals was a least six times higher than for similar detectors made from ground-grown crystals. Neither the structural nature of the differences nor their origins in crystal growth had been determined prior to the initiation of the current program. Since both issues are important to the realization of the space crystal growth program, and indeed to improvement in the effectiveness of crystal growth in general, we have begun to study highly selected high quality crystals in close collaboration with the crystal growers of NASA's Microgravity Sciences and Applications Program.

We have three principal goals in mind:

- Establishment of a base line of mesoscopic structural information on those crystals of greatest interest to the microgravity sciences program;
- Correlation of observed variation in characteristics with observed features in the mesoscopic structure;
- Determination of conditions optimum for growth, both on the ground and in microgravity.

For two materials, mercuric iodide and lead tin telluride, more than one phase (arrays of non diffracting inclusions) has already been observed. In the first case, the second phase forms as a widely dispersed precipitate that traps electrons and decreases the energy resolution of detectors made from it. Precipitate formation apparently is suppressed both in microgravity and on the ground when higher purity source material is used. Device performance appears to be correlated far more strongly with the absence of these precipitates than with a high degree of general lattice uniformity, which is in fact lower in devices that perform best to date than in those made from the most regular material.

By contrast, inclusions observed in lead tin telluride appear to be an additional phase of the major constituents. The boundaries between the two constituent structures are much less distinct than in mercuric iodide. Nevertheless, we have found that formation of this second phase also appears to be suppressed in microgravity. Lead tin telluride is of special interest because its growth in space was stimulated by the knowledge that its terrestrial growth is thermosolutally unstable. The initial diffraction imaging results confirm that this is indeed a dominant factor in terrestrial growth.

The growth of triglycine sulfate has been found to be dictated by the propagation of structures from the seed, particularly those created during the preparation of the periphery of the seed. Even where these can be avoided, the general lattice uniformity of the best triglycine sulfate has been found to be severely degraded by cleaving and polishing. As a result of these observations, future space growth of triglycine sulfate will be seeded only with virgin crystal surfaces. It is also of extraordinary interest that the x-ray diffraction acceptance angle for high quality untouched triglycine sulfate crystals has been found to be smaller that that of silicon, the most regular material previously known.

Although gallium arsenide crystals grown in space are not yet available, they are expected shortly. In preparation for their study, comparable terrestrial crystals have been imaged in high resolution diffraction. The resulting images show that the continuity of the Czochralski seed lattice is preserved in new Bridgman growth. However, the general lattice uniformity of the new growth is substantially lower than that of the seed. Nevertheless, seeding at the walls seems to be required for complete destruction of the initial lattice orientation.

Zinc cadmium telluride crystals, two grown in an highly sophisticated furnace and two grown in a furnace designed for space flight and growth according to space flight protocols, have been observed. The strain in crystals grown under the conditions projected for space growth was reflected principally by lattice irregularity within a single grain, while that in the other crystals was reflected in the formation of several grains, each with a more uniform lattice. The high degree of strain found in these two crystals grown under space protocols suggests that the cooling protocols might be modified for improved space growth experiments.

In-Situ X-Ray Diffraction Imaging of Non-Linear Optical Interactions in Photorefractive Crystals

B. Steiner, M. Cronin-Golomb,[1] G. Fogarty,[1] T. M. Garrett,[2] D. Anderson,[3] T. Pollack,[4] B. Wechsler,[5] U. Laor,[6] and R. C. Dobbyn[7]

[1]Electro-Optics Technology Center, Tufts University
[2]Massachussetts Institute of Technology
[3]University of Colorado/Joint Inst. for Laboratory Astrophysics
[4]Sanders, Inc.
[5]Hughes Research Laboratories
[6]Guest Scientist from the Nuclear Research Center of the Negev
[7]Consultant

Rapid signal processing may be facilitated by the development of optical approaches, which can incorporate parallelism with relative ease. One promising technique for processing optical signals in photorefractive crystals is complicated by photorefractive amplified scattering (fanning). The scattering centers responsible for seeding the fanning noise may be presumed to be traceable to crystal lattice irregularities. These defects have not been previously examined in detail, and the relative importance of various specific imperfections and the role that they play in crystal optics is not known. An understanding of these defects should lead to improvement in optical signal processing through growth of more satisfactory photorefractive crystals. We have set out to address these issues through direct, in situ, observation of photorefractive crystals and optical gratings established in them.

We have observed nine carefully selected crystals of barium titanate, which is the most generally satisfactory material, as well as samples of potassium niobate and strontium barium niobate in order to determine their overall uniformity and thus their suitability for real-time, high resolution x-radiation diffraction imaging. The results present a good picture of the current state of crystal perfection in these materials and indicate that real-time observation of optically induced photorefractive gratings is possible.

The overall uniformity of lattice orientation in all nine barium titanate crystals and in the potassium niobate was within the acceptance angle of the crystal for the beam, a few arc seconds. Diffraction was observed from virtually the entire surface of individual domains in each crystal in Bragg geometry. In Laue geometry, which places much higher restrictions on the diffraction condition because of the elimination of most kinematical diffraction, diffraction was observed in the best four barium titanate crystals, with extraordinarily interesting results. Ninety degree domains were clearly imaged in varous orientations in (100)-cut crystals, some in <100> directions, and other in <110> directions as they intersect the (100) surfaces. Some crystals contained two or three large domains. Other crystals displayed the narrow intrusion of long, thin domains into what is otherwise a single domain matrix.

In addition, many of the crystals display deviation in lattice orientation within individual domains. In some crystals, two relatively large areas of a single domain may be slightly misoriented with respect to one another by a few arc seconds. In other cyrstals, the relative misorientation may be restricted to small parts of an entire domain.

Probably most important of all was the observation of {110} interfaces separating what appear to have been 90° domains before poling. The observation that such interfaces can survive conventional poling provides an explanation for the reestablishment of domain walls in depoled crystals in the same locations at which the domains appeared before the initial poling.
Surface imperfections are far more serious than had been anticipated and indeed more than encountered in any other material. The surface of barium titantate appears to be more dufficult to polish than the surfaces of other optical materials, with the result that surface treatment requires particular attention and close correlation with the poling procedures. Dense networks of residual scratches are found in almost all crystals, even after conventional commercial surface preparation. Even with specal care taken in polishing, different types of surface can be distinguished.

Defects in Substrate Wafers and Epitaxial Layers: Their Genesis and Effects on Semiconductor Device Performance

B. Steiner, K. Rajan,[1] J. Comas,[2] and W. Tseng[2]

[1]Rensselaer Polytechnic Institute
[2]Electronics and Electrical Engineering Laboratory

Commercially available semi-insulating gallium arsenide and indium phosphide wafers have a very high density ($>10^3$ cm^{-2} etch pit density) of severely strain-inducing crystallographic irregularities such as dislocations, anti-phase boundaries, low angle grain boundaries, stacking faults, etc. Epitaxial layers grown on the surfaces of such irregular substrates contain defects, some of which propagate from the underlying wafers into the layers grown on them. In addition, other defects are introduced by device fabrication and processing. We are examining the various types of defects in such systems, both before and after layer deposition, and their propagation from the underlying substrates into epitaxial layers. In this way we intend to separate process-induced irregularities from those grown in. We want at the same time to determine which of these are electrically or optically active and therefore which need to be controlled most carefully. Where appropriate, these results will be compared with those obtained by electron microscopy.

We have demonstrated initially the feasibility of the observation of multiple layers by imaging two systems: silicon on germanium on silicon, and mercury cadmium telluride on cadmium telluride on gallium arsenide on silicon. High quality images are obtained on multiple layers, each of which retains its bulk lattice constant but at the same time also preserves epitaxial orientation. The results appear to suggest that lattice irregularity at an epitaxial interface is strongly affected not only by the degree of lattice mismatch but also by the presence of defects in the substrate.

This work has been extended to an aluminum gallium arsenide/gallium arsenide superlattice high electron mobility transistor (HEMT) on a gallium arsenide substrate, both before and after deposition of the layered structure. Two "lattice-matched" indium gallium arsenide/indium aluminum arsenide HEMT structures on indium phosphide substrates have been examined as well, one of these both before and after layer deposition. The gallium arsenide structure appears to be closely enough lattice-matched not to introduce severe defect structure at the interface. By contrast, the ostensibly lattice-matched indium phosphide structure displays sufficient strain to form a distinct, dense set of straight, parallel edge dislocations that contrast with the nest of wandering edge dislocations characteristic of the bulk substrate prior to layer formation.

The examination of test field effect transistor structures and of Hall-patterns is being planned. Electrical characteristics such as drain current and Hall mobility will be mapped for direct comparison with the diffraction images and correlation.

RESEARCH STAFF

POWDER CHARACTERIZATION AND PROCESSING

Cline, James P.	• Standard reference materials • High-temperature x-ray diffraction • Microstructural effects in x-ray diffraction • Rietveld Refinement of XRD data
Kelly, James F.	• Quantitative scanning electron microscopy • Image analysis • Microstructure analysis • Powder standards
Lum, Lin-Sien H.	• Powder characterization • Instrumental analysis
Malghan, Subhas G.	• Powder and dense slurry characterization • Colloidal processing and forming • Interfacial and surface chemistry of powders • Standards Development
Minor, Dennis B.	• Analytical SEM of ceramics and particulates • Powder test sample preparation • Powder characterization
Pei, Patrick T.	• Spectroscopic and thermal characterization • Chemical coating • Bulk chemical properties
Ritter, Joseph J.	• Chemistry of powders synthesis • Specialty powders synthesis • Powder preparation and compositional evaluation
Pechenik, Alexander	• Novel powder processing • High pressure, low temperature powder compaction • Powder processing science
Wallace, Jay S.	• Processing and microstructure • Silicon nitride densification • Thermal analysis
Wang, Pu Sen	• Solid state NMR • Surface characterization by x-ray photoelectron and Auger electron spectroscopy

MECHANICAL PROPERTIES

Chuang, Tze-Jer	• Creep/creep rupture • Fracture mechanics • Finite-element modeling • Lifetime predictions
Cranmer, David C.	• Ceramic and glass composite fabrication • Composite test development • Ceramic composite properties • Glass viscosity • Properties of glass
Hockey, Bernard J.	• Electron microscopy
Horn, Roger G.	• Surface forces • Fracture mechanics • Colloidal processing • Tribology • Adhesion
Kauffman, Dale A.	• Glass melting
Krause, Ralph F., Jr.	• Creep in flexure and tension • Fracture mechanics • Hot pressing • Chemical thermodynamics
Lawn, Brian R.	• Microstructure/strength relations • Fracture mechanics • Contact phenomena • Surface forces in fracture
Ostertag, Claudia P.	• Influence of heterogeneities on sintering • Processing and sintering of reinforced ceramics • Investigation of toughening mechanisms in pressureless sintered composites • Measurement of residual stresses by cathodoluminescence and in situ high temperature X-ray diffraction
Smith, Douglas T.	• Surface forces • Charge transfer at interfaces • Adhesion

TRIBOLOGY

Ives, Lewis K.	• Wear of materials • Transmission electron microscopy • Mechanical properties
Jahanmir, Said	• Wear mechanisms • Machining of advanced materials • Mechanical behavior of materials
Ku, Chia-Soon	• Lubrication of ceramics • Oxidation, thermal stability and volatility • Lubricant degradation mechanisms
Perez, Joseph M.	• Additive chemistry, deposits and engine emissions • Thermal and oxidation stability of fluids • Fuels, lubricants and diesel engines
Peterson, Marshall B.	• Wear of materials • Solid film lubricants • Mechanical behavior
Ruff, Arthur W.	• Wear of materials • Microstructure effects • Mechanical behavior
Whitenton, Eric P.	• Surface profilometry • Data processing • Computer interfaces

ELECTRONIC MATERIALS

Blendell, John E.	• Ceramic processing and clean-room processing • Sintering and diffusion controlled processes • Processing high T_c ceramic superconductors • Activation chemical analysis
Chiang, Chwan K.	• Electronic ceramics • Superconductivity • Electrical measurements
Clevinger, Mary A.	• Phase diagrams for ceramists • Computerized data
Cook, Lawrence P.	• High temperature chemistry • Phase equilibria • Electronic ceramic films

Hill, Michael D.	•	Superconducting materials
	•	Ceramic processing
Ondik, Helen M.	•	Phase diagrams for ceramists
	•	Database management systems
Piermarini, Gasper J.	•	Ceramic processing and high pressure sintering
	•	Pressure-induced transformation toughening
	•	High pressure physical properties and structures
	•	High pressure X-ray diffraction and spectroscopy
Rawn, Claudia J.	•	Phase diagrams
	•	X-ray diffraction
Raynes, Alan S.	•	Fracture
	•	Microstructure
Roth, Robert S.	•	Crystal chemistry
	•	Phase diagrams
	•	Phase equilibria
Vaudin, Mark D.	•	Electron microscopy of ceramic superconductors and of ceramic-ceramic and ceramic-metal composites
	•	Microscopy and diffraction studies of interfaces
	•	Computer modelling of grain boundary phenomena
White, Grady S.	•	Thin films
	•	Nondestructive evaluation
	•	Subcritical crack growth
Wong-Ng, Winnie	•	X-ray analysis
	•	X-ray standards
	•	Molecular orbital calculations

OPTICAL MATERIALS

Farabaugh, Edward N.	•	Chemical vapor deposition of diamond
	•	Structure and morphology analysis
	•	Scanning electron microscopy
	•	X-ray diffraction
	•	Thin film deposition
	•	Surface analysis
Feldman, Albert	•	Chemical vapor deposition of diamond
	•	Thermal properties
	•	Modelling thermal wave propagation
	•	Thin film optical properties

Kaiser, Debra L.	• Bulk single crystal growth • Phase equilibria • Physical properties and structures of high temperature superconductors • Interfaces in high temperature superconductors • Chemical vapor deposition of ferroelectric oxide thin films
Robins, Lawrence H.	• Defect identification and distribution in CVD diamond • Stress in ceramics • Cathodoluminescence imaging and spectroscopy • Photoluminescence spectroscopy • Optical properties • Raman spectroscopy • Scanning electron microscopy

MATERIALS MICROSTRUCTURE CHARACTERIZATION

Black, David R.	• Defect microstructure in diamond • Polycrystalline diffraction imaging • X-ray imaging of photonic materials
Bouldin, Charles E.	• X-ray absorption spectroscopy • Diffraction anomalous fine structure • GeSi heterojunction bipolar transistors
Burdette, Harold E.	• X-ray optics • X-ray diffraction imaging • Crystal growth • Instrumentation
Fischer, Daniel A.	• X-ray absorption fine structure • X-ray scattering • Surface science
Long, Gabrielle G.	• Small-angle x-ray and neutron scattering • Ceramic microstructure evolution as a function of processing • X-ray optics
Spal, Richard D.	• X-ray optics • Diffraction physics • X-ray scattering
Woicik, Joseph C.	• UV photoemission • X-ray standing waves • Surface and interface science

DATA BASE ACTIVITIES

Begley, Edward F.	• Database management methods • Engineering database structures • User-friendly interfaces
Munro, Ronald G.	• Material properties of advanced structural ceramics • Data evaluation and validation • Analysis of data relations

DIVISION OFFICE

Carpenter, Joseph A., Jr.,	• Functional ceramics applications • Technical assessments • Industrial liaisons
Dapkunas, Stanley J.	• Structural ceramics applications • Technical assessments
Freiman, Stephen W.	• Electronic ceramics • Mechanical properties • Superconductivity
Fuller, Edwin, R., Jr.	• Influence of microstructure on fracture and other physical properties of materials • Toughening mechanisms in ceramics and ceramic composites, and their relations to processing • Interfacial fracture and toughening mechanisms in reinforced ceramic composites • Processing/property relations and phase equilibria of high T_c ceramic superconductors
Gates, Richard S.	• Ceramic surface chemical interactions • Lubrication of advanced materials • Ceramic tribology
Hsu, Stephen M.	• Tribology of ceramics materials • Advanced high temperature lubrication concepts • Wear maps concepts and methodology
Steiner, Bruce W.	• High resolution diffraction imaging • Nature, genesis, distribution, and effects of irregularitites in monolithic crystals and multilayers

GUEST SCIENTISTS AND GRADUATE STUDENTS

Allen, Andrew	University of Maryland
Ananthanarayana, Venkatasurbramanian	Delco Products
Balasubramanian, Raghuraman	Clarkson University
Bender, Gerald	University of Groningen
Bennison, Stephen	Lehigh University
Blackburn, Douglas	Consultant
Block, Stanley	Consultant
Braun, Linda	Lehigh University
Butler, Elizabeth	Lehigh University
Carter, W. Craig	Postdoc (ex - University of California at Berkeley)
Cedeno, Christina	American Ceramic Society
Chang, Luke	University of Maryland
Chen, Yung-Mien	University of Maryland
Cheng, Herbert	Northwestern University
Coker, Eric	Worcester Polytechnic Institute
Coyle, Thomas	GPR Systems
Craig, Charles	Defense Tech Security
Czubarow, Pawel	American University
Dally, James	University of Maryland
Deckman, Doug	Pennsylvania State University
Domingues, Louis	Trans-Tech, Inc.
Dong, Xiaoyuan	University of Maryland
Dragoo, Alan	Department of Energy
Frederikske, Hans	Consultant
Green, Thomas	American Ceramic Society

Grabbe, Alexis	Postdoc (ex - University of North Carolina at Chapel Hill)
Hackley, Vince	University of Wisconsin
Hahn, Horst	Rutgers University
Haller, Wolfgang	Abbott Laboratories
Hamilton, Kenneth	Worcester Polytechnic Institute
Harmer, Martin	Lehigh University
He, Chuan	University of Maryland
Hong, William	Institute for Defense Analysis
Hu, Zu-Shao	East China University
Hwang, Nong-Moon	Korea Science and Engineering Institute
Inglehart, Lorretta	Johns Hopkins University
Ito, Osamu	Hitachi Research Lab
Jemian, Peter	Argonne National Laboratory
Jiang, Si-Juan	Tsinghua University
Kerch, Helen	Johns Hopkins University
Kessell, Kimberly	American Ceramic Society
Kim, Seock-Sam	Korea Science and Engineering Institute
Klaus, Elmer	Pennsylvania State University
Krebs, Lorrie	Johns Hopkins University
Kruger, Jerome	Johns Hopkins University
Kuwamoto, Hidehiko	Rockwell International
Lacey, Paul	University of Maryland
Larsen-Basse, Jorn	National Science Foundation
Lathabai, Srinivasarao	Lehigh University
Lee, Soo Wohn	University of Illinois

Lindsay, Curt	Postdoc (ex - Virginia Polytechnic Institute and State University)
Martin, Curtis	Naval Surface Warfare Center
McMurdie, Howard	Joint Center for Powder Diffraction Studies
Messina, Carla	American Ceramic Society
Padture, Nitin	Lehigh University
Paik, Ungyu	Clemson University
Paretzkin, Boris	Joint Center for Powder Diffraction Studies
Paulik, Steven	Northwestern University
Pryor, Caroline	American Ceramic Society
Reed, James	Alfred University
Rigdon, Michael	Institute for Defense Analysis
Ritter, Andrew	Martin Marietta
Rödel, Juergen	Lehigh University
Russell, Thomas	Naval Surface Warfare Center
Sater, Janet	Institute for Defense Analysis
Schioler, Liselotte	Air Force Office of Scientific Research
Shechtman, Dan	Johns Hopkins University
Shen, Ming	University of Illinois
Smith, Wallace	Office of Naval Research
Spooner, Stephen	Oak Ridge National Laboratory
Sun, Jian-Xia	Shanghai University of Science and Technology
Swanson, Nils	American Ceramic Society
Thanomkul, Srinuan	Chulalongkorn University
Trivedi, Sudhir	Brimrose Corporation
Vandiver, Pamela	Smithsonian Institute

Wachtman, John	Rutgers University
Wan, Kai-Tak	University of Maryland
Wang, Yushu	University of Maryland
Wilcox, William	Clarkson University
Wu, Dong-Di	East China University
Ying, Tsi-Neng	University of Maryland
Zhang, Yuming	University of Maryland
Zutshi, Ajoy	Rutgers University

OUTPUTS AND INTERACTIONS

TECHNICAL PUBLICATIONS

POWDER CHARACTERIZATION AND PROCESSING

Bennett, L. H., Turchinskaya, M., Swartzendruber, L. J., Roitburd, A., Lundy, D., Ritter, J. J. and Kaiser, D. L., "Flux Flow and Flux Dynamics in High T_c Superconductors," Advances in Materials Science and Applications of High Temperature Superconductors, L. H. Bennett et al., Eds., (NASA Conference Publication, Washington, D.C., 1990) pp. 213-229.

Carter, W.C. and Handwerker, C.A., "The Growth Morphologies of DIR Grains in Cubic Materials," to be submitted to Acta Metal. et Mater.

Freiman, S. W., Ritter, J. J. and Cline, J. P., "Molecular-Chemical Approach to High T_c Superconductors," Proceedings of 1991 5th Ultrastructure Processing Conference, J. K. West, Ed., to be published by John Wiley and Sons, New York, NY.

Malghan, S. G., "Silicon Nitride Powders and Their Processing," Advanced Materials Processing, P. Ganguli, Ed. (Elsevier Science Publishers B. V., Amsterdam, The Netherlands, 1991) pp. 562-576.

Malghan, S. G., "Chapter E. Comminution," Engineered Materials Handbook: Ceramics and Glasses (ASM International, Materials Park, OH, 1991) in press.

Malghan, S. G., "Characteristics of High Energy Agitation Ball Mills for Submicron Powders Milling," Powder and Bulk Engineering, June 1991, 44-48.

Malghan, S. G., "Dispersion of Si_3N_4 Powders -- Surface Chemical Interactions in Aqueous Media," accepted for publication in Colloids and Interfaces.

Malghan, S. G. and Dragoo, A. L., "Chapter D. Characterization of Ceramic Powders," Engineered Materials Handbook: Ceramics and Glasses (ASM International, Materials Park, OH) in press.

Malghan, S. G., Hsu, S. M., Dragoo, A. L., Hausner, H. and Pompe, R., "Analysis of Physical Properties of Ceramic Powders in an International Interlaboratory Comparison Program," accepted for publication in Ceramics for Heat Engines, R. Clausson, Ed. (Elsevier Science Publishers B. V., Amsterdam, The Netherlands).

Malghan, S. G. and Lum, L.-S., "An Analysis of Factors Affecting Particle Size Distribution of Hydraulic Cements," Cement, Concrete and Aggregate, 9 (30), 115-120 (1991).

Malghan, S. G., Minor, D. B. and Lum, L.-S., "Physical and Chemical Modifications During Agitation Milling of Si_3N_4 Powder," Ceramic Powder Processing Science, III, G. L. Messing, Ed. (American Ceramic Society, Westerville, OH, 1991).

Malghan, S. G., Pei, P. T. and Wang, P. S., "Analysis of Surface Chemistry of Silicon Nitride and Carbide Powders," Forming of Ceramics, M. Cima, Ed. (American Ceramic Society, Westerville, OH, 1991) in press.

Malghan, S. G., Pei, P. T. and Wang, P. S., "Interface Chemistry of Silicon Carbide Platelets During Alumina Coating," Ceramic Engineering and Science Proceedings, 12(9-10), 2115-2123 (1991).

Malghan, S. G., Sivakumar, A. and Wang, P. S., "A Surface Chemical Technique for Sintering Aid Addition," Forming of Ceramics, M. Cima, Ed. (American Ceramic Society, Westerville, OH, 1991) in press.

Malghan, S. G., Vaudin, M., Cline, J. P., Wang, P. S., Lum, L.-S. and Jain, M., "Characterization of Phase and Surface Composition of Silicon Carbide Platelets," Ceramic Transactions, 19, 253-261 (1991).

Pechenik, A., "Rapid Hot Pressing of Ultra Fine PSZ Powders," J. Am. Ceram. Soc., 74(7), 1547-53 (1991).

Pimienta, P.J.P., Bentz, D.P., Garboczi, E.J. and Carter, W.C., "Cellular Automaton Simulations of Gradients: Simulations of Surface Mass Transport Due to Curvature of Sintering," in Proceedings of Symposium Q: Synthesis and Processing of Ceramics: Scientific Issues, Fall Meeting of the Materials Research Society, Boston (1991), submitted.

Pimienta, P.J.P., Garboczi, E.J. and Carter, W.C., "Cellular Automaton Algorithm for Surface Mass Transport Due to Curvature Gradients: Simulations of Sintering," submitted to J. Mater. Res.

Shull, R. D., Ritter, J. J., Shapiro, A. J., Swartzendruber, L. J. and Bennett, L. H., "Magnetic Behavior of Nanocomposites Prepared in a Vitreous Alumina Gel," Proceedings of the Materials Research Society, Vol 206, R. S. Averback et al., Eds. (Materials Research Society, Pittsburgh, PA, 1991) pp. 455-60.

Shull, R. D., Ritter, J. J. and Swartzendruber, L. J., "Change in Magnetic State of Fe + Silica Gel Nanocomposites Due to Low Temperature Treatment in Ammonia," J. Applied Physics, 69, 5144-46 (1991).

Wang, P. S., Malghan, S. G. and Hsu, S. M., "The Effect of a Boron Impurity on the Surface Oxidation of Silicon Carbide as Studied by X-Ray Photoelectron Spectroscopy and Bremstrahlung-Excited Auger Electron Spectroscopy," submitted to Surface and Interface Analysis, 1991.

Wang, P. S., Malghan, S. G., Hsu, S. M., Bartenfelder, D. and Hegemann, B., "Surface Chemistry of α-Alumina Powders Treated by Aqueous and Nonaqueous Solvents," Ceramic Powder Processing Science, III, G. L. Messing, Ed. (American Ceramic Society, Westerville, OH, 1991).

Wang, P. S., Malghan, S. G., Wittberg, T. and Hsu, S. M., "Surface Oxidation Kinetics of SiC Platelets Studied by X-Ray Photoelectron and X-Ray Induced Auger Electron Spectroscopy," submitted to proceedings of Materials Research Society symposium, Boston, MA, Nov 26-29, 1990 (Materials Research Society, Pittsburgh, PA).

MECHANICAL PROPERTIES

Becher, P.F., Fuller, E.R., Jr. and Angelini, P., "Matrix-Grain-Bridging Contributions to the Toughness of Whisker-Reinforced Ceramics," J. Am. Ceram. Soc., 74 (9), 2131-2135 (1991).

Bennison, S. J., Padture, N. P., Runyan, J. L. and Lawn, B. R., "Flaw-Insensitive Ceramics", Philos. Mag., 64, 191-195 (1991).

Bennison, S. J., Rödel, J., Lathabai, S., Chantikul, P. and Lawn, B. R., "Microstructure, Toughness Curves and Mechanical Properties of Alumina Ceramics," Toughening Mechanisms in Quasi-Brittle Materials, S. P. Shah, Ed. (Kluwer Academic Publishers, Dordrecht, The Netherlands, 1991) p. 209.

Carter, W.C., Butler, E.P. and Fuller, E.R., Jr., "Micro-Mechanical Aspects of Asperity-Controlled Friction in Fiber-Toughened Ceramic Composites," Scripta Metall. et Mater., 25 (3), 579-584 (March 1991).

Cho, S.-J., Moon, H., Hockey, B. J. and Hsu, S., "The Transition from Mild to Severe Wear in Alumina During Sliding," Acta Met. et Mat., in press.

Chuang, T.-J., "Crack Growth Resistance of Strain-Softening Materials under Flexural Loading," Structures Congress, 1991, T. G. Williamson et al., Eds. (American Society of Civil Engineers, New York, NY, 1991) pp. 466-469.

Chuang, T.-J. and Fuller, E. R., "An Extended Charles-Hillig Theory for Stress Corrosion Cracking of Glass," J. Amer. Ceram. Soc., in press.

Chuang, T.-J., Liu, W. and Wiederhorn, S. M., "Steady-State Creep Behavior of Si-SiC C-rings," J. Amer. Ceram. Soc., 74(10), 2531-2537 (1991).

Chuang, T.-J., Shiue, S.-T. and Lee, S., "Asymmetric Tip Morphology of Creep Microcracks Growing Along Bi-material Interfaces," Acta Metall. et Mater., in press.

Conway, J. C., Jr., Mecholsky, J. J., Wiederhorn, S. M., Jadaan, O. M., Shelleman, D. L., Cranmer, D. C. and Krause, R. F., Jr., "Test Methodology for Tubular Components," in the Center for Advanced Materials Annual Report, CAM-9002 (Gas Research Institute, Chicago, IL, Mar 1991).

Cranmer, D. C., "Fiber Coatings and Properties in Ceramic Matrix Composites," Composite Materials and Coatings (American Electroplating and Surface Finishing Society, Orlando, FL, 1991) pp. 1017-1049.

Cranmer, D. C., Editor, "Fundamentals of Carbon/Carbon," NIST Special Publication, in preparation, 1991.

Cranmer, D. C., "Lifetime and Reliability Predictions of Advanced Ceramics Based on Creep and Creep Rupture Mechanisms," submitted to Journal of Statistical Planning and Inference, 1991.

Cranmer, D. C., Editor, "Mechanical Testing Methodology for Ceramic Design and Reliability," NIST Special Publication, in preparation, 1991.

Cranmer, D. C., Editor, Mechanical Testing Methodology for Ceramic Design and Reliability, to be published by Marcel Dekker, 1992.

Cranmer, D. C., "Overview of Technical, Advanced, and Engineering Ceramics," ASM Engineered Materials Handbook, Volume 4 (ASM International, Materials Park, OH) in press.

Cranmer, D. C., Editor, "Testing Methodology for Glass, Glass-Ceramic, and Ceramic Matrix Composites," NIST Special Publication, in preparation, 1991.

Cranmer, D. C., "An Assessment of Testing Methodology for Ceramic Matrix Composites," Advanced Composite Materials, M. Sacks, Ed. (American Ceramic Society, Westerville, OH, 1990) pp. 1003-1010.

Cranmer, D. C., "An Assessment of Testing Methodology for Glass, Glass-Ceramic, and Ceramic Matrix Composites," Journal of Research NIST, 94(4), 493-501 (1991).

Cranmer, D. C., Deshmukh, U. V. and Coyle, T. W., "Comparison of Methods for Determining Fiber/Matrix Interface Frictional Stresses in Ceramic Matrix Composites," Thermal and Mechanical Behavior of Ceramic Matrix and Metal Matrix Composites, ASTM STP 1080, J. M. Kennedy et al., Eds. (American Society for Testing and Materials, Philadelphia, PA, 1990) pp. 124-135.

Cranmer, D. C., Freiman, S. W., Chuang, T.-J. and Raynes, A. S., "Design Diagrams For Heavy Metal Fluoride Glasses," Proceedings of the Topical Meeting on High Power Laser Optical Components, 30-31, October 1989, NWC TP 7080, Part 1, December 1990, pp. 98-114.

Cranmer, D. C., Freiman, S. W., Fuller, E. R., Haller, W., Koczak, M., Barsoum, M. and Chou, J., "Mechanical Property Enhancement in Ceramic Matrix Composites," submitted for publication as NIST IR, 1990.

Cranmer, D. C., Hockey, B. J., Wiederhorn, S. M. and Yeckley, R., "Creep and Creep-Rupture of HIP-ed Silicon Nitride," Ceramic Engineering and Science Proceedings, 12 (9-10), 1862-72 (1991).

Cranmer, D. C., Freiman, S. W., White, G. S. and Raynes, A. S., "Moisture- and Water-Induced Crack Growth in Optical Materials," Optical Surfaces Resistant to Severe Environments, SPIE Volume 1330 (Society of Photo-optical Instrumentation Engineers, Bellingham, WA, 1990) pp. 152-163.

French, V. A., Powell, R. C., Blackburn, D. H. and Cranmer, D. C., "Refractive Index Gratings in Rare Earth-Doped Glasses," J. Appl. Phys., 69 (2), 913-917 (1991).

Fuller, E.R., Jr., Butler, E.P. and Carter, W.C., "Determination of Fiber-Matrix Interfacial Properties of Importance to Ceramic Composite Toughening," Toughening Mechanisms in Quasi-Brittle Materials, S. P. Shah, Ed. (Kluwer Academic Publishers, Dordrecht, The Netherlands, 1991) pp. 385-403.

Grabbe, A. and Horn, R. G., "Direct Measurements of Double-Layer and Hydration Forces Between Oxide Surfaces," to be published in Proceedings of NATO Advanced Research Workshop on Clay Swelling and Expansive Soils, P. Bavenge and M. B. McBride, Eds. (Kluwer Academic Publishers, Dordecht, The Netherlands).

Handwerker, C. A., Deshmukh, U. V. and Cranmer, D. C., "Fabrication and Interface Debonding of Al_2O_3-Cr_2O_3-Cr Composites," Metal and Ceramic Matrix Composites: Processing, Modeling, and Mechanical Behavior, R. B. Bhagat et al., Eds. (The Minerals, Metals and Materials Society, Warrendale, PA, 1990) pp. 457-465.

Hicho, G. E., Smith, L. C., Handwerker, C. A. and Kauffman, D. A., "Determination of the Prior-Austenitic Grain Size of Selected Steels Using a Molten Glass Etch," Journal of Heat Treating, 9, 37-47 (1991).

Horn, R. G., "Surface Forces and Adhesion," to be published in Metals Handbook, Vol. 4, 10th Edition (ASM International, Materials Park, OH).

Horn, R. G. and Smith, D. T., "Analytic Solution for the General Three-Layer Interferometer," Applied Optics, 30, 59-65 (1991).

Krause, R. F., Jr., "Observed and Theoretical Creep Rates for an Alumina and a Silicon Nitride Ceramic in Flexure," submitted to J. Amer. Cer. Soc.

Krause, R. F., Jr. and Chuang, T.-J., "A Test Method for Tensile Creep of Structural Ceramics Using Flexure Beams," Ceramics Today - Tomorrow's Ceramics, P. Vincenzi, Ed. (Elsevier Science Publishers B. V., Amsterdam, The Netherlands, 1991) pp. 1865-1874.

Lathabai, S., Rödel J. and Lawn, B. R., "Cyclic Fatigue from Frictional Degradation at Bridging Grains in Alumina," J. Amer. Ceram. Soc., 74, 1340 (1991).

Lathabai, S., Rödel, J., Lawn, B. R. and Dabbs, T., "Fracture Mechanics Model for Subthreshold Indentation Flaws I. Equilibrium Fracture," J. Mater. Sci., 26, 2157 (1991).

Lathabai, S., Rödel, J., Lawn, B. R. and Dabbs, T., "Fracture Mechanics Model for Subthreshold Indentation Flaws II. Nonequilibrium Fracture," J. Mater. Sci., 23, 2313 (1991).

Lawn, B. R., Fracture of Brittle Solids, Second Edition (Cambridge University Press, London) to be published in 1991.

Lawn, B. R., "Friction Processes in Brittle Fracture," Fundamentals of Friction (Kluwer Academic Publishers, Dordrecht, The Netherlands) in press.

Lawn, B. R., "Fundamental Condition for Existence of Microcrack Clouds in Monophase Ceramics," J. Europ. Ceram. Soc., 7, 17 (1991).

Ostertag, C. P., "Differential Sintering," Science of Sintering, D. P. Ustotovic et al., Eds. (Plenum Press, New York, NY, 1990) p. 453.

Ostertag, C. P., Charalambides, P. G. and Evans, A. G., "Observations and Analysis of Sintering Damage," Sintering of Advanced Ceramics, C. A. Handwerker et al., Eds., Ceramic Transactions Volume 7 (American Ceramic Society, Westerville, OH, 1990) pp. 710-732.

Ostertag, C. P., Robins, L. H. and Cook, L. P., "Cathodoluminescence Measurements of Strained Alumina Single Crystals," J. Europ. Ceram. Soc., 7, 109-116 (1991).

Padture, N. P., Chan, H. M., Bennison, S. J., Runyan, J. L., Rödel, J. and Lawn, B. R., "Fabrication of Flaw Tolerant $A\ell_2O_3$-$A\ell_2TiO_5$ Composites," Symposium on Composites: Processing, Microstructure and Properties (American Ceramic Society, Westerville, OH, 1991) p. 715.

Padture, N. P., Chan, H. M., Lawn, B. R. and Readey, M. J., "The Role of Crystallization of an Intergranular Glassy Phase in Determining Grain Boundary Residual Stresses in Debased Aluminas," Mater. Res. Soc. Sympos. Proc., 170, 245 (1990).

(Quinn, G. D. et al.) "Flexural Strength of Advanced Ceramics at Ambient Temperatures," ASTM Standard C-1161, Dec. 1990.

(Quinn, G. D. et al.) "Flexural Strength of High Performance Ceramics at Ambient Temperature," MIL STD 1942(A), Nov. 1990.

Quinn, G. D., "Chapter 8H. Strength and Proof Testing," Handbook of Engineered Materials: Ceramics and Glasses (ASM International, Materials Park, OH) in press.

Quinn, G. D., "Refinements to Flexure Testing," submitted to J. Europ. Ceram. Soc.

Quinn, G. D., "Fracture Mechanism Maps for Advanced Structural Ceramics Part 1, Methodology and Hot Pressed Silicon Nitride Results," J. Mat. Sci., 25, 4361-76 (1990).

Quinn, G. D. and Braue, W., "Fracture Mechanism Maps for Advanced Structural Ceramics. Part 2, Sintered Silicon Nitride," J. Mat. Sci., 25, 4277-92 (1990).

Quinn, G. D. and Morrell, R., "Design Data for Engineering Ceramics: A Review of the Flexure Test," J. Am. Ceram. Soc., 74, 2037-2066 (1991).

Quinn, G. D., Swab, J. and Slavin, M., "A Proposed Standard Practice for Fractographic Analysis of Monolithic Advanced Ceramics," to be published in the proceedings of the 37th Army Sagamore Conference, "Structural Ceramics", Oct. 1990.

Quinn, G. D., Swab, J. J. and Slavin, M. J., "A Proposed Standard Practice for Fractographic Analysis of Monolithic Advanced Ceramics," Fractography of Glasses and Ceramics, Part II, V. D. Frechette and J. R. Varner, Eds. (American Ceramic Society, Westerville, OH, 1991) pp. 309-362.

Rödel, J., Fuller, E.R., Jr. and Lawn, B.R., "In Situ Observations of Toughening Processes in Alumina Reinforced with Silicon Carbide Whiskers," J. Am. Ceram. Soc., 75 (1), (1992), in press.

Rödel, J., Kelly, J. and Lawn, B. R., "In Situ Measurements of Bridged Crack Interfaces in the SEM," J. Amer. Ceram. Soc., 73, 3313 (1990).

Rödel, J., Kelly, J., Stoudt, M. and Bennison, S., "A Loading Device for Fracture Testing of Compact Tension Specimens in the SEM," Scanning Microscopy, 5, 29 (1991).

Runyan, J. and Bennison, S., "Fabrication of Flaw-Tolerant Aluminum Titanate-Reinforced Alumina," J. Europ. Ceram. Soc., 7, 93-99 (1991).

St. John, W. D., Taheri, B., Wicksted, J. P., Powell, R. C., Blackburn, D. H. and Cranmer, D. C., "Time Dependent Thermal Lensing in Lead Oxide Modified Silicate Glass," submitted to J. Opt. Sci. B, 1991.

Stone, C. A., Blackburn, D. H., Kauffman, D. A., Cranmer, D. C., Olmez, I. and Rossbach, M., "^{6}Li-doped Silicate Glass for Thermal Neutron Shielding," submitted to Nuclear Science and Engineering.

Stone, C. A., Mildner, D. F. R., Zeisler, R. and Cranmer, D. C., "Capture Gamma-ray Spectroscopy Using Cold Neutron Beams," to be published in Proceedings of the 7th International Conference on Capture Gamma-ray Spectroscopy and Related Topics, 1991.

Swab, J., Quinn, G. D. and Slavin, M., "A Proposed Standard Practice for Fractographic Analysis of Monolithic Advanced Ceramics," submitted to Ceramic Materials and Components for Engines, proceedings of the 4th Conference, Goteburg, Sweden, June 1991.

Swab, J. J., Quinn, G. D. and Snoha, D. J., "Mechanical Behavior of a SiC-Fiber/Si_3N_4 Composite," U. S. Army MTL TN 90-2, September 1990.

Taheri, B., Munoz F., A., St. John, W. D., Wicksted, J. P., Powell, R. C., Blackburn, D. H. and Cranmer, D. C., "Effects of the Structure and Composition of Lead Glasses on the Thermal Lensing of Pulsed Laser Radiation," submitted to J. Applied Physics, 1991.

Vandiver, P., Swann, C. and Cranmer, D., "A Review of Mid-Second Millennium B.C. Egyptian Glass Technology at Tell el-Amarna," Materials Issues in Art and Archaeology, II, P. Vandiver et al., Eds., MRS Symposium Volume 185 (Materials Research Society, Pittsburgh, PA, 1991) pp. 335-347.

Wan, K. T., Aimard, N., Lathabai, S., Horn, R. G. and Lawn, B. R., "Interfacial Energy States of Moisture-Exposed Cracks in Mica," J. Mater. Res., 5, 172-182 (1990).

Wan, K. T., Lathabai, S. and Lawn, B. R., "Crack Velocity Functions and Thresholds in Brittle Solids," J. Europ. Ceram. Soc., 6, 259 (1990).

Wan, K. T. and Lawn, B. R., "Surface Forces at Crack Interfaces in Mica in the Presence of Capillary Condensation," Acta Mater., 38, 2073 (1990).

Wan, K. T., Smith, D. T. and Lawn, B. R., "Fracture and Contact Adhesion Energies of Mica-Mica, Silica-Silica and Mica-Silica Interfaces in Dry and Moist Atmospheres," J. Amer. Ceram. Soc., in press.

White, G. S., Freiman, S. W. and Fuller, E. R., Jr., "Chemically Enhanced Fracture of Brittle Materials: Effects of Atomic Bonding," Environmental Effects on Advanced Materials, R. H. Jones and R. E. Ricker, (The Minerals, Metals and Materials Society, Warrendale, PA, 1991), pp. 147-158.

Wiederhorn, S. M., Cranmer, D. C., Kauffman, D. A., Krause, R. F., Jr. and Roberts, D. E., "Standard Tensile Test Development," in Ceramic Technology for Advanced Heat Engine Project, Semi-Annual Report for the Period October 1, 1990 Through March 30, 1991 (Oak Ridge National Laboratory, Oak Ridge, TN, July 1991), in press.

Wiederhorn, S. M. and Hockey, B. J., "High Temperature Degradation of Structural Composites," Ceramics International, 17, 243-252 (1991).

Wiederhorn, S., Hockey, B. and Chuang, T.-J., "Creep and Creep Rupture of Structural Ceramics," Toughening Mechanisms in Quasi-Brittle Materials, S. P. Shah, Ed. (Kluwer Academic Publishers, Dordecht, The Netherlands, 1991), pp. 555-576.

Wiederhorn, S. M., Hockey, B. J., Cranmer, D. C. and Yeckley, R., "Transient Creep of Hot-Isostatically Pressed Silicon Nitride," submitted to Journal of Materials Science, 1991.

Wiederhorn, S. M., Hockey, B. J., Liu, W., Baldoni, J. G. and Buljian, S.-T., "Tensile Creep of Whisker Reinforced Silicon Nitride," J. Mater. Sci., 26, 3931-39 (1991).

TRIBOLOGY

Cho, S. J., Moon, H. and Hsu, S. M., "Wear Transition Mechanism in Alumina during Sliding," accepted for publication in Acta Metal. et Mater.

Deckman, D., Jahanmir, S. and Hsu, S., "Wear Mechanisms of Alpha Alumina Lubricated with Paraffin Oil," accepted for publication in Wear.

Dong, X., Jahanmir, S. and Hsu, S. M., "Tribological Characteristics of Alpha Alumina at Elevated Temperatures," J. Am Ceram. Soc., 74, 1036-1044 (1991).

Gates, R. S. and Hsu, S. M., "Effect of Selected Chemical Compounds on the Lubrication of Silicon Nitride," Tribology Transactions, 34 (3), 417-425 (1991).

Gangopadhayay, A. and Jahanmir, S., "Friction and Wear Characteristics of Silicon Nitride-Graphite and Alumina-Graphite Composites," Tribology Trans., 34, 257-265 (1991).

Hsu, S. M. and Hu, Z., "Copper Surface Interacting with Lubricant Studied by Laser Raman Spectroscopy," STLE Annual Meeting, Montreal, Canada, April 29-May 2, 1991, to be published by the Society of Tribologists and Lubrication Engineers.

Hsu, S. M. and Hu, Z., "Tribochemical Reactions of Stearic Acid on Copper Surface Studied by Infrared and Raman Spectroscopy," ACS Symposium on Surface Chemistry in Tribology, Atlanta, GA, April 15-17, 1991, to be published by American Chemical Society.

Hsu, S. M., Lacey, P. I., Wang, Y. S. and Lee, S. W., "Wear Mechanism Maps of Ceramics," Proceedings of the 1990 International Symposium on Industrial Tribology, STLE SP-31 (Society of Tribologists and Lubrication Engineers, Park Ridge, IL, 1991) pp. 123-132.

Hsu, S. M., Lim, D. S., Wang, Y. S. and Munro, R. G., "Ceramic Wear Maps: Concepts and Method Development," Lub. Engr., 47(1), 49-54 (1991).

Hsu, S. M. and Perez J. M., "A Critical Assessment of Lubrication Technology for Engines," Coatings for Advanced Heat Engines, U. S. DOE Pub. # CONF 9008151 (U. S. Dept. of Energy, Washington, DC, 1991) pp. III-9 thru III-16.

Hu, Z., Hsu, S. M. and Wang, P. S., "Tribochemical and Thermochemical Reactions of Stearic Acid on Copper surface Studied by Infrared Microscopy," STLE Preprint 91-AM-3B-1, 1991.

Ives, L. K., "Abrasive Wear by Coal-Fueled Engine Particles," Proceedings of Corrosion-Erosion-Wear of Materials at Elevated Temperatures, A. V. Levy, Ed. (National Association of Corrosion Engineers, Houston, TX, 1991) pp. 29-1 thru 29-20.

Ives, L. K., "Wear by Coal-Fueled Diesel Engine Particles," Proceedings of the Conference on Fossil Energy Materials, Oak Ridge, TN, May 14-16, 1991, in press.

Jahanmir, S., "Ceramic Bearing Technology," NIST Special Publication, in press.

Jahanmir, S., "Development of Wear Test Methods for Advanced Materials," Proceedings of International Symposium on Pre-Standards Research for Advanced Materials, in press.

Jahanmir, S. and Dong, X., "Mechanism of Mild to Severe Wear Transition in Alpha Alumina," ASME Paper No. 91-Trib-28, to be published in Journal of Tribology.

Jahanmir, S., Ives, L. K., Ruff, A. W. and Peterson, M. B., "Ceramic Machining: An Assessment of Current Technology and Research Needs," NIST Special Publication, in press.

Ku, C. S., Pei, P. and Hsu, S. M., "A Modified Thin-Film Oxygen Uptake Test for the Evaluation of Lubricant Stability in ASTM IIIE Engine Sequence Test," SAE Paper No. 902121, Society of Automotive Engineers, Warrendale, PA, 1990.

Lacey, P., Hsu, S. M., Gates, R. S., Lee, S., Ives, L., Ku, C., Pei, P., Wang, Y., Whitenton, E. P. and Munro, R. G., "Wear Mechanisms of Valves and Valve Seat Inserts in a Gas-Fired Reciprocating Engine," to be published by the Gas Research Institute, Chicago, IL.

Lee, S. W., Hsu, S. M. and Munro, R. G., "Ceramic Wear Maps: SiC Whisker Reinforced Alumina," in Tribology of Composite Materials Proceedings of a Conference, Oak Ridge, TN, May 1-3, 1990 (ASM International, Materials Park, OH, 1990) pp. 35-41.

Perez, J. M., "High Temperature Liquid Lubricants," Coatings for Advanced Heat Engines, U. S. DOE Pub. # CONF 9008151 (U. S. Dept. of Energy, Washington, DC, 1991) pp. III-41 thru III-50.

Perez, J. M., Ku, C. S. and Hsu, S. M., "High Temperature Liquid Lubricant for Advanced Engines," SAE Technical Paper 910454, International Congress and Exposition, Detroit, MI, Feb. 25-March 1, 1991.

Perez, J. M., Ku, C. S., Pei, P., Hegemann, B. E. and Hsu, S. M., "Characterization of Tricresyl Phosphate Lubricating Films by Micro-Fourier Transform Infrared Spectroscopy," STLE Tribology Trans., 33, 131-139 (1990).

Perez, J. M., Pei, P., Zhang, Y. and Hsu, S. M., "Diesel Deposit Forming Tendencies-Microanalysis Methods," SAE Technical Paper 910750, International Congress and Exposition, Detroit, MI, Feb. 25-March 1, 1991.

Peterson, M. B., Jahanmir, S. and Ives, L. K., "Lubrication of Mechanical Components at High Temperatures," Coatings for Advanced Heat Engines, U. S. DOE Pub. # CONF 9008151 (U. S. Dept. of Energy, Washington, DC, 1991) pp. III-65 thru III-74.

Ruff, A. W., "Considerations on Data Requirements for Tribological Modeling," Tribological Modeling for Mechanical Designers, K. C. Ludema and R. G. Bayer, Eds., STP 1105 (American Society for Testing and Materials, Philadelphia, PA, 1991) pp. 127-142.

Ruff, A. W. and Lashmore, D. S., "Effect of Layer Spacing on Wear of Nickel-Copper Multi-layer Alloys," Wear of Materials - 1991, K. C. Ludema, Ed. (American Society of Mechanical Engineers, New York, NY, 1991) pp. 137-142.

Ruff, A. W. and Peterson, M. B., "Wear Mechanisms in Self-Lubricating Metal Matrix Composites," Tribology of Composite Materials, P. J. Blau and C. S. Yust, Eds. (ASM International, Materials Park, OH, 1990) pp. 43-50.

Wang, Y. S., Hsu, S. M. and Munro, R. G., "Ceramic Wear Maps: Alumina," Lub. Engr., 47(1), 63-69 (1991).

Wang, Y. S., Hsu, S. M. and Munro, R. G., "A Wear Model for Alumina Sliding Wear," Proceedings of the Japan International Conference on Tribology, Nagoya, 1990, Vol. II, (JST, Tokyo, Japan, 1990) pp. 1225-1230.

Wang, F. X., Lacey, P., Gates, R. S. and Hsu, S. M., "A Study of the Relative Surface Conformity between Two Surfaces in Sliding Contact," ASME preprint, 90-Trib-61, October 1990.

Zhang, Y. and Hsu, S. M., "Inhibition Mechanisms of Some Antioxidants in Lubricant Oxidation Using a Chemiluminescence Technique," to be published in Tribology Trans. of STLE.

ELECTRONIC MATERIALS

Brody, P. S., Rod, B. J., Bennett, K. W., Cook, L. P., Schenck, P. K., Vaudin, M. D., Wong-Ng, W. and Chiang, C. K., "Preparation, Microstructure and Ferroelectric Properties of Laser-Deposited thin $BaTiO_3$ and Zirconate-Titanate Films," to be published in Ferroelectrics.

Carpenter, J. A., Jr., "Measurement of Properties of Materials in Multilayer Ceramic Capacitors and Microelectronic Packaging," Metal-Ceramic Joining, P. Kumar and V. A. Greenhut, Eds., (The Minerals, Metals and Materials Society, Warrendale, PA, 1991) pp. 205-217.

Carpenter, J. A., Jr., "NIST Program on Measurements of the Properties of Materials in Electronic Packaging," Electronic Packaging Materials Science, E. D. Lillie et al., Eds., MRS Symposium Proceedings, Vol. 203 (Materials Research Society, Pittsburgh, PA 1991), pp. 119-128.

Chiang, C. K., Wong-Ng, W., Schenck, P. K., Cook, L. P., Vaudin, M. D., Brody, P. S., Rod, B. J. and Benedetto, J. M., "Characterization of Lead Zirconate-Titanate Thin Films Prepared by Pulsed Laser Deposition," to be published in Material Research Society Symposium Series, 1991.

Cook, L. P. "Thermodynamic Calculations of Phase Equilibria and Enthalpy-Yield During Progressive Oxidation of SCEPS Fuels," in proceedings of 27th JANNAF Combustion Symposium, Nov. 5-9, 1990, Chemical Propulsion Agency, Laurel, Md, in press.

Cook, L. P., Vaudin, M. D., Schenck, P. K., Wong-Ng, W., Chiang, C. K. and Brody, P. S., "Microstructural Changes During Processing of Laser-Deposited $BaTiO_3$ and PZT Thin Films," Evolution of Thin-Film and Surface Microstructure, C. V. Thomson et al., Eds., MRS Symposium Proceedings, Vol. 202 (Materials Research Society, Pittsburgh, PA, 1991) pp. 241-246.

Cook, L. P., Wong-Ng, W., Chiang, C. K. and Bennett, L. H., "Stoichiometric Variations in the 2122 (Tl:Ca:Ba:Cu Oxide) High T_c Phase," Proceedings of ACerS Symposium on Ceramic Superconductors, Orlando, FL, Nov. 1990, K. M. Nair, Ed., in press.

Cook, L. P., Wong-Ng, W., Huang, T., Schenck, P. K., Vaudin, M. D., Chiang, C. K. and Brody, P. S., "Thermal Processing of Laser-Deposited $BaTiO_3$," to be published in Proceedings of the International Conference on Material and Process Characterization for VLSI, Shanghai, 1991.

Cook, L. P., Wong-Ng, W., Schenck, P. K., Chiang, C. K. and Vaudin, M. D., "Thallia Based Superconducting Thin Films by a Two-Stage Laser Deposition/Vapor Transport Process," to be published in Proceedings of International Conference on Material and Process Characterization for VLSI, Shanghai, 1991.

Deb, K. K., Hill, M. D., Roth, R. S. and Kelly, J. F., "Dielectric and Pyroelectric Properties of Doped PZN Ceramic Materials," submitted to B. Amer. Ceram. Soc.

Etz, E. S., Schroeder, T. D. and Wong-Ng, W., "Raman and Fluorescence Spectra Observed in Laser Microprobe Measurements of Several Compositions in the Ln-Ba-Cu-O System," submitted to Microbeam Analysis-1990, J. R. Michael and Peter Ingram, Eds.

Freiman, S. W., "Stress-Corrosion Cracking of Glasses and Ceramics," Stress-Corrosion Cracking: Materials Performance and Evaluation, (ASM International, Materials Park, OH) in press.

Freiman, S.W. and Fuller, E.R., Jr., "Mechanical Reliability of High T_c Superconductors," Superconductivity II (The American Ceramic Society, Inc., Westerville, OH, 1991), pp. 547-559.

Gatehouse, B. M., Platts, S. N. and Roth, R. S., "The Crystal Structure of Low-$Ba_3P_4O_{13}$," submitted to Acta Cryst. C.

Hill, M. D., Wong-Ng, W., Chiang, C. K., Fuller, E. R., Jr., Paretzkin, B., Lagergren, E. and Kacker, R., "Effect of Composition on Superconducting Properties in the System Ba-Y-Gd-Cu-O," submitted to the Journal of the American Ceramic Society.

Kacker, R., Lagergren, E., Hill, M., Wong-Ng, W., Chiang, C. K., and Fuller, E., "Alternate Formulation of High Temperature Superconducting Ceramics," Communications in Statistics (Theory and Methods), 20 (2), 441 (1991).

Piermarini, G. J. and Block, S., "Energetic Materials Under High Pressure I. 1,4 Dinitrocubane," to be published in Propellants, Explosives, and Pyrotechnics.

Piermarini, G. J., Block, S., Russell, T. P. and Miller, P. J., "High Pressure Phase Transition in γ Hexanitrohexaazaisowurtzitane," submitted to J. Phys. Chem.

Rawn, C. J., Roth, R. S. and McMurdie, H. F., "Powder X-Ray Diffraction Data for $Ca_2Bi_2O_5$ and $Ca_4Bi_6O_{13}$," submitted to Powder Diffraction.

Raynes, A. S., Freiman, S. W., Gayle, F. W. and Kaiser, D. L., "Fracture Toughness of $YBa_2Cu_3O_{6+x}$ Single Crystals: Anisotropy and Twinning Effects," Journal of Applied Physics, in press.

Roth, R. S., Editor, "Chemistry of Electronic Materials," Proceedings of the International Conference on the Chemistry of Electronic Ceramic Materials, Jackson Hole, WY, August 17-22, 1990, NIST Special Publication 804, January 1991 .

Roth, R. S., Rawn, C. J., and Hill, M. D., "Synthesis and Characterization of Phases in the System Ba-Au-Ag-O_2," Chemistry of Electronic Materials, R. S. Roth, Ed., NIST Special Publication 804, January 1991, pp. 225-236.

Russell, T. P., Miller, P. J., Piermarini, G. J., Block, S., Gilardi, R. and George, G., "Investigation of Hexanitrohexaazaisowurtzitane," Proceedings of Joint Army, Navy, NASA, Air Force (JANNAF) Meeting, to be published by CPIA-Chemical Propulsion Information Agency.

Torardi, C. C., Parise, J. B., Santoro, A., Rawn, C. J., Roth, R. S. and Burton, B. P., "$Sr_2Bi_2O_5$: A Structure Containing 3-Coordinated Bismuth," Journal of Solid State Chemistry, 93, 228-235 (1991).

Vaudin, M. D. and Carter, C., "Studies of Ceramics Using Back Scatter Diffraction Patterns in the SEM," to be published in Proceedings of 25th Anniversary Meeting of Microbeam Analysis Society, 1991.

White, G. S., Raynes, A. S. and Freiman, S. W., "Fracture Behavior of Cyclically Loaded PZT. II.," submitted to J. Amer. Ceramic Society.

Wong-Ng, W. and Cook, L. P., "Oxidation/Reduction Melting Reactions in The System BaO-Y_2O_3-CuO_x. I. Methods," Proceedings of the ACerS Symposium on Ceramic Superconductors, Orlando, FL, Nov. 1990, K. M. Nair, Ed., in press.

Wong-Ng, W. and Bennett, L. H., "Effects of Oxygen on Yttrium-and Bismuth-Type Superconductors," submitted to TMS-AIME Proceedings.

Wong-Ng, W., Cook, L. P., Chiang, C. K., Vaudin, M., Bennett, L. H. and Fuller, Jr., E. R., "Correlations of the Structural Phase Transformation of the High T_c Superconducting Materials, $Ba_2RCu_3O_{6+x}$, in Air," to be published in J. Amer. Ceramic Soc.

Wong-Ng, W., Cook, L. P., Schenck, P. K., Vaudin, M. D. and Chiang, C. K., "PZT Films Prepared by the Laser Deposition Technique," to be published in Proceedings of International Conference on Material and Process Characterization for VLSI, Shanghai, 1991.

Wong-Ng, W. and Mighell, A. D., "Crystallographic Databases for Chemical and Material Analyses," distributed at the Pacific-International Congress on X-Ray Analytical Methods, Hawaii, August 1991.

Wong-Ng, W., Paretzkin, B. and Fuller, E. R., Jr., "Crystal Chemistry and Phase Equilibria Studies of the BaO-R_2O_3-CuO Systems. X-Ray Characterization of BaR_2O_4, R = Lanthanides," submitted to Powder Diffraction.

Wong-Ng, W., White, G. S. and Freiman, S. W., "Application of Molecular Orbital Calculations to Fracture Mechanics: Effect of Applied Strain on Charge Distribution in Silica," submitted to Journal American Ceramics Society.

OPTICAL MATERIALS

Bennett, L. H., Swartzendruber, L. J. and Kaiser, D. L., "Meissner, Shielding and Flux Loss Behavior in Single-Crystal $YBa_2Cu_3O_{6+x}$," J. Appl. Phys., 69, 4889 (1991).

Bennett, L. H., Swartzendruber, L. J., Kaiser, D. L., Gayle, F. W., Blendell, J., Habib, M. and Seyoum, H. M., "Thermoremanance and Meissner Effect in QMG and Single Crystal YBCO," submitted to J. Magnetism and Magnetic Matls.

Bohandy, J., Kim, B. F., Moorjani, K., Adrian, F. J., Kaiser, D. L., Swartzendruber, L. J., Gayle, F. W. and Bennett, L. H., "Twin Planes, Impurities, and Anisotropy in YBa_2CuO_{7-x} Single Crystals," submitted to Appl. Phys. Lett.

Farabaugh, E. N., Feldman, A. and Robins, L. H., "Effects of Multiple Filament Geometry in the Hot Filament Deposition of Diamond Films," Applications of Diamond Films and Related Materials, Y. Tzeng et al., Eds., Elsevier Monograph 73 (Elsevier Science Publishers, Amsterdam, The Netherlands, 1991) pp. 483-488.

Farabaugh, E. N., Feldman, A. and Robins, L. H., "Influence of Filament Geometry on Hot Filament CVD Growth of Diamond Films," New Diamond Science and Technology, R. Messier and J. T. Glass, Eds., MRS International Conference Proceedings Series (Materials Research Society, Pittsburgh, PA, 1991) pp. 449-454.

Feldman, A., Frederikse, H.P.R. and Norton, S. J., "Analysis of Thermal Wave Propagation in Diamond Films," Diamond Optics III, A. Feldman and S. Holly, Eds., SPIE Vol. 1325 (Society pf Photo-optical Instrumentation Engineers, Bellingham, WA, 1990) pp. 304-314.

Feldman, A., Frederikse, H.P.R. and Norton, S. J., "Thermal Wave Propagation in Diamond Films," New Diamond Science and Technology, R. Messier and J. T. Glass, Eds., MRS International Conference Proceedings Series (Materials Research Society, Pittsburgh, PA, 1991) pp. 881-886.

Feldman, A. and Holly, S., Editors, Diamond Optics IV, SPIE Vol.1534, (Society of Photo-optical Instrumentation Engineers, Bellingham, WA) in press.

Feldman, A. and Robins, L. H., "Critical Assessment of Optical Properties of CVD Diamond," Applications of Diamond Films and Related Materials, Y. Tzeng et al., Eds., Elsevier Monograph 73 (Elsevier Science Publishers, Amsterdam, The Netherlands, 1991) pp. 181-188.

Gayle, F. W. and Kaiser, D. L., "The Nature of [001] Tilt Boundaries in $YBa_2Cu_3O_{7-x}$," J. Mater. Res., 6, 908 (1991).

Kaiser, D. L., Gayle, F. W., Swartzendruber, L. J., Bennett, L. H. and McMichael, R., "Effect of Twin Boundaries on Flux Pinning in YBa_2CuO_{7-x} at Low and Intermediate Magnetic Fields," J. Appl. Phys., in press.

Robins, L. H., Farabaugh, E. N. and Feldman, A., "Determination of the Optical Constants of Thin Chemical-vapor-deposited Diamond Windows from 0.5 to 6.5 eV," Diamond Optics IV, A. Feldman and S. Holly, Eds., SPIE Vol.1534 (Society pf Photo-optical Instrumentation Engineers, Bellingham, WA) in press.

Robins, L. H., Farabaugh, E. N., Feldman, A. and Cook, L. P., "Inverse Correlation between the Intensity of Luminescence Excited by Electrons and by Visible Light in Chemical-vapor-deposited Diamond Films," Phys. Rev. B, 43, 9102-9107 (1991).

Robins, L. H., Farabaugh, E. N. and Feldman, A., "Line Shape Analysis of the Raman Spectrum of Diamond Films Grown by Hot-filament and Microwave-plasma Chemical Vapor Deposition," J. Mater. Res., 5, 2456-2468 (1990).

Robins, L. H., Farabaugh, E. N. and Feldman, A., "Spatially and Spectrally Resolved Cathodoluminescence of Hot-filament Chemical-vapor-deposited Diamond Particles," J. Mater. Res., in press.

Robins, L. H., Farabaugh, E. N. and Feldman, A., "Spatially and Spectrally Resolved Cathodoluminescence Measurements of CVD-grown Diamond Particles and Films," Proceedings of the 2nd International Symposium on Diamond Materials (The Electrochemical Society, Pennington, NJ, 1991) in press.

Robins, L. H., Farabaugh, E. N. and Feldman, A., "Studies of Defects in Diamond Films and Particles by Raman and Luminescence Spectroscopies," Diamond Optics III, A. Feldman and S. Holly, Eds., SPIE Vol. 1325 (Society pf Photo-optical Instrumentation Engineers, Bellingham, WA, 1990) pp. 130-141.

Robins, L. H., Tjossem, P.J.H., Smyth, K. C., Barnes, P. Y., Farabaugh, E. N. and Feldman, A., "Photoluminescence Excitation by Band-gap Optical Absorption in Chemical Vapor Deposition of Diamond Films," J. Appl. Phys., 69, 3702-3708 (1991).

Robins, L. H., Whitenton, E. P., Farabaugh, E. N. and Feldman, A., "Surface Roughness Evaluation of Diamond Films Grown on Substrates with a High Density of Nucleation Sites," New Diamond Science and Technology, R. Messier and J. T. Glass, Eds., MRS International Conference Proceedings Series (Materials Research Society, Pittsburgh, PA, 1991) pp. 619-624.

Shechtman, D., Farabaugh, E. N., Robins, L. H., Feldman, A. and Hutchison, J. L., "High Resolution Electron Microscopy of Diamond Film Growth Defects and Their Interactions," Diamond Optics IV, A. Feldman and S. Holly, Eds., SPIE Vol.1534 (Society pf Photo-optical Instrumentation Engineers, Bellingham, WA) in press.

Swartzendruber, L. J., Kaiser, D. L., Gayle, F. W., Bennett, L. H. and Roitburd, A., "Low Field Flux Pinning in Twinned and Detwinned Single Crystals of YBa_2CuO_{7-x}," Appl. Phys. Lett., 58, 1566 (1991).

Tzeng, Y., Yoshikawa, M., Murakawa, M. and Feldman, A., Editors, Applications of Diamond Films and Related Materials, Elsevier Monograph 73 (Elsevier Science Publishers, Amsterdam, The Netherlands, 1991).

MATERIALS MICROSTRUCTURE CHARACTERIZATION

Black, D. R., Burdette, H. E., Dobbyn, R. C., Spal, R. D. and Kuriyama, M., "Advanced X-ray Imaging Methods for Ceramics," Ceramics Bulletin, 70, 1004 (1991).

Black, D. R., Burdette, H. E., Kuriyama, M. and Spal, R. D., "Diffraction Imaging of Polycrystalline Materials," J. Mater. Research, 6, 1469 (1991).

Black, D. R., Posthill, J. B., Rudder, R. A., Hudson, G. C., Malta, D. P., Fountain, G. G., Thomas, R. E., Markunas, R. J., Humphreys, T. P. and Nemanich, R. J., "Substrate Effects and the Growth of Homoepitaxial Diamond (100) Layers Using Low Pressure rf Plasma Enhanced Chemical Vapor Deposition," Proceedings of the 2nd International Symposium on Diamond Materials, A. J. Purdes et al., Eds. (The Electrochemical Society, Pennington, NJ, 1991) p. 274.

Bouldin, C. E., Kim, K. H., Bell, M. I., Dozier, C. M. and Frietag, R. K., "Correcting for the X-ray Energy Calibration Error Caused by Misalignment of a Right-Angle Linkage Monochromator," Rev. Sci. Inst., 62, 982 (1991).

Bouldin, C. E., Webb, A. W. and Kim, K. H., "The Valence of Copper in $LaCuO_3$: An X-ray Absorption Study," Solid State Comm., 79(6) 507-508 (1991).

Fischer, D. A., Donovan, R., Jiang, L. Q. and Strongin, M., "Deuteration of Propylene Over Palladium Overlayers on Tantalum," to be submitted to Surface Science.

Fischer, D. A., Gland, J. L. and Rufael, T., "Ultra-Soft X-ray Absorption Detected by Fluorescence Yield: An In Situ Method for Characterizing Adsorbates and Surface Reactions," Surface Science of Catalysis: In-Situ Probes and REaction Kinetics, F. Hoffman, Editor (American Chemical Society, Washington, DC) submitted.

Fischer, D. A. and Phillips, W., "Soft X-ray Transmission of Thin Film Diamond: Applications to Detectors and High Pressure Gas Cells," to be submitted to J. of Vacuum Science and Technology.

Fogarty, G., Cronin-Golomb, M. and Steiner, B., "Synchrotron X-ray Diffraction Imaging of Photorefractive Crystals," Proceedings of Photorefractive Materials Conference, 1991, Technical Digest Series (Optical Society of America, Washington, D. C., 1991) pp. 162-165.

Long, G. G., Black, D. R., Feldman, A., Farabaugh, E. N., Spal, R. D., Tanaka, D. K. and Zhang, Z., "Structure of Vapor-deposited Yttria and Zirconia Thin Films," Thin Solid Films, in press.

Long, G. G., Davis, G. D., Moshier, W. C. and Black, D. R., "Passive Film Structure of Super-Saturated Al-Mo Alloys," J. Electrochem. Soc., 138, 3194-3199 (1991).

Long, G. G., Jemian, P. R., Weertman, J. R. and Spal, R. D., "Characterization of Modified Fe9CrlMo Steel by Anomalous Small-Angle X-Ray Scattering," Acta Metallurgica, in press.

Long, G. G., Krueger, S., Black, D. R., Minor, D., Jemian, P. R., Nieman, G. and Page, R. A., "Evolution of the Pore Size Distribution in Final Stage Sintering of Alumina Measured by Small-Angle X-Ray Scattering," J. Am. Ceram. Soc., accepted.

Steiner, B., Dobbyn, R. C., Black, D., Burdette, H., Kuriyama, M., Spal, R., van den Berg, L., Fripp, A., Simchick, R., Lal, R., Batra, A., Matthiesen, D. and Ditchek, B., "High Resolution Synchrotron X-Radiation Diffraction Imaging of Crystals Grown in Microgravity and Closely Related Terrestrial Crystals," J. Res. NIST, 96, 305-331 (1991).

Steiner, B. and Dobbyn, R. D., "Crystal Regularity with High-Resolution Synchrotron X-Radiation Diffraction Imaging," Bull. Am Cer. Soc., 70, 1017-1023 (1991).

Steiner, B., Dobbyn, R. C., Black, D., Burdette, H., Kuriyama, M., Spal, R., van den Berg, L., Fripp, A., Simchick, R., Lal, R., Batra, A., Matthiesen, D. and Ditchek, B., "High Resolution Diffraction Imaging of Crystals Grown in Microgravity and Closely Related Terrestrial Crystals," NIST Technical Note 1287 (1991).

Steiner, B., Dobbyn, R. C., Black, D., Burdette, H., Kuriyama, M., Spal, R., van den Berg, L., Fripp, A., Simchick, R., Lal, R., Batra, A., Matthiesen, D. and Ditchek, B., "High Resolution Synchrotron X-radiation Diffraction Imaging of Crystals Grown in Microgravity and Closely Related Terrestrial Crystals," Proceedings of SPIE (Society of Photo-optical Instrumentation Engineers, Bellingham, WA) in press.

Steiner, B., Dobbyn, R., Black, D. R., Burdette, H., Kuriyama, M., Spal, R., Simchick, R. and Fripp, A., "High Resolution Diffraction Imaging of Lead Tin Telluride Grown in Microgravity on Space Shuttle STS 61A and on the Ground," J. Crystal Growth, in press.

Steiner, B., Dobbyn, R. C., Black, D., Burdette, H., Kuriyama, M., Spal, R. and van den Berg, L., "High Resolution Diffraction Imaging of Mercuric Iodide Crystals Grown in Spacelab III and on the Ground," submitted to the J. Cryst. Growth.

Steiner, B., Kuriyama, M. and Dobbyn, R.C., "Insight into the Genesis of Irregularity during Crystal Growth Achieved through High Sensitivity Monochromatic Synchrotron X-radiation Diffraction Imaging (Topography)," Prog. Crystal Growth and Charact., 20, 189-216 (1990).

Woicik, J. C., Bouldin, C. E., Bell, M. I., Cross, J. O., Tweet, D. J., Swanson, B. D., Zhang, T. M., Sorensen, L. B., King, C. A., Hoyt, J. L., Pianetta, P. and Gibbons, J. F., "Conservation of Bond Lengths in Strained Ge-Si Layers," Phys. Rev. B, 43, 2419 (1991).

Woicik, J. C., Bouldin, C. E., Cross, J. O., Sorensen, L. B. and King, C. A., "Extended X-ray Absorption Fine Structure and X-ray Diffraction Study of Strain and Bond Distortions in Epitaxial Semiconductor Layers," J. Vac. Sci. Technol. B, 9, 2194 (1991).

Woicik, J. C., Karlin, B. A. and Cowan, P. L., "X-ray, Soft X-ray, and VUV Beam Position Monitor," Rev. Sci. Instrum., in press.

Woicik, J. C., Kendelewicz, T., Miyano, K. E., Bouldin, C. E., Meissner, P. L., Pianetta, P. and Spicer, W. E., "Local Bonding Structure of Sb on Si(111) by Surface Extended X-ray Absorption Fine Structure and Photoemission," Phys. Rev. B, 43, 4331 (1991).

Woicik, J. C., Kendelewicz, T., Miyano, K. E., Bouldin, C. E., Meissner, P. L., Pianetta, P. and Spicer, W. E., "Structure of the Si(111) $\sqrt{3}$x$\sqrt{3}$-Sb Interface by Surface X-ray Absorption Fine Structure and Photoemission," J. Vac. Sci. Technol. A, 9, 1956 (1991).

Woicik, J. C., Kendelewicz, T., Miyano, K. E., Cowan, P. L., Bouldin, C. E., Karlin, B. A., Pianetta, P. and Spicer, W. E., "Determination of the Sb/Si(111) Interfacial Structure by Back-Reflection X-ray Standing Wave and Surface Extended X-ray Absorption Fine Structure Techniques," Phys. Rev. B, 44, 3475 (1991).

Woicik, J. C., Kendelewicz, T., Miyano, K. E., Cowan, P. L., Bouldin, C. E., Karlin, B. A., Pianetta, P. and Spicer, W. E., "Synchrotron X-ray Standing Wave Study of Sb on GaAs(110) and InP(110)," J. Vac. Sci. Technol. B, 9, 2290 (1991).

Woicik, J. C., Kendelewicz, T., Miyano, K. E., Cowan, P. L., Bouldin, C. E., Karlin, B. A., Pianetta, P. and Spicer, W. E., "X-ray Standing Wave Measurement of the InP(110) Surface Relaxation," submitted for publication to Phys. Rev. Lett.

Woicik, J. C., Kendelewicz, T., Miyano, K. E. Cowan, P. L., Bouldin, C. E., Karlin, B. A., Pianetta, P. and Spicer, W. E., "X-ray Standing Wave Study of Monolayers of Sb on (110) Surfaces of III-V Semiconductors," to be submitted to J. of Vacuum Science and Technology.

Woicik, J. C., Kendelewicz, T., Miyano, K. E., Cowan, P. L., Bouldin, C. E., Richter, M., Karlin, B. A., Pianetta, P. and Spicer, W. E., "Extended X-ray Absorption Fine Structure and X-ray Standing Wave Study of the Clean InP(110) Surface Relaxation," to be submitted to J. of Vacuum Science and Technology.

Woicik, J. C. and Pianetta, P., "Studies of Si-Ge Interfaces with Surface EXAFS and Photoemission," Synchrotron Radiation Research: Advances in Surface Science, R. Z. Bachrack, Ed. (Plenum Press, New York, NY) in press.

Woicik, J. C., Richter, M., Nogami, J., Pianetta, P., Miyano, K. E., Baski, A. A., Kendelewicz, T., Bouldin, C. E., Spicer, W. E., Quate, C. F. and Lindau, I., "Surface Extended X-ray Absorption Fine Structure and Scanning Tunneling Microscopy of Si(001) 2x1 - Sb," Phys. Rev. Lett., 65, 3417 (1990).

DATA BASE ACTIVITIES

Begley, E. F., "Program Infrastructure," Building of Materials Databases, C. Newton, Ed., ASTM Special Publication (American Society for Testing and Materials, Philadelphia, PA) to be published in 1992.

Begley, E. F. and Munro, R. G., "Issues in the Development of a Materials Selector Expert System," Proceedings of the Third International Symposium on Computerization and Use of Materials Property Data (Cambridge, UK, Sept. 9-11, 1991), in press.

Begley, E. F. and Munro, R. G., "The Structural Ceramics Database," NISTIR 4601 (National Institute of Standards and Technology, 1991).

Munro, R. G., "Ceramic Properties Data Base Systems," Engineered Materials Handbook: Ceramics & Glasses, S. J. Schneider, Jr., Ed. (ASM International, Materials Park, OH) in press.

Munro, R. G., "Characterizing Materials Properties for Ceramic Matrix Composites," Proceedings of the Advanced Materials and Processing Technology Workshops, C. Y. Ho and S. K. El-Rahaiby, Eds. (1991) in press.

Munro, R. G. and Begley, E. F., "Materials Properties for Advanced Structural Ceramics," NISTIR 4602 (National Institute of Standards and Technology, 1991).

Munro, R. G. and Begley, E. F., "The Structural Ceramics Database: Data Acquisition Format for Monolithic Ceramics," ASTM J. Testing and Evaluation, 19 (3), 250-255 (1991).

Munro, R. G. and Begley, E. F., "Update on the Structural Ceramics Database," Center for Advanced Materials Newsletter, 5 (1), 18 (1991).

CERAMICS DIVISION PATENTS

1991

Diamond Coated Laminates and Methods of Producing Same	A. Feldman E. N. Farabaugh
High Resolution X-Ray Microtomographic Detector	R. D. Spal R. C. Dobbyn M. Kuriyama
A Colloidal Processing Method for Coating Ceramic Reinforcing Agents U.S. Patent No. 5,039,550, August 1991	S. Malghan C. Ostertag
Process for the Fabrication of Ceramic Monoliths by Laser-Assisted Chemical Vapor Infiltration U.S. Patent No. 5,001,001, March 19, 1991	J. Ritter
A Method for Making Translucent High Purity Transparent Silicon Nitride	A. Pechenik G. Piermarini S. Block S. Danforth

1990

Novel Synergistic Additive Packages Containing High Molecular Weight Antioxidants for High Temperature Lubricants	S. Hsu J. Perez C. Ku Y. Zhang
Low Energy (Thermal) Neutron Absorbing Glass	D. Blackburn (Retired) C. Stone D. Cranmer D. Kauffman J. Grudl
Process for Elimination of Twins in Perovskite-Type Superconducting Single Crystals	D. Kaiser F. Gayle
A Method for Fabrication of Materials from Nano-Sized Particles Using High Pressure and Cryogenic Temperatures	A. Pechenik G. Piermarini
Aluminum Hydroxides as Solid Lubricants U.S. Patent 4919829, issued April 24, 1990	R. Gates S. Hsu

1989

Ultraviolet Transmitting Glass for 308mm Ring Dye Laser	D. Blackburn D. Cranmer D. Kauffman
Buffered Cell for Sintering of High T_c Thallium Containing Ceramics	L. Cook
Polished Plates of Chemical Vapor Deposited Diamond	A. Feldman E. Farabaugh
Additive Packages Containing High Molecular Weight Antioxidants for High Temp Lubricant	S. Hsu J. Perez C. Ku
A Novel Fluid to Solubilize High Temperature Liquid Lubricant Antioxidants	J. Perez C. Ku S. Hsu
A Process for the Controlled Preparation of a Composite of Ultra-Fine Magnetic Particles Homogeneously Dispersed in a Dielectric Matrix	J. Ritter R. Shull
Optical Sensor: Molecular Orientation and Viscosity of Polymeric Materials	A. Bur R. Lowry R. Roth
Elimination of Twins in Perovskite-Type Superconducting Single Crystals	F. Gayle D. Kaiser

1988

Stress-Free Sintering of Fiber-Reinforced Ceramic Composites	C. Ostertag
Electrode Array for Analysis of Particles in Slurries	A. Dragoo
Quantitative & Qualitative Technique for Assessing Stresses During Densification	C. Ostertag
Process for the Preparation of Fiber-Reinforced Ceramic Matrix Composites	W. Haller U. Deshmukh
A Process for the Chemical Synthesis and Forming of BiPbSrCaCuO and BiSrCaCuO High Temperature Superconductors Materials	J. Ritter

Co-Precipitation Synthesis of Precursors to Bismuth Containing Superconductors	J. Ritter
Low Temperature Chemical Synthesis of Precursors to $BiCaSrCuO_x$ High Temperature Superconductor Powders	J. Ritter
High Pressure Process for Producing Transformation Toughened Ceramics	S. Block G. Piermarini
Superconductor-Polymer Composite	A. DeReggi C. Chiang G. David

"Applications of Diamond Films and Related Materials, ADC91", Auburn University, Auburn, AL, A. Feldman, Organizer, August 20-22, 1991. Conference cosponsored by NIST to review applications of the new diamond technology.

Symposium on Diamond Optics IV, at 35th Annual International Technical Symposium on Optical and Optoelectronic Applied Science and Engineering, A. Feldman, Organizer, July 21-26, 1991. Conference to review applications of diamond to optics.

The NASA Microgravity Sciences Diffraction Imaging Program: Accomplishments and Future Directions, Washington, D.C., Bruce Steiner, February 5, 1991, 25 attendees. Full review of initial program results and formation of consensus on crystals to be studied this year.

High Resolution Diffraction Imaging of Space Related Crystals: The Second Generation, Huntsville, Bruce Steiner, September 19, 1991, 20 attendees. Initial review of second year program results and discussion of crystals to be studied this coming year.

Microanalysis of Electronics, J. A. Carpenter, Jr., Organizer, May 29-30, 1991, NIST, Gaithersburg, MD. Symposium/Short Course sponsored by Washington, D.C. Chapter of ASM International. Reviewed current state-of-the-art in techniques for elemental and microstructural characterization of electronics at the microscale.

Fundamentals of Carbon/Carbon, D. C. Cranmer, Organizer, December 6-7, 1990, Gaithersburg, MD. Workshop sponsored by Air Force Office of Scientific Research, to review current state-of-the-art and future research needs in carbon.carbon composites in structural applications.

Ceramic Bearing Technology Workshop, Said Jahanmir, Organizing Chairman, April 17-18, 1991. The workshop was co-sponsored by DARPA and NIST, to review the state-of-the-art in ceramic bearing technology and recommend research areas to enhance the utilization of silicon nitrite bearings.

STANDARD REFERENCE MATERIALS

The Division provides science, industries, and government a central course of well characterized materials certified for chemical composition of physical or chemical properties. These materials are issued with a certification and are used to calibrate instruments, to evaluate analytical methods, or to produce scientific data which can be referred to a common base.

DESCRIPTION	SRM NUMBER
Alumina Elasticity	718
Alumina Glass Anneal Point	714
Alumina Glass Anneal Point	715
Alumina Melting Point	742
Aluminum Magnetic Susceptibility	763-1
Aluminum Magnetic Susceptibility	763-2
Aluminum Magnetic Susceptibility	763-3
Barium Glass Anneal Point	713
Borosilicate Glass Composition	93(A)
Borosilicate Glass Thermal Expansion	731L1
Borosilicate Glass Thermal Expansion	731L2
Borosilicate Glass Thermal Expansion	731L3
Cadmium Vapor Pressure	746
Chlorine in Base Oil	1818
Container Glass Composition	621
Container Glass Leaching	622
Container Glass Leaching	623
Copper Thermal Expansion	736L1
Fused Silica Thermal Expansion	739L1
Fused Silica Thermal Expansion	739L2
Fused Silica Thermal Expansion	739L3
Glass Analytical Standard	1835
Glass Dielectric Constant	774
Glass Electrical Resistance	624
Glass Fluorescence Source	477
Glass Liquidus Temperature	773
Glass Refractive Index	1820
Glass Sand (High Iron)	81A
Glass Sand (Low Iron)	165A
Glass Stress Optical Coefficient	708
Glass Stress Optical Coefficient	709
Glass Viscosity Standard Renewal	717
Gold Vapor Pressure	745
High Boron Glass Viscosity	717
Intensity XRD Set	674
Lead Barium Glass Composition	89
Lead Glass Anneal Point	712
Lead-Silica Glass High Temperature Resistivity	1414*
Lead Glass Viscosity	711
Line Profile	660
Liquids Refractive Index	1823
Low Boron Glass Composition	92
Lube Oil Oxidation Test Kit	1817

Lube Oil Oxidation Test Kit	1817b
Lube Oxidation Catalysts	8500
Lube Oxidation Catalysts	8501*
Lubricant Oxidation Research Test Kit	8500a
MNF_2 Magnetic Susceptibility	766-1
Mica X-Ray Diffraction	675
Neutral Glass Anneal Point	716
Nickel Magnetic Susceptibility	772
Opal Glass Composition	91
Palladium Magnetic Susceptibility	765-1
Palladium Magnetic Susceptibility	765-2
Palladium Magnetic Susceptibility	765-3
Platinum Magnetic Susceptibility	764-1
Platinum Magnetic Susceptibility	764-2
Platinum Magnetic Susceptibility	764-3
Refractive Index Glass	1822
Respirable Cristobalite	1879
Respirable Quartz	1878
Ruby EPR Absorption	2601
Sapphire Thermal Expansion	732
Silicon X-Ray Diffraction	640(b)
Silver Vapor Pressure	748
Soda Lime Flat Glass Composition	S620
Soda Lime Float Composition	1830
Soda Lime Float Viscosity	710
Soda Lime Sheet Composition	1831
Soda-Lime-Silica Glass	710a*
Sulfur in Base Oil	1819
Toluene 5 ML	211C
Total Nitrogen in Lubricating Base Oil	1836
Tungsten Thermal Expansion	737
Total Nitrogen in Base Oils	1836
X-Ray Diffraction Intensity Set	674a
Wear Metals in Oil	1084a
Wear Metals in Oil	1085a

*New in FY-1991

SELECTED TECHNICAL/PROFESSIONAL COMMITTEE LEADERSHIP

American Association for the Advancement of Science

- Physics Committee
  - B. Steiner, Representative of the Optical Society of America

American Ceramic Society

- Program and Meetings Committee
  - S. Freiman, Incoming Chairman
- Glass Division
  - Committee on Glass Standards Classification and Nomenclature
    - M. Cellarosi, Chairman
  - Editorial Committee
    - S. Wiederhorn, Subchairman
- Basic Science Division
  - Editorial Committee
    - B. Lawn, Chairman
  - Program Committee
    - E. Fuller, Jr., Chairman
- Communication of the American Ceramic Society
  - E. Fuller, Jr., Contributing Editor
- Engineering Ceramics Division
  - D. Cranmer, Vice-Chairman

ASM International

- Energy Division
  - S. Dapkunas, Chairman
- Journal of Engineering Materials
  - S. Dapkunas, Associate Editor
- Washington D.C. Chapter Education Committee
  - J. A. Carpenter, Jr., Chairman

American Society for Engineering Education

- Postdoctoral Review Committee
  - A. Feldman, Member

American Society for Testing and Materials

- C14: Glass and Glass Product
  - M. Cellarosi, Chairman
- C14.01: Nomenclature of Glass and Glass Products
  - M. Cellarosi, Chairman
- C28. Advanced Ceramics
  - G. D. Quinn, Vice-Chairman
- C28.05: Task Group on Powder Characterization
  - S. Malghan, Working Group Chairman
- C28.07: Ceramic Matrix Composites
  - D. C. Cranmer, Chairman
- D2: Petroleum Products and Lubricants

American Society for Testing and Materials (cont'd)

D2.09G: Response of Base Oils to Oxidation Inhibitors
J. Perez, Chairman
C. Ku, Secretary

E24.07: Fracture Toughness of Brittle Nanmetallic Materials
G. D. Quinn, Member

E29.01: Advanced Ceramics, Organizational Meeting
M. Cellarosi

E42: Surface Science
G. G. Long, Member

Fl:02: Lasers
A. Feldman, Subcommittee Editor

G2.2.02: Solid Particle Erosion
A. Ruff, Task Group Leader

G2.4.04: Pin-on-Disk
A. Ruff, Chairman

G2.92: Computerization in Wear and Erosion,
A. Ruff, Chairman

American Society of Mechanical Engineers

Journal of Tribology
S. Jahanmir, Associate Editor

Research Committee on Tribology
S. Jahanmir, Chairman
S. Hsu, Member

Wear of Materials Conference Steering Committee
A. Ruff, Member

COMAT Subcommittee on Structural Ceramics
S. Hsu, Member

COMAT Subcommittee on Superconductivity
S. Dapkunas, Member

Diamond Films and Technology
Editorial Advisory Board
A. Feldman, Member

IEEE Lasers and Electrooptics Society
Washington-Northern Virginia Chapter
B. Steiner, Treasurer

International Energy Agency
Task II - International Standards
S. Hsu, Overall Task Leader on Powder Characterization
Subtask 6 Powder Characterization Subgroup
S. Malghan, U. S. Task Leader
Assignment II-O-3 Ceramic Characterization
E. Fuller, Jr., Member

International Union of Crystallography (IUCr)
Commission on Crystallographic Studies at Controlled Pressures and Temperatures
G. Piermarini, Chairman

Materials Research Society
Washington-Baltimore Chapter
A. Feldman, President

Minerals and Metallurgical Processing Journal
Editorial Board
S. G. Malghan, Member

National Materials Advisory Board, National Academy of Sciences
Committee on Ceramic Tribology
S. Hsu, Member
S. Jahanmir, Member
Committee on Superhard Materials
A. Feldman, Member

National Synchrotron Light Source
Housing Committee
C. E. Bouldin, Member
User Executive Committee
G. G. Long, Member
EXAFS Special Interest Group
C. E. Bouldin, Chairman
Proposal Study Panel
D. A. Fischer, Member
Housekeeping Committee
J. C. Woicik, Member

NIST Cold Neutron Research Facility
G. G. Long, Program Advisory Committee Member

Optical Society of America
Meggers Award Committee
B. Steiner, Member (ex officio as past chairman)

Powder and Bulk Engineering Journal
S. Malghan, Member Editorial Advisory Board

Society of Automotive Engineers
Task Group on Recommended Practices for the Measurement of Unregulated Diesel Emissions
J. Perez, Chairman

Society of Photooptical Instrumentation Engineers
Kingslake Award Committee
B. Steiner, Chairman

Society of Tribologists and Lubrication Engineers
Annual Meeting Program Committee
S. Jahanmir, Member
Board of Directors
S. Hsu, Director
Ceramics and Composite Committee
S. Jahanmir, Chairman

Strategic Defense Initiative Organization Technology Applications Office (SDIO/TA)
Materials and Electronics Panel
J. A. Carpenter, Jr., Member

Superconductor Applications Association
E. Fuller, Jr., Member of Advisory Board

Versailles Project on Advanced Materials and Standards (VAMAS)
Technical Working Area on Ceramics
G. D. Quinn, U. S. Representative and International Chairman

Technical Working Area on Wear Test Methods
S. Jahanmir, U. S. Representative and International Leader

INDUSTRIAL

ACTIS, Inc.

An agreement has been signed between NIST and ACTIS, Inc. for a joint research and development activity related to comprehensive computerized tribology databases. These databases will be evaluated by NIST and marketed by ACTIS, Inc. Other participants in the program are DOE, U.S. Army, U.S. Air Force, ASME and STLE.

Adiabatics, Inc.

As part of the Gas Research Institute joint study, research on valve materials selection and wear mechanisms in gas-fired engines was conducted (L. K. Ives and E. P. Whitenton, NIST; R. Kamo, Adiabatics).

Advanced Technology Materials (ATM)

A collaboration between NIST (L. H. Robins) was begun with Advanced Technology Materials (C. Beetz) to characterize chemically doped diamond specimens from ATM by cathodoluminescence imaging and spectroscopy.

AKZO Chemical Co.

A Cooperative Research and Development Program is in progress to utilize the NIST technology (J. M. Perez and C. S. Ku, NIST; T. Marolewski, AKZO) in development of a high temperature liquid lubricant for evaluation in low heat rejection engines.

Allied Signal Corporation

The Tribology Group (S. Jahanmir) is participating in a joint program with Allied in research aimed at using silicon nitride in diesel engine applications. The purpose of this program is to define the role of surface condition and finishing methods on tribological performance. The samples are prepared and characterized by Allied Signal Aerospace Company (M. Meiser), and subsequently tested and analyzed by NIST.

A joint research program is underway to determine the role of impurities in superconducting ceramic powders on limiting the critical current density in the final product. Allied (A. Trivedi) is supplying superconducting powders containing various quantities of carbon and other impurities. NIST (S. Freiman) is processing these powders and determining critical current densities. The work will be published as a joint paper.

S. G. Malghan is conducting collaborative studies with B. Busovne and J. Pollinger of Garrett Ceramic Components (an Allied subsidiary) on the interactions of powder-binder-sintering aid in the processing of silicon nitride powders. Garrett intends to utilize the results developed at NIST.

Allison

D. C. Cranmer has been collaborating in a program started to completely evaluate the creep and creep rupture behavior of PY6, a grade of silicon nitride made by GTE. This work is being done in collaboration with Pramod Khandelwal of Allison Gas Turbine.

Applied Physics Laboratory (APL)

A collaboration between NIST (L.H. Robins) and Johns Hopkins Applied Physics Laboratory (A. Wickendon) to characterize the optoelectronic properties of epitaxial films and heterostructures of the aluminum gallium nitride ($Al_xGa_{1-x}N$) system. These films, grown at APL by metalorganic chemical vapor deposition, show promise for applications as blue-violet/UV laser and non-laser light sources, photoconductive light detectors, and electro-optic modulators. Spectroscopic characterization techniques to be applied to these films include cathodoluminescence, photoluminescence, photoconductivity, and electroabsorption; preliminary cathodoluminescence measurements have already been carried out.

The magnetic properties of superconducting $YBa_2Cu_3O_{6+x}$ single crystals fabricated at NIST (D. Kaiser) are being measured at Johns Hopkins Applied Physics Laboratory (K. Moorjani, J. Bohandy, B. Kim, F. Adrian) to study details of the superconducting transition in twinned and detwinned crystals.

Argonne National Laboratory

P. R. Jemian is collaborating with G. G. Long and S. Krueger (Reactor Division) on neutron and x-ray scattering by novel materials.

AT&T (Bell Laboratories)

There is a joint research program on the phase relations in superconducting ceramics between AT&T Bell Laboratories (S. Sunshine) and NIST (R. Roth). Specimens are exchanged and x-ray diffraction data analyzed to determine crystal structure. Several joint papers have resulted from the ongoing interaction between NIST and AT&T.

Dr. Cliff King is collaborating with J. C. Woicik (NIST) and C. E. Bouldin (NIST) on the structure of boron-doped SiGe heterojunction bipolar transistors.

Battelle Columbus Laboratories

A joint activity is underway to prepare a wear atlas from selected literature and research findings at Battelle Columbus Laboratories, NIST, and the West German Bundesanstalt fur Materialprufung. Battelle (W. Glaeser) and NIST (A. W. Ruff) are evaluating publications in wear and friction to select authoritative findings that relate wear and friction with materials properties and surface morphology.

Carborundum Company

Dr. Divakar is a Research Associate in the Tribology Group, participating in a joint research program with NIST (S. Jahanmir) on the wear mechanisms of advanced ceramics and composites at elevated temperatures. The aim of this program is to define the controlling effect of microstructure on friction and wear behavior of silicon carbide.

Catalyst Research Corp.

D. Schrodt (CRC) has obtained laboratory procedures from J. Ritter for designing tests for Li-batteries.

Caterpillar Corporation

Discussions and an exchange of visits has taken place with technical staff from Caterpillar Corporation (F. A. Kelley) in connection with wear of certain types of equipment bearings. The company is considering establishing a Research Associate at NIST (A. W. Ruff) in the area of wear-resistant coatings and galling wear.

CPS Superconductor

A joint research program has been established to determine the link between melt processing procedures and phase equilibria in superconducting ceramics, as well as to determine the strength of superconducting ceramic fibers. CPS Superconductor (J. Hodge) is supplying materials, while NIST (S. Freiman) will develop the necessary test procedures and phase diagrams. The work will result in joint publications.

Crystallume

Unique samples of thick homoepitaxial diamond films were provided to D. R. Black, The defect microstructure of these films was examined by x-ray topography and correlated to the substrate microstructure.

Delco Products (Division of General Motors)

Dr. V. Ananthanarayanan, Delco Products, has collaborated with S. Malghan in developing test procedures for evaluating the dispersion of strontium ferrite in aqueous environment. Two scientists spent two months at NIST to conduct experimental research. Based on these results, a development program is being carried out at the Delco Products production facility.

EG&G Energy Systems

Collaboration in diffraction imaging on irregularities in mercuric iodide crystals and detectors grown in space and on the ground. (Bruce Steiner, NIST, and Lodewijk van den Berg, EG&G)

E. I. DuPont de Nemours & Co.

DuPont (D. Roach) has provided alumina and alumina-zirconia fibers to C. Ostertag for incorporation into ceramic, ceramic-metal, and glass matrix composites.

Edge Technology Inc.

Artificial diamonds to be used as machine tools were supplied to D. R. Black. Topographic examination of these crystals was correlated to optically observed defects for quality control.

Electric Power Research Institute

EPRI (W. Bakker) is funding a program in the Ceramics Division (S. Freiman) to develop superconducting ceramics for conductor applications. The program involves determining the effects on critical current density of substituting other rare earth ions for yttrium in Ba-Y-Cu-O superconducting ceramics. Phase equilibria and processing data relevant to the production of these materials are being obtained.

Ford Motor Company

Ford Motor Company (K. Carduner and M. Rokosz) have been active in the application of NMR spectroscopy and imaging to characterize ceramic materials. Collaborative effort with P. S. Wang involves data exchange of Si-27 CP/MAS NMR for phase composition determination of silicon nitride and carbide powders. In the future, we plan to exchange imaging capabilities.

Gas Research Institute and Center for Advanced Materials, Pennsylvania State University

The Structural Ceramics Database project was funded in part by the Gas Research Institute through the Center for Advanced Materials at Pennsylvania State University, as an important step towards the use of advanced ceramics in heat exchangers and gas-fueled engines.

General Electric Corporate Research and Development

A collaborative research program to study the microstructure of large artificial diamond has been established with D. R. Black in the Materials Microstructure Characterization Group.

Grumman Corporation

Collaboration in diffraction imaging on the crystal perfection of zinc cadmium telluride crystals grown in space and on the ground. (Bruce Steiner, NIST, and David Larson, Grumman)

GTE Laboratories, Inc.

GTE (J. Baldoni) has provided whisker-reinforced and whisker-free silicon nitrides to S. Wiederhorn and D. Cranmer for evaluation of creep and creep rupture, and changes in microstructure as a result of creep.

Collaboration in diffraction imaging on irregularities in gallium arsenide. (Bruce Steiner, NIST, and David Matthiesen and Brian Ditchek, GTE)

Hughes Research Laboratories

Collaboration in the crystal growth of barium titanate. (Bruce Steiner, NIST, Mark Cronin-Golomb and Gerard Fogarty, Tufts University, and Barry Wechsler, Hughes)

Infrared Fiber Systems, Inc.

A collaboration between NIST (E.N. Farabaugh) and Infrared Fiber Systems (D. Tran) to develop corrosion resistant diamond coatings for crucibles used in melting heavy metal fluoride glasses.

Matec Applied Sciences

This cooperative research is related to the development of electrokinetic sonic amplitude measurement for dispersion of powders in dense slurries. Research at NIST under the direction of S. Malghan will be utilizing hardware and software developed by Matec Applied Sciences for on-line measurement of dispersion.

Naval Research Laboratory

S. Lawrence and B. Bender (NRL) are collaborating with J. Wallace on the thermochemical treatment of polymer-derived SiC fibers and the degradation mechanisms of these fibers during high temperature heat treatments. A joint publication is planned.

Norton Company

In one collaborative project V. Pujari and C. Willkens of Norton Company, and S. Malghan of NIST are studying the characteristics of agitation milled silicon nitride powders in aqueous environment. Norton Company has provided silicon nitride powder samples. Based on the results of first stage of collaboration, a second stage of research was initiated with an intent to compare the performance of agitation ball milling to large-scale processing by conventional methods.

Thermal conductivity measurements are important for characterizing diamond films. Interaction with Norton (K. Grey) involved learning to use the NIST (A. Feldman and H.P.R. Frederikse) photothermal radiometry facility for the purpose of setting up such a facility at Norton. We plan to collaborate in the analysis of the data generated at Norton.

Norton/TRW Co.

Norton/TRW (R. Yeckley) has provided a Y_2O_3-containing silicon nitride to S. Wiederhorn and D. Cranmer for evaluation of creep and creep rupture, and changes in microstructure as a result of creep.

Oak Ridge National Laboratory (ORNL)

A collaboration between NIST (L.H. Robins) and Oak Ridge National Laboratory (ORNL) to characterize the microstructure of thin diamond films on optical glass substrates by the method of photon scanning tunneling microscopy. This method was recently developed by the ORNL researchers.

Research Triangle Institute

A joint research project was developed with D. R. Black to study the microstructure of diamond substrates to be used for homoepitaxial growth of diamond films by chemical vapor deposition.

Rockwell International

A collaboration between NIST (A. Feldman) and Rockwell International (S. Holly) to organize the Diamond Optics IV conference sponsored by the Society of Photo-Optical Instrumentation Engineers (SPIE).

Sanders Corporation

Collaboration on the crystal growth of barium titanate single crystals (Bruce Steiner, NIST, Mark Cronin-Golomb and Gerard Fogarty, Tufts University, and Tom Pollack, Sanders)

Schmidt Instruments

A collaborative research project was initiated with D. R. Black to grow heteroepitaxial diamond films and characterize their crystal perfection.

Southwest Research Institute

R. A. Page, Southwest Research Institute and S. Krueger, Reactor Division, NIST, are collaborating with G. G. Long on multiple angle small angle neutron scattering (MSANS) studies of pore evolution in alumina.

Ube Industries, Japan

Ube Industries (T. Yamada) has collaborated with S. Malghan by providing powder samples for studying the high energy agitation milling of silicon nitride powders. The specific interest lies in the development of an understanding of morphological and surface chemical changes taking place to the milled powders.

Uniroyal/Ciba Geigy/R. T. Vanderbilt/Shell Ltd.

Development of high temperature liquid lubricants involves cooperative efforts with several additive manufacturers. This cooperative research (C. S. Ku and J. M. Perez) has resulted in several candidate lubricants for evaluation in low heat rejection engines.

USSR Academy of Science

Cooperative activities under the NIST-USSR Academy of Science Agreement have continued in the areas of tribology and materials science. Current emphasis is on a joint US-USSR book on tribology (A. W. Ruff and S. Jahanmir). Future benefits to NIST and the Division include exchange of tribology data, exchange of computer software for surface analysis, and future exchange of technical staff.

ACADEMIA

Alabama A&M University

Collaboration on the crystal growth of triglycine sulfate in space and on the ground (Bruce Steiner, NIST, and Ravindra Lal and Ashok Batra, Alabama A&M)

Auburn University

A collaboration between NIST (A. Feldman) and Auburn University (Y. Tzeng) to organize the First International Conference on the Applications of Diamond Films and Related Materials, ADC'91.

Clemson University

B. I. Lee is collaborating with S. Malghan on surface chemical characteristics of silicon nitride powders in aqueous environment in the presence of organic surface active agents.

Columbia University

P. Somasundaran has been collaborating with S. Malghan on a research project to study basic parameters affecting the preparation of dense suspensions of silicon nitride powder containing sintering aids.

Drexel University

This is a joint program between Drexel University (M. Barsoum) and NIST (D. Cranmer) to investigate and control the fracture behavior of ceramic and glass matrix composites.

East China University of Chemical Technology

This is a joint effort to use finite-element techniques to analyze creep behavior of ceramic c-rings at elevated temperatures. ECUCT (D. Wu and Z-D Wang) is developing the finite element model for C-rings and a computational algorithm for creep and NIST (T.-J. Chuang) is providing a theoretical framework and experimental data to support the program.

Johns Hopkins University

Professor J. Kruger and L. Krebs are collaborating with G. G. Long, NIST, and C. Majkrazak (Reactor Division, NIST) on in situ polarized neutron reflectometry studies of the nature and structure of passive films.

The magnetic properties of superconducting $YBa_2Cu_3O_{6+x}$ single crystals fabricated at NIST (D. Kaiser) are being measured at Johns Hopkins (K. Moorjani, J. Bohandy) using the recently-developed, magnetically modulated microwave absorption (MAMMA) technique. The crystals have produced the cleanest, sharpest spectra of any superconducting sample measured by this technique. The objective of this effort is to study the details of the superconducting transition in twinned and detwinned crystals in order to further the understanding of the mechanism of high temperature superconductivity.

Dan Shechtman of Johns Hopkins is collaborating with NIST (A. Feldman and E. Farabaugh) in the high resolution TEM analysis of CVD diamond nucleation and growth.

Lehigh University

This is a collaboration to determine the effect of microstructure on the fracture resistance of monolithic ceramic materials. The materials under study have been manufactured at Lehigh University (H. Chan, M. Harmer) and are being characterized at NIST (B. Lawn).

Louisiana State University

Crystal structure determinations on a detwinned single crystal of $YBa_2Cu_3O_{6+x}$ (T_c = 89 K) were performed in this joint activity between Louisiana State University (S. Watkins, F. Fronczek) and NIST (D. Kaiser, F. Gayle). The results indicated that the oxygen atoms in the O(4) chain sites are offset from the crystallographic b-axis, leading to zig-zag rather than linear Cu-O chains. Weak superlattice reflections were observed, indicating a possible superstructure linked to three-dimensional ordering of oxygen and/or gold atoms.

Massachusetts Institute of Technology

Collaboration in diffraction imaging on the crystal growth of barium titanate (Bruce Steiner, NIST, and Mark Garrett, MIT)

National Tsing Hua University

S.B. Lee and J.L. Chu are collaborating with T.-J. Chuang, NIST on the diffusional crack growth along a bimaterial interface.

North Carolina State University

A joint research project with D. R. Black has been developed to supply and characterize copper single crystal substrates for use as substrates for heteroepitaxial growth of diamond films.

Northwestern University

J. Weertman and P. Jemian are collaborating with G. G. Long, NIST, on anomalous small angle x-ray scattering to separate contributions from various scattering species in a complex material.

J. R. Weertman is collaborating with G. G. Long, NIST, on high-resolution x-ray scattering measurements of nanophase materials.

Northwestern University/Pennsylvania State University

Joint research involves lubrication modeling between NIST, E. E. Klaus (PSU) and H. S. Cheng (NWU). The research focuses on the microelastohydrodynamic theories under wearing conditions. This is the first attempt at combining surface chemistry with surface mechanics to create a predictive wear model.

Oklahoma State University

Collaborative research between OSU and NIST (R. Powell and D. Cranmer) is being conducted to investigate the properties of permanent, laser-induced refractive index gratings based on Eu-containing glasses. The end result of this effort will be a device for processing optical signals.

Pennsylvania State University

The Tribology Group has several joint research projects with the Department of Chemical Engineering and the Materials Research Laboratory at PSU. The research projects include fundamental studies on the vapor phase lubrication of ceramic materials at high temperature; microstructural effects in ceramic wear processes; high temperature friction and wear tribometer design; and ceramic wear modeling which seeks to establish a theoretical understanding of ceramic wear processes.

Rensselaer Polytechnic Institute

Collaboration on the diffraction imaging of semiconducting multilayers (Bruce Steiner, NIST, and Krishna Rajan, RPI)

Rutgers University

S. C. Danforth (Rutgers) has provided A. Pechenik (NIST) with nano-sized Si_3N_4 powder. The powder is processed at NIST using our diamond cell.

Stanford University

Professor W. Spicer is collaborating with J. C. Woicik, NIST, on the structure of metal/semiconductor interfaces and clean semiconductor interfaces.

Tufts University

Collaboration on the observation of four wave mixing and related optical phenomena in non linear optical crystals (Bruce Steiner, NIST, and Mark Cronin-Golomb and Gerard Fogarty, Tufts)

University of California at Berkeley

A.M. Glaeser is collaborating with T.J. Chuang, NIST, on microdesign of interfacial defects to be implemented in alumina and sapphire for creep rupture studies.

University of California at Santa Barbara

Joint experiments between University of California (J. N. Israelachvili, P. McGuiggan) and NIST (R. Horn and D. Smith) are being conducted to investigate frictional properties of silica surfaces under dry conditions and with a variety of thin ($<$ 10 nm) intervening liquid films.

University of Colorado/Joint Institute for Laboratory Astrophysics

Collaboration in the surface treatment of barium titanate single crystals (Bruce Steiner, NIST, Mark Cronin-Golomb and Gerard Fogarty, Tufts University, and Dana Anderson, U. Col.)

University of Dayton Research Institute

Using UDRI's x-ray photoelectron spectrometer (XPS) and Auger electron spectrometer (AES), T. Wittberg, UDRI, is conducting studies on surface structures and reactivities with P. S. Wang, NIST. A variety of powders and ceramic materials have been investigated and the results have been published.

University of Florida

B. Moudgil is studying the characterization techniques and structure of flocs in dense slurries with G. G. Long and S. G. Malghan. Primary emphasis is placed on interfacial, rheological, and scattering (neutron and x-ray) techniques.

University of Houston

In this joint effort between the University of Houston (S. Moss, P. Wochner) and NIST (D. Kaiser, F. Gayle), detwinned single crystals of $YBa_2Cu_3O_{6+x}$ are being measured by high resolution x-ray diffraction techniques to search for a structural transition associated with the onset of superconductivity.

University of Illinois

Soo Wohn Lee of the Department of Civil Engineering, Mechanics, and Metallurgy are conducting joint research with NIST. The project centers on an investigation of the fundamental mechanisms of friction, wear, and surface damage in tribological applications of advanced ceramics.

University of Maryland

A collaborative study between the University of Maryland (A. Roitburd) and NIST (D. Kaiser, F. Gayle, L. Swartzendruber, L. Bennett) involves theoretical aspects of twin boundary migration under an applied stress and flux pinning by twin boundaries in $YBa_2Cu_3O_{6+x}$. A model has been developed to calculate the velocity of boundary migration as a function of temperature and applied stress. Magnetization measurements demonstrating an effect of twin boundaries on flux pinning have been understood in terms of vortex/twin boundary interactions.

Three projects in the area of tribology are also underway: on wear models of ceramics, on the determination of residual stresses in ceramics by x-ray techniques, and on modeling of indentation of a solid surface. The project on wear models (S. Jahanmir, NIST; J. Dally, U. MD) deals with the application of photoelastic techniques for analysis near surface cracks. The results of this research are used to develop a wear model for ceramics. The project on indentation modeling will compare results with NIST nanoindentation measurements of selected materials and tribological films (A. W. Ruff, NIST; J. Stewart, U. MD).

L. Chang and Y. Zhang, U. MD, are collaborating with P. S. Wang on a project to investigate ceramic surface reactivities with surface lubricants at high temperature by TGA/DSC as well as surface film formations. The lubricant oxidation is studied through free radical formation and recombinations by the electron spin resonance (ESR) method.

R. K. Khanna is conducting joint research with S. Malghan on the Raman and FTIR Spectroscopy of silicon nitride, silicon carbide, zirconia and aluminum nitride powders.

A collaborative study between the University of Maryland (A. Roitburd) and NIST (D. Kaiser, F. Gayle, L. Swartzendruber, L. Bennett) involves theoretical aspects of twin boundary migration under an applied stress and flux pinning by twin boundaries in $YBa_2Cu_3O_{6+x}$.

University of Michigan

J. Schwank is carrying out specialized characterization of conductive ceramic powders by ESCA and Auger spectroscopy in collaboration with J. Ritter, NIST. These powders are synthesized at NIST for NASA.

University of Utah

A collaboration was begun between NIST (L. Robins) and the University of Utah (J. Viner) to measure the optical absorptance of CVD diamond films by the method of photothermal deflection spectroscopy (PTDS), using the PTDS apparatus developed at the University. Initial results for one sample show that PTDS is a promising technique.

University of Virginia

Samples of SiC reinforced metal matrix composite materials were provided to D. R. Black as part of a continuing collaborative research project to measure the thermally induced residual strain.

University of Washington

Professor Larry Sorenson is collaborating with C. E. Bouldin and J. C. Woicik on XAFS and diffraction studies of strained semiconductor materials.

University of Western Ontario

A collaboration was initiated this year between H. H. Schloessin and R. A. Secco of the Geophysics Department and R. D. Spal, NIST, involving the study of geological samples by means of x-ray diffraction topography and the asymmetric Bragg diffraction microscope.

University of Wisconsin

V. Hackley, Water Chemistry Program, Civil Eng. Department at the University of Wisconsin is conducting joint research with NIST on the electrokinetic sonic amplitude (ESA) measurement technique for dispersion of powders. The results of this research are to be used for the application of ESA technique for on-line monitoring of ceramic slurry properties.

A joint activity is underway between the University of Wisconsin (S. Babcock, X. Cai, D. Larbalestier) and NIST (D. Kaiser) to characterize the magnetic and electrical transport properties of single crystals and bicrystals of superconducting $YBa_2Cu_3O_{6+x}$.

FACILITIES

FACILITIES

POWDER CHARACTERIZATION AND PROCESSING

High Temperature X-ray Diffraction - J. P. Cline

The x-ray diffraction facility at NIST consists of a high temperature machine of theta-two theta geometry equipped with an incident beam monochromator and a position sensitive proportional counter. The furnace is an enclosed high vacuum chamber capable of reaching 3000 K; it is equipped with a mass flow controller for atmospheric control. The incident beam monochromator removes the $K\alpha_2$ radiation and results in diffraction profiles that are more sensitive to effects of sample character such as particle size and micro-strain. The position sensitive detector allows for data collection at rates of speed, and from a proportion of particles, two orders of magnitude greater than with conventional detectors. An automatic sample changer/sample spinner can be installed to allow for highly accurate powder measurements suitable for Rietveld refinement. Also on site are four automated and updated conventional diffractometers, some with automatic sample changers and sample spinners.

Electrokinetic Sonic Amplitude Measurement - L.-S. Lum and S. G. Malghan

The Matec ESA-8000 system has the unique capability for measuring colloidal properties in dense slurries. The analytical capabilities of the ESA system include performance in the following modes: potentiometric titration, conductometric titration, time-series titration, and concentration series titration. In the selected mode, the equipment can monitor: electrokinetic sonic amplitude, zeta-potential, electrophoretic mobility, electrical conductivity, isoelectric point, surface charge density, and phase angle of the material with the specified experimental conditions.

Slurry Rheology - S. G. Malghan

The RTI rheometer allows for viscosity as well as rheology characterization of ceramic slurries. Rheological measurements are more informative and flexible with respect to the various slurry properties: Newtonian, pseudoplastic, plastic, dilatant, and thixotropic. The modeling of these rheological properties as a function of sample treatment, surface chemical properties is paramount in developing and improving the slurry processing technology.

Physical Properties Characterization Laboratory - L. Lum, D. Minor, P. Pei and S. Malghan

The physical properties characterization laboratory is equipped with state-of-the-art techniques for the measurement of particle size distribution, specific surface area, specific gravity, tap density, and porosity. The particle size distribution is measured by three techniques -- gravity sedimentation by Sedigraph, centrifugal sedimentation by Joyce-Loeble, laser diffraction by Horiba LA-500. The range of particle size distribution covered by these techniques is 0.01 micron to 200 microns. The specific surface area determination is carried out by nitrogen adsorption and the BET method. The porosity of powders and ceramics is measured by mercury intrusion.

Agitation Milling of Powders - D. Minor and S. Malghan

High energy agitation milling of silicon nitride powders is carried out with a minimum contamination by the use of a specially designed milling system. This milling device allows for the size reduction of silicon nitride powder by milling at high slurry densities in approximately 1/6th to 1/10th of the time required by the conventional tumbling ball mill. The mill is lined with silicon nitride and the media are made of silicon nitride materials. Hence, external sources of contamination can be minimized.

Nuclear Magnetic Resonance (NMR) - P. S. Wang

The solid state NMR facility includes a Bruker MSL-400 NMR system capable of studying almost all NMR active nuclei in the periodic table in both solid and liquid states as well as performing NMR imaging in proton and carbon-13 frequencies. Currently, the operation parameters for both states at proton, deuterium, carbon-13, and aluminum-27 have been defined and proved by documented NMR spectra of organic and inorganic molecules. The equipment has been tuned to Si-29, Cu-63, and Y-89.

Scanning Electron Microscope/Image Analysis (SEM) Facility - J. F. Kelly

This laboratory is equipped with an Amray 1830 digital scanning electron microscope with LaB_6 source and a Leitz optical microscope. The SEM is equipped with a solid state backscatter detector and an ultrathin window x-ray detector. A Kevex Delta V EDS x-ray analysis and image analysis system is interfaced to both the SEM and optical microscopes. Automated imaging capabilities enable rapid size and shape analysis of a variety of imaged features, including ceramic powder particles and second phase regions in composite structures. Fracture stages have been developed for real time observation and measurement of in-situ crack propagation in ceramic specimens. The addition of an interior mounted phosphor screen with video camera imaging provides the capability of imaging single grain electron backscatter diffraction patterns from bulk specimens. This permits the measurement of crystallographic orientation in ceramic specimens.

Time-Resolved Micro-Raman - P. S. Wang

This versatile facility consists of a pulsed Nd-YAG laser, a CW Ar-ion laser, a triple monochromator, and a gated intensified diode array detector. This facility, therefore, provides a wide variety of Raman analysis techniques in both time-resolved and continuous operation modes, using either visible or ultra-violet excitation sources for either operation mode. In addition, either bulk macro-Raman or 5 μm resolution micro-Raman analysis is available.

Thermal Analysis Facility - J. Wallace and J. Blendell

A thermal analysis facility has been set up for measurement of behavior of ceramic materials in a wide range of atmospheres and temperatures. The equipment is comprised of a computer-controlled differential pushrod dilatometer capable of measuring thermal expansion or sintering shrinkage in vacuum, inert, oxidizing or reducing conditions from room temperature to 1600 °C. The atmosphere can be monitored using either a zirconia oxygen cell or an external mass spectrometer using its own associated computerized data acquisition system.

The second major piece of equipment is a simultaneous thermal analysis (STA) system which is capable of performing simultaneous thermogravimetric and differential thermal analysis from room temperature to 1700 °C. Atmospheres can be varied from vacuum to single and mixtures of gases using a four channel mass flow controller. The STA is also connected to the mass spectrometer system and it's associated data acquisition system. The quadrapole mass spectrometer system has a capability of analyzing to 512 AMU.

Chemical Laboratory Facilities - J. J. Ritter

Chemical synthesis of powders is carried out in a well-equipped laboratory, which consists of controlled atmosphere glove boxes, preparative chemical vacuum systems, and a chemical flow reactor. A range of powders can be synthesized for exploratory purposes.

Ceramics Powder Processing Laboratory - J. Wallace and J. Blendell

A processing laboratory for processing and sintering well controlled ceramic powders has been assembled. This facility consists of: equipment for chemical powder synthesis routes; attrition mills; ball mill; jet mill; pressure slip caster; uniaxial presses; cold isostatic press; spray dryers; drying ovens; hot presses; air furnaces to 1700 °C; controlled atmosphere furnaces with associated gas flow systems and oxygen sensors for temperatures to 1600 °C; graphite furnace for temperatures to 2300 °C and a hot isostatic press/gas pressure sintering furnace capable of 2300 °C and 200 MPa using graphite elements and insulation.

MECHANICAL PROPERTIES

Instrumented Indenter - D. Cranmer

This apparatus is designed to enhance our ability to measure the properties of the fiber/matrix interface in ceramic matrix composites. The instrumented indenter permits us to measure the force on and displacement of a fiber directly during loading and unloading. Previous methods for examining these properties could only measure the maximum applied load and inelastic displacement.

High Temperature Creep Apparatus - D. Cranmer and S. Wiederhorn

A series of four high temperature creep rigs (T_{max} = 1550 °C) equipped with laser displacement sensors are available to determine the behavior of materials at elevated temperatures. Additionally, a rig capable of 1800 °C in air equipped with the same laser displacement sensor is available.

Surface Forces Laboratory - R. Horn

The surface forces laboratory consist of a semi-clean room preparation facility and a crossed-cylinders surface forces apparatus. The crossed cylinder apparatus permits measurements of the forces associated with surfaces brought to within ~2 nm of one another through contact. It can be operated with a variety of liquid or gaseous environments, thus allowing investigations of the effects of chemical changes on forces between two surfaces.

Analytical Electron Microscopy - B. Hockey

Several transmission and scanning electron microscopes are available for analysis of the changes in microstructure as a result of creep.

Glass Melting - D. Cranmer and D. Kauffman

Extensive glass melting and annealing facilities for production of melts up to 1600 °C are available. Batch sizes up to about 2.5 -3 kg can be produced using this equipment. Special facilities for melts containing heavy metals such as thallium and lead are also available.

Viscometers - D. Cranmer

Rotating bob, fiber elongation, and bending beam apparatuses for determining the complete range of viscosity from about 10^{14} to 10^{1} poise over the temperature range from room temperature to 1600 °C are available.

Microsphere Fabrication - D. Cranmer

This special facility is available to make relatively uniform diameter spheres of about 1 - 10 micrometers. Virtually any glass composition which can be melted below 1600 °C can be made into spheres with this apparatus.

TRIBOLOGY

Friction and Wear Testing - S. W. Ruff

More than twenty different tribometers are available for the measurement of friction and wear of materials under different test conditions and environments. Examples include: high temperature unidirectional reciprocating tribometer, modified four ball wear tester with a special ball-on-three-flats adaptation, computer controlled pin-on-disk and single stroke pin-on-flat, high temperature erosion system, cross-cylinder standard test machine, dry sand and wet sand rubber wheel abrasion tester, and ferrograph for wear particle analysis. These tribometers can be used to simulate and analyze almost any desired test condition and environment.

Surface Analysis - J. Perez

Many analytical instruments are available for the chemical and morphological characterization of surfaces. These include: time resolved micro-Raman laser system for in-situ analysis of tribochemical reactions, room temperature and high temperature microindentation apparatus, computer controlled 3-D surface profilometer, computer controlled nanoindentation and scratch hardness tester, optical microscopes for surface analysis, unique liquid chromatography refractive index/UV atomic absorption surface film analyzer for organo-metallic compound identification and quantification, surface analyzer with Fourier transformed infrared and multi-photodiode ultra-violet spectroscopy, and other analytical instruments such as HPLC, LC, GC, GC-MS.

Tribo-System Simulation/Degradation Mechanisms - J. Perez

Various special lubricant simulation devices include: hot-tube, panel coker, oxidation, free radical titration, bearing corrosion, thin film oxidation test apparatus, thin film micro-oxidation apparatus for interface chemistry investigation, NIST modified thermal analyzer with high pressure differential scanning calorimeter (DSC) and thermogravimetric analyzer (TGA) for surface reaction products analysis, and NIST designed chemiluminescence apparatus to relate molecular structures to oxidation and surface reactions.

ELECTRONIC MATERIALS

Ceramics Processing Laboratory - J. Blendell, J. Wallace, S. Malghan

A processing laboratory for the synthesis and production of well controlled ceramics has been assembled. Equipment includes: cold isostatic process, hot presses, furnaces, milling equipment, a sinter forge and tape caster.

Level 10 Clean Room - J. Blendell

A Level 10 Clean Room has been constructed for the processing of ceramics in a controlled environment where the presence of air low contaminants can seriously affect the final products properties. The room is provided with separated work stations to allow simultaneous conduct of experiments.

Thermal Wave Analysis Facility - A. Feldman and G. White

This facility is used for characterizations based on variations of thermal diffusivities. Equipped with both an Ar-ion and CO_2 laser, the facility permits analyses by infrared and Mirage methods. It is especially useful as a nondestructive method of detecting flaws in ceramics especially in near-surface regions.

OPTICAL MATERIALS

Diamond Film Deposition - E. Farabaugh and A. Feldman

Facilities consist of two hot filament CVD reactors, a microwave enhanced CVD reactor. The hot filament reactors can deposit diamond onto substrates up to 2.5 cm x 2.5 cm. The microwave reactor can accommodate substrates up to 10 cm in diameter. The reactant gases are hydrogen and methane. Growth rates typically range from 0.1 to 0.6 μm/hr.

Optical Characterization - L. Robins and A. Feldman

Facilities include a Cary spectrophotometer for measuring optical transmittance in the spectral range 0.2 μm to 2.5 μm, optical spectrometers for measuring photoluminescence and Raman spectra, and an argon ion laser.

Defect and Morphology Characterization - L. Robins and L. Cook

Facility consists of a scanning electron microscope (SEM) equipped with mirrors for cathodoluminescence detection allowing for simultaneous electron and cathodoluminscence imaging. A spectrometer for optical spectrum analysis of the cathodoluminescence radiation is attached to the SEM.

Single Crystal X-Ray Diffractometer - W. Wong-Ng

A commercial automated x-ray diffractometer suitable for single crystals is available. It is used by researchers from the Reactor Radiation and Polymers Divisions, in addition to those from the Ceramics Division, in investigations of the crystal structures of materials.

Thin Film Deposition and Characterization - E. Farabaugh

Facility consists of an electron beam deposition system equipped with multiple sources for codeposition. Attached to the deposition system is surface analysis chamber with capabilities for Auger spectroscopy, electronic energy loss spectroscopy, x-ray photoelectron spectroscopy, and secondary ion mass spectroscopy. Facility includes a HP-1000 computer for data acquisition.

Metallorganic Chemical Vapor Deposition (MOCVD) System - D. Kaiser

The system has been designed for depositing selected oxide materials by the method of MOCVD. The materials that can be deposited depend on the availability of metallorganic precursor materials. At present precursors suitable for depositing titanium dioxide and barium oxide are available. The substrate area is approximately 1 cm x 1 cm.

MATERIALS MICROSTRUCTURE CHARACTERIZATION

Synchrotron Radiation Beamlines - G. G. Long

The Materials Microstructure Characterization Group operates two beamstations on the X23A port at the National Synchrotron Light Source at Brookhaven National Laboratory in New York. These two beamstations offer access to dedicated instrumentation for small-angle x-ray scattering, x-ray diffraction imaging (topography) and EXAFS.

Small-angle x-ray scattering can be carried out in the energy range from 5 to 11 keV. The minimum wavevector is 4 x 10^{-3} nm^{-1} and the wavelength resolution is $\Delta\lambda/\lambda = 10^{-4}$, nomalous small-angle scattering with excellent resolution. Diffraction imaging of single crystals and powders is carried out with monochromatic photons between 5 and 30 keV. An energy-tunable x-ray image magnifier enables imaging of microstructure down to less than 1 μm. EXAFS experiments are also performed over an energy range from 5 - 30 keV.

Small-angle scattering measurements on ceramic and metallurgical materials are being used to characterize the microstructure in the 2 nm to 1 μm size range as a function starting chemistry and processing parameters. Diffraction imaging is being used to study imperfections and strains in single crystals and powder compacts. EXAFS is being used to study the structure of strained semiconductor interfaces and metal multilayers. A combination of EXAFS and diffraction will provide a capability for site-specific local structure determination in crystals.

SANS - Ceramics Furnace - G. Long

The SANS-Ceramic furnace is a unique facility that is now coming together. This system will allow in-situ densification studies of ceramic powders and SANS application. The experimental system has been designed to carry out densification studies of oxide powders at temperatures up to 2000 °C. In addition, the furnace will be equipped with a dilatometer.

APPENDIX

National Institute of Standards and Technology
ORGANIZATIONAL CHART

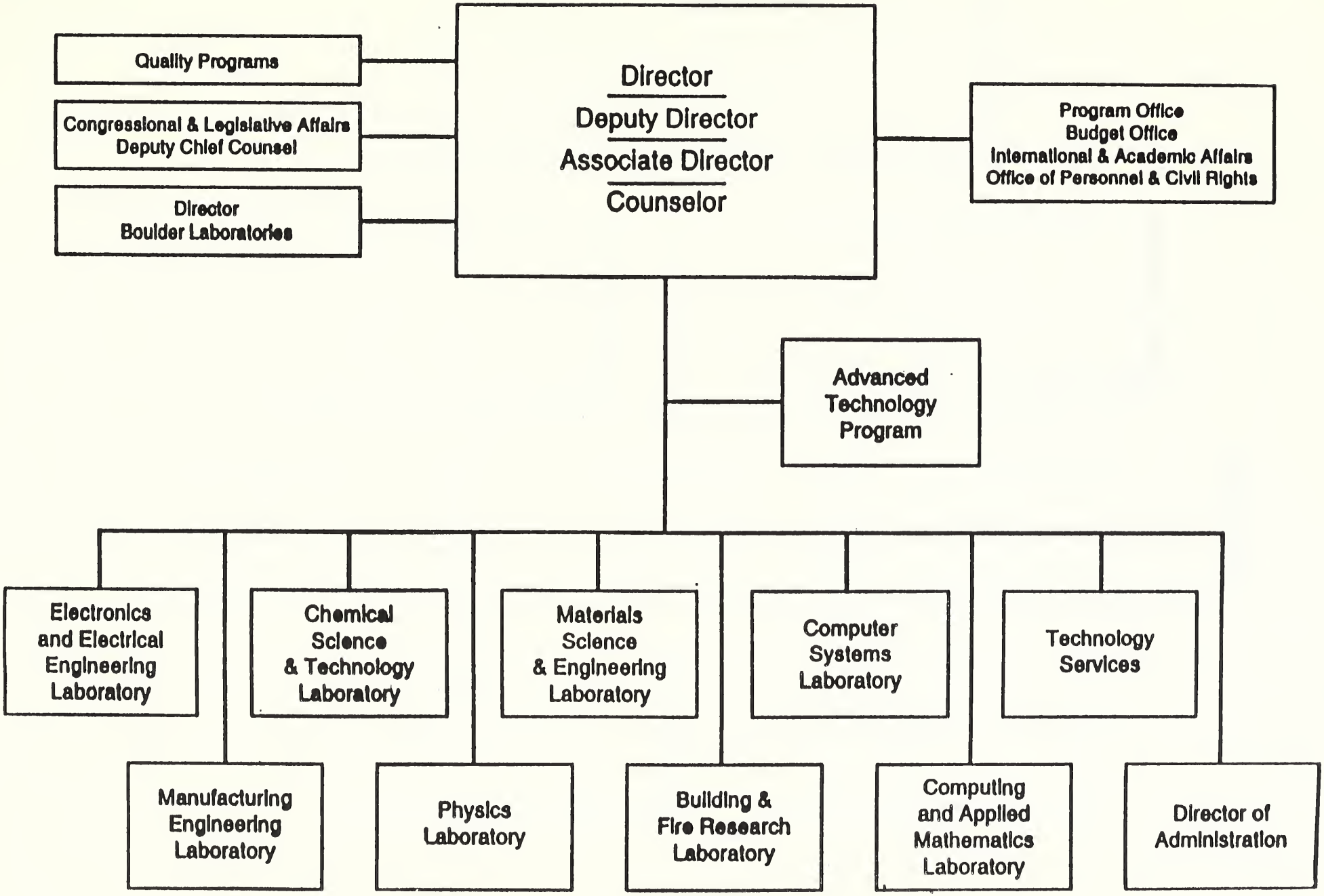

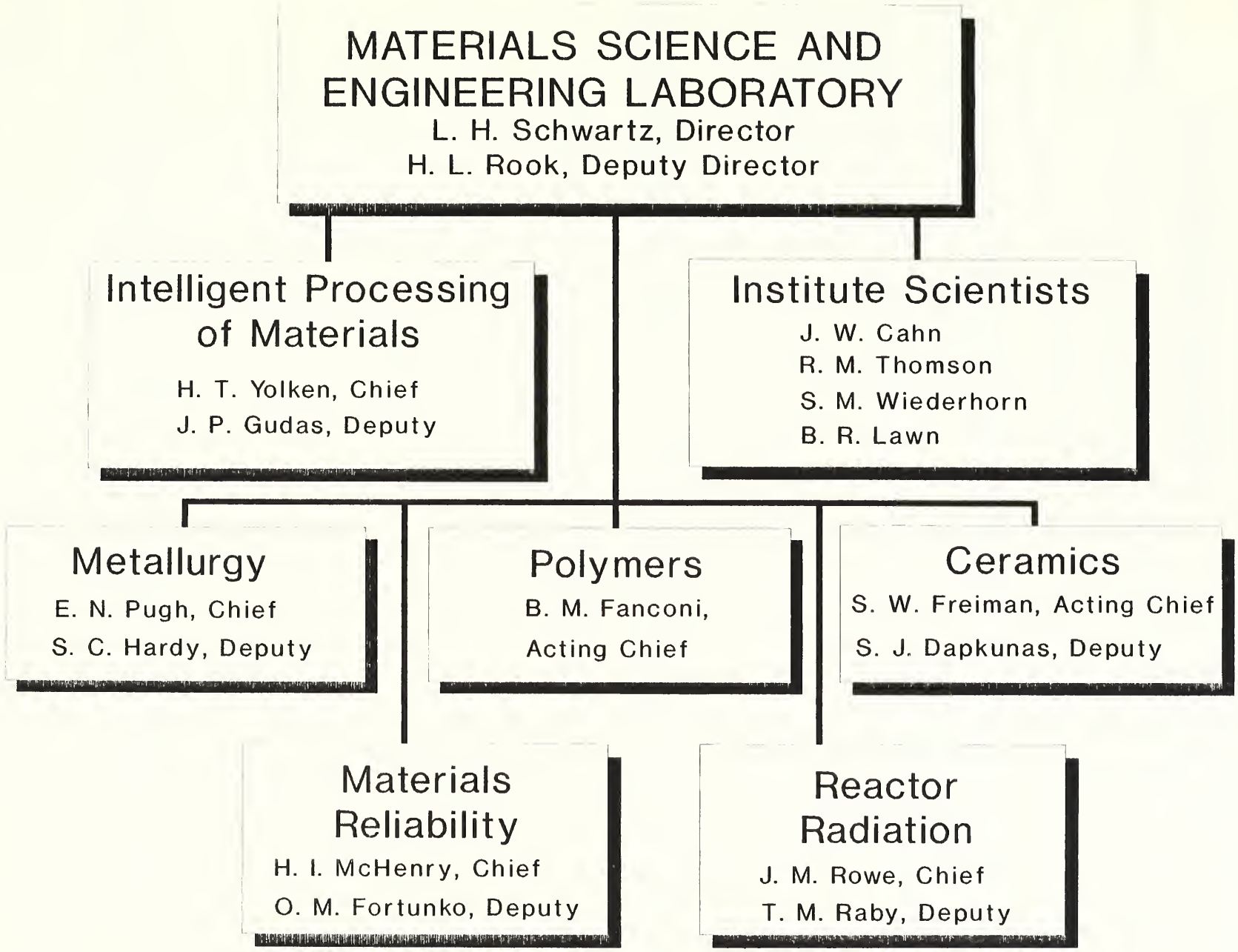
MATERIALS SCIENCE AND ENGINEERING LABORATORY
L. H. Schwartz, Director
H. L. Rook, Deputy Director
Intelligent Processing of Materials
H. T. Yolken, Chief
J. P. Gudas, Deputy
Institute Scientists
J. W. Cahn
R. M. Thomson
S. M. Wiederhorn
B. R. Lawn
Metallurgy
E. N. Pugh, Chief
S. C. Hardy, Deputy
Polymers
B. M. Fanconi,
Acting Chief
Ceramics
S. W. Freiman, Acting Chief
S. J. Dapkunas, Deputy
Materials Reliability
H. I. McHenry, Chief
O. M. Fortunko, Deputy
Reactor Radiation
J. M. Rowe, Chief
T. M. Raby, Deputy

NIST-114A
(REV. 3-90)

U.S. DEPARTMENT OF COMMERCE
NATIONAL INSTITUTE OF STANDARDS AND TECHNOLOGY

BIBLIOGRAPHIC DATA SHEET

1. PUBLICATION OR REPORT NUMBER
NISTIR 4694

2. PERFORMING ORGANIZATION REPORT NUMBER

3. PUBLICATION DATE
February 13-14, 1992

4. TITLE AND SUBTITLE

Ceramics Division - Technical Activities 1991

5. AUTHOR(S)

S. W. Freiman

6. PERFORMING ORGANIZATION (IF JOINT OR OTHER THAN NIST, SEE INSTRUCTIONS)

U.S. DEPARTMENT OF COMMERCE
NATIONAL INSTITUTE OF STANDARDS AND TECHNOLOGY
GAITHERSBURG, MD 20899

7. CONTRACT/GRANT NUMBER

8. TYPE OF REPORT AND PERIOD COVERED

9. SPONSORING ORGANIZATION NAME AND COMPLETE ADDRESS (STREET, CITY, STATE, ZIP)

NIST - Ceramics Division 852
Building 223/A256
Gaithersburg, MD 20899

10. SUPPLEMENTARY NOTES

11. ABSTRACT (A 200-WORD OR LESS FACTUAL SUMMARY OF MOST SIGNIFICANT INFORMATION. IF DOCUMENT INCLUDES A SIGNIFICANT BIBLIOGRAPHY OR LITERATURE SURVEY, MENTION IT HERE.)

Current programs of the Ceramics Division are reviewed.

12. KEY WORDS (6 TO 12 ENTRIES; ALPHABETICAL ORDER; CAPITALIZE ONLY PROPER NAMES; AND SEPARATE KEY WORDS BY SEMICOLONS)

Advanced Ceramics; Data Bases; Electronic Ceramics; Mechanical Properties; Optical Materials; Powder Characterization and Processing; Reference Data; Superconductors; Synchrotron Radiation; Tribology

13. AVAILABILITY

[X] UNLIMITED

[ ] FOR OFFICIAL DISTRIBUTION. DO NOT RELEASE TO NATIONAL TECHNICAL INFORMATION SERVICE (NTIS).

[ ] ORDER FROM SUPERINTENDENT OF DOCUMENTS, U.S. GOVERNMENT PRINTING OFFICE, WASHINGTON, DC 20402.

[X] ORDER FROM NATIONAL TECHNICAL INFORMATION SERVICE (NTIS), SPRINGFIELD, VA 22161.

14. NUMBER OF PRINTED PAGES
175

15. PRICE
A08

ELECTRONIC FORM